20

SOME STUDIES ON CHLOROCUPRATES

A Thesis submitted for the degree
of Doctor of Philosophy,
University of Stirling.

by Judith Murray-Rust

Stirling. April, 1971.

ACKNOWLEDGEMENTS

I would like to thank everyone who has helped me during this work and in the preparation of this thesis. I am particularly grateful to my supervisor, Dr. R. M. Clay, for his kindness, help and encouragement, and to my husband, both for his instruction in the technique of X-ray crystallography and for his patience during the last three years.

ABSTRACT

The work in this thesis is concerned with alkylammonium chlorocuprates and their solid solutions. The stoichiometries and structures of various chlorocuprate anions are considered in terms of the influence of the size and shape of the cation on the compounds formed. The determination of the structure of $(Me_3NH)_3Cu_2Cl_7$ by X-ray crystallography is described; it is unusual because it contains two distinct chlorocuprate anions, $CuCl_4^{2-}$ tetrahedra and $(CuCl_3^-)_n$ chains. The symmetry of the $CuCl_4^{2-}$ tetrahedron is approximately C_{3v}, and this is attributed to the effect of the packing of $(CuCl_3^-)_n$ chains, together with interactions between $CuCl_4^{2-}$ and the cations. The $CuCl_4^{2-}$ ion in this compound is replaceable by $CoCl_4^{2-}$ and $ZnCl_4^{2-}$, while the $(CuCl_3^-)_n$ chains are not disturbed. This led to a consideration of the possible effects of replacing the Jahn-Teller distorted ion in simple tetrachlorocuprates by ions not affected by this distortion, and hence to the preparation of solid solutions $A_2(M,M')Cl_4$.

The formation of solid solutions from a system of two salts having a common ion and a solvent is discussed, with particular emphasis on systems which deviate from ideal behaviour.

The preparations of solid solutions $(Me_4N)_2(Cu,Co)Cl_4$, $(Me_4N)_2(Cu,Zn)Cl_4$ and $(Me_4N)_2(Co,Zn)Cl_4$ from ethanol and water are described, and related to the general conditions for solid solution formation. Solid solutions $(Me_3NH)_3Cu(Cu,Co)Cl_7$ are also given.

Differential scanning calorimetry has been used in an attempt to elucidate the nature of the thermal transitions in $(Me_4N)_2MCl_4$ and in the solid solutions. The crystal structures of $(Me_4N)_2CuCl_4$, and $(Me_4N)_2(Cu,Co)Cl_4$ (Cu:Co = 1:1) have been determined, and compared with that of $(Me_4N)_2CoCl_4$. It has been shown that $CuCl_4^{2-}$ and $CoCl_4^{2-}$ each retain their characteristic configuration in the solid solution, so that $CuCl_4^{2-}$ is the more distorted, because of the Jahn-Teller effect.

Contents

Contents cont'd

CHAPTER I

INTRODUCTION

INTRODUCTION

The work contained in this thesis developed from an interest in the variety of stoichiometries and structures which are exhibited by chlorocuprate(II) complexes. Both the stoichiometries and structures of these anionic complexes are strongly dependent on the associated cation. This work is concerned with monovalent cations, and particularly the alkali metals and ammonium or substituted ammonium ions. Only the anhydrous salts have been considered.

Within these limits the various possible stoichiometries which occur are $ACuCl_3$, A_2CuCl_4, A_3CuCl_5 and $A_3Cu_2Cl_7$, where A is the monovalent cation.[1] Table I.1 shows which of these stoichiometries are found with various monovalent cations.

There is often more than one possibility for the coordination geometry of the chlorocuprate anion of a particular stoichiometry. Chlorocuprates are known in which the geometry around the copper(II) ion is formally octahedral, square planar, square pyramidal, tetrahedral or trigonal bipyramidal. As a d^9 ion, Cu^{2+} in a cubic field would have an orbitally degenerate ground state (^2E or ^2T); it is therefore expected, according to the Jahn-Teller theorem, that the ion will distort in order to remove the orbital degeneracy. The distortion splits the degenerate levels such that their centre of gravity remains constant, as shown in Fig.I.1 for a d^9 ion in an octahedral environment distorted towards D_{4h} symmetry. There is a net lowering of energy from the splitting of the e_g orbitals, provided these are not fully occupied. Similar lowering of energy occurs if the t_{2g} orbitals of the tetrahedral case are split. This type of distortion has been found in the chlorocuprate anions. An octahedral complex is not usually regular, but most commonly has four equatorial ligands at approximately the same Cu-Cl distance, which is shorter than the Cu-Cl distance for the two axial ligands and tetrahedral complexes do not have strict T_d symmetry.

The types of geometry found for the several chlorocuprate stoichiometries are given below.

$ACuCl_3$

(i) $(CuCl_3^-)_n$ chains formed by octahedra sharing faces as in $CsCuCl_3$[2] (Fig. I.2a).

(ii) $(Cu_2Cl_6)^{2-}$ dimers. The Cu$\overset{Cl}{\diagup\diagdown}$Cu bridge may either be symmetrical as in $KCuCl_3$[3] or non-symmetrical as in $(Me_2NH_2)CuCl_3$.[4] In $KCuCl_3$ the copper coordination is octahedral (Fig. I.2b); in $(Me_2NH_2)CuCl_3$ it is square pyramidal (Fig. I.2c).

A_2CuCl_4

(i) square planar $CuCl_4^{2-}$ ions with interactions between the ions producing distorted octahedral coordination for the copper as in $(NH_4)_2CuCl_4$[5] (Fig. I.2d).

(ii) tetrahedral $CuCl_4^{2-}$ ions in which the bond angles deviate from 109°28', as in Cs_2CuCl_4[6].

A_3CuCl_5

(i) trigonal bipyramidal $CuCl_5^{3-}$ ions as in $[Co(NH_3)_6]CuCl_5$[7].

(ii) a square planar $CuCl_4^{2-}$ ion (with axial interactions) and an isolated Cl^- ion as in $[(NH_2.CH_2.CH_2)_2NH_2]Cl(CuCl_4)$[8].

(iii) a tetrahedral $CuCl_4^{2-}$ ion and an isolated Cl^- ion as in Cs_3CuCl_5[9].

ACu_2Cl_5

The only known compound of this stoichiometry is $(Me_3NH)Cu_2Cl_5$,[10] and the structure is analogous to the $Cu_2Cl_6^{2-}$ dimer, i.e. a planar $[Cu_4Cl_{10}]^{2-}$ ion (Fig. I.2e).

$A_3Cu_2Cl_7$

The only known compound with this stoichiometry has $A = Me_3NH^+$. There are several possible arrangements of two copper^{2+}

and seven chloride ions which are chemically reasonable (Fig. I.3) and a structure determination was felt to be of interest. In order to appreciate some of what follows, it is necessary to mention briefly that this structure was found to contain two types of chlorocuprate coordination; $(CuCl_3^-)_n$ chains similar to those in $CsCuCl_3$ and tetrahedral $CuCl_4^{2-}$ ions.

During preparative work on the Me_3NHCl-$CuCl_2$ system an observation was made which led to much of the subsequent work. It was found that the $CuCl_4^{2-}$ ion in $(Me_3NH)_3Cu_2Cl_7$ could be replaced by $CoCl_4^{2-}$ or $ZnCl_4^{2-}$, while the $(CuCl_3^-)_n$ chains were not affected. In fact a series of solid solutions $(Me_3NH)_3Cu(Cu,M)Cl_7$ could be prepared.

This raised the question of whether the ions introduced into the lattice would be distorted in a similar manner to $CuCl_4^{2-}$ or not. There is no general reason why $CoCl_4^{2-}$ or $ZnCl_4^{2-}$ should be distorted from T_d symmetry, since they are not subject to Jahn-Teller distortion. However, distortion of the ions might be brought about by crystal-packing effects. The distortion of $CuCl_4^{2-}$ is normally attributed to the Jahn-Teller effect rather than lattice forces. If this is the case, then it might be expected that the $CoCl_4^{2-}$ or $ZnCl_4^{2-}$ ions (which are of similar size to $CuCl_4^{2-}$) would be undistorted when they replace $CuCl_4^{2-}$ in the lattice. Conversely if lattice forces were more important in the distortion of the $CuCl_4^{2-}$ ion, then the $CoCl_4^{2-}$ and $ZnCl_4^{2-}$ ions should also be distorted in the lattice. Study of the solid solutions should therefore give some indication of the nature of the forces causing distortion of the $CuCl_4^{2-}$ ion. These arguments should hold for any lattice containing $CuCl_4^{2-}$ ions and it was decided to study in the first instance simpler compounds containing only MCl_4^{2-} ions, such as $(Et_4N)_2MCl_4$ or $(Me_4N)_2MCl_4$.

Some measure of the ease of replacement of one ion by another can be gained from a study of the equilibrium between the two

salts in solution and in the solid phase. If in the system A_2MCl_4-$A_2M'Cl_4$-solvent the MCl_4^{2-}:$M'Cl_4^{2-}$ ratio at equilibrium is much greater in the solid phase than in solution, it can be considered that MCl_4^{2-} is energetically preferred over $M'Cl_4^{2-}$ in the lattice. The phase diagrams of various pairs of salts plus a solvent were therefore studied. Previous work on the classification and description of solid solution formation in this type of situation is discussed, and used to form a basis for comparison of the results obtained.

The solid products from this sort of experiment are expected to be homogeneous solid solutions, so that the effect of variation of composition on the geometry of the anion could be studied by such techniques as visible-ultraviolet spectroscopy, differential scanning calorimetry and X-ray crystallography.

Differential scanning calorimetry (DSC) has been used to detect thermal transitions in $(Me_4N)_2ZnCl_4$ and $(Et_4N)_2MCl_4$.[11] These have been tentatively assigned to the onset of rotation of the anions and cations, but are not understood in detail. It might be expected that alterations in the lattice as a result of solid solution formation would affect the transition temperature and ΔH and ΔS of the transitions, and it was hoped that DSC would help to elucidate the nature of the transitions.

X-ray crystallography is valuable in detecting any ordering which might occur in the solid solutions and in providing detailed information on bond lengths and angles. Clearly a full structure determination could not be attempted for each solid solution produced, but a study of a crystal of $(Me_4N)_2(Cu,Co)Cl_4$ containing approximately equal amounts of Co^{2+} and Cu^{2+} was undertaken.

REFERENCES FOR CHAPTER I

1. Colton & Canterford, "Halides of First Row Transition Elements" Wiley 1969
2. A. W. Schuleter, R. A. Jacobson & R. E. Rundle, Inorg.Chem. 1966, 5, 277
3. R. D. Willett, C. Dwiggins, R. F. Kruh & R. E. Rundle, J.Chem.Phys. 1963, 38, 2429
4. R. D. Willett, J.Chem.Phys. 1966, 44, 39
5. R. D. Willett, J.Chem.Phys. 1964, 41, 2243
6. B. Morosin & E. C. Lingafelter, J.Phys.Chem. 1961, 65, 50
7. K. N. Raymond, D. W. Meek & J. A. Ibers, Inorg.Chem. 1968, 7, 1111
8. B. Zaslow & G. L. Ferguson, Chem.Comm. 1967, 822
9. D. M. Adams & P. J. Lock, J.Chem.Soc. 1967(A), 620
10. R. D. Willett & R. Caputo, personal communication
11. T. P. Melia & R. Merrifield, J.Chem.Soc. 1970(A), 1166.

Figure I.1

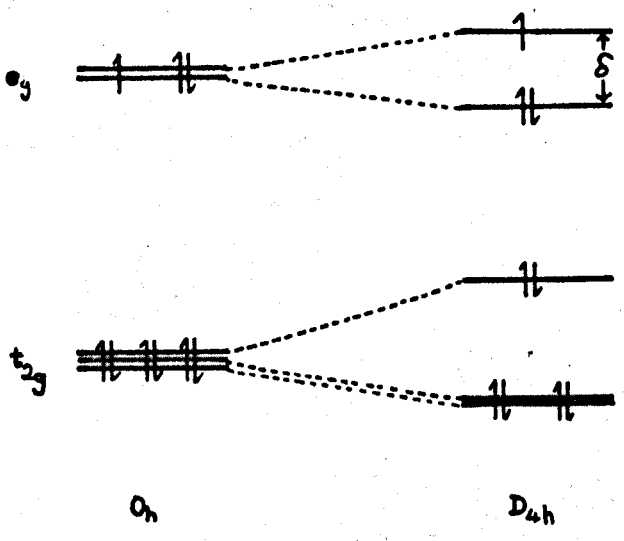

The Jahn-Teller effect for Cu^{2+}.

The distortion is from O_h to D_{4h} symmetry by stretching along z. A centre of gravity rule is obeyed for splitting of both e_g and t_{2g} sets. There is no net energy change for the t_{2g} electrons, but a net gain of $\frac{1}{2}\delta$ from the e_g electrons.

Figure I.2

The geometry of the copper ion environment in some chlorocuprates(II).

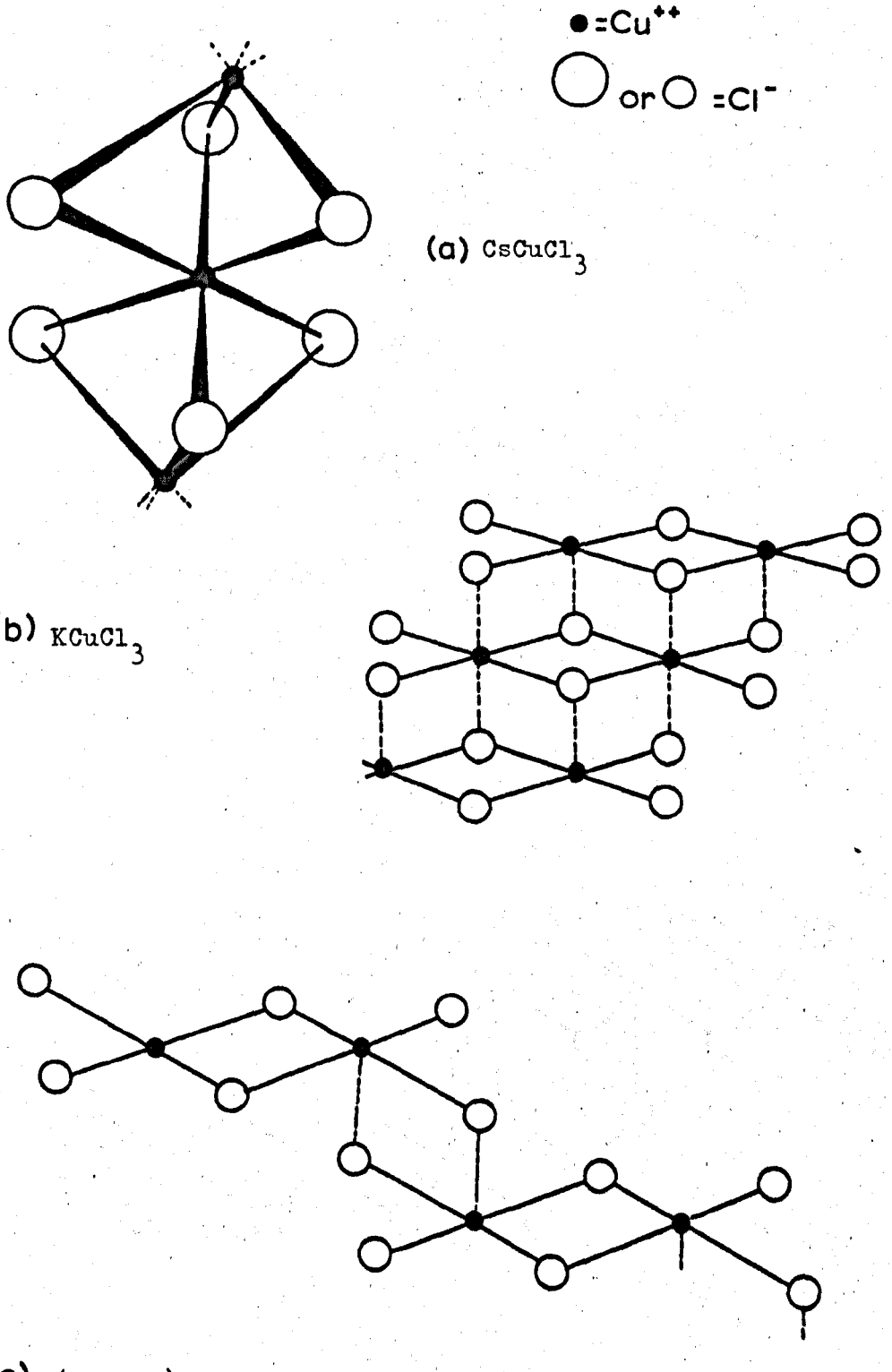

Figure I.2 cont'd

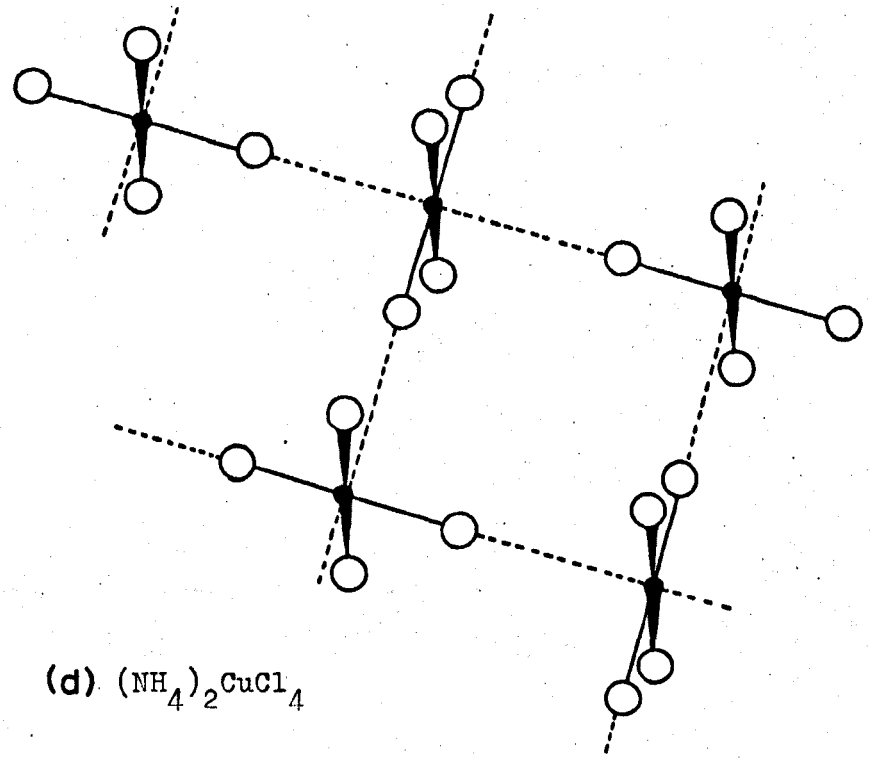

(d) $(NH_4)_2CuCl_4$

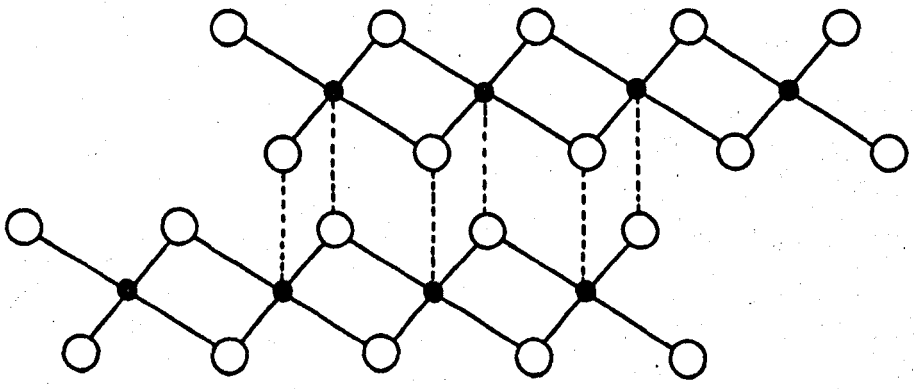

(e) $(Me_3NH)Cu_2Cl_5$

Figure I.3

Some possible arrangements of $Cu_2Cl_7^{3-}$ stoichiometry

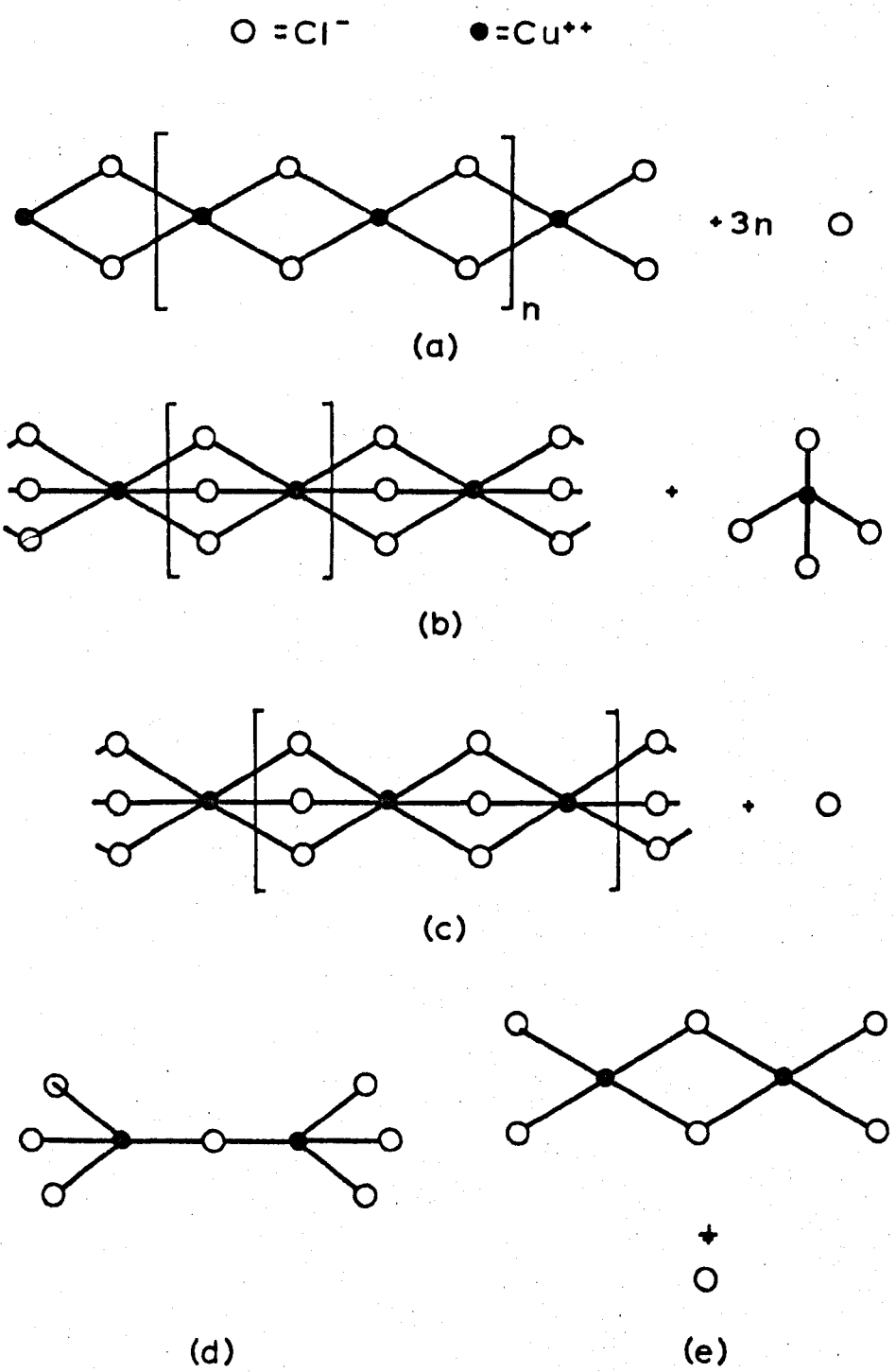

TABLE I.1

The chlorocuprates formed with a number of monovalent cations (A)

A = H^+	$HCuCl_3.2H_2O$, H_2CuCl_4, $H_2CuCl_4.5H_2O$, $H_3CuCl_5.nH_2O$
A = Li^+	$LiCuCl_3.2H_2O$, $LiCuCl_3.HCOOH$, $LiCuCl_3.CH_3CN$
A = Na^+	no complex formation
A = K^+	$KCuCl_3$, $KCuCl_3.2H_2O$, $K_2CuCl_4.2H_2O$
A = Rb^+	$Rb_2CuCl_4.2H_2O$
A = Cs^+	$CsCuCl_3$, Cs_2CuCl_4, $Cs_2CuCl_4.2H_2O$, $Cs_3Cu_2Cl_7.2H_2O$
A = NH_4^+	$(NH_4)CuCl_3$, $(NH_4)CuCl_3.2H_2O$, $(NH_4)_2CuCl_4$
A = $Me_2NH_2^+$	$Me_2NH_2CuCl_3$, $(Me_2NH_2)_2CuCl_4$, $(Me_2NH_2)_3CuCl_5$

Data taken from Pascal, "Traité Nouveau de Chimie Minerale", Sidgwick, "The Chemical Elements and Their Compounds" and Colton and Canterford "Halides of the First-Row Transition Elements" and references therein.

CHAPTER II

THE STRUCTURE AND PROPERTIES OF $(Me_3NH)_3Cu_2Cl_7$

CRYSTAL STRUCTURE OF $(Me_3NH)_3Cu_2Cl_7$

The crystals were prepared as described in Chapter III. They were in the form of orange needles, typically hexagonal in cross-section and often hollow. The compound was hygroscopic, and crystals for X-ray analysis were sealed into thin-walled glass capillary tubes together with a small amount of phosphorus pentoxide.

Diffraction pattern of the crystal

The first crystal selected was mounted with its needle axis coincident with the oscillation axis of a Weissenberg camera. Oscillation photographs (CuKα) showed a repeat distance along the needle axis of about 630 pm. A hk0 Weissenberg photograph exhibited hexagonal (6 mm) symmetry (Fig.II.1) with $a \approx 1430$ pm. The hkl photograph, however, showed that each spot had in fact six components arranged in a small hexagon (Fig.II.2). This crystal was therefore a six-fold twin and unsuitable for data collection.

Examination of several crystals eventually produced one for which the hkl and higher level spots were not split. The crystal was monoclinic, and systematic absences hkℓ ($h + k = 2n + 1$), h0ℓ ($\ell = 2n + 1$ ($h = 2n + 1$) and (0k0: $k = 2n + 1$) indicated space groups Cc(N°9) or C2/c (N°15). Lattice parameters were obtained from precession photographs. These and other parameters for the crystal are given in Table II.1.

The closeness of the lattice parameters to those for a hexagonal crystal ($\sqrt{3}.a = 2478$ pm $\approx b$; $\beta \approx 90^\circ$) explains the ease of twinning. This can be described as an example of pseudomerohedral twinning, which occurs when the lattice is almost of higher symmetry than the crystal system to which it belongs.[1] An empirical law due to Mallard states that the twin can be described in terms of either a twin plane parallel to a lattice plane which is almost a symmetry plane or a twin axis parallel to a lattice row which is almost a

symmetry axis. For example, a monoclinic crystal with β close to 90° has almost orthorhombic symmetry and twinning is facilitated. Examples of reflection and rotation twins of this type are shown in Fig.II.3. For pseudomerohedral twinning to occur, the obliquity angle (θ) is usually less than 5°.[2] The reflections of the two zero levels coincide, but those on higher levels are separated, the separation being related to θ . An orthorhombic crystal with $b \approx \sqrt{3}.a$ is almost hexagonal, and is likely to form six-fold twins. This is illustrated in Fig.II.4. Three orthorhombic individuals with 2 mm symmetry are combined so that each pair of neighbours is related by reflection; the twin produced has 6 mm symmetry. The diffraction pattern of the complete twin will have hexagonal symmetry on the zero level. On higher levels the reflections will not coincide exactly, the extent of separation being dependent on the deviation of the lattice parameters from exactly hexagonal values. $(Me_3NH)_3Cu_2Cl_7$ has a monoclinic lattice with $\beta \approx 90°$ and $b \approx \sqrt{3}.a$, and might be expected to form both two-fold and six-fold twins, but the sixfold twins appear strongly predominant in all the samples examined.

Fig.II.5 is the hk0 photograph of the untwinned crystal, which shows that the intensity distribution is very close to that for a hexagonal crystal. Together with the oscillation photograph, which shows close to mirror symmetry perpendicular to c, this shows that the pseudo-symmetry exhibited by the diffraction pattern is a mirror plane ab and a six-fold axis (c). If this symmetry were strictly obeyed (and $\beta = 90°$, $b = \sqrt{3}.a$) the crystal would belong to Laue group 6/mmm and thus to the hexagonal space groups $P6_3mc$ or $P6_3/mmc$. The closeness of the intensity distribution to hexagonal symmetry is most clearly illustrated on hk0. The a*b* plane of the monoclinic reciprocal lattice is shown in Fig.II.6. From this it is found that if the lattice were hexagonal, the following reflections

would be equal

$$h,k,0 \quad h',k',0 \ (h' = \tfrac{1}{2}(h+k) \quad (k' = \tfrac{1}{2}(3h-k)) \qquad h'',k'',0 \ (h'' = \tfrac{1}{2}(h-k)) \quad (k'' = \tfrac{1}{2}(3h+k))$$

These reflections would not be equivalent for a monoclinic crystal, and an attempt was made to estimate the deviation of the measured hk0 intensities from hexagonality.

The percentage deviation from hexagonality for each set of three reflections was defined as

$$\Delta = \frac{(|F - M| + |F' - M| + |F'' - M|)}{(F + F' + F'')} \times 100$$

where $F = \sqrt{F^2_{hk0}}$ etc. and M is the mean of F, F' and F''. Also calculated was $R = \Sigma M\Delta / \Sigma M$.

R and Δ were calculated for 41 cases in which all three symmetry-related reflections were measured and 29 cases where two of the three possible reflections were available (Table II.2). This gave a mean Δ of 12% (maximum 65%, minimum 0%) and a mean R of 6.6%. A mean discrepancy of this order would not be unexpected if equivalent reflections of a hexagonal crystal were measured visually from photographic data, but close examination of Fig.II.5 shows that the crystals are in fact monoclinic.

Data Collection

Data were collected from the non-twinned crystal. Layers hk0 through hk5 were collected using equiinclination Weissenberg geometry (CuKα) and a multiple-film, multiple exposure technique. h0ℓ, h1ℓ and h2ℓ were collected by precession photography. The intensities of the Weissenberg photographs were estimated visually by comparison with a calibrated strip, and those of the precession photographs using a Joyce-Loebl flying spot microdensitometer. No absorption or spot-shape corrections were made. Interfilm scaling of each 5-film pack of Weissenberg photographs used the published value of the transmission coefficient,[3] and interpack scaling was

on the basis of exposure times. Scaling of the precession photographs was on a time basis. The cross-level data from the precession photographs were used to determine approximate layer scale factors; the layer scale factors were later included in the least-squares refinement.

Structure Determination

The hexagonal distribution of hk0 intensities suggested that the atomic arrangement might also have six-fold or 6_3 symmetry, at least for the heavy atoms. It was also observed that c is approximately equal to twice the Cu-Cu distance for the chains in $CsCuCl_3$.[4] These two facts suggested that the structure probably contains $(CuCl_3^-)_n$ chains parallel to c, and it was therefore postulated that the structure was composed of these chains and isolated chloride ions (Fig.II.7a).

Data reduction was followed by a two-dimensional Patterson synthesis. A sharpened hk0 projection was calculated, assuming cmm symmetry, and using the sharpening function $(1/\hat{f}^2)^2 \exp(2B \sin^2\theta/\lambda^2)$ where $\hat{f}^2 = \sum N_i f_i^2 / \sum N_i$ and $B = 3 \times 10^4$ pm^2. This was interpreted in terms of $(CuCl_3^-)_n$ chains and Cl^- ions. A two-dimensional Fourier synthesis phased on the Cu^{2+} and Cl^- ions in these produced a map indicating that the structure in fact contained $CuCl_4^{2-}$ ions and $(CuCl_3^-)_n$ chains (Fig.II.7b). A difference map afforded more accurate heavy atom positions, and two-dimensional synthesis phased on these also showed the three trimethyl ammonium groups. The location and orientation of the $CuCl_4^{2-}$ tetrahedron on b determined the space group as Cc, since it could not be placed on the two-fold axis of C2/c in this orientation.

In the absence of a three-dimensional Fourier program, the z coordinates of the heavy atoms were determined by trial and error. The origin was fixed by placing the Cu atom of the chain at 0, y, $\frac{1}{2}$ ($y \approx \frac{1}{2}$). The x and y coordinates of all the heavy atoms were known, and z coordinates of the chain chloride ions could be estimated approximately. The Cu-Cl bond distance in the tetrahedron could be

estimated, but the z height of the tetrahedron was indeterminate. Using assumed temperature factors of $B = 3 \times 10^4$ pm^2 for Cu and $B = 4 \times 10^4$ pm^2 for Cl^-, the R factor was calculated for a series of structures with the fractional z coordinate of the whole tetrahedron being varied in steps of 0.1. There was a clear minimum with the Cu atom at about 0.6.

A similar procedure was adopted for the Me_3NH^+ tetrahedra, initially assuming that all three tetrahedra in the asymmetric unit were at the same z height. There were two possible orientations for the N-H vectors of these groups, which can be described as 'up' and 'down' with respect to the positive sense of c. Keeping the heavy atom parameters constant, the z height of the three tetrahedra were varied and the R factor calculated at intervals of z = 0.1; at each z height R had to be calculated for both 'up' and 'down' positions. A minimum R of 27% was found with the groups 'up' and the N atoms at z = 0.16. (Fig.II.8).

A three-dimensional Fourier program was now obtained. A Fourier synthesis phased on the heavy atoms showed that the three trimethyl ammonium ions in the 'up' position with $\bar{z}(N) = 0.16$.

Structure Refinement

The course of the least squares refinement is shown in Table II.3.

The failure of the block diagonal refinement to converge below 18.3% was attributed to an "inverse overlap" effect[5] because of the pseudohexagonal symmetry of the structure. An attempt to eliminate this was made by refining only the positional parameters of one of the Me_3NH^+ groups, but R increased slightly. Full matrix refinement was therefore employed. The correlation matrix in fact shows some quite strong interactions, but in general the strongest of them are not necessarily between parameters related by pseudohexagonal symmetry.

Refinement was considered complete when $\Delta < \sigma$ for all

parameters. Structure factors are given in Appendix A. Positional and thermal parameters with their standard deviations are given in Table II.4.

Discussion of the Structure

The structure has essentially three components; the $(CuCl_3^-)_n$ chain, the $CuCl_4^{2-}$ tetrahedron and the Me_3NH^+ groups. Each of these can be compared with the same component in other environments, and the relationship between the components can be considered. The unit cell is illustrated in Fig.II.9. Bond lengths and angles are given in Table II.5, together with their standard deviations; no difference is treated as significant unless it is greater than 3σ.

The $(CuCl_3^-)_n$ chain is extremely similar to the chain in $CsCuCl_3$,[4] for which the bond lengths and angles are given in Table II.6. The only large difference is that in the length of the longest Cu-Cl bond. The distortion of the coordination around the Cu atom from O_h symmetry is explained on the basis of Jahn-Teller distortion. The Cu-Cu distance in the chain is similar to that in $CsCuCl_3$; these two distances are shorter than those in other chloride-bridged copper compounds because in $(Me_3NH)_3Cu_2Cl_7$ the $CuCl_6$ octahedra are joined by face-sharing, while in the other compounds octahedra are linked by sharing edges.

The $CuCl_4^{2-}$ tetrahedron may be compared with those found in Cs_2CuCl_4,[6] $(Me_4N)_2CuCl_4$[7] and $(TMBA)_2CuCl_4$,[8] whose parameters are given in Table II.7. In each of the latter compounds, the general shape of the ion is that of a 'squashed' tetrahedron, with two Cl-Cu-Cl angles much greater than $109^\circ 28'$ and four much less; bond lengths vary between 218 and 227 pm. In $(Me_3NH)_3Cu_2Cl_7$, however, the symmetry is significantly different. All the bond angles are within 1 esd of $109^\circ 28'$, and the only deviation from T_d symmetry is caused by bond length differences. Three bond lengths are relatively short (223,220,223 pm) compared with the fourth distance of 230 pm.

This reduces the symmetry of the copper atom environment to approximately C_{3v}. The reason for the distorted ion taking up this shape instead of the more usual form (approximately D_{2d}) is clearly intimately bound up with the surroundings of the $CuCl_4^{2-}$ ion in the lattice, and is discussed in more detail below.

The Me_3NH^+ ion can be compared with the Me_3N group in Me_3NHCl [9] and gaseous Me_3N.[10] Me_3NHCl has N-C distances of 147 and 149 (± 1) pm and C-N-C angles of 110° and 112° (± 1). In Me_3N the distances are 147 (± 2) pm, but the angles are 108° (± 4). The smaller angle in Me_3N is ascribed to the repulsion due to the lone pair of Me_3N being greater than that exerted by the bonding electrons of N-H in Me_3NHCl. The mean distance in $(Me_3NH)_3Cu_2Cl_7$ is 146 (± 5) pm and the mean angle is 111° (± 3), which is in agreement with the data for Me_3NHCl.

Relationship between different parts of the structure

The $(CuCl_3^-)_n$ chains have approximately sixfold symmetry, and their influence on structures containing them is very clear. In $CsCuCl_3$ there is a fairly simple problem in packing, since there are no very stringent packing requirements for the cation and the packing of $(CuCl_3^-)_n$ chains essentially determines the structure. In consequence $CsCuCl_3$ belongs to a hexagonal space group ($P6_122$). The packing problem in $(Me_3NH)_3Cu_2Cl_7$ is more complex, but the dominant effect determining the symmetry of the structure is evidently the arrangement of $(CuCl_3^-)_n$ chains, giving the very close approach to hexagonal symmetry which is illustrated in the ab projection (Fig.II.10).

In considering the individual ions the most obvious feature was the unusual type of distortion shown by the $CuCl_4^{2-}$ ion. In a single crystal structure it is difficult to distinguish between the effects of crystal packing on the ions concerned and the influence of the electronic structures of the ions on their environment. However there seems to be sufficient evidence in this case that $CuCl_4^{2-}$ usually exists as a squashed tetrahedron, so that its shape in this structure must be explained in terms of crystal packing.

The imposition of approximately three-fold symmetry around $CuCl_4^{2-}$ by the $(CuCl_3^-)_n$ chains suggests that an ion with C_{3v} symmetry may be more easily accommodated than one with D_{2d}. The N-H vector of Me_3NH^+ is directed towards $CuCl_4^{2-}$, and there is therefore a possibility of N-H-Cl bond formation, which might stabilize the three-fold symmetry of $CuCl_4^{2-}$.

If a model is constructed of the $CuCl_4^{2-}$ tetrahedron and its surrounding Me_3NH^+ groups, with H atoms being introduced to complete the tetrahedral coordination of the N atoms, then the N-H vectors are directed approximately towards the central Cu atom. A sketch of this arrangement is given in Fig.II.11. This arrangement has three-fold symmetry with mean distances of Cl(2)-N = 351 ($\pm$ 2), Cl(3)-N = 350 ($\pm$ 2) and Cl(4)-N = 350 ($\pm$ 2) pm, so that only the atoms N(3), H(3), Cl(1'), Cl(3) and Cl(4) need be considered. The N(3)- Cl(1') distance is 327 ($\pm$ 2) pm. These distances are short enough for some electrostatic interaction between Me_3NH^+ and Cl^- to occur, but it is less certain that hydrogen bonding takes place. The length of the hydrogen bond is dependent on the coordination and hybridization of the nitrogen atom, so that the sum of the van der Waals' radii ($\sim$ 330 pm) is not a satisfactory criterion. In the ammonium and alkylammonium halides[11] the N-Cl distance varies between 335 pm (NH_4Cl (CsCl structure)) and 300 pm in Me_3NHCl. In various -onium chlorocuprates N-Cl contacts of 309-380 pm have been reported, but no distinction has been made between electrostatic interaction and hydrogen bond formation.

Not only the N-Cl distance, but also the hybridization of the atoms and the spatial orientation of the orbitals are important in hydrogen bond formation. As shown in the sketch none of the N-H-Cl angles are 180°, but the postulated hydrogen atom position is roughly equidistant from Cl(1'), Cl(3) and Cl(4). If the chlorine atoms are sp^3 hybridized, and therefore have a tetrahedral arrangement of orbitals, then filled orbitals could be directed approximately towards

the hydrogen atom. There then seems no reason why Cl(1'), Cl(3) or Cl(4) should hydrogen bond preferentially, so that a trifurcated bond would be produced. This would be extremely unusual, and there is no strong evidence in its favour, so that only electrostatic interaction can be assumed to exist in this case.

It is therefore concluded that the threefold symmetry of the $CuCl_4^{2-}$ tetrahedron in this structure is imposed basically by the packing of the $(CuCl_3^-)_n$ chains, and reinforced by interaction with the Me_3NH^+ groups.

REFERENCES FOR CHAPTER II

1. Cahn, Advances in Physics 1954, 3, 363.
2. Grainger, Acta Cryst. 1969, A25, 435.
3. Morimoto & Uyede, Acta Cryst. 1963, 16, 1107.
4. Schuleter et al., Inorg.Chem. 1966, 5, 277.
5. Srinivasan, Acta Cryst. 1961, 14, 1163.
6. Morosin & Lingafelter, J.Phys.Chem. 1961, 65, 50.
7. See Chapter IV.
8. Bonamico et al., Theoret.Chim Acta 1967, 7, 367.
9. Lindgren & Olovsson, Acta Cryst. 1968, B24, 554.
10. Brockway & Jenkins, J.A.C.S. 1936, 58, 2036.
11. Lindgren & Olovsson, Acta Cryst. 1968, B24, 557.

Figure II.1

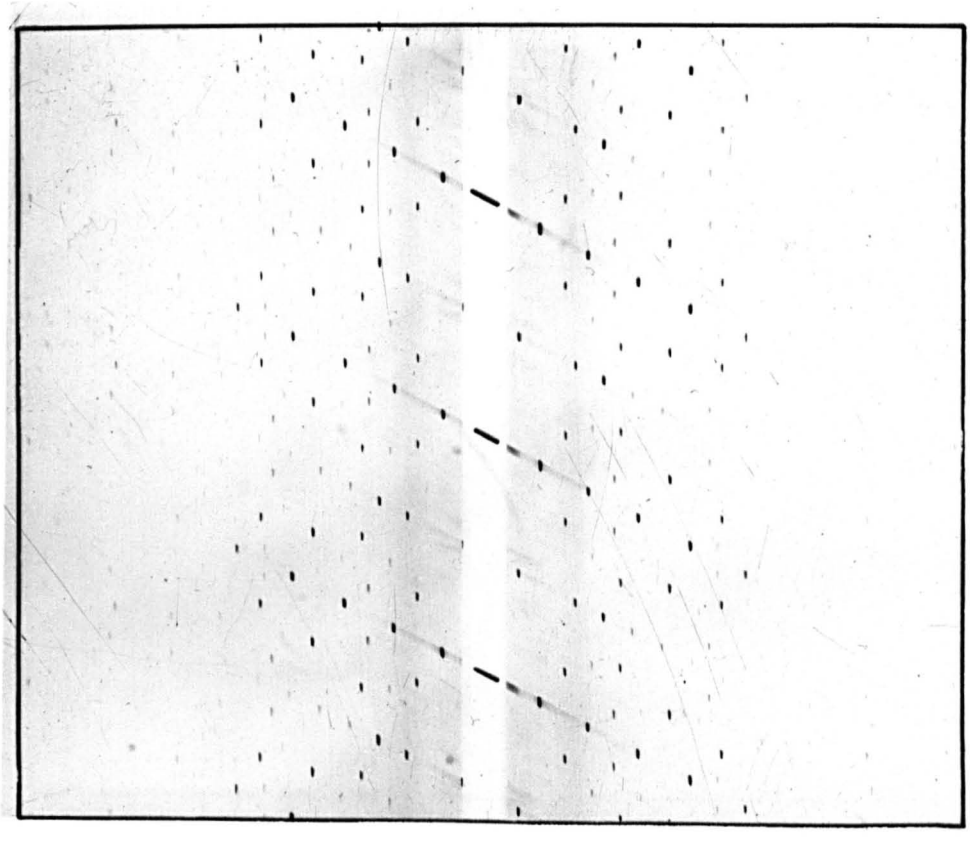

The hk0 Weissenberg photograph of a twinned crystal of $(Me_3NH)_3Cu_2Cl_7$. The three marked axes are 60 degrees apart, and they appear to be identical.

Figure II.2

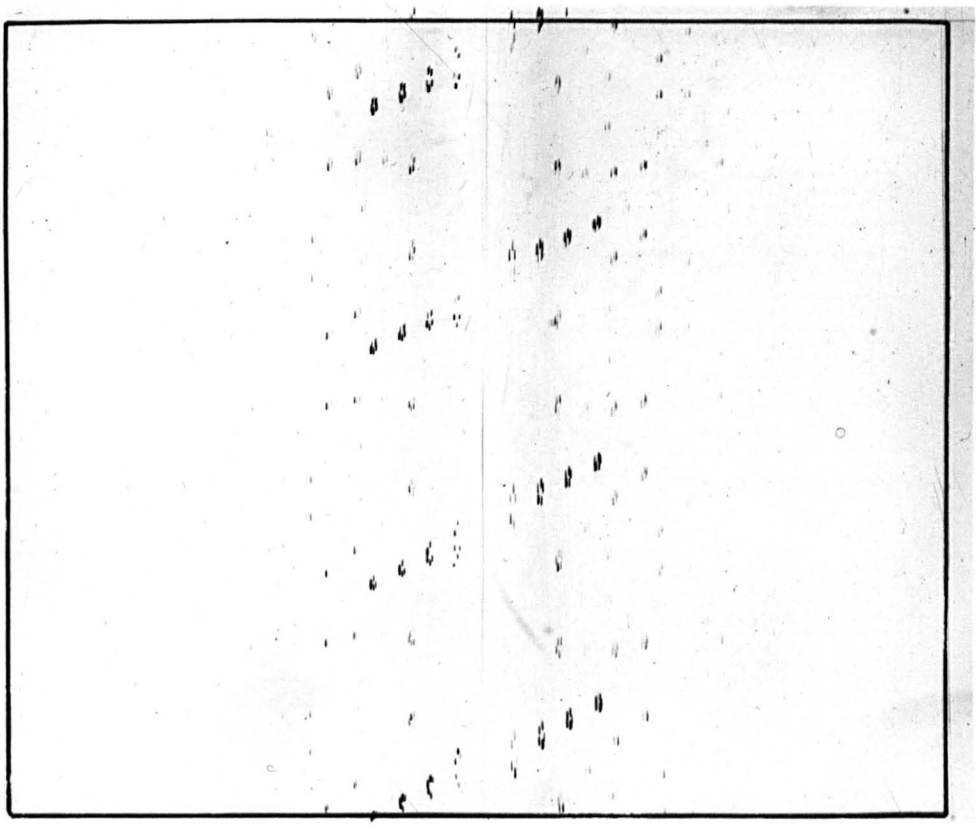

The hkl Weissenberg photograph of a twinned crystal of $(Me_3NH)_3Cu_2Cl_7$.

Figure II.3

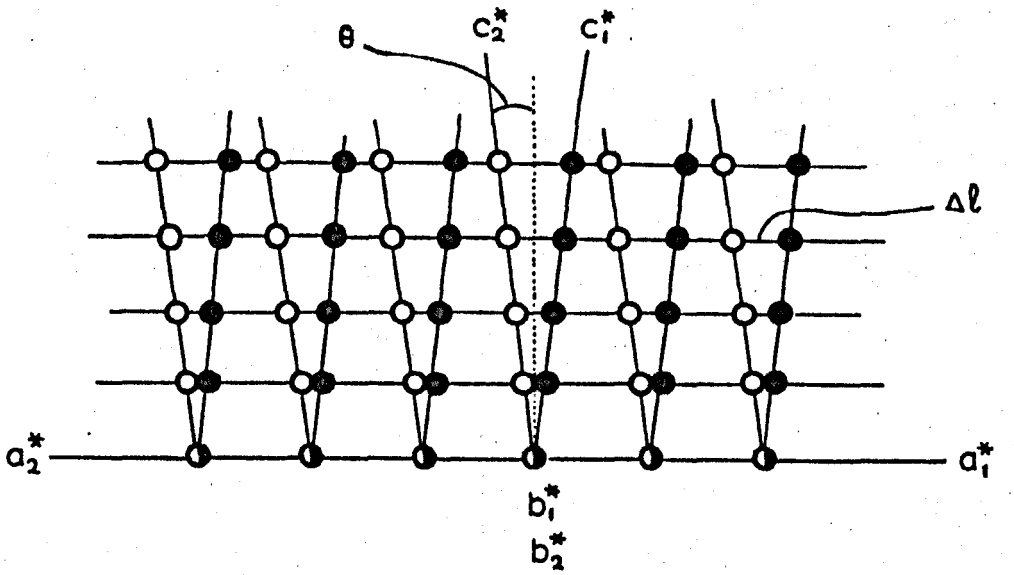

Pseudomerohedral twinning

b* is common to both individuals, the a* axes coincide, and the c* axes almost coincide. The diagram represents either a rotation twin with c as the twin axis, or a reflection twin with 100 as the twin plane.
Pairs of reflections along lines parallel to a* are twin-pairs of separation $\Delta\ell = 2p\tan\theta$, where p is the perpendicular distance of the lattice row from the origin.

Figure II.4

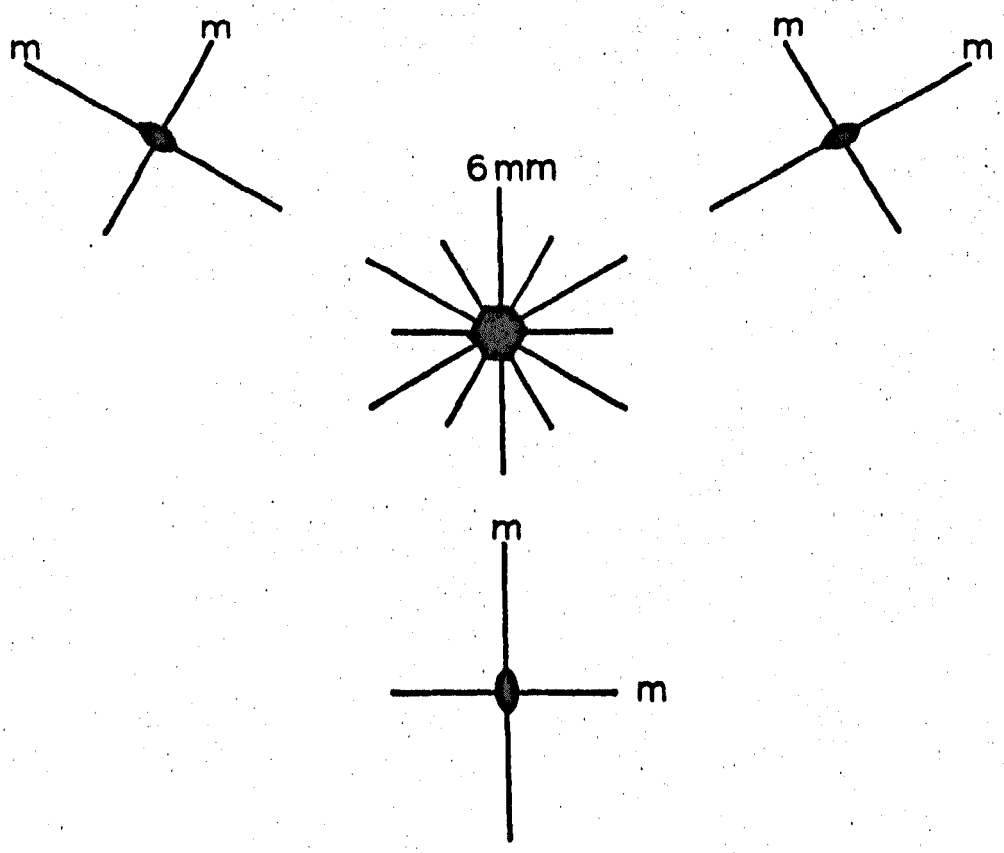

Twinning of orthorhombic individuals to mimic hexagonal crystals

Each pair of orthorhombic individuals of 2mm symmetry is related by a mirror plane; the resultant twin has 6mm symmetry.

Figure II.5

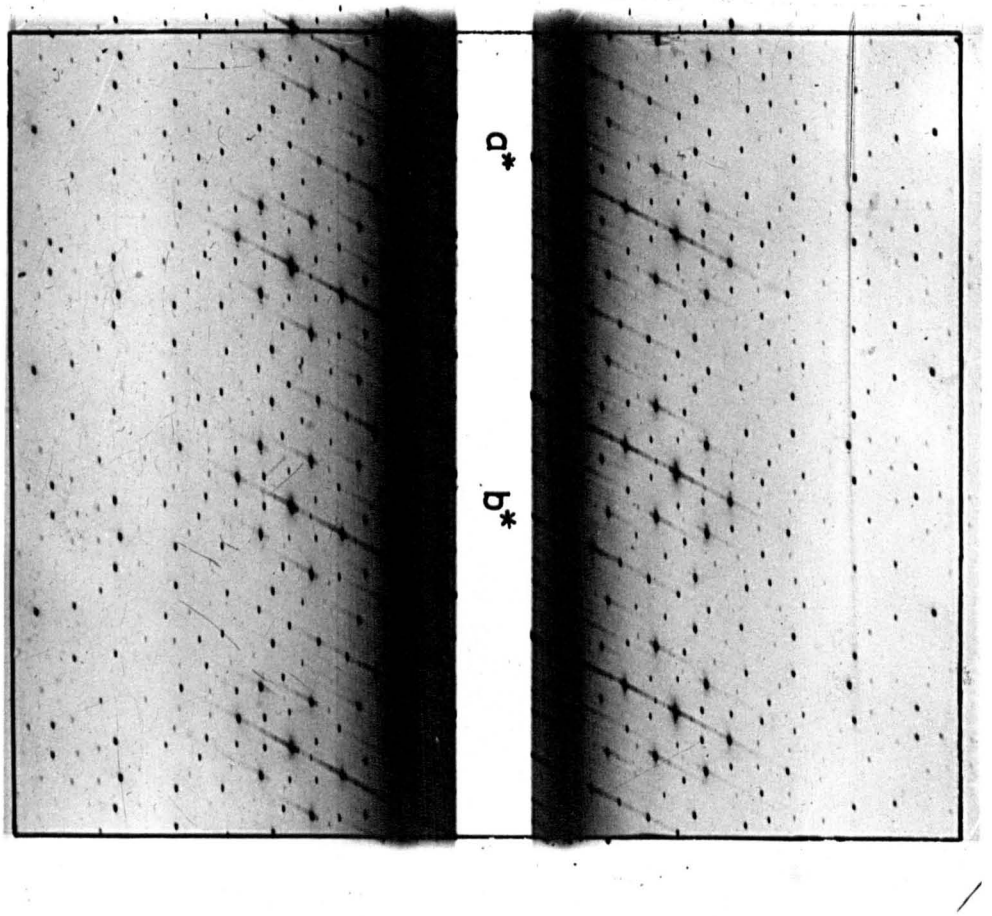

The hkO Weissenberg photograph of a single crystal of $(Me_3NH)_3Cu_2Cl_7$, showing the almost hexagonal intensity distribution.

Figure II.6

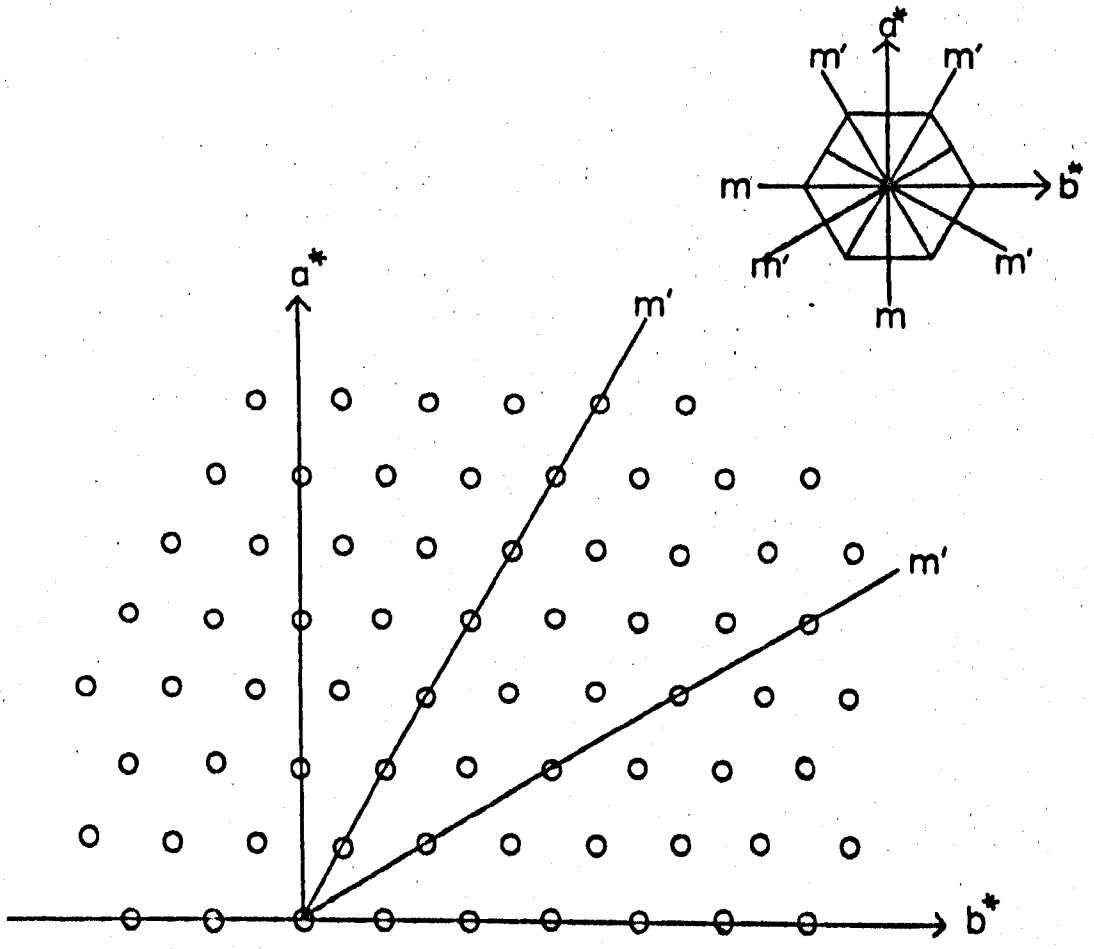

The centred orthorhombic reciprocal lattice in relation to hexagonal axes

Figure II.7

The two asymmetric units considered for $(Me_3NH)_3Cu_2Cl_7$

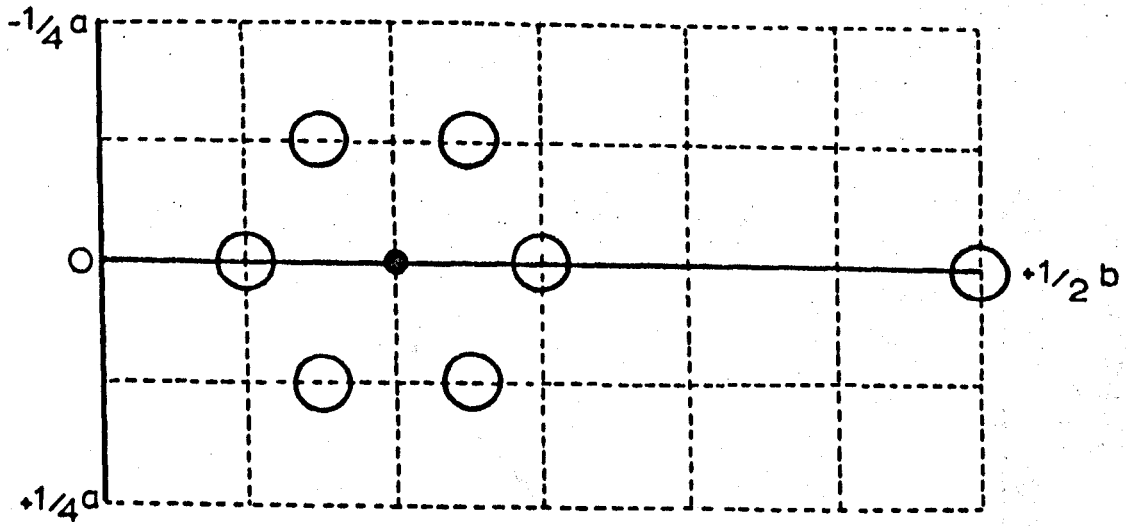

(a)

○ =Cl ● =Cu

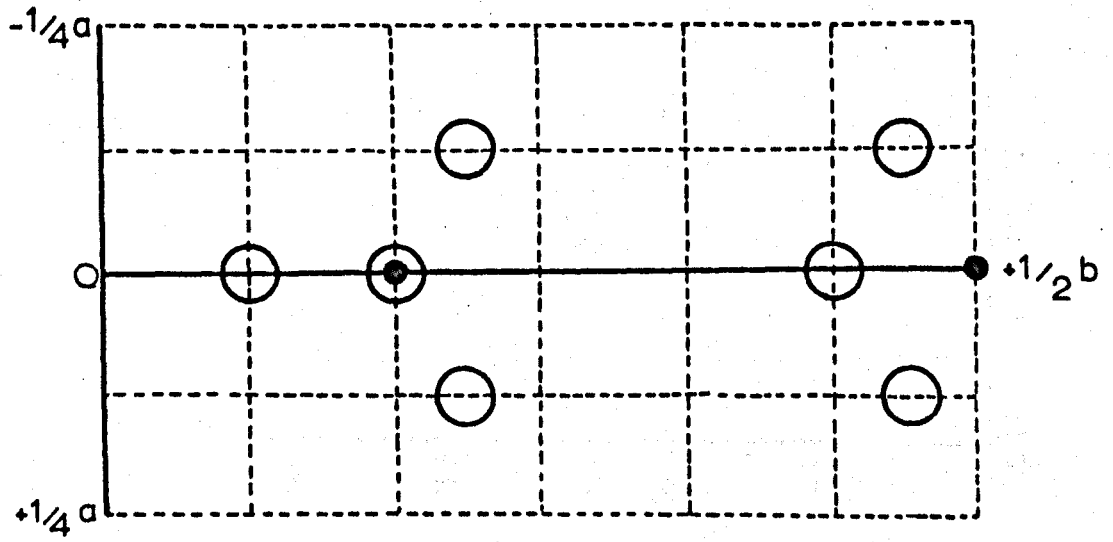

(b)

Figure II.8

Approximate determination of light atom positions

A – groups "down" with respect to c.

B – groups "up" with respect to c.

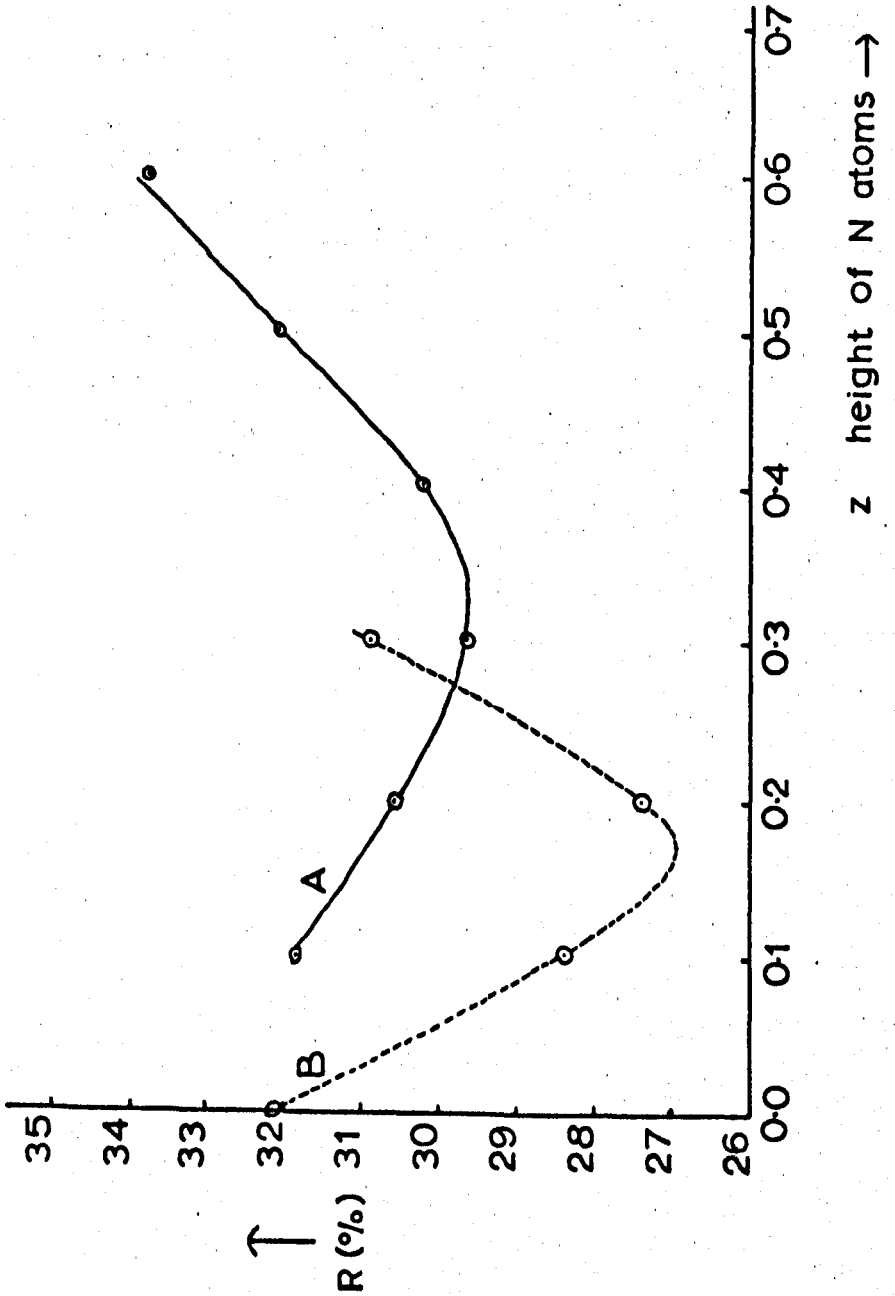

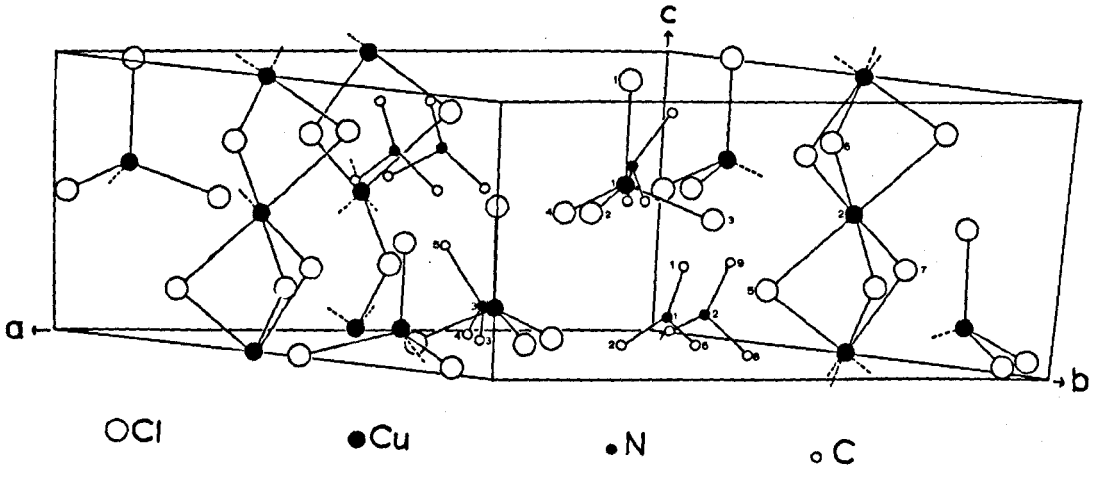

Figure II.9

Figure II.10

ab projection of $(Me_3NH)_3Cu_2Cl_7$.

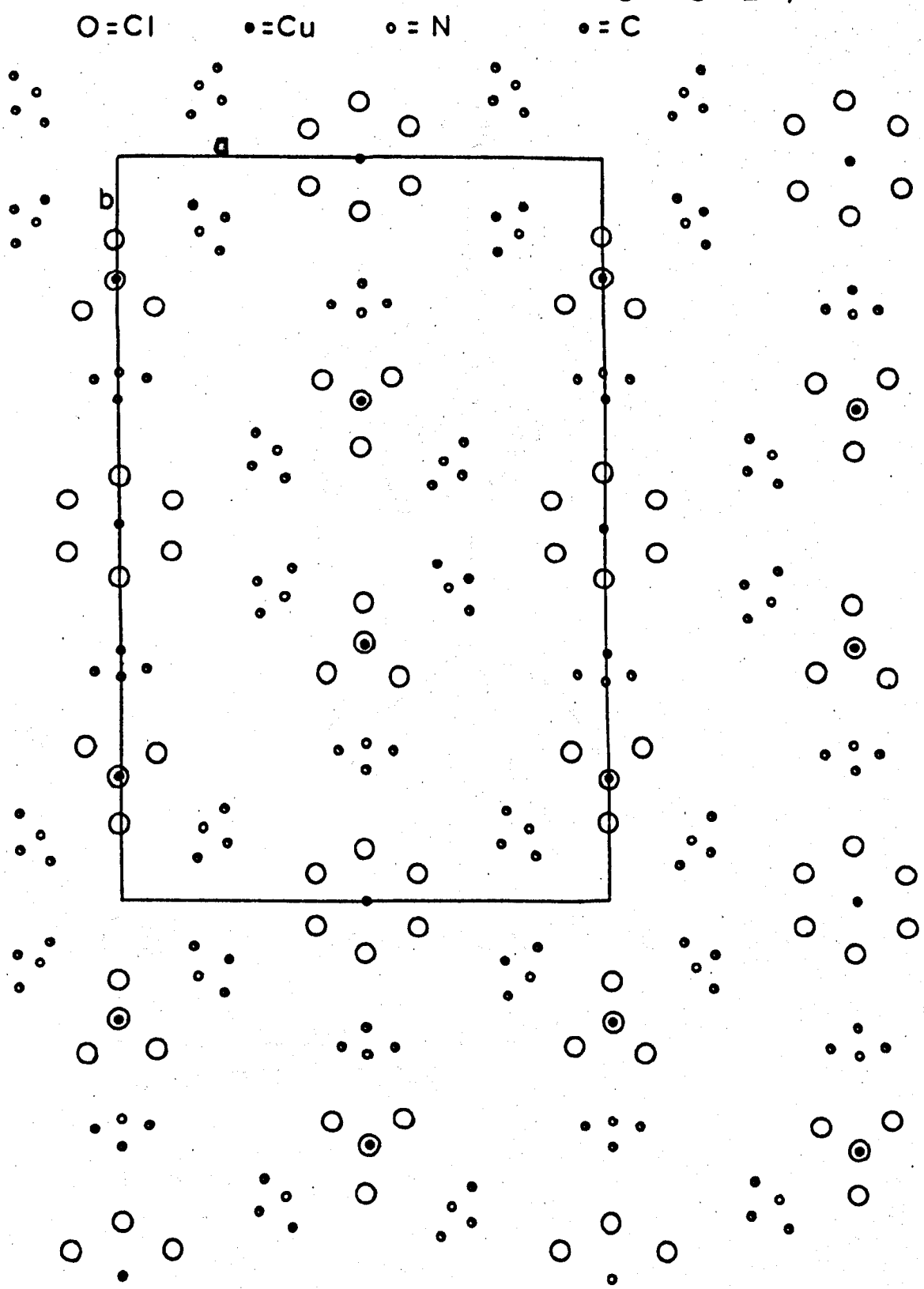

Figure II.11

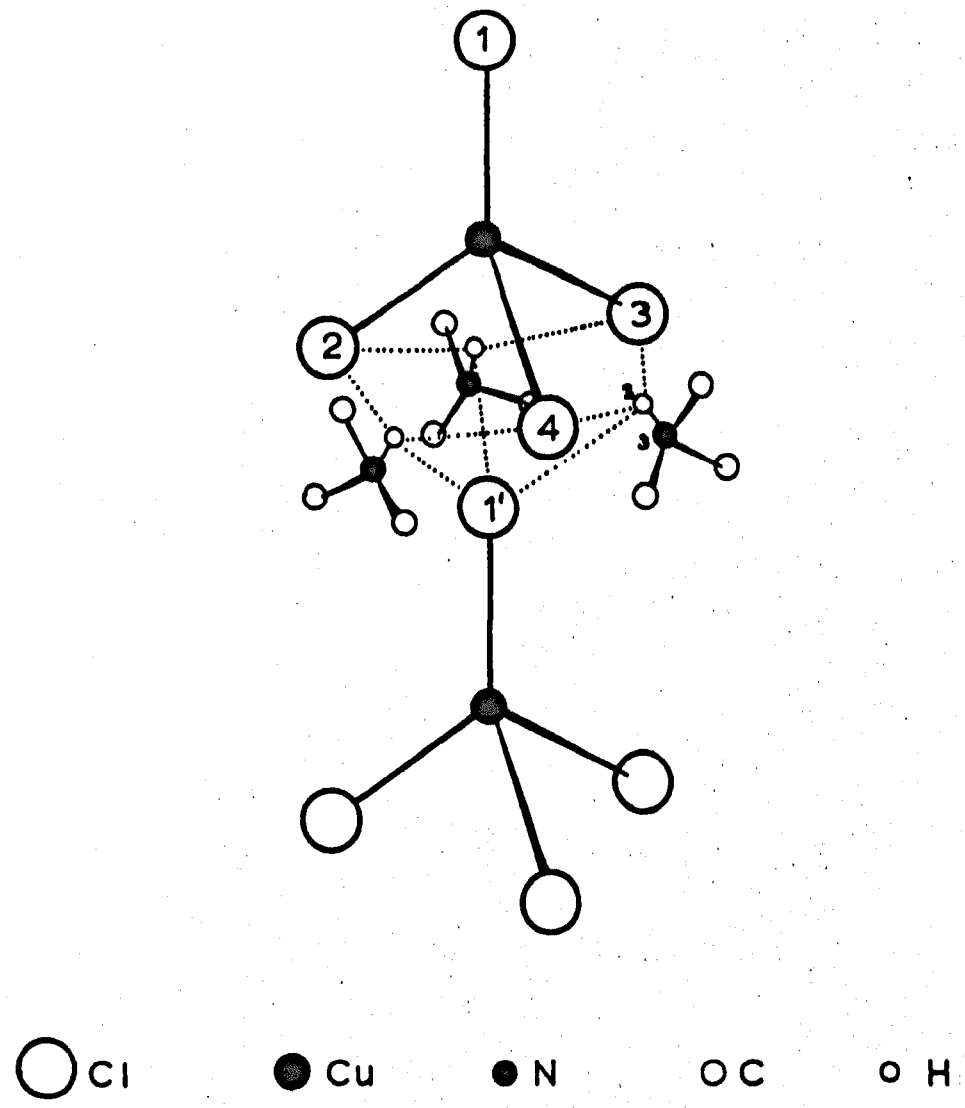

Sketch of the relation between $CuCl_4^{2-}$ and the light atom tetrahedra (not to scale)

TABLE II.1

SOME PROPERTIES OF $(Me_3NH)_3Cu_2Cl_7$

Linear absorption coefficient $\mu = 97.46\ cm^{-1}$ (CuKα)

Density $\rho_{obs} = 1.65$ $\rho_{calc} = 1.65\ g\ cm^{-3}$

Approximate dimensions 0.1 x 0.1 x 0.2 mm.

Cell parameters a = 1430 b = 2467 c = 630 pm

α = 90° β = 92.52° ϒ = 90°

Space group Cc

Z = 4

N° of reflections measured = 1490

N° of reflections included in refinement = 1480

TABLE II.2

Comparison of reflections on hk0 which are related by pseudo-hexagonal symmetry

Each line contains h, k and F_{obs} for the two or three related reflections, and Δ (%) for the group, where

$$\Delta\ (\%) = \frac{(\,|F-M| + |F'-M| + |F''-M|\,)}{(F + F' + F'')} \times 100$$

and M is the mean of F, F' and F''.

Table II.2

H	K	F	H	K	F	H	K	F	DELTA(%)
3	1	19.5	2	4	18.8	1	5	19.5	1.6
5	1	17.7	3	7	16.4	2	8	22.2	12.2
7	1	8.2	4	10	7.5	3	11	5.7	13.4
9	1	15.3	5	13	3.5	4	14	14.3	45.5
11	1	5.1	6	16	6.4	5	17	5.1	10.4
4	2	10.7	3	5	10.7	1	7	10.4	1.3
6	2	10.1	4	8	9.2	2	10	8.1	7.5
8	2	7.7	5	11	6.0	3	13	6.6	9.2
10	2	10.9	6	14	9.7	4	16	10.6	4.5
12	2	4.1	7	17	4.4	5	19	4.4	3.1
18	2	3.6	10	26	2.6	8	28	2.6	15.2
5	3	25.8	4	6	25.8	1	9	22.7	5.2
7	3	46.4	5	9	46.5	2	12	43.3	3.1
9	3	38.8	6	12	36.8	3	15	43.0	5.8
11	3	11.3	7	15	13.7	4	18	12.0	7.4
13	3	5.8	8	18	6.0	5	21	3.5	20.9
15	3	11.7	9	21	10.1	6	24	7.8	14.0
17	3	9.2	10	24	7.0	7	27	8.1	9.1
6	4	1.0	5	7	1.4	1	11	4.7	65.7
8	4	12.5	6	10	11.3	2	14	11.5	4.2
10	4	4.2	7	13	3.5	3	17	4.0	5.6
12	4	6.9	8	16	5.0	4	20	7.4	14.9
7	5	6.1	6	8	6.9	1	13	6.8	5.1
11	5	10.5	8	14	10.5	3	19	11.5	4.1
8	6	21.7	7	9	20.6	1	15	22.0	2.6
10	6	13.1	8	12	13.1	2	18	14.9	5.8
12	6	5.0	9	15	9.2	3	21	7.0	20.1
14	6	9.1	10	18	8.5	4	24	4.7	24.5
16	6	3.7	11	21	3.0	5	27	3.3	7.3
9	7	2.2	8	10	1.4	1	17	3.5	31.9
11	7	5.1	9	13	5.8	2	20	5.0	6.3
10	8	3.0	9	11	3.7	1	19	2.0	20.7
11	9	17.1	10	12	16.0	1	21	14.7	5.2
13	9	18.5	11	15	20.8	2	24	15.2	10.9
15	9	5.1	12	18	5.1	3	27	4.1	9.3
12	10	3.7	11	13	3.5	1	23	2.0	23.2
14	10	5.4	12	16	6.5	2	26	4.1	15.4
16	10	2.4	13	19	2.6	3	29	3.0	8.3
13	11	6.2	12	14	6.2	1	25	3.0	27.7
14	12	11.1	13	15	11.4	1	27	10.8	1.8
16	12	3.2	14	18	3.7	2	30	3.8	6.9

Table II.2 cont'd

H	K	F	H	K	F	DELTA(%)
2	0	65.0	1	3	62.0	2.4
4	0	45.0	2	6	46.1	1.2
6	0	49.6	3	9	51.3	1.7
8	0	75.6	4	12	79.8	2.7
10	0	35.4	5	15	37.0	2.2
12	0	14.9	6	18	15.9	3.2
14	0	10.8	7	21	7.1	20.7
16	0	16.7	8	24	13.3	11.3
18	0	6.1	9	27	4.7	13.0
13	1	1.4	6	20	2.8	33.3
17	1	4.2	8	26	1.4	50.0
2	2	2.2	0	4	1.7	12.8
14	2	2.8	6	22	2.0	16.7
3	3	22.8	0	6	22.9	0.2
4	4	35.0	0	8	35.0	0.0
5	5	16.3	0	10	14.7	5.2
9	5	3.6	2	16	4.1	6.5
13	5	2.4	9	17	3.2	14.3
15	5	1.7	5	25	1.7	0.0
6	6	16.5	0	12	14.7	5.8
7	7	12.2	0	14	13.1	3.6
15	7	2.8	11	19	2.4	7.7
8	8	14.4	0	16	10.2	17.1
9	9	9.2	0	18	10.8	8.0
10	10	2.0	0	20	3.6	28.6
12	12	24.7	0	24	20.3	9.8
13	13	5.6	0	26	3.9	17.9
14	16	3.7	1	29	3.7	0.0
14	14	5.9	0	28	5.1	7.3

TABLE II.3

LEAST SQUARES REFINEMENT OF $(Me_3NH)_3Cu_2Cl_7$

(1) Block diagonal matrix; all observations at unit weights

No of cycles	Parameters refined	$R = \frac{\sum \lvert \lvert F_o \rvert - \lvert F_c \rvert \rvert}{\sum \lvert F_o \rvert}$ for all observed refls.
5	all atom positions, B_{iso} for all atoms	18.3%
2	atom positions for one $(CH_3)_3NH^+$ group	18.3%
2	B_{ij} for Cu and Cl atoms	18.6

(2) Full matrix; weighting scheme $w = 1$ for $F \leqslant F^*$; $w = \frac{1}{F-\left(\frac{F-F^*}{G^*}\right)^2}$ for $F > F^*$

1	atoms positions and B_{iso} for Cu, Cl atoms (unit weights)	17.9
1	all atom positions and individual layer scales (unit weights)	15.7
2	all atom positions and B_{iso} for all atoms (unit weights)	14.0
2	some positions and B_{iso} for all atoms (unit weights)	12.7
2	all atom positions and individual layer scales ($F^* = 45$, $G^* = 48$)	12.5
1	all B_{iso} and layer scales ($F^* = 45$, $G^* = 48$)	12.1
	at this stage some errors in the data were corrected and structure factor calculations gave R = 11.7	
2	positions, layer scales ($F^* = 45$, $G^* = 35$)	11.5
1	positions, layer scales B_{iso} for all atoms ($F^* = 35$, $G^* = 45$)	11.4
2	B_{ij} for Cu and Cl atoms ($F^* = 35$, $G^* = 35$)	10.3
1	all atom positions and layer scales ($F^* = 35$, $G^* = 35$)	10.1
1	B_{ij} for Cu and Cl atoms ($F^* = 35$, $G^* = 35$)	10.1

Table II.4

(a) Positional parameters ($x10^4$) for $(Me_3NH)_3Cu_2Cl_7$.

Standard deviations are given in parentheses.

ATOM	X		Y		Z	
CU1	15	(3)	1669	(1)	6382	(8)
CU2	0	*	4999	(1)	5000	*
CL1	27	(5)	1672	(2)	31	(17)
CL2	5	(6)	814	(3)	5229	(15)
CL3	-1254	(6)	2090	(3)	5117	(15)
CL4	1294	(5)	2098	(3)	5402	(14)
CL5	1164	(5)	4605	(2)	2116	(12)
CL6	-2	(5)	4266	(2)	7519	(13)
CL7	-1151	(4)	4607	(2)	2953	(12)
N1	25	(12)	2920	(6)	1846	(24)
N2	-1364	(14)	1043	(8)	1576	(34)
N3	1884	(11)	1054	(7)	1974	(27)
C1	-6	(19)	3269	(10)	3722	(45)
C2	850	(27)	3003	(15)	681	(65)
C3	1623	(20)	607	(11)	662	(50)
C4	2421	(21)	1426	(12)	792	(54)
C5	2468	(19)	859	(11)	3933	(47)
C6	-766	(23)	3019	(12)	376	(56)
C7	-1566	(23)	561	(13)	509	(58)
C8	-2404	(19)	1421	(11)	254	(48)
C9	-2367	(18)	874	(11)	3506	(45)

* FIXED TO DETERMINE ORIGIN, THEREFORE ESD IS ZERO.

Table II.4

(b) Thermal parameters for $(Me_3NH)_3Cu_2Cl_7$.

ANISOTROPIC THERMAL PARAMETERS ($\times 10^3$)

ATOM	B		ESD	ATOM	B		ESD
CU1	11	5.5	(0.2)	CL4	11	5.5	(0.3)
	22	1.8	(0.1)		22	2.3	(0.1)
	33	26.0	(0.8)		33	39.8	(2.4)
	12	-0.1	(0.1)		12	-0.6	(0.2)
	13	0.8	(0.3)		13	2.4	(0.7)
	23	0.1	(0.2)		23	0.7	(0.4)
CU2	11	4.2	(0.1)	CL5	11	4.7	(0.3)
	22	1.5	(0.1)		22	1.6	(0.1)
	33	18.3	(0.8)		33	24.9	(1.9)
	12	0.1	(0.1)		12	-0.1	(0.1)
	13	-0.6	(0.2)		13	-2.0	(0.5)
	23	0.2	(0.1)		23	0.5	(0.3)
CL1	11	4.8	(0.3)	CL6	11	4.7	(0.2)
	22	1.7	(0.1)		22	1.7	(0.1)
	33	22.7	(1.7)		33	28.8	(1.7)
	12	-0.2	(0.1)		12	-0.1	(0.2)
	13	-0.9	(0.5)		13	-0.1	(0.5)
	23	-0.3	(0.4)		23	-0.2	(0.4)
CL2	11	7.7	(0.4)	CL7	11	4.0	(0.2)
	22	1.6	(0.1)		22	1.5	(0.1)
	33	39.8	(2.3)		33	22.5	(1.7)
	12	0.1	(0.2)		12	-0.3	(0.1)
	13	0.8	(0.7)		13	-2.2	(0.5)
	23	-2.1	(0.4)		23	-0.9	(0.3)
CL3	11	5.7	(0.3)				
	22	2.3	(0.1)				
	33	45.4	(2.7)				
	12	0.7	(0.2)				
	13	-2.9	(0.7)				
	23	1.5	(0.4)				

B_{11} etc are coefficients in the expression for the anisotropic temperature factor

$$\exp\{-(B_{11}h^2 + B_{22}k^2 + B_{33}l^2 + 2B_{12}hk + 2B_{13}hl + 2B_{23}kl)\}.$$

ISOTROPIC THERMAL PARAMETERS

ATOM	T	ESD	ATOM	T	ESD
N1	2.9	(0.3)	C4	5.9	(0.7)
N2	4.3	(0.4)	C5	5.4	(0.7)
N3	3.1	(0.3)	C6	6.2	(0.7)
C1	5.2	(0.6)	C7	6.6	(0.8)
C2	7.6	(0.9)	C8	5.2	(0.6)
C3	5.3	(0.6)	C9	4.9	(0.6)

T is the coefficient in the expression for the isotropic temperature factor

$$\exp - \left(T \cdot \frac{\sin^2\theta}{\lambda^2}\right).$$

TABLE II.5

Bond distances and angles in $(Me_3NH)_3Cu_2Cl_7$

e.s.d's are given in parentheses

(a) Selected bond distances (p.m).

Cu(1) - Cl(1)	230(1)	Cu(2) - Cl(5)	269(1)		
- Cl(2)	223(1)	- Cl(6)	240(1)		
- Cl(3)	220(1)	- Cl(7)	226(1)		
- Cl(4)	223(1)	- Cl(5')	230(1)		
		- Cl(6')	239(1)		
		- Cl(7')	273(1)		

N(1) - C(1)	146(4)	N(2) - C(7)	148(5)	N(3) - C(3)	140(4)
- C(2)	142(5)	- C(8)	140(5)	- C(4)	145(5)
- C(6)	141(5)	- C(9)	154(4)	- C(5)	157(4)

(b) Selected bond angles

Cl(1) - Cu(1) - Cl(2)	109.7(0.4)
Cl(1) - Cu(1) - Cl(3)	109.7(0.4)
Cl(1) - Cu(1) - Cl(4)	109.2(0.4)
Cl(2) - Cu(1) - Cl(3)	109.6(0.4)
Cl(2) - Cu(1) - Cl(4)	110.6(0.4)
Cl(3) - Cu(1) - Cl(4)	110.0(0.4)

TABLE II.5 (continued)

C(1) - N(1) - C(2)	105(3)
C(1) - N(1) - C(6)	111(3)
C(2) - N(1) - C(6)	113(3)
C(3) - N(3) - C(4)	114(3)
C(3) - N(3) - C(5)	113(3)
C(4) - N(3) - C(5)	107(2)
C(7) - N(2) - C(8)	115(3)
C(7) - N(2) - C(9)	107(3)
C(8) - N(2) - C(9)	114(3)

Cl(5) - Cu(2) - Cl(5)	96.1(0.5)
Cl(5) - Cu(2) - Cl(6)	100.8(0.3)
Cl(5) - Cu(2) - Cl(6')	79.6(0.5)
Cl(5) - Cu(2) - Cl(7)	85.2(0.3)
Cl(5') - Cu(2) - Cl(6)	92.3(0.5)
Cl(5') - Cu(2) - Cl(6')	89.1(0.5)
Cl(5') - Cu(2) - Cl(7')	104.3(0.5)
Cl(6) - Cu(2) - Cl(7)	91.6(0.3)
Cl(6) - Cu(2) - Cl(7')	100.9(0.5)
Cl(6') - Cu(2) - Cl(7)	88.3(0.5)
Cl(6') - Cu(2) - Cl(7')	98.0(0.5)
Cl(7) - Cu(2) - Cl(7')	95.6(0.5)

TABLE II.6

Bond Length and Angles in the $(CuCl_3^-)_n$ chain of $CsCuCl_3$

(a) bond lengths (p.m).

Cu - Cl(1) 235.5 Cu - Cl(2) 277.6 Cu - Cl(2') 228.1

(b) Cl - Cu - Cl angles

90.52, 89.30, 95.52, 95.44, 91.74, 90.32.

TABLE II.7

Bond distances and angles in tetrachlorocuprates

Trimethylbenzylammonium tetrachlorocuprate

Bond distances (p.m)	Bond angles	
222.9	100.3°	99.1°
226.3	132.1°	98.3°
226.3	132.8°	99.7°
226.6		

Caesium tetrachlorocuprate

Bond distances (p.m)	Bond angles	
218, 225	124.9	102.5
	123.3	102.9

Tetramethylammonium tetrachlorocuprate

Bond distances (p.m)	Bond angles	
225, 221, 223	101.1	132.1
	100.8	126.6

CHAPTER III

EXPERIMENTAL

PREPARATIONS AND ANALYSES

This chapter describes the preparation and analyses of the chlorometallates and chlorometallate solid solutions, together with the construction of the phase diagrams. Spectral and DSC data are also given.

(1) The trimethylammonium chlorocuprates

The various trimethylammonium chlorocuprates were prepared by the methods given by Remy and Laves,[1] which are summarized below, and their stoichiometries were confirmed by copper and chloride analyses. (Chloride was determined gravimetrically as AgCl, and copper titrimetrically with EDTA, in pyridine-buffered solution with pyrocatechol violet as indicator).

System $CuCl_2$:Me_3NHCl:solvent (figures given are the $CuCl_2$:Me_3NHCl molar ratio)

water=solvent

1:1, 1:2, 1:3

↓ mix hot solutions and crystallize

$Me_3NHCuCl_3.2H_2O$ (green)

↓ dry in vacuum desiccator oven H_2SO_4 or by heating

$Me_3NHCuCl_3$ (brown)

1:4, 1:5, 1:6

↓ evaporate to point of crystallization on the water-bath

$(Me_3NH)_3CuCl_5$ (orange)

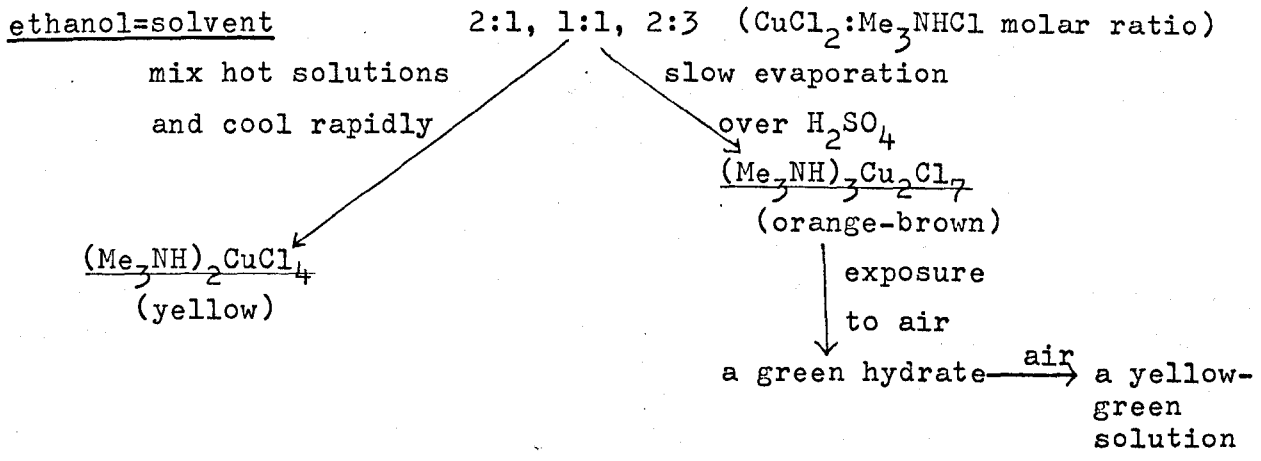

$(Me_3NH)_3Cu_2Cl_7$

The compound was prepared by the method shown above using a solution containing a 2:3 molar ratio of $CuCl_2$ and Me_3NHCl in dry ethanol. It was deposited as fine orange needles; these were hygroscopic, but could be handled in the open laboratory for periods of up to about 15 min. The crystals were dried in a vacuum desiccator over P_2O_5. The copper was estimated titrimetrically with EDTA, and the chloride gravimetrically as AgCl.

Found Cu = 23.15% Cl = 44.06%

Calculated for $(Me_3NH)_3Cu_2Cl_7$ Cu = 22.86% Cl = 44.73%

Under the microscope the crystals are found to be hexagonal in cross-section; many of them had a hollow centre running the length of the needle axis, giving the cross-section

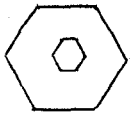

Less frequently individuals were found which were completely solid and almost rectangular in cross-section; X-ray examination of a number of these showed that they were usually single crystals. The crystals were slightly pleochroic, changing from orange to greenish-orange, and there was an extinction parallel to the needle axis.

The electronic spectrum was measured from 700 to 350 nm using the diffuse reflectance attachment of a Unicam SP800 spectrophotometer, and is shown in Fig.III.6.

Before the magnetic properties could be examined, it was necessary to calibrate the Gouy balance; this calibration is described at the end of this chapter. The magnetic susceptibility was measured from 100 to 300K. The magnetic moment per copper atom (including a correction for temperature independent paramagnetism of 60 cgsu for Cu^{2+}) was 2.02 BM at 294 K. This is in agreement with values found for other Cu^{2+} complexes. $1/\chi_m$ ($\chi_m = \frac{M}{2}\chi_g$, where M is the molecular weight and χ_g is the gram susceptibility) varied linearly with temperature and the Weiss constant was 1°.

(2) Solid solution formation

The first experiments involved crystallization of Me_3NHCl, $CuCl_2$ and $CoCl_2$ or $ZnCl_2$ such that $Me_3NHCl:MCl_2 = 3:2$, using ethanol as solvent. The results are exemplified for the case of M = Co:-

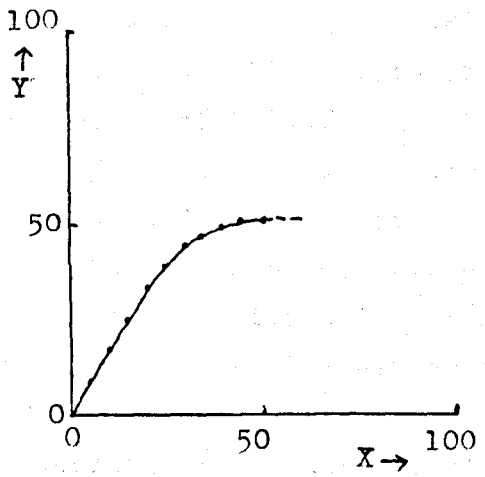

X = % Co in initial mixture.
Y = % Co in solid solution.

(The percentages refer to the cobalt concentration as a percentage of the total metal ion concentration.)

The product with much greater than 50% of Co in the original mixture apparently contained impurities, since its total metal content was less than that expected for $(Me_3NH)_3(CuCo)_2Cl_7$.

The replacement of $CuCl_4^{2-}$ by another MCl_4^{2-} ion was felt to be of interest, but the $(Me_3NH)_3(Cu,M)_2Cl_7$ system is rather complicated, so that a series of solid solutions of stoichiometry $A_2(Cu,M)Cl_4$ was sought. The main requirements were that a series of solid solutions, continuous if possible, were formed without by-products; that some structural data on the compounds were available; and preferably that more than one solvent could be used. A could be Me_4N^+, Et_4N^+ and Cs^+, since all of these ions form at least some solid solutions of the appropriate stoichiometry. The most complete structural data ~~was~~ were available for A = Me_4N^+ and Cs^+.

The differences between Me_4N^+ and Cs^+, which finally resulted in the choice of Me_4N^+, were in the number of solvents available and the purity of the products obtained.

The caesium compounds are very insoluble in ethanol, whereas the Me_4N^+ compounds will crystallize from water, ethanol or mixtures of the two. Attempts to produce $Cs_2(Cu,Co)Cl_4$ from aqueous solution produced green crystals, but these were contaminated with the various caesium chlorocuprates. Experiments in aqueous solution over a range of $CsCl:CuCl_2$ ratios showed the formation of $CsCuCl_3$, Cs_2CuCl_4, $Cs_2CuCl_4.2H_2O$ and $Cs_3Cu_2Cl_7.2H_2O$, often with two of these products formed simultaneously. All these compounds are well known; however another compound (X), not previously reported, was persistent in crystallizing in small amounts from systems with $CuCl_2:CsCl > 2:1$. Elemental analyses of X gave the ratios Cs:Cu:Cl = 2:2:5; it was apparently anhydrous. The presence either of OH^- in the coordination sphere or of Cu(I) was suspected, but attempts to prepare X from solutions containing appropriate quantities of CsCl and $CuCl_2$ in presence of OH^- or Cu(I) were not successful.

The cell dimensions of X were a = 1180, b = 970, c = 677 pm, $\beta = 95.5^{\circ}$. This differs from both $CsCuCl_3$ and Cs_2CuCl_4. Cell dimensions obtained for $Cs_3Cu_2Cl_7.2H_2O$ were a = 1090, b = 830, c = 888 pm, $\gamma = 106.8^{\circ}$. Since structure determination of $Cs_3Cu_2Cl_7.2H_2O$ was already in progress elsewhere, and further investigation of X was irrelevant to the main line of research on solid solutions, the caesium chlorocuprates were abandoned.

The $(Me_4N)_2(M,M')Cl_4$ solid solutions were homogeneous and easily reproduced, and are available from water, ethanol and mixtures of the two, and these systems were therefore chosen for further study.

Preparation of solid solutions. Two systems have been described for the formation of homogeneous samples of solid solutions.[2] Both of these rely on the same principle:

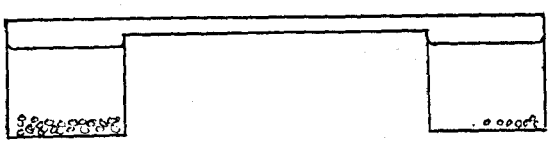

$T_1 > T_2$

at temperature T_1 at temperature T_2

In each of the vessels V_1 and V_2 solid solution is in equilibrium with saturated solution, and T_1 is greater than T_2 by 1-2°K. The solution is therefore more concentrated in V_1 than in V_2. Some arrangement is provided to transfer the more concentrated solution from V_1 to V_2, where it is allowed to equilibrate at the lower temperature T_2, so that some crystals of solid solution are deposited. Some of the less concentrated solution from V_2 is then returned to V_1 and again allowed to equilibrate, so that some of the solid in V_1 dissolves. The process is thus cyclic, and results in a gradual transfer of solid from V_1 to V_2. Since the temperatures of

V_1 and V_2 are very nearly equal, the composition of the two solids is similar and the crystals grown in V_2 should be very nearly homogeneous.

In the present experiments a similar effect was produced by allowing temperature fluctuations in the surroundings of a single vessel, while constantly grinding the samples.

The preparations of the starting materials are given first, and then the solid solutions.

Preparation of $(Me_4N)_2MCl_4$ (M = Cu,Co,Zn)

Boiling ethanolic solutions of tetramethylammonium chloride and the appropriate metal chloride in stoichiometric proportions were mixed, stirred at boiling point for 5 minutes, and allowed to cool. The products were collected, washed with ethanol and dried in a vacuum desiccator over P_2O_5.

Several batches of each compound were prepared, and each was analysed for the metal by atomic absorption. In each case the metal content was within 2% of the calculated value. Some batches were analysed gravimetrically for chloride, and were within 1% of the calculated chloride content. This method was considered to produce sufficiently pure compounds for further recrystallization to be unnecessary.

Preparation of the solid solutions $(Me_4N)_2(M,M')Cl_4$

Mixtures of $(Me_4N)_2MCl_4$ and $(Me_4N)_2M'Cl_4$ (total weight 5g.) were prepared covering the composition range 0-100% $(Me_4N)_2MCl_4$. The solids were ground together and placed in a screwtop glass jar. Solvent was added to each jar so that not more than 50% of the solid mixture (estimated visually) was dissolved. A short length of Teflon rod was placed in each jar and the jars were shaken on a mechanical shaker for about two weeks. The Teflon rods prevented the formation of large aggregates of crystals or large single crystals.

For a further period of between six weeks and three months the jars were allowed to stand with intermittent shaking at room temperature. This aided dissolution and recrystallization of the solid, and the initial powdered samples in water and ethanol-water rapidly become crystalline.

The pairs with M = Cu, M' = Co and M = Co, M' = Zn were equilibrated in ethanol, water and 50% ethanol-water, and the pair M = Cu, M' = Zn in water and 50% ethanol-water. The latter pair was also equilibrated in ethanol, but a complicated mixture of products resulted, which was not further examined.

Microscopic examination of the solid solutions $(Me_4N)_2(M,M')Cl_4$

The texture of the solids varied dependent on the solvent from which they were crystallized; the samples from water and 50% ethanol-water showed individual crystals up to 0.5 mm in length, while those from ethanol were powdery. The colour of each of the samples was homogeneous. In those cases where large enough crystals were formed, sections were cut through them, and these showed no gradation in colour and extinction from the middle to the outside. The crystals were somewhat rounded by abrasion, but the morphology was generally similar to that of the single-metal compounds.

Preparation of $(Me_3NH)_3Cu(Cu,Co)Cl_7$ solid solutions

Solid solution formation effectively takes place between $(Me_3NH)_3Cu_2Cl_7$ and $(Me_3NH)_3CuCoCl_7$. It was found difficult to produce large quantities of $(Me_3NH)_3CuCoCl_7$, so that the method was not exactly the same as that for $(Me_4N)_2(M,M')Cl_4$.

The preliminary experiments showed that if hot ethanolic solutions of Me_3NHCl and the metal chlorides were mixed and allowed to cool, solid solutions were produced having a greater Co:Cu ratio than the original mixture. This method cannot be expected to give a homogeneous product, but the average Co:Cu ratio was obtained by atomic

absorption analysis. In this way ten samples were prepared with average compositions between 10 and 100% $(Me_3NH)_3CuCoCl_7$. Addition of pure $(Me_3NH)_3Cu_2Cl_7$ where necessary allowed the compositions of the mixture to be adjusted so as to be in steps of 10% $(Me_3NH)_3CuCoCl_7$ between 10 and 100%. From this stage the equilibration with ethanol was analogous to that for $(Me_4N)_2(M,M')Cl_4$ except that each initial mixture of solids weighed only 1g.

$(Me_3NH)_3Cu(Cu,Co)Cl_7$. The morphology is identical to that of $(Me_3NH)_3Cu_2Cl_7$; however the crystallinity of the samples decreased as the cobalt content increased, and all the crystals were severely damaged by abrasion. The hkO Weissenberg photograph of a crystal of intermediate composition was almost identical to that of $(Me_3NH)_3Cu_2Cl_7$.

(3) Analysis of the solid solutions

To construct the phase diagram it was necessary to know the composition of the solid phase and of the supernatant liquor. The samples were analysed for both metal ions by atomic absorption, and the stoichiometry of the solids deduced from this was consistent with the formula $(Me_4N)_2(M,M')Cl_4$. In all cases samples were taken when the systems had been at 293 $\pm$ 2K for 3-4 hours.

Atomic absorption analysis

All measurements were carried out using a Unicam SP90 atomic absorption spectrophotometer. Standard solutions were prepared containing 2-20 mg dm^{-3} of Cu^{++}, Co^{++} and Zn^{++}, and calibration curves of peak height vs. metal ion concentration determined for each analysis. Checks were also made to ensure that there was no interference with one metal ion by another, even in presence of 1000 fold excess. Since no interferences were apparent the standard solution for each metal ion contained only that ion, rather than a mixture approximating to that in the unknown solution.

The error in these analyses is estimated at about ± 2% for each metal ion percentage which is slightly greater than might be expected for a carefully conducted classical analysis. Atomic absorption was used because of its convenience for the large number of analyses to be performed, and because of the wide concentration ranges to be covered from fairly small samples of the solid solutions.

(a) $(Me_4N)_2(M,M')Cl_4$ from water. A sample of mother liquor (about 0.5g) was removed and made up in a standard flask. The solid product was filtered off, and as much mother liquor as possible removed by pressing between filter papers. A sample of this wet residue (about 0.1g) was dissolved in water and made up in a standard flask. Analysis for the two metal ions led to the amounts of the two salts in a solid contaminated by mother liquor of known composition. From the weight of solid taken for analysis and the amounts of the two salts present in it the weight of water in the wet residue was found. A correction was then applied for the weights of the two salts in this weight of water, enabling the composition of the pure solid solutions to be found.

This method was satisfactory for determination of the phase diagram and Roozeboom plot, but made it difficult to obtain pure samples of the solid solutions for physical measurements.

(b) $(Me_4N)_2(M,M')Cl_4$ from 50% ethanol-water. The mother liquor was sampled as before. After filtration the solid was washed with solvent to remove adhering mother liquor and then dried at 373K to constant weight. The composition of the solid solution was then obtained directly from the two metal ion analyses, and there was no contamination by mother liquor.

The disadvantage of this method is that up to 40% of the solid product was lost during washing; however no satisfactory alternative was devised which produced pure solid solution.

(c) $(Me_4N)_2(M,M')Cl_4$ from ethanol. The solid was filtered off. A sample of mother liquor was immediately weighed out ($\sim$ 10g.), and then allowed to evaporate to dryness. The resultant solid ($\sim$ 0.1g.) was then dissolved in water for atomic absorption analysis. This procedure was necessary to remove the large bulk of ethanol which would have interfered with the atomic absorption analysis. The analysis then proceeded as for the solid solutions formed in 50% ethanol-water.

(d) $(Me_3NH)_3Cu(Cu,Co)Cl_7$ from ethanol. The solid was filtered off. A sample of mother liquor was immediately weighed out and made up in water for analysis. The solid solutions were washed with a small amount of dry ethanol and dried in a vacuum desiccator over P_2O_5. The analyses were performed as before.

(4) Phase diagrams (Fig.III.1)

The results of these experiments were plotted in the form of Gibbs triangular diagrams, and are also recorded in Table III.1. Roozeboom and Hill-Durham-Ricci diagrams (see Chapter V) are plotted in Figs. III.2 and III.3.

(5) Spectra

The reflectance spectra of $(Me_4N)_2CuCl_4$ and $(Me_4N)_2CoCl_4$ are given in Fig.III.4. The spectra of the solid solutions were also recorded; they were independent of the solvent used and only one series for each pair of metal ions is given (Fig.III.5). The reflectance spectra of $(Me_3NH)_3Cu(Cu,Co)Cl_7$ are shown in Fig.III.6.

(6) DSC measurements of $(Me_4N)_2MCl_4$ and $(Me_4N)_2(M,M')Cl_4$

All measurements were carried out using the DSC attachment of a Dupont 3000 Thermal Analyser. Essentially this attachment consists of a constantan disc which serves both as the heat transfer

path to and from the sample and as one half of a differential thermocouple system.[4] The disc is attached to a silver heating block and has raised sample and reference platforms symmetrically placed on it. A chromel wire is connected to each platform to complete the chromel-constantan differential thermocouple system. The sample position is totally surrounded by a block of high thermal conductivity. With the small size of the sample chamber and its surrounding block temperature gradients in the cell are minimised and the sample temperature is easily controlled. The graph produced is of ΔT (the difference between sample and reference temperature) vs T (the temperature of the reference).

The sample was held in a small aluminium cup with a lid and the reference was a similar cup and lid. Sample sizes of 20-30 mg were employed, and data ~~was~~ were recorded over the range 150-330K. In all cases the heating rate was 6^{o}/min and the initial sample temperature was about 100K. A time-base record was also obtained from an external chart-recorder; the area beneath a peak on this was about five times that from the standard temperature base record. The area beneath the peaks on the time-base record were measured using an Allbrit planimeter.

Traces for the solid solutions were independent of solvent, and only one example of each series is given (Fig.III.7). The DSC of 50:50 mechanical mixtures of the pure compounds were also run, for the sake of comparison and are given in Fig.III.8.

The transition temperature is most closely approximated by the extrapolated onset temperature (T_{EOT}):-

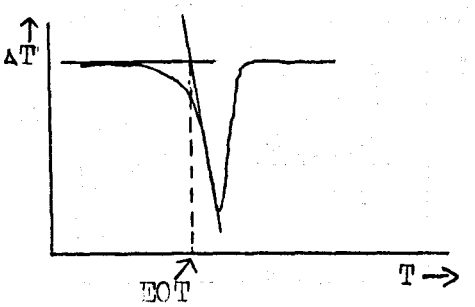

The area under the peak is proportional to ΔH for the transition; in theory if the machine is calibrated using substances with transitions of known ΔH at a number of temperatures, values of ΔH for the unknown transitions can be found. In practice the calibration constant is temperature-dependent; there is also a slight difference depending on whether the calibrant is a metal, or a polymer, or an inorganic salt etc. Insufficient calibrants of appropriate nature were found for the low-temperature part of the range, so that absolute ΔH measurements were not made. However the area under a peak per unit weight of sample was measured, and for transitions at similar temperature will give some measure of the relative ΔH of transition for the two compounds. In particular the area per unit weight for the broad transitions was plotted against composition for various solid solutions, and the results are shown in Fig.III.9.

(7) Calibration of the Gouy balance

The Gouy balance was of a standard design (Newport Instruments) except for the inclusion in the sample chamber of two thermocouples for more accurate monitoring of the sample temperature than that provided by the control system. One thermocouple junction was at the bottom of the sample space and the other about 10 cm above this. The reference junctions of the two thermocouples were in an ice-water mixture.

The thermocouples were calibrated against a platinum resistance thermometer, which was introduced into the space normally occupied by the sample tube and midway between the two thermocouple junctions. This thermometer had already been calibrated at NBS. The emf's generated in the thermocouples were measured by the potentiometer supplied with the instrument; the resistance of the thermometer was measured using the circuit

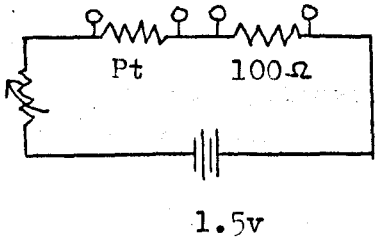

with the variable resistance adjusted to give a current of about 3×10^{-3} amp.

The temperature measured by the platinum resistance thermometer was given by

$$t_{pt} = \frac{R_t - 21.1733}{0.00392011 \times 21.1733} \ ^{o}C.$$

This was converted to give the temperature (t) in ^{o}C on the International Practical Temperature Scale by use of the equation

$$t = t_{pt} + \underbrace{\delta t(t - 100).10^{-4}}_{A} + \underbrace{\beta t^3(t - 100).10^{-8}}_{B} ,$$

where $\delta = 1.492$ and $\beta = 0.1113$ (but 0 above $0^{o}C$). This equation was solved for t by the method of successive approximations and the result converted to ^{o}K.

The emf of both thermocouples and T(K) were measured over the range 90 - 370K at approximately 10^{o} intervals. The two thermocouple emf's at any particular temperature did not differ by more than 1×10^{-5} volt ($= 0.30^{o}$) i.e. the temperature is constant along the length of the sample. The mean thermocouple emf was plotted against T(K) and the resulting smooth curve used to determine intermediate temperatures.

Magnetic field calibration used the standard compounds $Nien_3S_2O_3$ and $HgCo(CNS)_4$ at $20^{o}C$ (293K).

For $Nien_3S_2O_3$ at 293K $X_g = 11.03 \times 10^{-6}$ cgsu

" $HgCo(CNS)_4$ $X_g = 16.44 \times 10^{-6}$ cgsu

All measurements were done in an atmosphere of nitrogen, so that no correction for the displaced medium was necessary.

Therefore $$X_g = \frac{2wg\ell}{WH^2} \text{ and hence } H^2 = \frac{2wg\ell}{X_g W} ,$$

where W is the mass of the sample (g)

w is the change in weight (g) on application of a magnetic field of strength H

g is the gravitational constant = 980.6 cm sec^{-1}

ℓ is the sample length (cm)

H is the magnetic field (Oersted)

X_g is the gram susceptibility (cm^3 g^{-1}).

Values of H^2 were thus obtained for several values of the electromagnet current I amp ($H^2 \alpha I$) and there was good agreement between results for the two calibrants.

REFERENCES FOR CHAPTER III

1. Remy & Laves, Berichte 1933, 66, 401.

2. Flatt, Wilhelm & Burkhardt, Helv.Chim.Acta 1944, XXVII, 1600.

3. Rousset & Paris, Bull.Soc.Chim. 1970.

4. Baxter, Thermal Analysis 1, 65.

Figure III.1

Phase diagrams

Diagrams are plotted using the weight percentage of each component. For figures (g), (h) and (i), the low solubilities of the solids necessitated expansion of the upper part of the diagram to show the solution curve clearly and dotted lines are used to indicate the breaks in the tie-lines.

Figure III.1

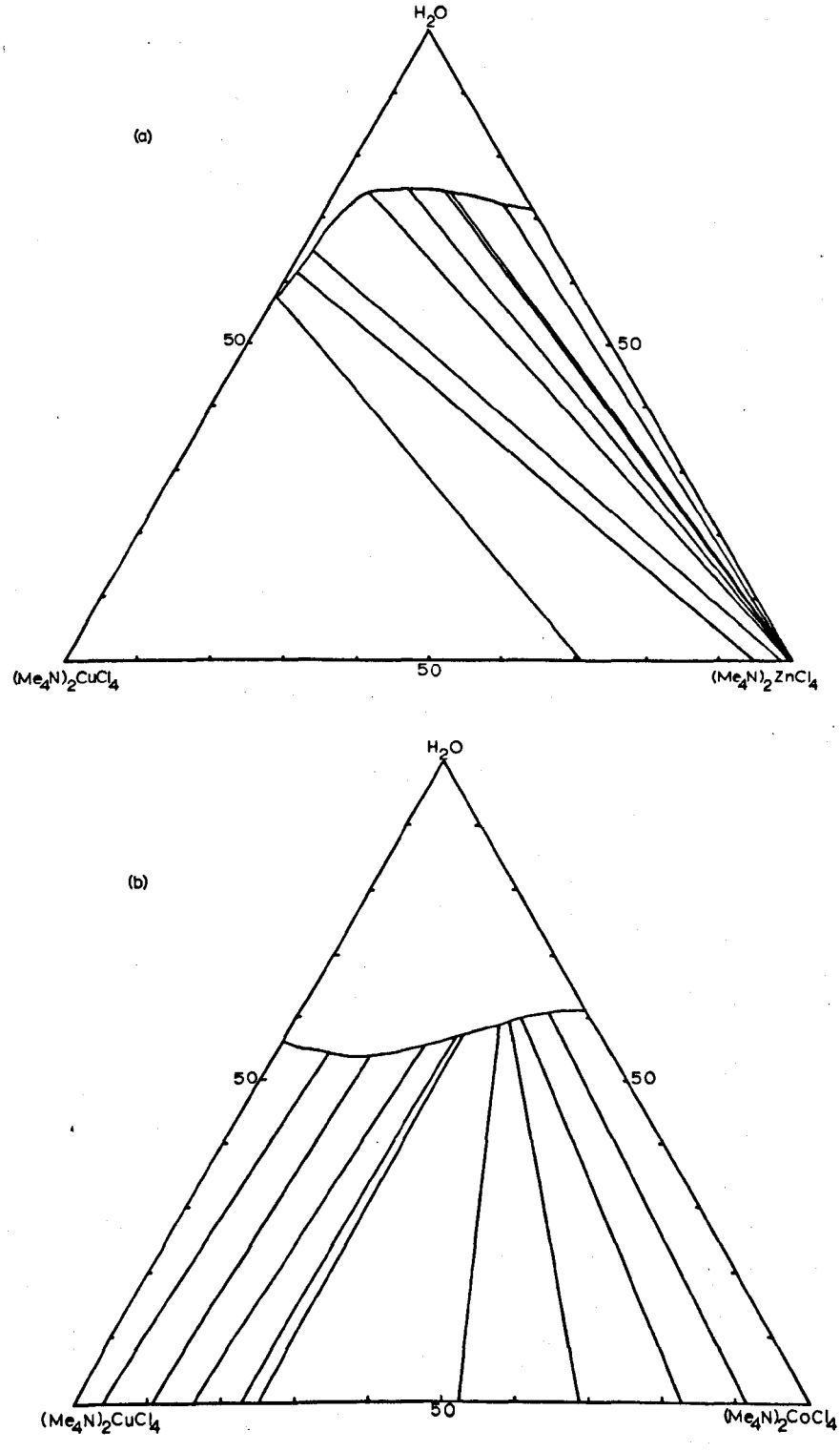
H2O
(a)
50
50
50
(Me4N)2CuCl4
(Me4N)2ZnCl4
H2O
(b)
50
50
50
(Me4N)2CuCl4
(Me4N)2CoCl4

Figure III.1 cont'd

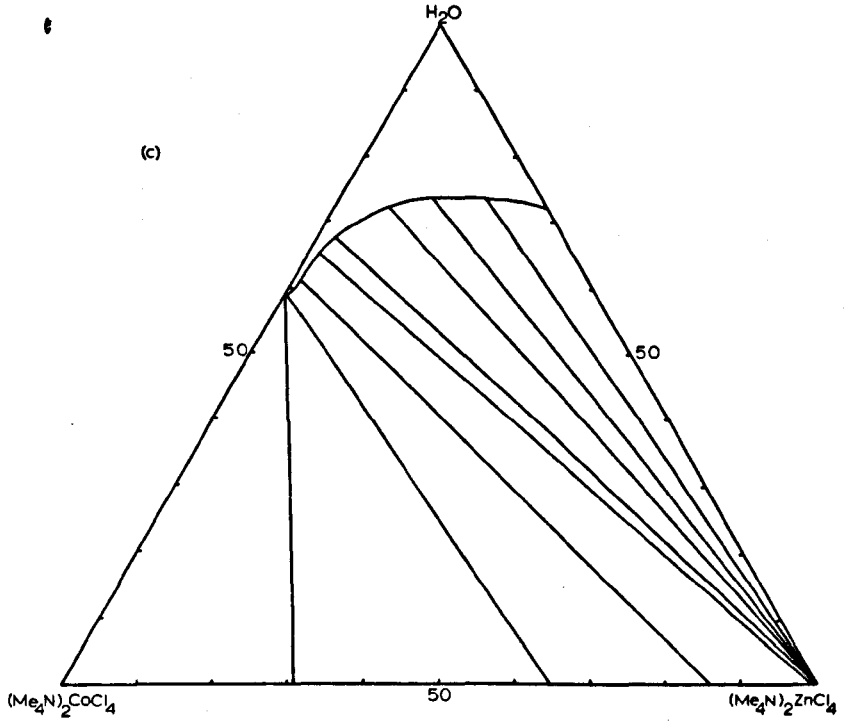

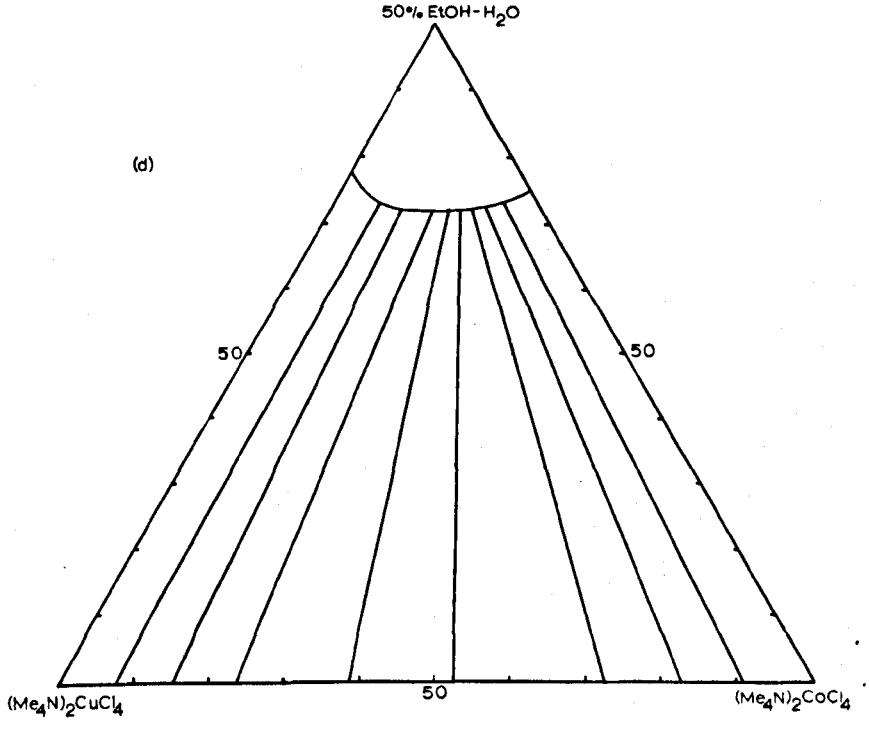

Figure III.1 cont'd

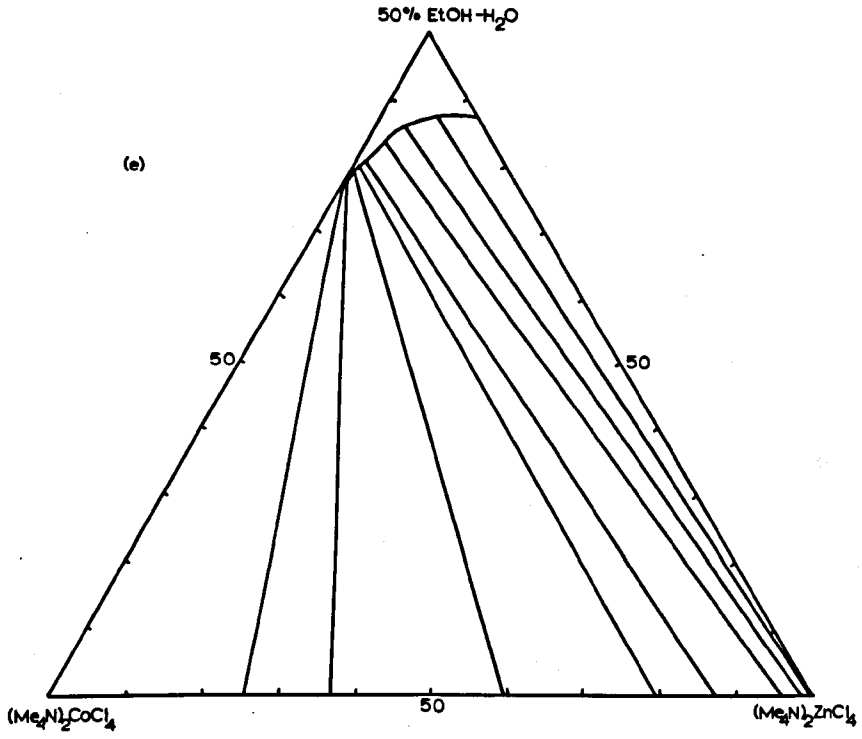

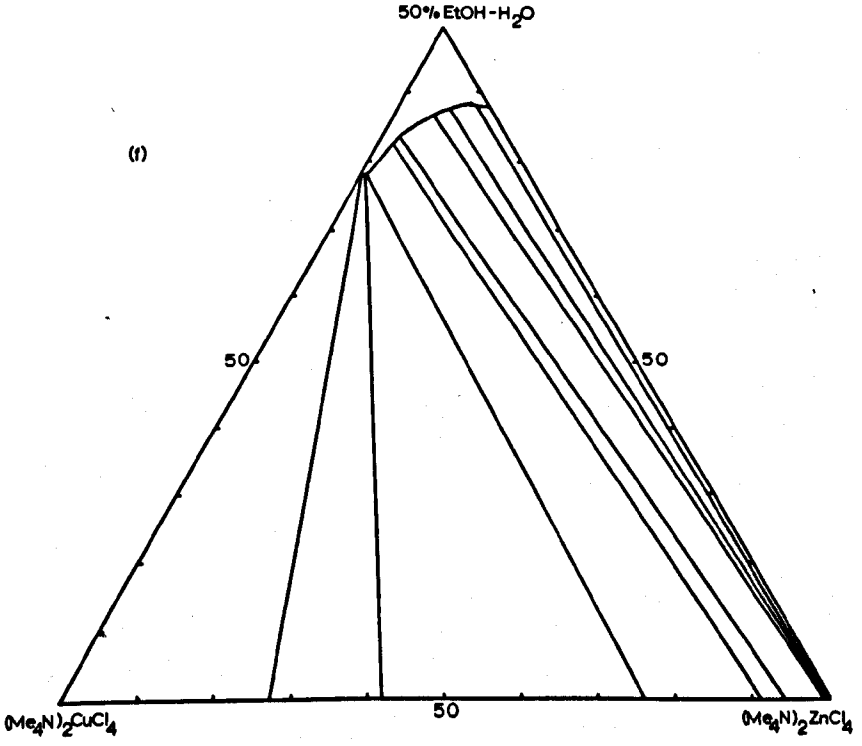

Figure III.1 cont'd

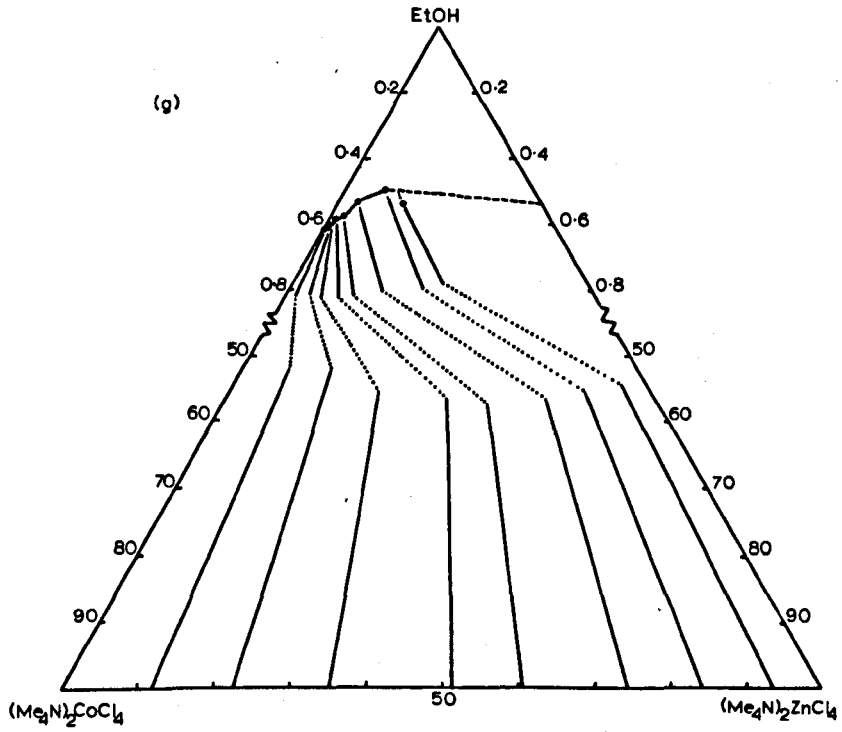

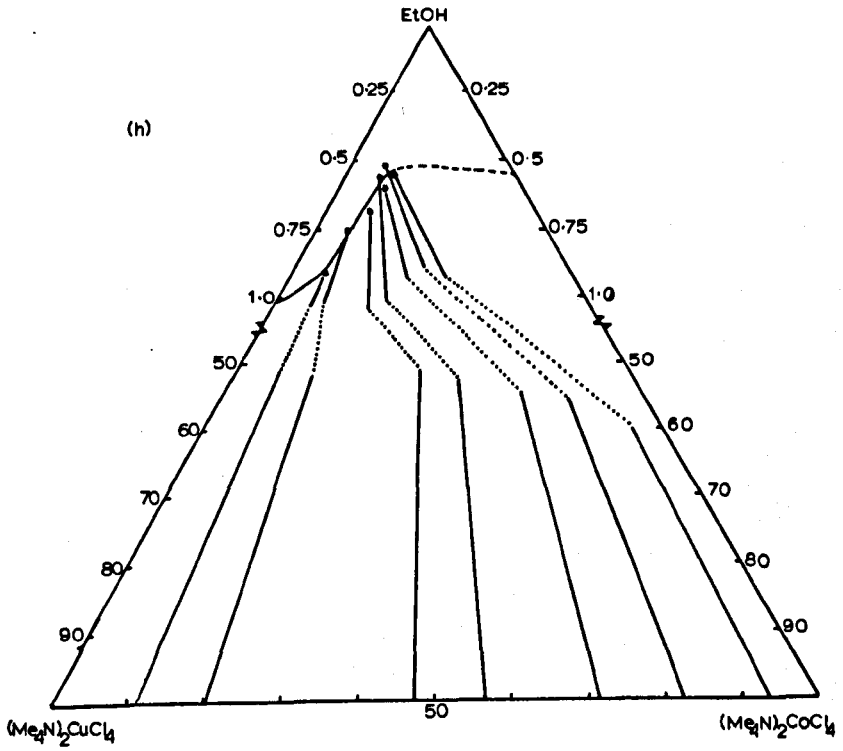

Figure III.1 cont'd

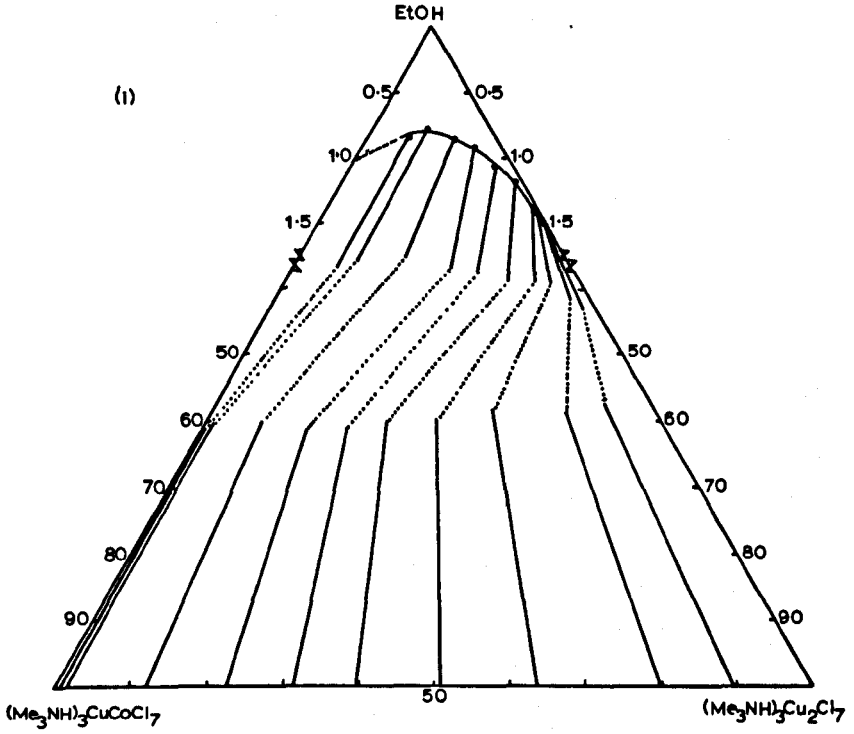

Figure III.2

Roozeboom plots

The ordinate is always the mole fraction (%) of the more soluble salt in the solute; the abscissa is the mole fraction of the more soluble salt in the solid solution. The continuous curve represents the experimental results; the dotted line represents the curve calculated from the solubilities as discussed in Chapter VI.

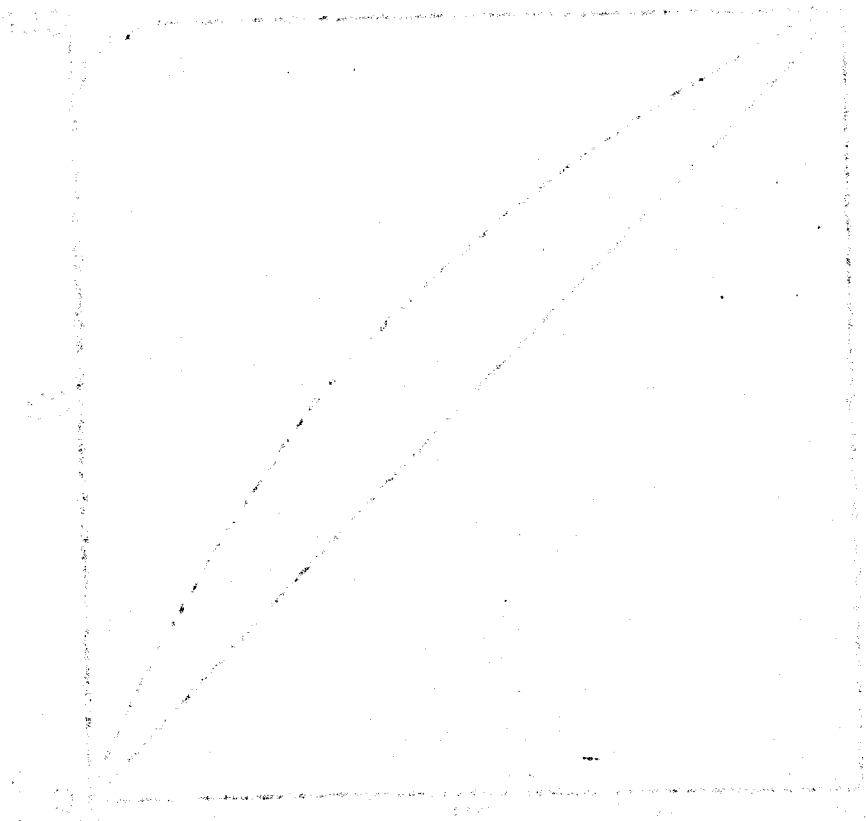

Figure III.2

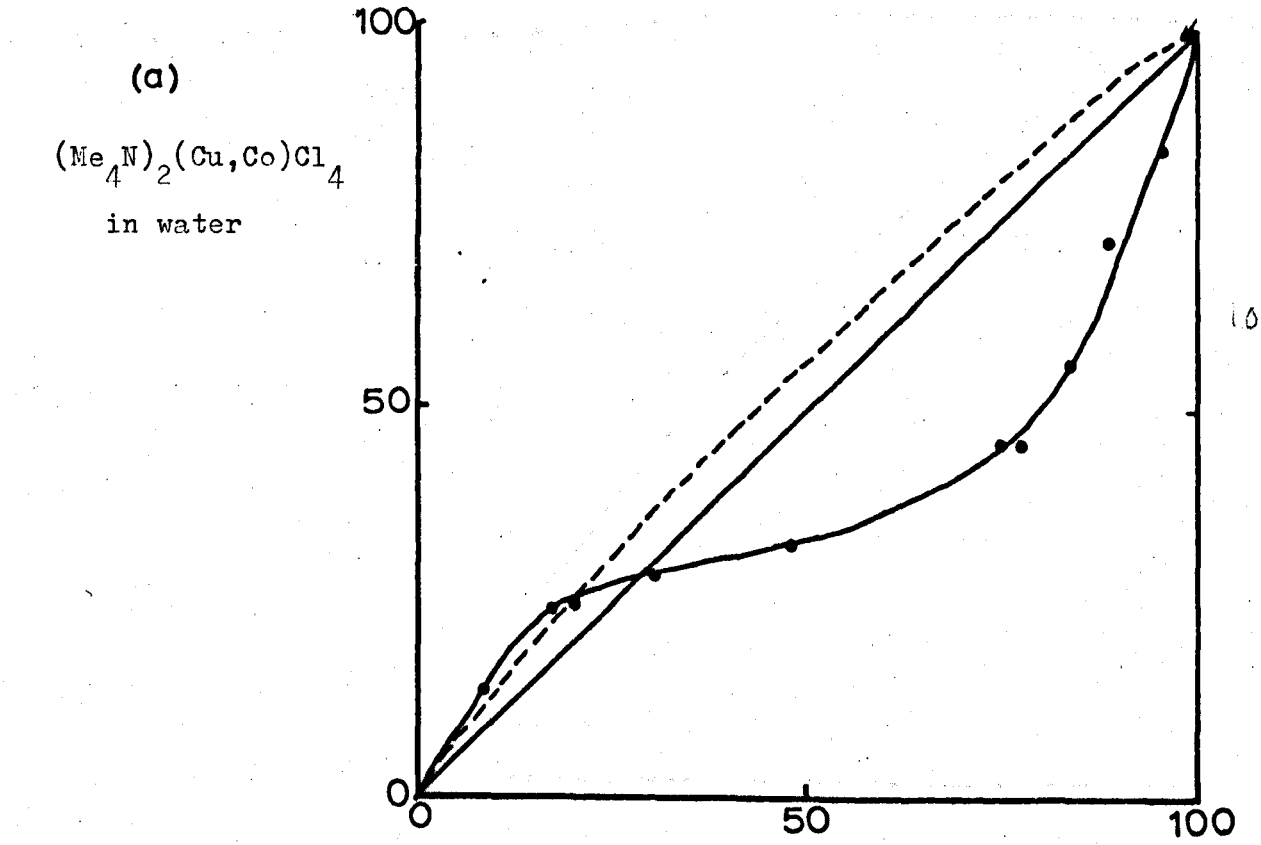

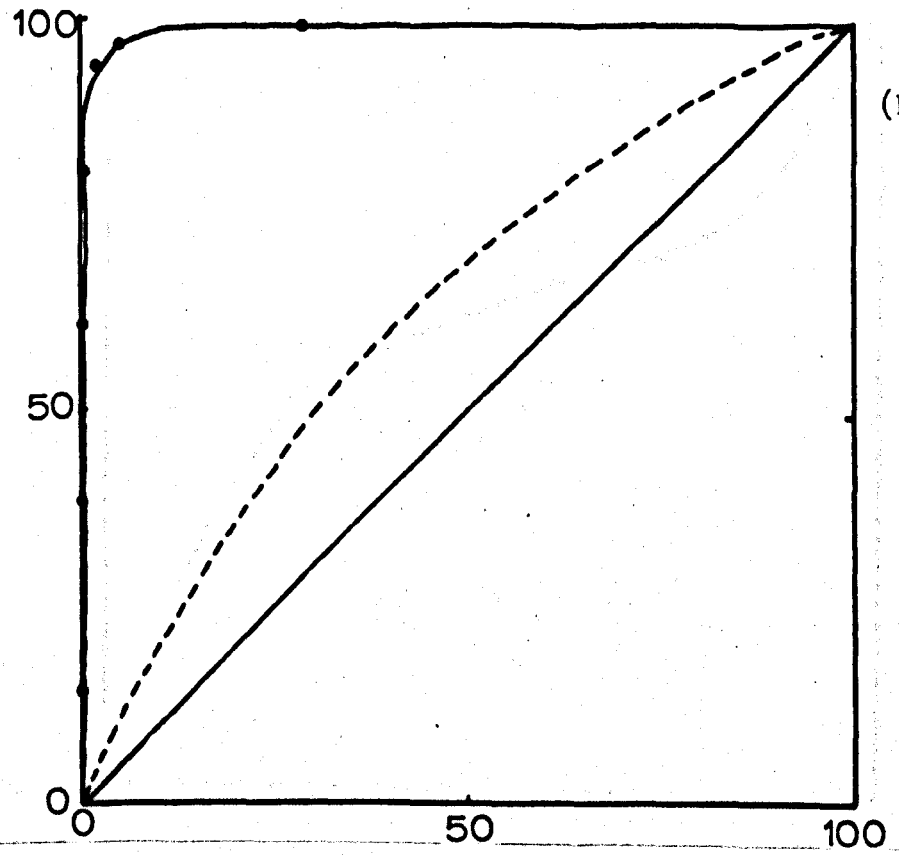

(b)

$(Me_4N)_2(Cu,Zn)Cl_4$
in water

Figure III.2 cont'd

(c)

$(Me_4N)_2(Co,Zn)Cl_4$ in water

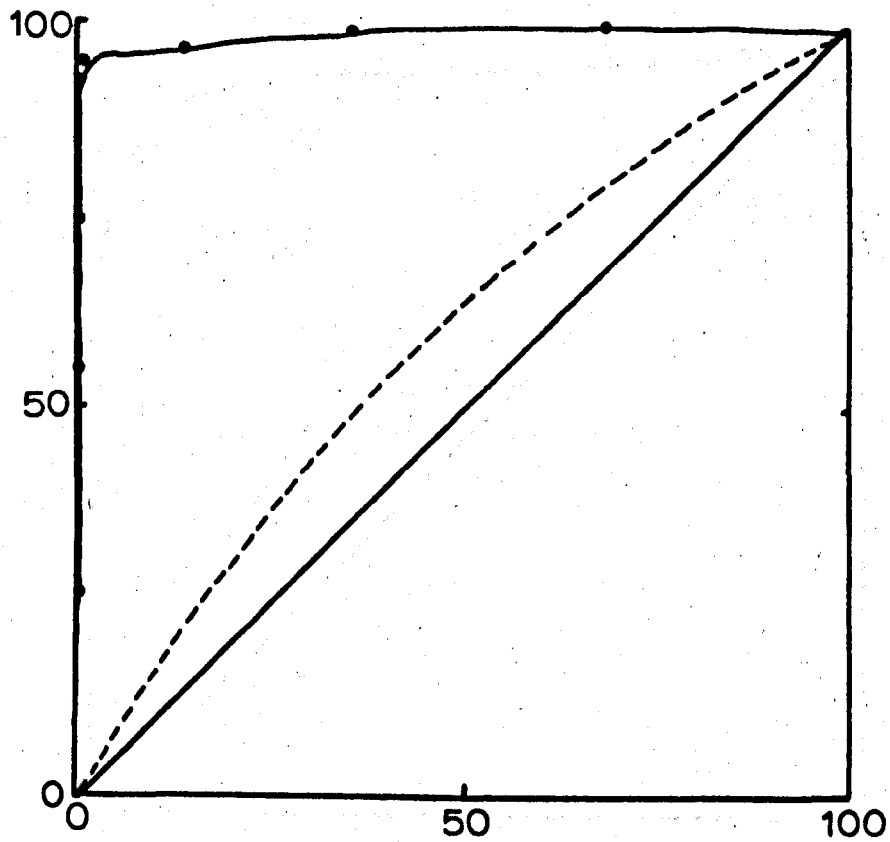

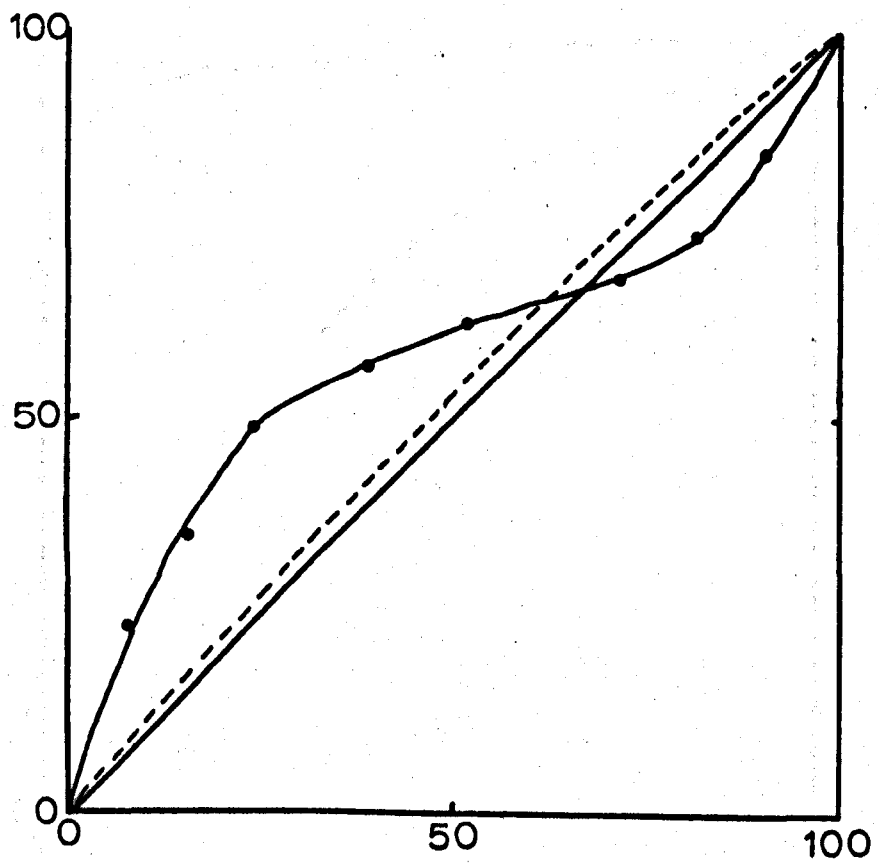

(d)

$(Me_4N)_2(Cu,Co)Cl_4$ in 50% ethanol-water

Figure III.2 cont'd

(e)

$(Me_4N)_2(Cu,Zn)Cl_4$ in 50% ethanol-water

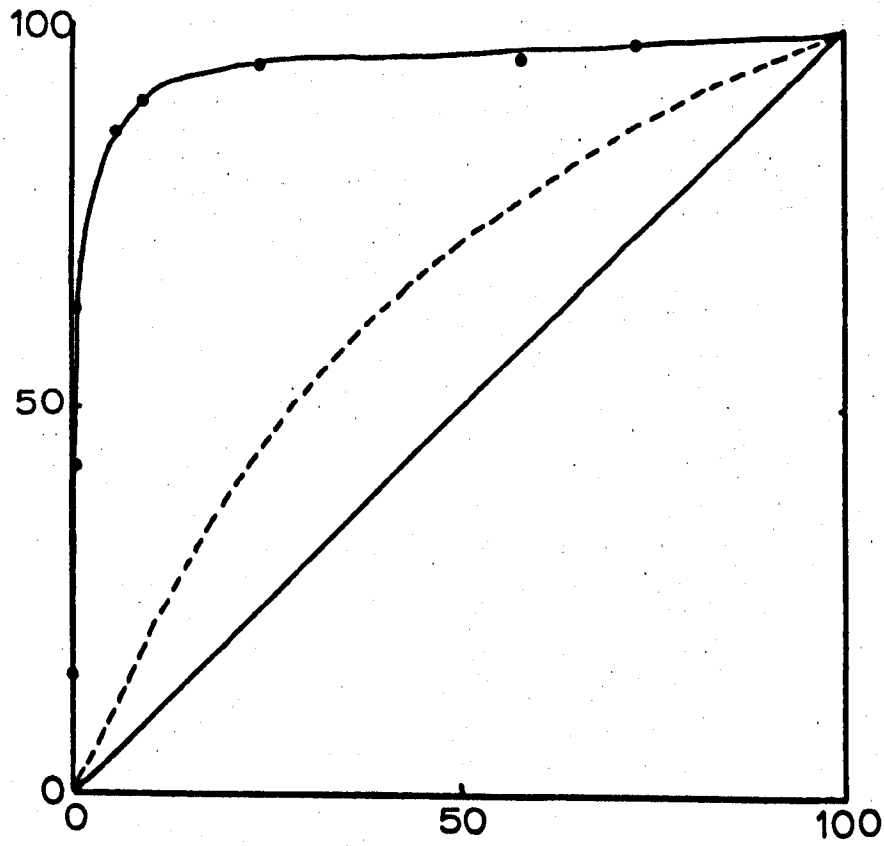

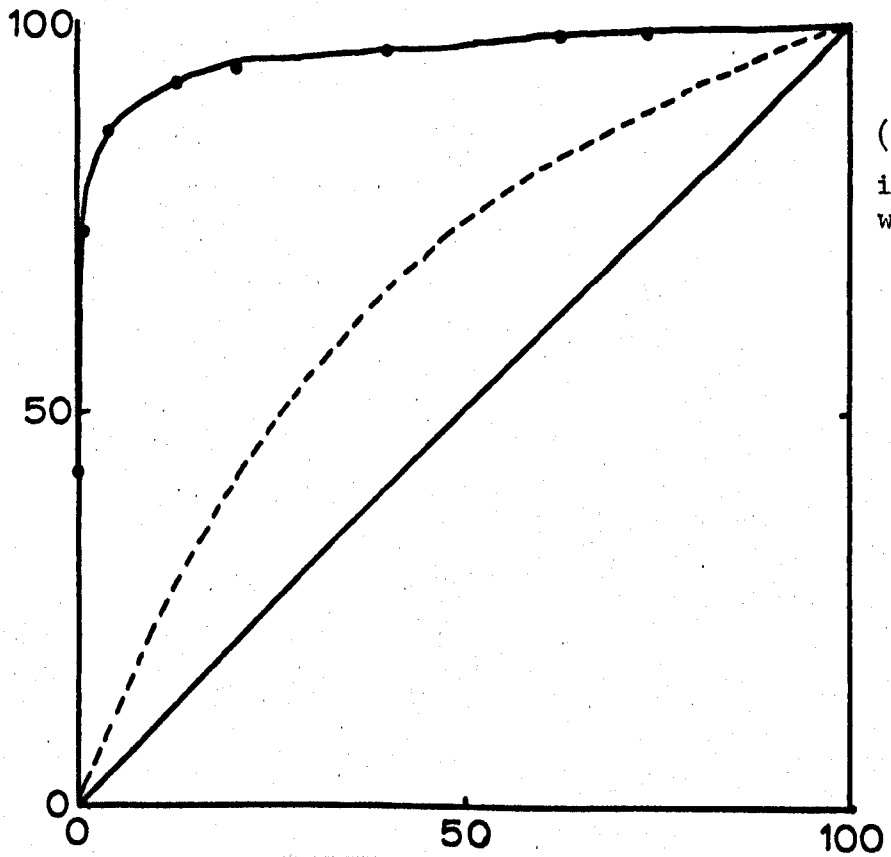

(f)

$(Me_4N)_2(Co,Zn)Cl_4$ in 50% ethanol-water

Figure III.2 cont'd

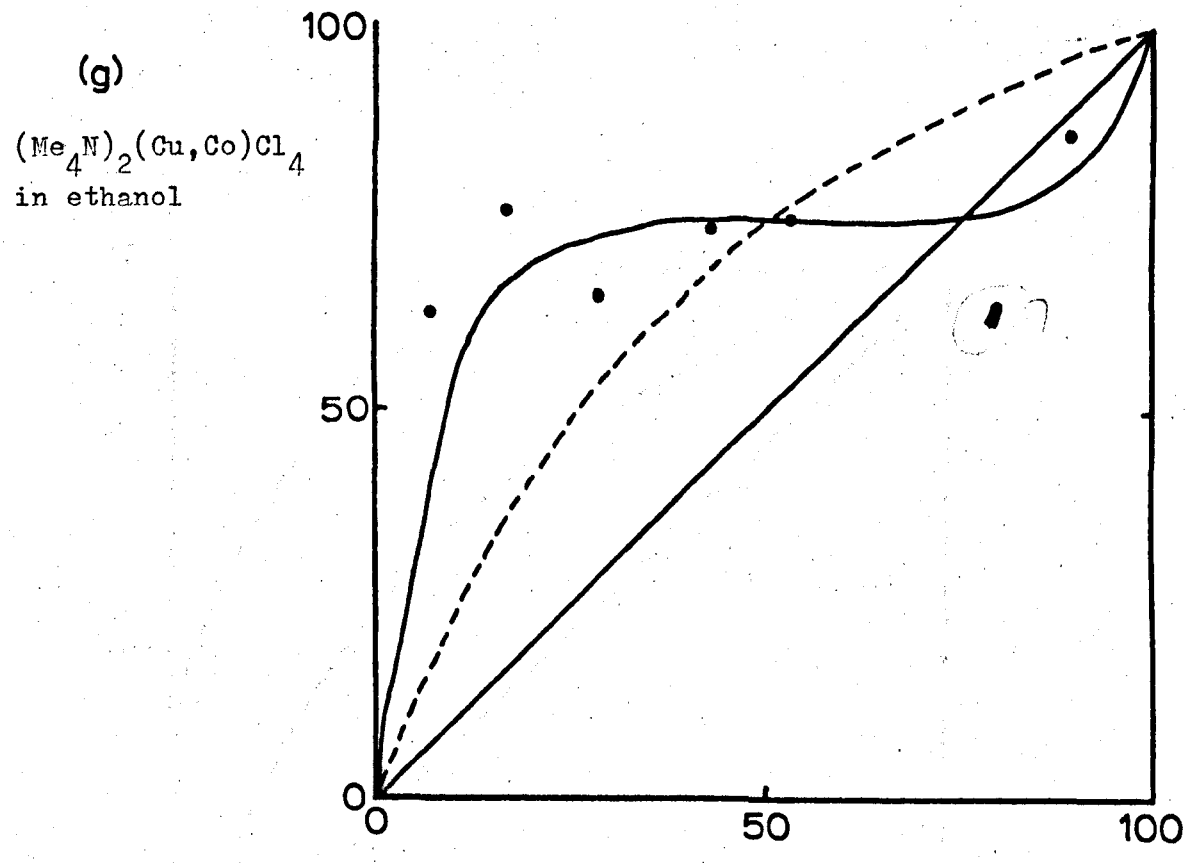

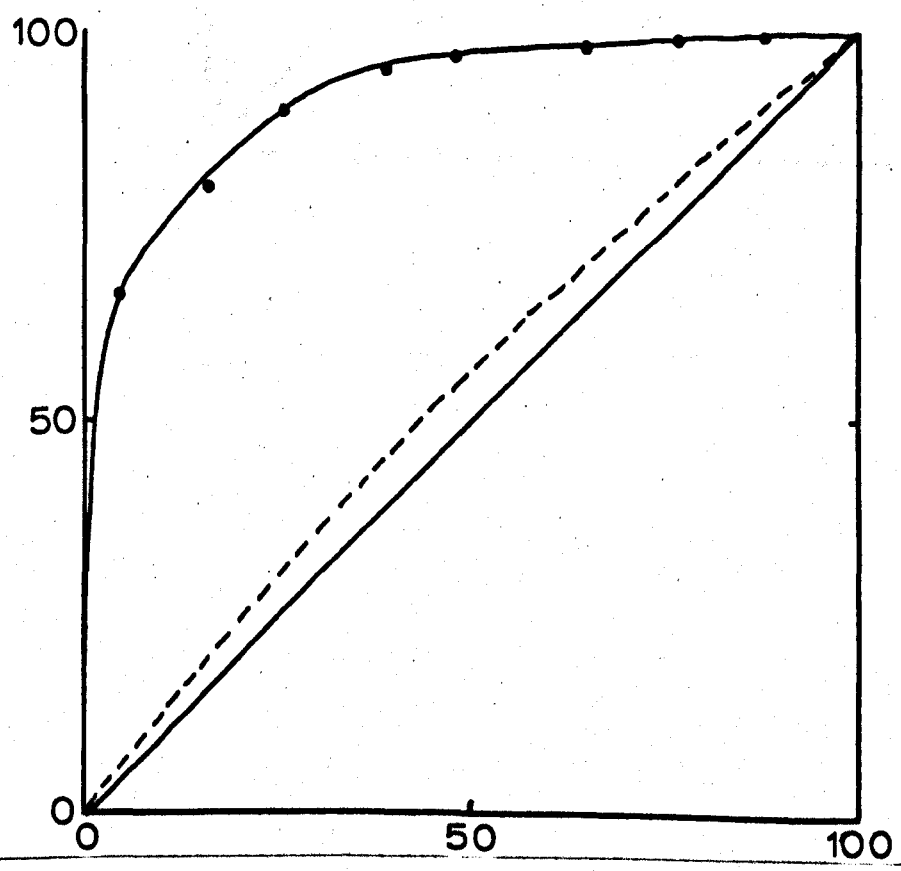

(h)

$(Me_4N)_2(Co,Zn)Cl_4$
in ethanol

Figure III.2 cont'd

(i)

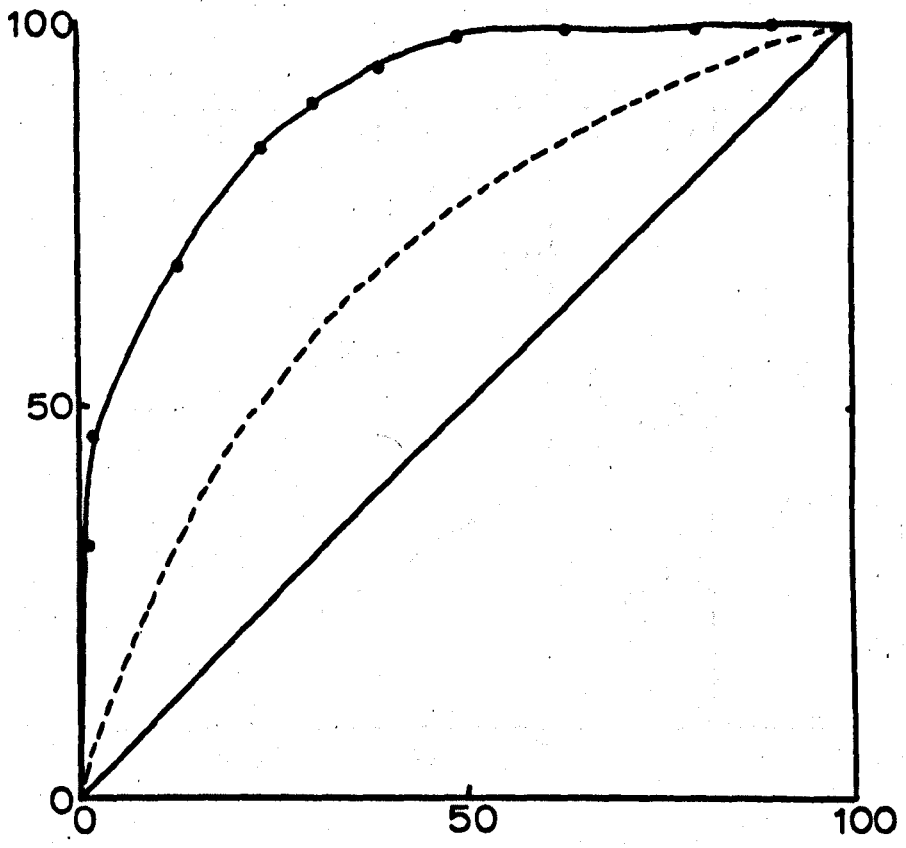

$(Me_3NH)_3Cu(Cu,Co)Cl_7$ in ethanol

Figure III.3

HDR plots ($R_\ell = \log_{10} R_\ell$; $R_s = \log_{10} R_s$)

The order in which the diagrams are presented corresponds with Figure III.2.

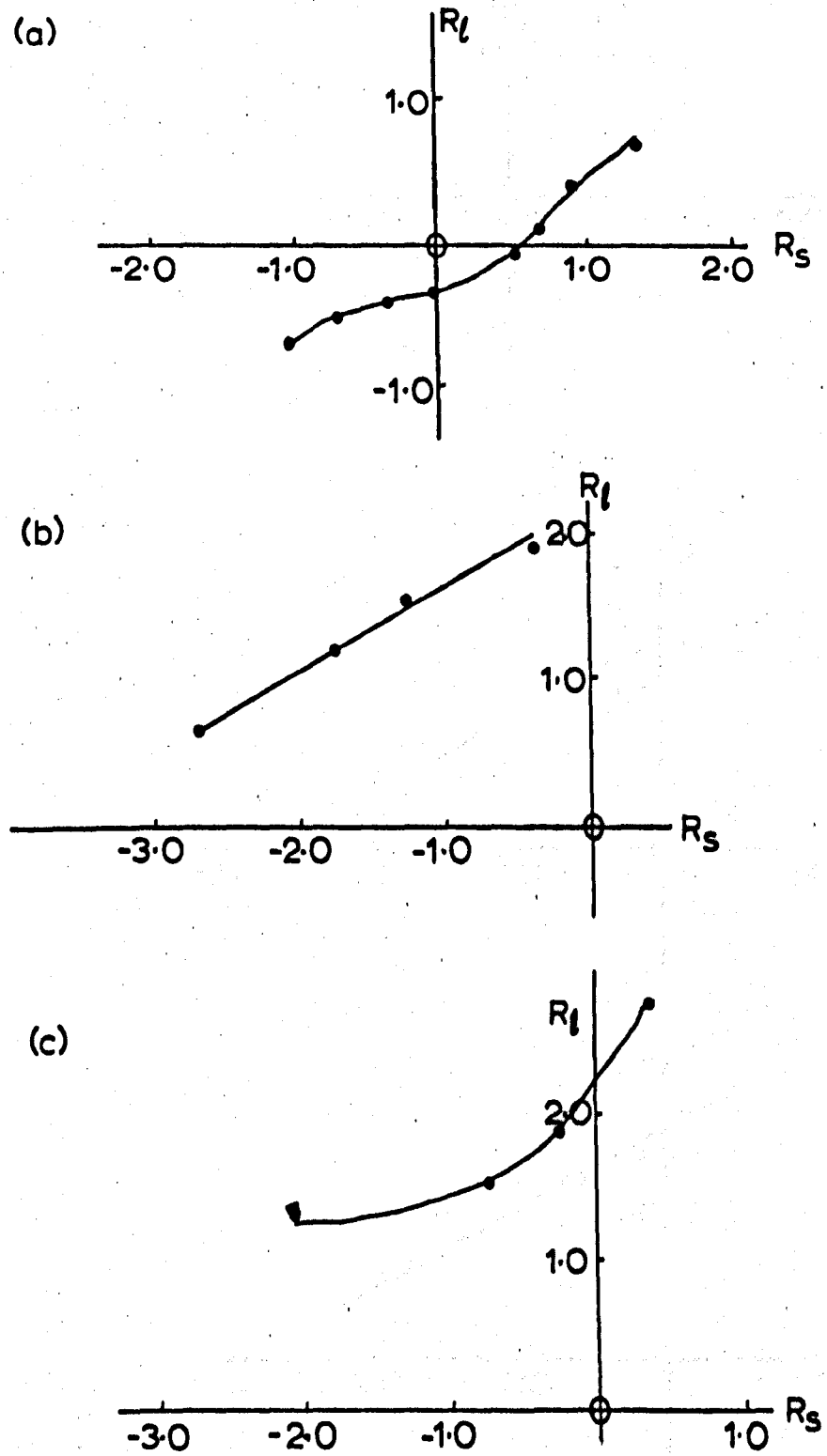

Figure III.3 cont'd

(d)

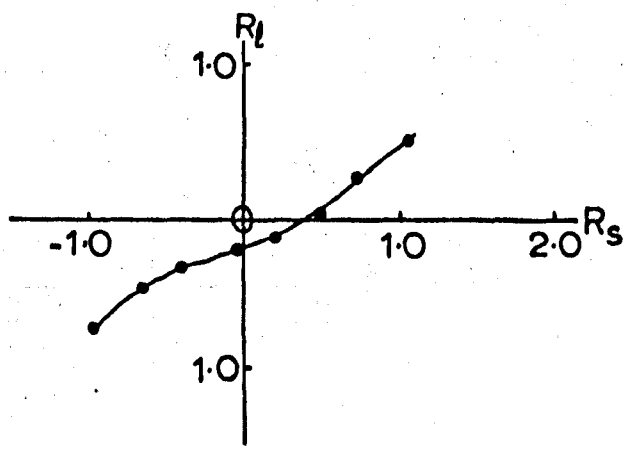

(e)

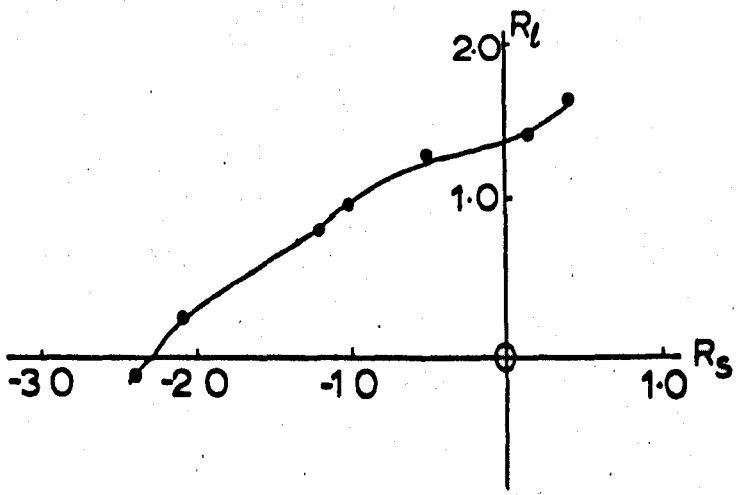

(f)

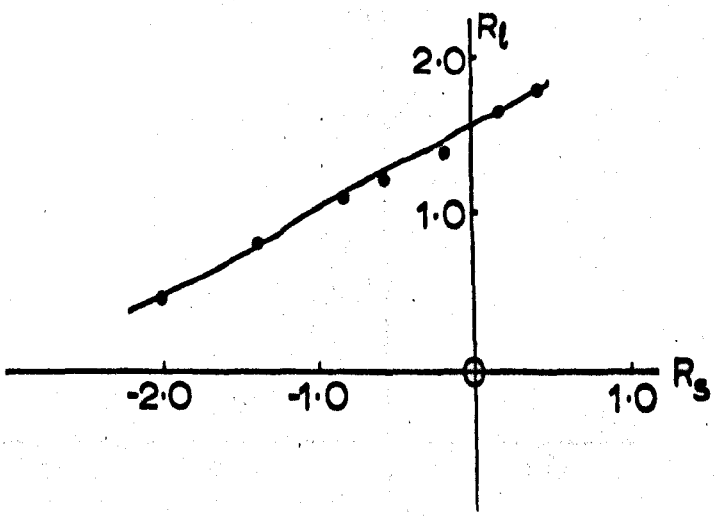

Figure III.3 cont'd

(g)

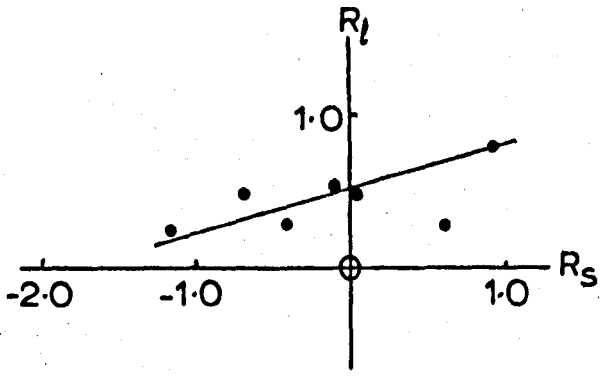

(h)

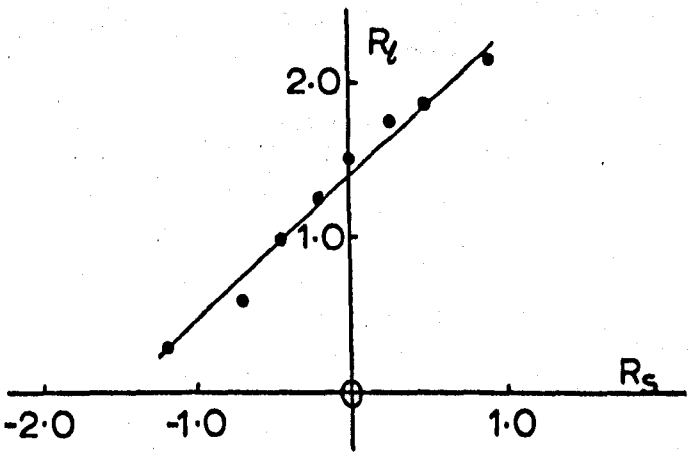

(i)

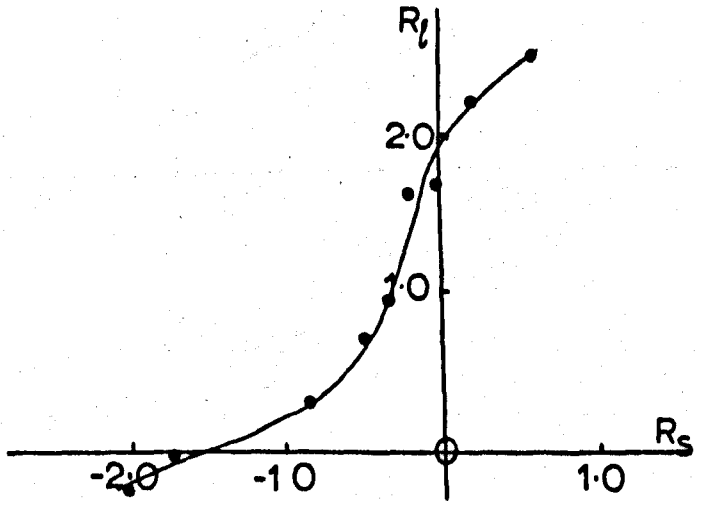

Figure III.4

Reflectance spectra

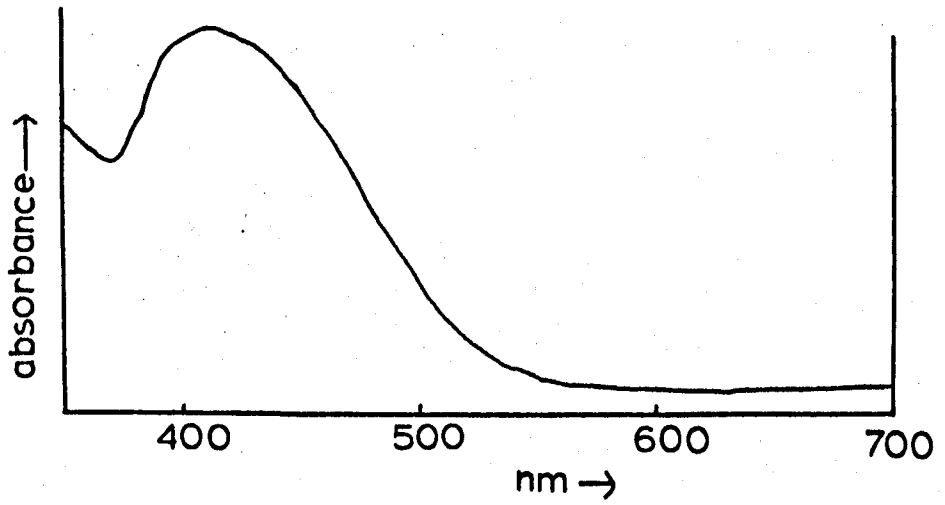

$(Me_4N)_2CuCl_4$

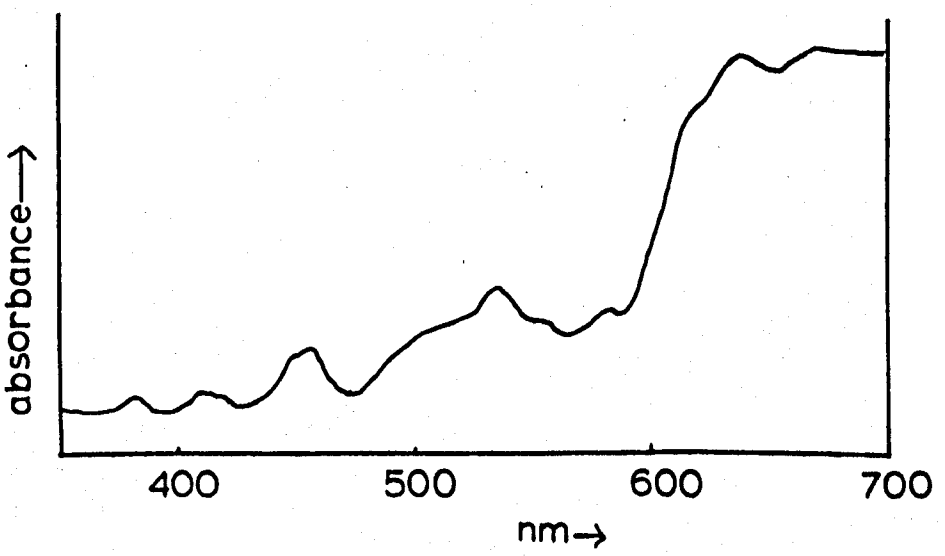

$(Me_4N)_2CoCl_4$

Figure III.5

Reflectance spectra of $(Me_4N)_2(M,M')Cl_4$.

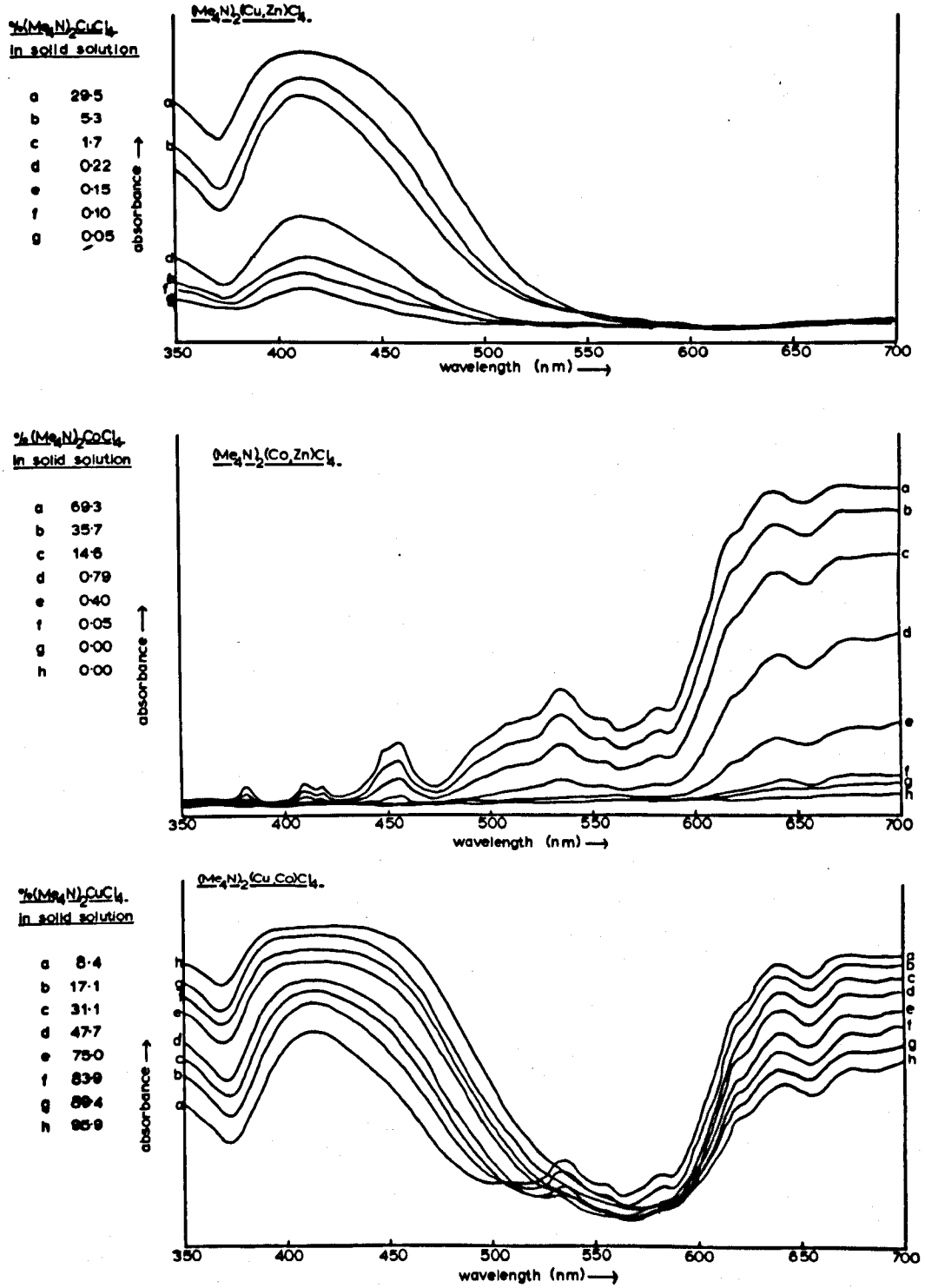

Figure III.6

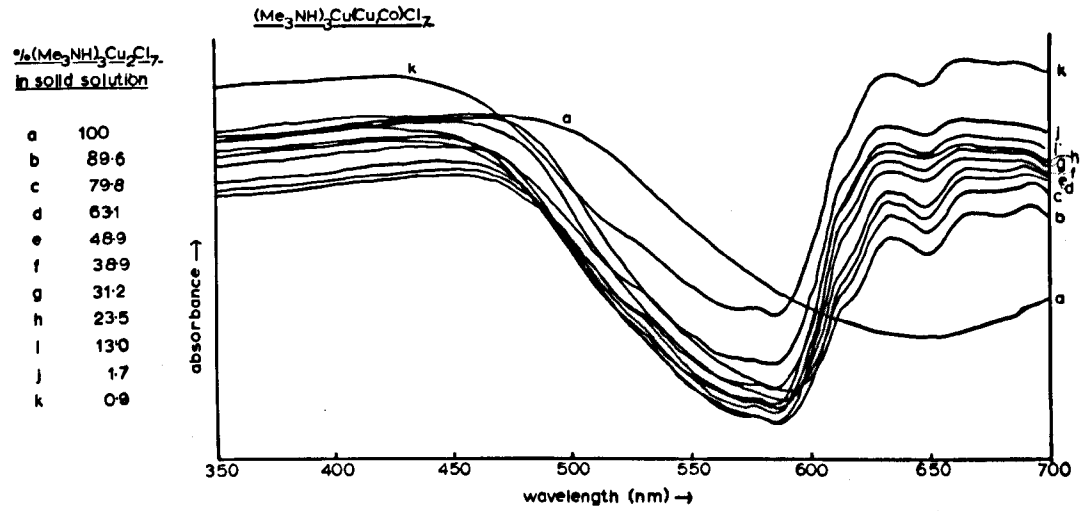

Reflectance spectra of $(Me_3NH)_3Cu(Cu,Co)Cl_7$.

Figure III.7

DSC of $(Me_4N)_2(Co,Zn)Cl_4$.

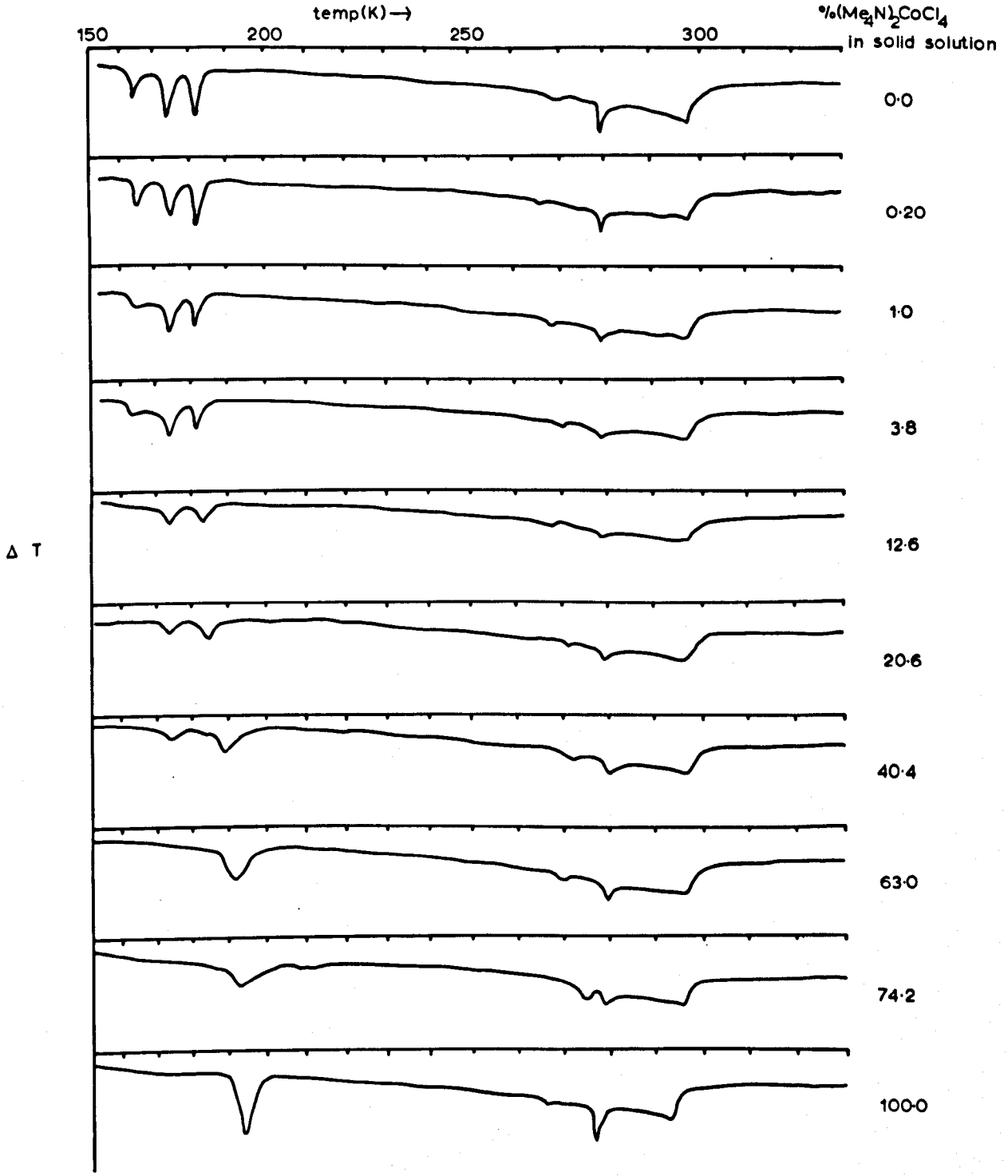

Figure III.7 cont'd

DSC of $(Me_4N)_2(Cu,Zn)Cl_4$.

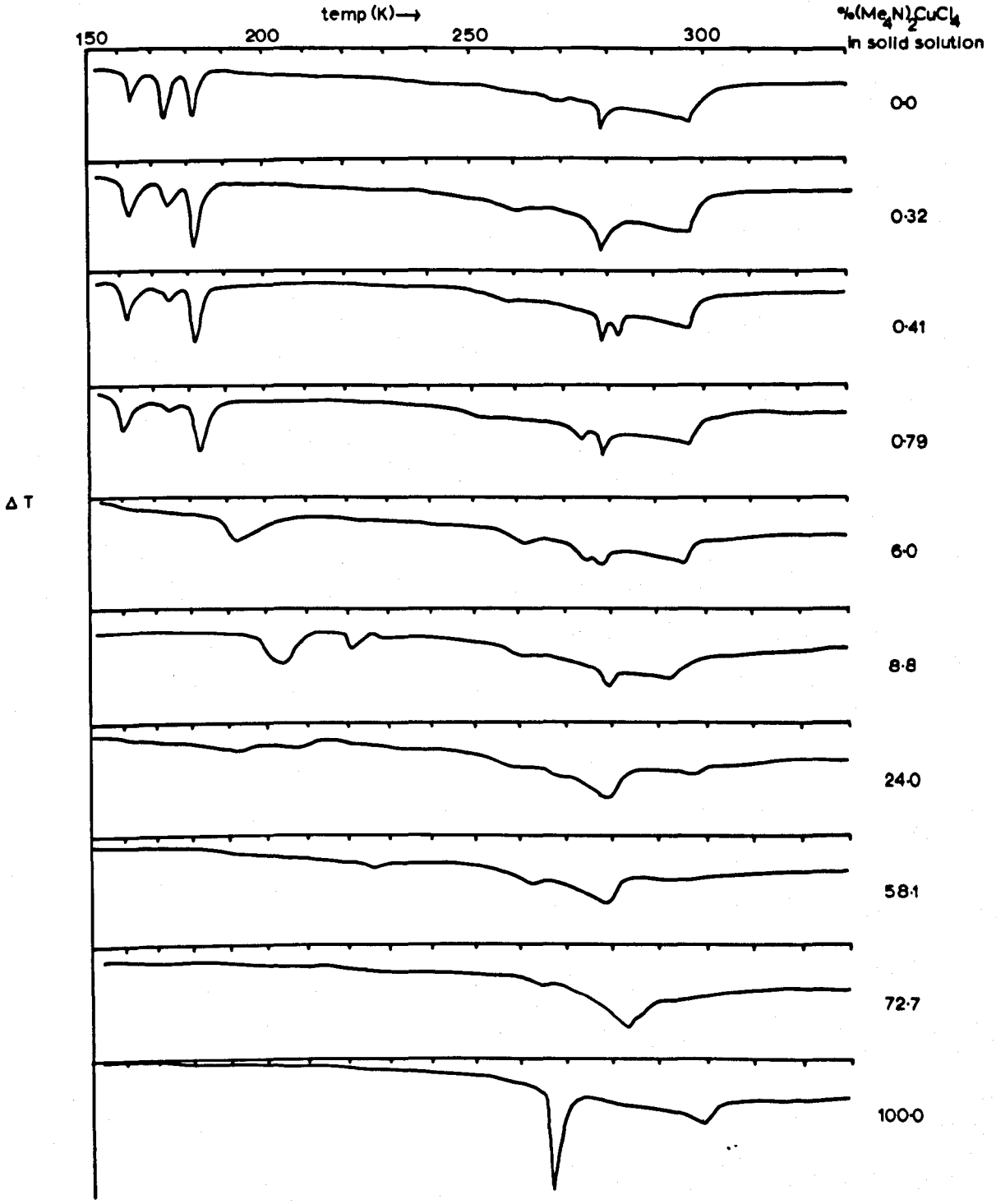

Figure III.7 cont'd

DSC of $(Me_4N)_2(Cu,Co)Cl_4$.

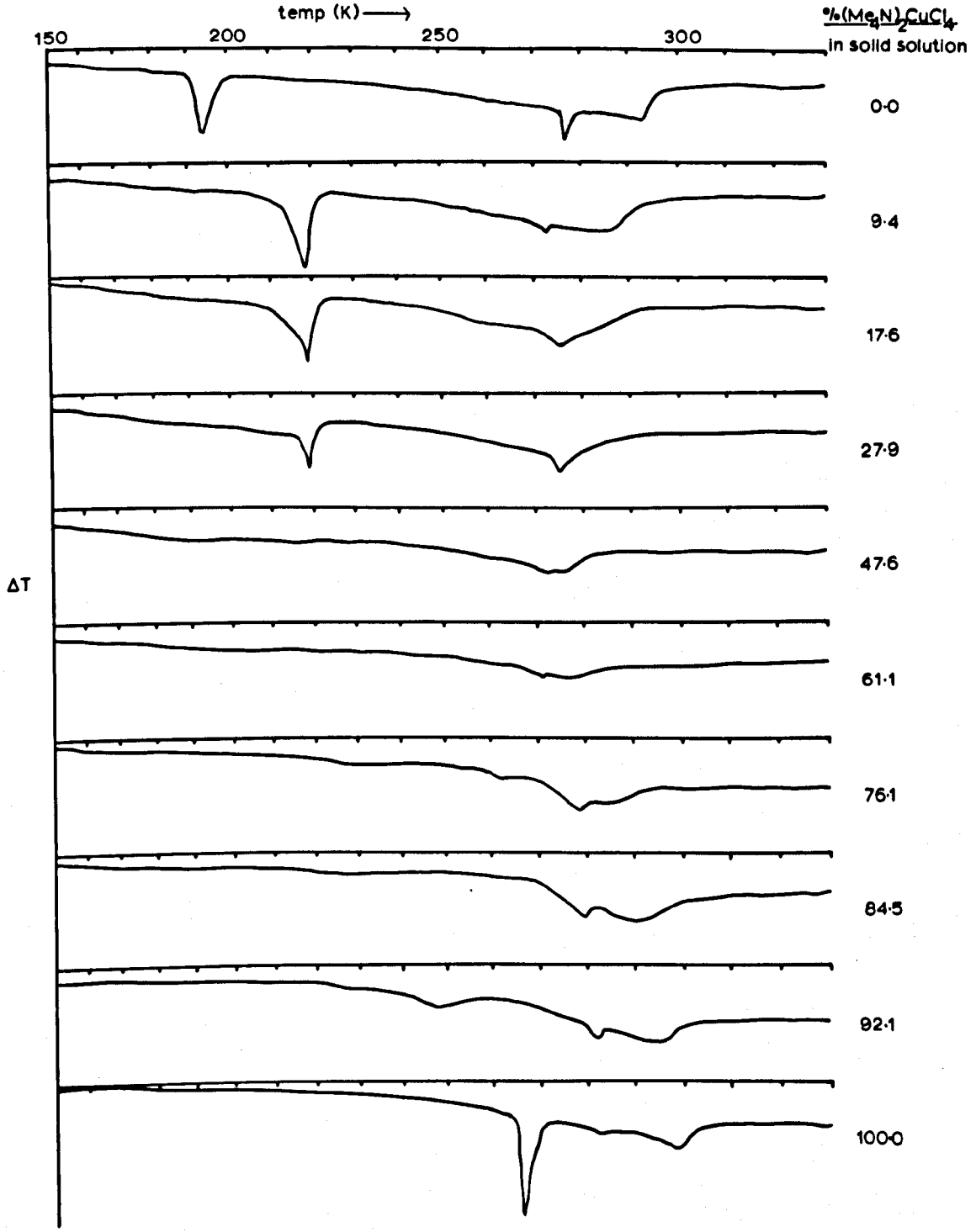

Figure III.8

DSC of mixtures of compounds

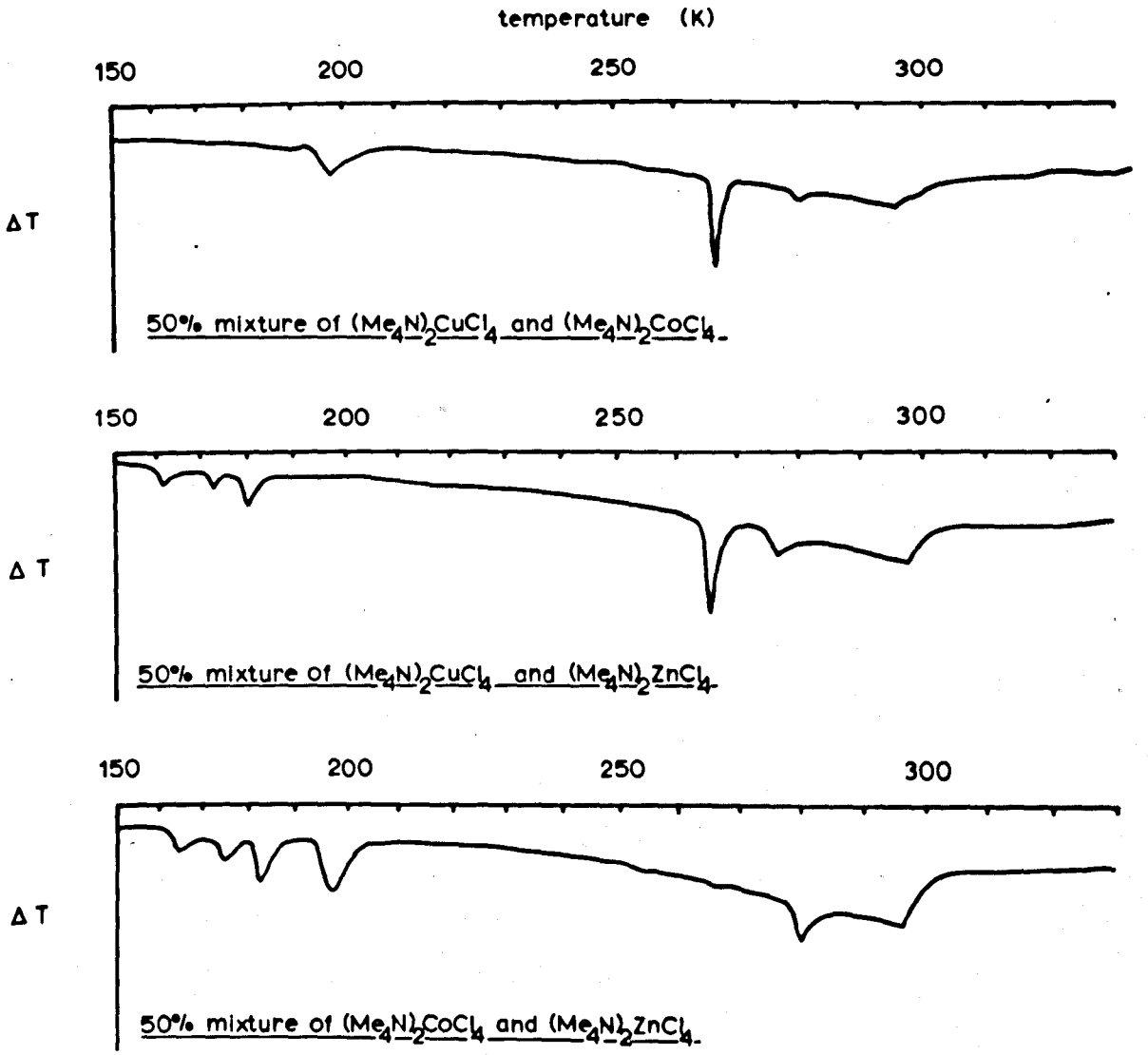

Figure III.9

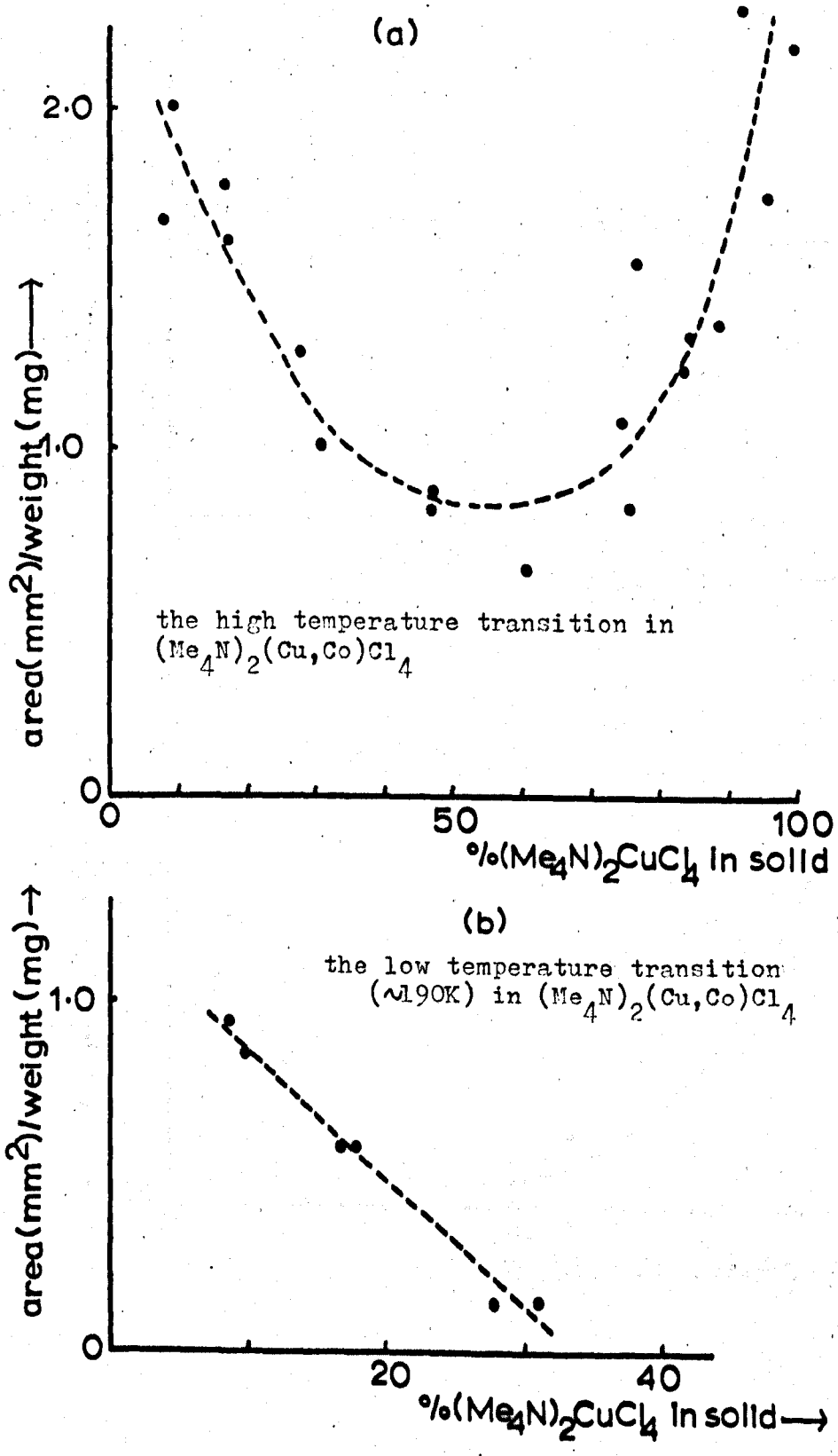
(a)
2·0
1·0
0
area(mm²)/weight (mg) ⟶
the high temperature transition in
(Me4N)2(Cu,Co)Cl4
0
50
100
%(Me4N)2CuCl4 in solid
(b)
the low temperature transition
(~190K) in (Me4N)2(Cu,Co)Cl4
1·0
0
area(mm²)/weight (mg) ⟶
20
40
%(Me4N)2CuCl4 in solid ⟶

Figure III.9 cont'd

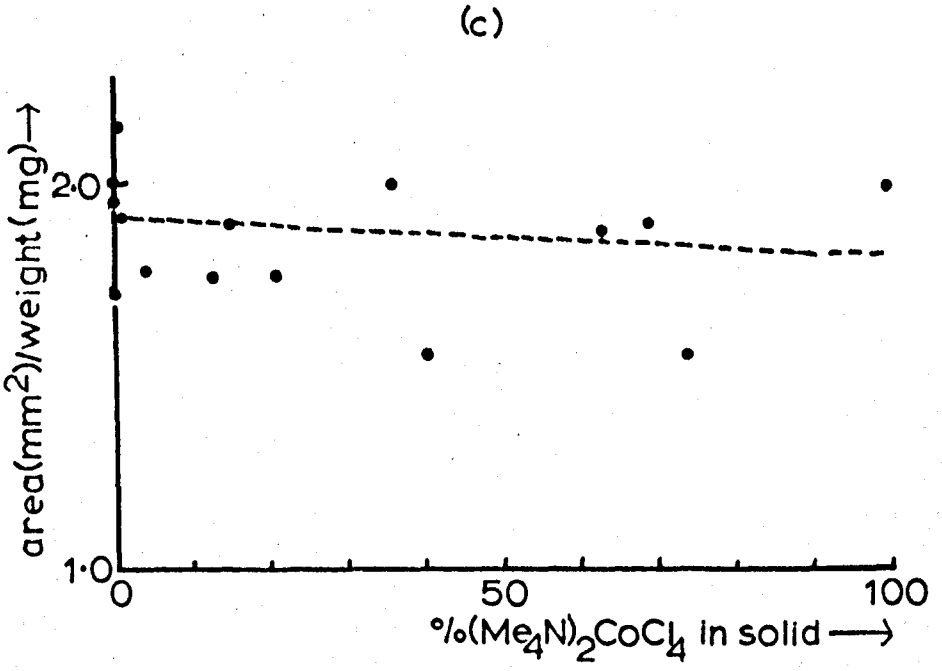

the high temperature transition in $(Me_4N)_2(Co,Zn)Cl_4$

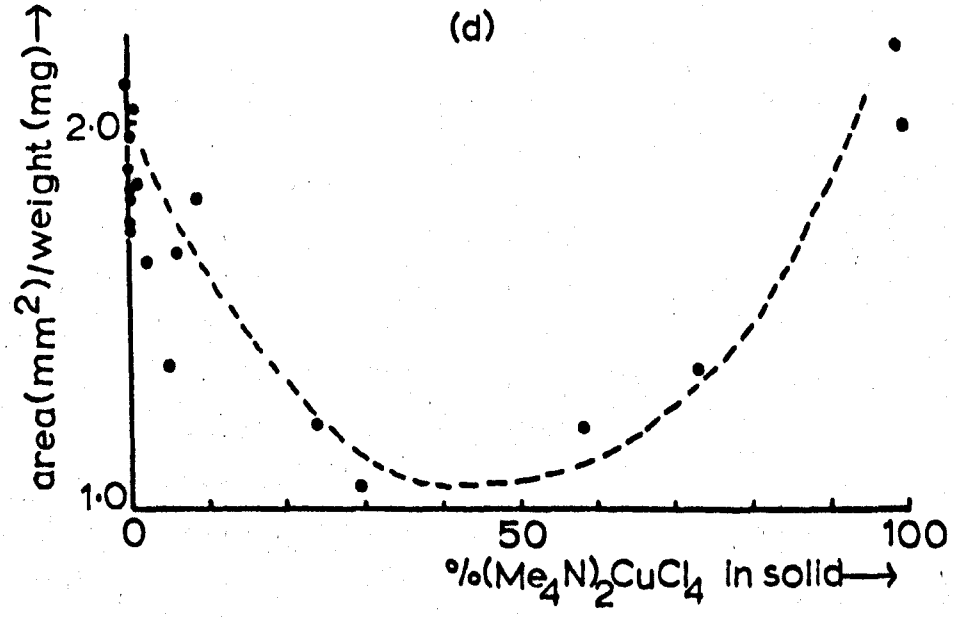

the high temperature transition in $(Me_4N)_2(Cu,Zn)Cl_4$

TABLE III.1

Results of equilibration experiments in the systems $(Me_4N)_2MCl_4$-$(Me_4N)_2M'Cl_4$-solvent

Data given are the weight percentages; for each solvent the three columns are (a) the % of compound (1) in the mother liquor, (b) the % of compound (2) in the mother liquor and (c) the % of compound (1) in the solid solution. Abbreviations used are CU = $(Me_4N)_2CuCl_4$, CO = $(Me_4N)_2CoCl_4$ etc.

WATER			50% ETHANOL-WATER			ETHANOL		
(1) CU-CO system								
CU	CO	CU	CU	CO	CU	CU	CO	CU
5.3	34.1	8.42	4.1	22.6	9.42	.41	.18	6.6
9.5	30.5	17.10	7.0	20.2	17.63	.42	.13	17.17
11.4	29.2	31.06	8.9	18.9	27.85	.44	.14	28.74
13.3	28.5	47.70	10.5	17.3	47.60	.54	.15	43.44
19.6	23.5	77.18	11.8	15.8	61.13	.47	.15	52.89
19.2	23.7	75.01	14.1	13.7	76.08	.66	.13	79.69
25.0	19.5	83.93	18.1	9.8	84.48	.81	.13	88.69
33.3	13.0	89.40	24.2	6.2	92.13			
38.5	7.3	85.93						
(2) CU-ZN system								
CU	ZN	CU	CU	ZN	CU	CU	ZN	CU
3.9	23.9	0.05	1.8	9.9	0.32			
10.0	16.3	0.09	5.3	7.3	0.41			
10.0	15.2	0.10	8.0	4.7	0.79			
15.6	9.8	0.15	14.0	2.3	5.96			
21.1	4.9	0.22	15.5	1.7	8.78			
33.9	2.2	1.74	21.0	1.1	24.02			
37.8	1.1	5.32	21.0	0.8	58.08			
42.3	0.5	29.47	21.5	0.5	72.74			

TABLE III.1 (cont.)

WATER			50% ETHANOL-WATER			ETHANOL		
(3) CO-ZN System								
CO	ZN	CO	CO	ZN	CO	CO	ZN	CO
7.1	19.6	0	5.3	7.1	0.2	.36	0.18	6.4
14.2	12.5	0	10.4	3.8	1.0	.39	0.10	15.9
20.7	7.1	0.05	14.0	2.2	3.8	.48	0.05	25.6
30.2	2.2	0.40	17.7	1.4	12.6	.54	0.03	39.2
34.3	1.6	0.19	19.1	1.2	20.6	.56	0.02	48.3
37.9	1.1	14.6	20.9	0.9	40.4	.59	0.01	64.7
40.9	0.05	69.3	23.8	0.4	74.2	.59	0.004	88.1

CHAPTER IV

THE CRYSTAL STRUCTURES OF $(Me_4N)_2CuCl_4$, $(Me_4N)_2CoCl_4$ and $(Me_4N)_2(Cu,Co)Cl_4$.

THE CRYSTAL STRUCTURES OF $(Me_4N)_2CuCl_4$, $(Me_4N)_2CoCl_4$ and $(Me_4N)_2(Cu,Co)Cl_4$.

The three-dimensional structure of $(Me_4N)_2(Cu,Co)Cl_4$ was determined in order to compare the distortions of the $CuCl_4^{2-}$ and $CoCl_4^{2-}$ ions with those found in $(Me_4N)_2CuCl_4$ and $(Me_4N)_2CoCl_4$. The structure of $(Me_4N)_2CoCl_4$ was already known with reasonable accuracy,[1] and the preliminary work on $(Me_4N)_2CuCl_4$[2] indicated that the two were isomorphous. This work had taken the form of examination of projection data, and had shown $(Me_4N)_2CuCl_4$ to be in the same space group as $(Me_4N)_2CoCl_4$, and with similar atomic coordinates except for a greater degree of distortion of the MCl_4^{2-} ion. A full determination of $(Me_4N)_2CuCl_4$ was therefore necessary for a detailed comparison of the three structures.

All three sets of data (those of $(Me_4N)_2CuCl_4$ and $(Me_4N)_2(Cu,Co)Cl_4$ from the measured intensities, and $(Me_4N)_2CoCl_4$ from the published values of F_{obs}) were treated by the same least-squares refinement procedure. This was done to eliminate slight differences in the weighting schemes used by Wiesner and those available in the CRYSTAL 69[3] programs used here, and to check the abnormally high isotropic temperature factors found for $(Me_4N)_2CoCl_4$. The data collection for $(Me_4N)_2CuCl_4$ and $(Me_4N)_2(Cu,Co)Cl_4$ is described first, followed by the least-squares refinement of all three structures.

Diffraction patterns of $(Me_4N)_2CuCl_4$ and $(Me_4N)_2(Cu,Co)Cl_4$

The appearance of both diffraction patterns was extremely similar. They each had orthorhombic cells with dimensions of about a = 1200, b = 900 and c = 1500 pm, and systematic absences hk0 h = 2n + 1 and 0kℓ k + ℓ = 2n + 1 indicating space groups Pnma or $Pn2_1a$ (as ~~did~~ in $(Me_4N)_2CoCl_4$). Two features are worthy of mention:-

the apparent tripling in length of a in $(Me_4N)_2CuCl_4$ and the streaking shown on both sets of photographs.

The tripling of a in $(Me_4N)_2CuCl_4$ to give an axis about 3600 pm long was noted by Morosin and Lingafelter[2] and confirmed here. The faint reflections indicating this were found on the hk0 net, but not on h0ℓ. They were mainly localized in one area of reciprocal space, and the indices of the strongest of them on hk0 were

	$\ell = 0$	
$0\frac{2}{3}$,2	$0\frac{2}{3}$,4	$3\frac{1}{3}$,4
$1\frac{1}{3}$,2	$1\frac{1}{3}$,4	$4\frac{2}{3}$,4
$0\frac{2}{3}$,3	$2\frac{2}{3}$,4	$2\frac{1}{3}$,5
		$0\frac{2}{3}$,6

This tripling is clearly of some importance in elucidation of the spectral and magnetic properties of $(Me_4N)_2CuCl_4$; for example six magnetically non-equivalent sites for the copper atom have been shown to exist, which is unlikely if the smaller cell is chosen. Morosin and Lingafelter concluded that the structure consisted of three sub cells, each with a = 1200, b = 900, c = 1500 pm, which differed mainly in the coordinates of the nitrogen and carbon atoms. However, the main interest in the present study was in the configuration of the $CuCl_4^{2-}$ tetrahedron and for this purpose the tripling of the axis was ignored.

Examination of hk0, h0ℓ and 0kℓ for $(Me_4N)_2(Cu,Co)Cl_4$ gave no evidence of tripling; nor did any of the higher levels. This was an additional reason for ignoring its existence in $(Me_4N)_2CuCl_4$.

The patterns of the streaks on Weissenberg photographs of $(Me_4N)_2CuCl_4$ and $(Me_4N)_2(Cu,Co)Cl_4$ were not similar. In the case of $(Me_4N)_2CuCl_4$ the streaking was on hk0, parallel to a* (i.e. perpendicular to bc) and was closely associated with the reflections

indicating tripling; that is, mainly on the lines K = 2,4,6 and 10.

In the case of $(Me_4N)_2(Cu,Co)Cl_4$ the strongest streaking was on Okℓ and was parallel to c*. The streaks were not continuous, but were associated with particular reciprocal lattice points, although the streak was sometimes present when the reflection itself was unobserved, but not when the reflection was systematically absent. Weaker streaks parallel to c* were also shown on 1kℓ and 2kℓ. There was also much fainter streaking on hOℓ parallel to both a* and c*. This streaking in $(Me_4N)_2(Cu,Co)Cl_4$ was attributed to the disordered nature of the solid solution. There was no evidence of superlattice formation on hkO, hOℓ or Okℓ, or on any of the higher levels examined.

Data Collection for $(Me_4N)_2(Cu,Co)Cl_4$

A solid solution containing approximately 50% each of $(Me_4N)_2CuCl_4$ and $(Me_4N)_2CoCl_4$ was prepared (51% $(Me_4N)_2CuCl_4$ by atomic absorption analysis). The crystal selected was approximately 0.3 x 0.3 x 0.25 mm. (μ = 18 cm^{-1} (MoK$\bar{\alpha}$)). The cell dimensions found from Weissenberg and oscillation photographs were a = 1230, b = 904, c = 1552 pm.

Data ~~was~~ were collected for layers hOℓ through h5ℓ and Okℓ through 2kℓ using MoK$\bar{\alpha}$ radiation and a multiple-film, multiple-exposure Weissenberg technique. Intensities were estimated visually by comparison with a calibrated strip using a reflection from the same crystal. The transmission coefficient for the film was estimated experimentally (T_o = 1.68) and experimental values were also used for higher layers. Since the generator used was unstabilized, experimental values for the interpack values for the various layers were used; in general these were in reasonable agreement with the exposure times.

After data reduction (which did not include spot-shape or absorption corrections), a scaled and merged set of 667 independent reflections was obtained, and was placed on an absolute scale by the Wilson plot method.

Data Collection for $(Me_4N)_2CuCl_4$

The crystal selected was approximately 0.4 x 0.4 x 0.4 mm. The cell dimensions of a = 1230, b = 903, c = 1519 pm were in agreement with those found by Morosin and Lingafelter. Data was collected for layers $0k\ell$ through $6k\ell$ and $h0\ell$ through $h3\ell$ using a Hilger-Watts linear diffractometer[7] and MoK$\bar{\alpha}$ radiation from a stabilized source. After rejection of all reflections with a peak count less than three times the standard deviation of the total count, Lorentz and polarization corrections were applied. The use of varying oscillation angles on different levels necessitated the determination of interlayer scalefactors; these were in good agreement with the variation in oscillation angle. A scaled and merged set of 670 independent reflections was obtained, and was placed on an absolute scale by the Wilson plot method. No absorption or spot-shape corrections were applied.

Data for $(Me_4N)_2CoCl_4$

Th~~is~~ data ~~was~~ were collected by Wiesner et al using FeKα radiation, an integrating Weissenberg camera and densitometric intensity measurement. Lorentz and polarization, but not absorption, corrections were applied. Interlayer scalefactors for $0k\ell$ through $6k\ell$ were initially obtained from exposure times, and later refined during the least squares procedure. The cell dimensions found were a = 1227.6, b = 900.1, c = 1553.9 pm.

The published values of F_{obs} for this compound (487 non-zero reflections) were used, without alteration of the inter-layer scalefactors.

Least-squares refinement of the three structures

The program used throughout was an adaptation of the ORFLS full-matrix least-squares routines made by Powell and Griffith of Portsmouth Polytechnic.

Since the data for both $(Me_4N)_2CuCl_4$ and $(Me_4N)_2(Cu,Co)Cl_4$ were merged from two axes, individual layer scalefactors were not refined. No systematic discrepancies between F_{obs} and F_{calc} for blocks of reflections to which a particular scalefactor had been applied were apparent at any stage in the refinements. The aim in re-refining $(Me_4N)_2CoCl_4$ was to compare the results with those obtained by Wiesner et al. The anisotropic thermal factors and individual layer scalefactors might not be completely independent, so to minimize differences the layer scalefactors were not refined.

The main feature found by Wiesner et al during refinement of $(Me_4N)_2CoCl_4$ was the unusually high values reached by the isotropic temperature factors, and particularly those of the carbon atoms, the highest of which was about 17×10^4 pm^2. In order to see if this behaviour was reproduced in the present refinement, the initial parameters chosen for refinement were the atom positions found by Wiesner et al together with "reasonable" values for the isotropic temperature factors. The course of the refinement is shown in Table IV.1. During the initial cycles the isotropic temperature factors of some carbon atoms increased rapidly, the highest reaching about 18×10^4 pm^2. The temperature factors were then converted to anisotropic values[8] and refinement continued. The final unweighted R factor for observed reflections was 11.1% i.e. identical to that found by Wiesner. The 315 unobserved reflections of Wiesner were not included at any stage.

The Wiesner positional parameters for $(Me_4N)_2CoCl_4$ were used as a starting point for refinement of $(Me_4N)_2CuCl_4$, together with estimated isotropic temperature factors. Isotropic temperature factors for the copper, chloride and nitrogen atoms were taken from the best values found for $(Me_4N)_2CoCl_4$, and those of the carbon atoms arbitrarily set at 8×10^4 pm^2. The course of the refinement is shown in Table IV.2. The behaviour was similar to that of $(Me_4N)_2CoCl_4$, with large values for the carbon isotropic thermal parameters. There were quite large positional shifts for the chloride ions compared with their positions in $(Me_4N)_2CoCl_4$. The final R factor was 7.5%.

Refinement of $(Me_4N)_2(Cu,Co)Cl_4$ used the same initial parameters as for $(Me_4N)_2CuCl_4$, except that the scattering factor of the metal atom was that of a fictitious average atom with $f = 0.5f_{Cu^{2+}} + 0.5f_{Co^{2+}}$. The MCl_4^{2-} ion refined was an average structure corresponding to the mean of the $CuCl_4^{2-}$ and $CoCl_4^{2-}$ positions. The positional parameters of the MCl_4^{2-} ion were between those of $CuCl_4^{2-}$ and $CoCl_4^{2-}$; the temperature factors tended to be larger than those of either $CuCl_4^{2-}$ or $CoCl_4^{2-}$. A similar situation held for the Me_4N^+ tetrahedra, where there were some quite large positional differences between the light atoms in $(Me_4N)_2CuCl_4$ and $(Me_4N)_2CoCl_4$. With this model the final unweighted R factor was 10.6%.

Since there was no evidence of ordering in the solid solution, the disordered solid solution might be better represented by including both a $CuCl_4^{2-}$ and a $CoCl_4^{2-}$ tetrahedron, each with an occupancy of 0.5. The parameters of all the atoms could be treated in this way, which would exactly double the number of parameters to be refined. Doubling either all the heavy atom parameters, or the parameters of all the atoms in the asymmetric unit would in itself cause a decrease in R. To see if the introduction of additional parameters led to a significant decrease in R, the Hamilton R-factor significance test[4] was employed. If n_1 parameters give R-factor R_1 and n_2 parameters give R_2 $(n_1 < n_2)$, then tables are available to test that r $(= R_1/R_2)$ is significant at levels from 1% to 50%. Extrapolation from these showed that at the 1% significance level $r = 1.105$ for doubling all the parameters and 1.042 for doubling of the heavy atom parameters only. In this case R_1 = ~~10.6~~ 8.9%, so that for a significant improvement in the model at the 1% level $R_2 \leqslant 8.05\%$ for the structure with two complete sets of atoms, and $R_2 \leqslant 8.54\%$ for two sets of heavy atoms only. Both these models were therefore used in the refinement as shown in Table IV.3. For the case where all the parameters were doubled, the final R factor was 8.2%, giving $r = 1.085$.

This is not below the 1% confidence level, but between 5% and 10%. In the case where two sets of heavy atom parameters only were used, the final R factor was ~~also~~ 8.3%, which is well below the 1% confidence level. It would therefore seem that the structure is best described as a random arrangement of $CuCl_4^{2-}$ and $CoCl_4^{2-}$ on the MCl_4^{2-} positions, surrounded by MCl_4^{2-} tetrahedra in average positions.

Structure factors for $(Me_4N)_2CuCl_4$ and $(Me_4N)_2(Cu,Co)Cl_4$ are given in Appendices B and C.

The positional and thermal parameters of $(Me_4N)_2CoCl_4$ obtained by Wiesner (W) and JMR are compared in Table IV.4. Positional and thermal parameters for $(Me_4N)_2CuCl_4$ and $(Me_4N)_2(Cu,Co)Cl_4$ are given in Table IV.5 and IV.6.

On completion of refinement, an F_{obs} map of CuCo was calculated, phased on the structure having two sets of heavy atom parameters and one set of light atom parameters. The electron density sections through the MCl_4^{2-} tetrahedron are shown in Fig. IV.2. The atoms Cu, Co, $Cl(1)_{Cu}$, $Cl(1)_{Co}$, $Cl(3)_{Cu}$, $Cl(3)_{Co}$ are on the mirror plane at $y = \frac{1}{4}$; $Cl(2)_{Cu}$ and $Cl(2)_{Co}$ are at approximately at $y = 15/480$; the positions of these atoms are also shown on Fig. IV.1. The distortion of the average electron density about any particular "atom" due to different atom positions is well illustrated, as is the much greater distortion in the $CuCl_4^{2-}$ than in the $CoCl_4^{2-}$ tetrahedron.

F_{obs} and F_{diff} maps were also calculated for $(Me_4N)_2CuCl_4$ and $(Me_4N)_2CoCl_4$. These showed atoms which were not completely spherical, but were less distorted than those found in $(Me_4N)_2(Cu,Co)Cl_4$. In particular the light atoms were rather diffuse and not well resolved; this is attributed to the large anisotropic thermal parameters found for the carbon atoms.

Comparison of the structures of $(Me_4N)_2CuCl_4$, $(Me_4N)_2CoCl_4$ and $(Me_4N)_2(Cu,Co)Cl_4$

The features which may be compared are the positional and anisotropic thermal parameters, and the bond distances and angles.

Positional parameters. The esd's for $(Me_4N)_2(Cu,Co)Cl_4$ are larger than those for $(Me_4N)_2CuCl_4$ or $(Me_4N)_2CoCl_4$, and are used whenever $(Me_4N)_2(Cu,Co)Cl_4$ is discussed.

(i) parameters for $CoCl_4^{2-}$ obtained by W and JMR. The two sets of parameters are given in Table IV.4. There is only one outstanding difference; that in the x coordinate of C(4), where the positional difference amounts to about 12 pm. The differences in the refinements were that Wiesner included unobserved reflections in the least-squares refinement (but not in calculation of R) and the weighting schemes were slightly different. These two factors may account for the differences in atomic parameters.

(ii) MCl_4^{2-} parameters. The $CuCl_4^{2-}$ parameters of $(Me_4N)_2CuCl_4$ and $(Me_4N)_2(Cu,Co)Cl_4$ are not in complete agreement, but five of the nine parameters are within three e.s.d's. For $CoCl_4^{2-}$ in $(Me_4N)_2CoCl_4$ and $(Me_4N)_2(Cu,Co)Cl_4$, six of the nine parameters are within three e.s.d's.

(iii) light atom parameters. For $(Me_4N)_2CuCl_4$ - $(Me_4N)_2(Cu,Co)Cl_4$ and $(Me_4N)_2CoCl_4$ - $(Me_4N)_2(Cu,Co)Cl_4$ the parameters generally agree within three e.s.d's, but many of those for $(Me_4N)_2CoCl_4$ - $(Me_4N)_2CuCl_4$ are outside those limits. For all parameters except x and z of C(2) and x of C(4) the value for $(Me_4N)_2(Cu,Co)Cl_4$ is between those of $(Me_4N)_2CuCl_4$ and $(Me_4N)_2CoCl_4$.

Anisotropic thermal parameters

(i) parameters for $(Me_4N)_2CoCl_4$ found by Wiesner and JMR. The two sets of parameters are given in Table IV.4. Agreement is generally very good, as is that for the orientations and root mean square displacements of the thermal ellipsoids.

(ii) parameters for all three structures. These are notably larger, in the cases of the chloride and nitrogen atoms, than those normally found for this sort of compound.[5] Fig. IV.2 shows that the values for $(Me_4N)_2CuCl_4$ tend to be larger than those for $(Me_4N)_2CoCl_4$, as do those of $(Me_4N)_2(Cu,Co)Cl_4$; those of $(Me_4N)_2(Cu,Co)Cl_4$ are similar to those of $(Me_4N)_2CuCl_4$. This may be a result of the lack of cross-level scaling data for $(Me_4N)_2CoCl_4$. The anisotropic thermal parameters (B_{11}) and layer scalefactors are then totally degenerate;[6] values of B_{11} may include a scalefactor component, making them unreliable for comparison with $(Me_4N)_2CuCl_4$ and $(Me_4N)_2(Cu,Co)Cl_4$. This effect cannot therefore be attributed to a greater degree of disorder in $(Me_4N)_2CuCl_4$ and $(Me_4N)_2(Cu,Co)Cl_4$ than in $(Me_4N)_2CoCl_4$.

The anisotropic thermal parameters and rms displacements of M,N(1) and N(2) are less than those for the chloride and carbon atoms. This is consistent with rotation or oscillation of the heavy and light atom tetrahedra about their central atoms, as suggested by Wiesner.

Bond lengths and angles

These are given in Tables IV.7, .

(i) $CoCl_4^{2-}$ as determined by Wiesner and JMR. Wiesner quoted distances with and without correction for thermal motion; only those without correction are considered here. The two sets of distances and angles all agree within two e.s.d's.

(ii) $CoCl_4^{2-}$ and $CuCl_4^{2-}$ in the single-metal compounds. The mean bond lengths for the MCl_4^{2-} tetrahedra are close (223 pm for $(Me_4N)_2CuCl_4$, 225 pm for $(Me_4N)_2CoCl_4$), and the chief difference between the two ions is in the degree of distortion. $CoCl_4^{2-}$ is slightly distorted, having two angles greater than 109°28', although only by 3° at most. The $CuCl_4^{2-}$ tetrahedron has angles of 132.1° and 126.6°, as well as four less than 109.5°, i.e. it is quite strongly distorted towards approximate D_{2d} symmetry. The degree of

distortion is similar to that found in $(TMBA)_2CuCl_4$ (Table 1.7); that found in Cs_2CuCl_4 is somewhat smaller. This may be attributable to crystal packing effects due to the greater size of Me_4N^+ and $TMBA^+$.

(iii) $CoCl_4^{2-}$ in $(Me_4N)_2CoCl_4$ and $(Me_4N)_2(Cu,Co)Cl_4$ and $CuCl_4^{2-}$ in $(Me_4N)_2CuCl_4$ and $(Me_4N)_2(Cu,Co)Cl_4$

The bond distances in the two $CoCl_4^{2-}$ ions are similar except that Co-Cl(3) is slightly greater in $(Me_4N)_2(Cu,Co)Cl_4$. The $CoCl_4^{2-}$ tetrahedron is rather more distorted in $(Me_4N)_2(Cu,Co)Cl_4$.

For $CuCl_4^{2-}$, Cu-Cl(1) is greater in $(Me_4N)_2(Cu,Co)Cl_4$ and Cu-Cl(3) is less, but these differences are less than three e.s.d's. The degree of distortion is similar, with Cl(2)-Cu-Cl(2') larger in $(Me_4N)(Cu,Co)Cl_4$ than in $(Me_4N)_2CuCl_4$.

(iv) light atom tetrahedra. In all three compounds these are distorted, but in $(Me_4N)_2CoCl_4$ the C(6)-N(2)-C(6') angle of 129.4° is unlikely to be very reliable. Typically the N-C bond length for a single bond has been found to be about 147 pm; many of the N-C distances in $(Me_4N)_2CuCl_4$ are greater than this, but the reason for this is not known. In general, the accuracy of nitrogen and carbon atom parameters in the presence of heavy atoms is not expected to be very high.

REFERENCES FOR CHAPTER IV

1. Wiesner et al., Acta Cryst. 1967, 23, 565.
2. Morosin & Lingafelter, J.Phys.Chem. 1961, 65, 50.
3. Powell & Griffiths, Portsmouth Polytechnic 1969.
4. Hamilton, Acta Cryst. 1965, 18, 502.
5. Cochran & Lipson, 'The Determination of Crystal Structures", Bell, 1968.
6. Lingafelter, Acta Cryst. 1966, 20, 321.
7. Arndt & Willis, "Single Crystal Diffractometry", Cambridge 1966.

Figure IV.1

b axis projection of the electron density map for the MCl_4^{2-} ion in $(Me_4N)_2(Cu,Co)Cl_4$. The positions of $CoCl_4^{2-}$ in $(Me_4N)_2CoCl_4$ (blue) and $CuCl_4^{2-}$ in $(Me_4N)_2CuCl_4$ (red) are also shown.

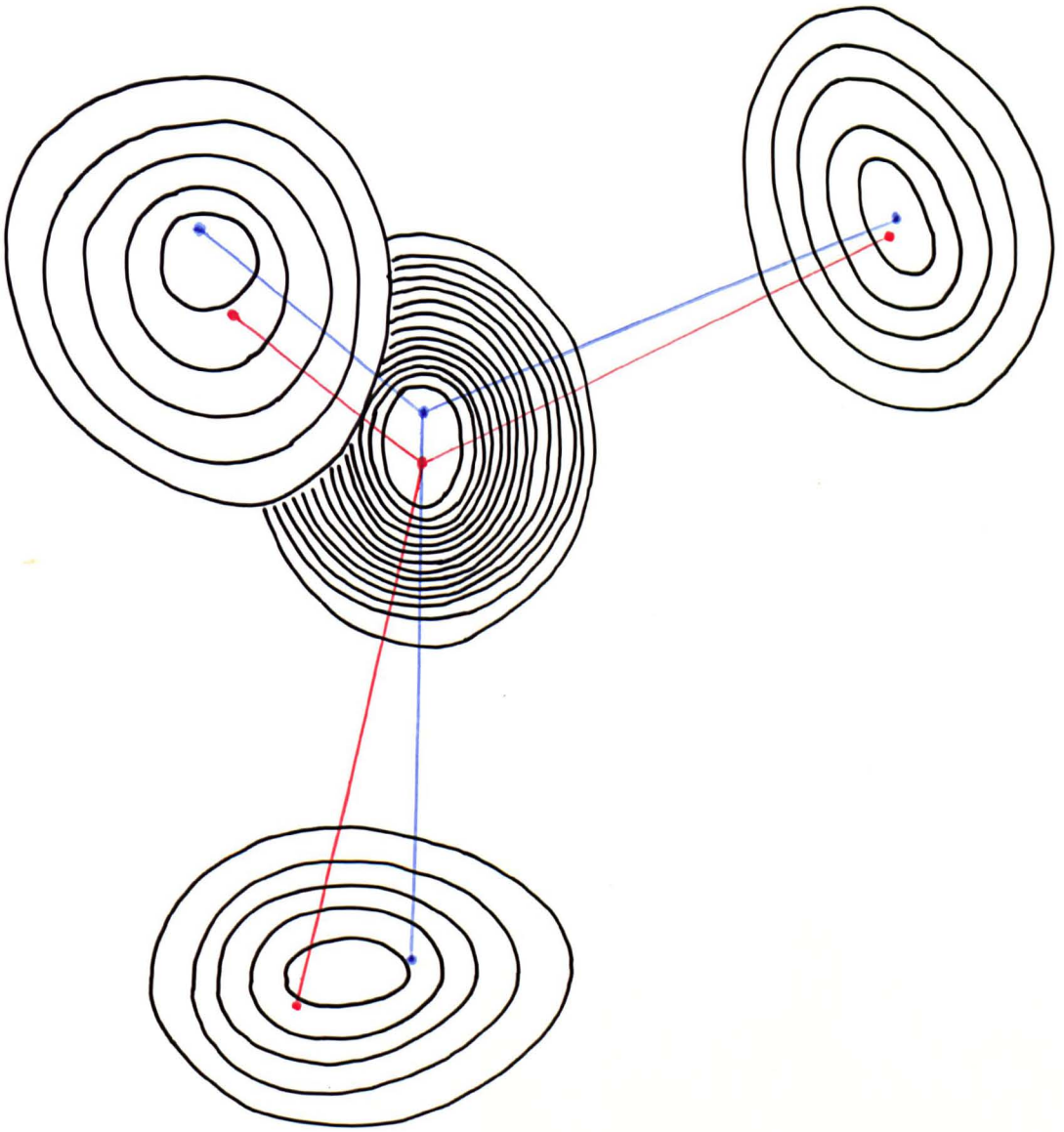

Figure IV.2

Comparison of anisotropic thermal parameters

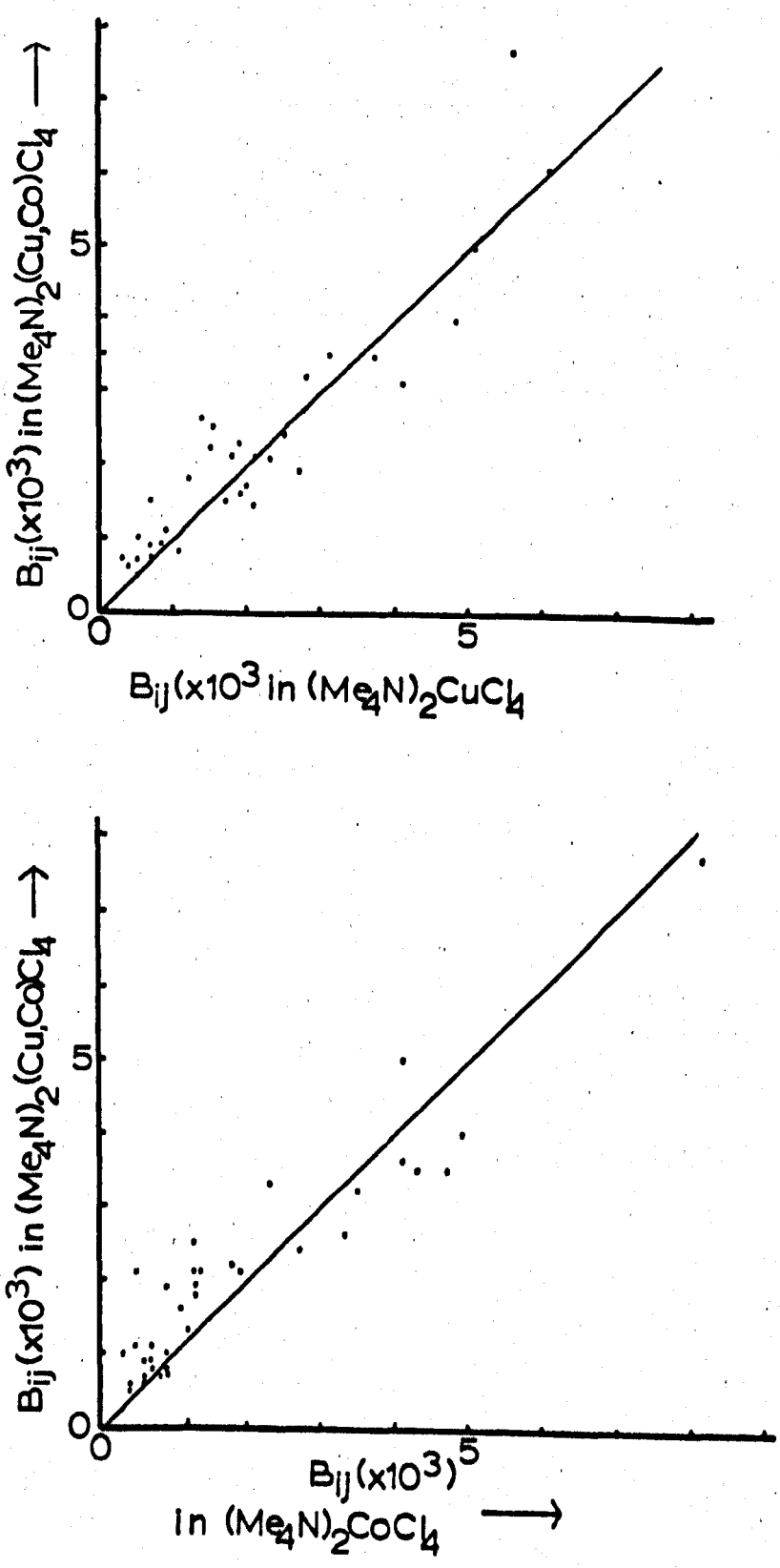

TABLE IV.1

The least-squares refinement of $(Me_4N)_2CoCl_4$

Full-matrix refinement; weighting scheme $w = 1$ for $F < F^*$, $w = \frac{1}{F-\left(\frac{F-F^*}{G^*}\right)^2}$ for $F \geqslant F^*$ (except where table has $F^* = G^* = 0$, when unit weights were applied).

No. of cycles	Parameters refined	F*	G*	$R = \frac{\sum \lvert\lvert Fo\rvert - \lvert Fo\rvert\rvert}{\sum \lvert Fo\rvert}$ for all observed reflections
3	Biso	0	0	21.5%
2	Positions	0	0	21.2
2	Biso	0	0	20.5
5	Bij	40	30	11.3
2	Positions	40	30	11.1
2	Positions, Bij	40	30	11.1

TABLE IV.2

The least-squares refinement of $(Me_4N)_2CuCl_4$

Full-matrix refinement; weighting scheme $w = 1$ for $F < F^*$,

$w = \dfrac{1}{F - \left(\dfrac{F-F^*}{G^*}\right)^2}$ for $F \geqslant F^*$ (except where table has $F^* = G^* = 0$, when unit weights were applied).

No. of cycles	Parameters refined	F^*	G^*	$R = \dfrac{\sum \lvert \lvert F_o \rvert - \lvert F_c \rvert \rvert}{\sum \lvert F_o \rvert}$ for all observed reflections
4	Positional, Biso	0	0	17.3%
2	Positional, Biso	25	50	16.1
2	Bij	25	50	8.1
2	Positional, Bij	25	50	7.5
1	Positional, Bij	25	50	7.5

TABLE IV.3

The least-squares refinement of $(Me_4N)_2(Cu,Co)Cl_4$

Full matrix refinement; weighting scheme $w = 1$ for $F < F^*$,

$w = \frac{1}{F-\left(\frac{F-F^*}{G^*}\right)^2}$ for $F \geq F^*$ (except where table has $F^* = G^* = 0$, when unit weights were applied).

No. of cycles	Parameters refined	F^*	G^*	$R = \frac{\sum\|\|F_o\|-\|F_c\|\|}{\sum\|F_o\|}$ for all observed reflections
(I) Refinement of the average set of atoms				
2	Positions, Biso	0	0	25%
1	Positions, Biso	40	35	22.5
2	Positions	25	50	16.7
2	Biso	25	60	16.0
1	Bij	25	60	12.5

(II) At this stage three sets of parameters were used independent for refinement, as explained in the text:

(a) an average set of atoms

(b) two complete sets of parameters, one taken from $(Me_4N)_2CuCl_4$ and one from $(Me_4N)_2CoCl_4$, each with occupation numbers of 0.5.

(c) metal and chlorine atom parameters as in (b), light atom parameters as in (a).

TABLE IV.3 (continued)

No. of cycles	Parameters refined	F*	G*	$R = \frac{\sum \| \|F_o\| - \|F_c\| \|}{\sum \|F_o\|}$
(a)				
4	Positions, Bij	25	60	9.0
2	Positions, Bij	25	60	8.9
2	Positions, Bij	25	60	8.9
(b)				
4	Positions, Bij	25	60	8.9
2	Positions, Bij	25	60	8.3
(c)				
2	Positions, Bij	25	60	9.6
2	Positions, Bij	25	60	8.2
2	Positions, Bij	25	60	8.2

Table IV.4

Atomic parameters for $(Me_4N)_2CoCl_4$. The values given are those found by Wiesner et al (W) and in the present study (JMR).

(a) Positional parameters ($x10^4$).

ATOM	W	JMR	ESD	ATOM	W	JMR	ESD
CO	2447	2448	(4)	C(1)	2614	2614	(34)
	2500*	2500*			2500*	2500*	
	4070	4069	(3)		992	991	(28)
CL(1)	631	628	(3)	C(2)	1118	1123	(35)
	2500*	2500*			2500*	2500*	
	4055	4056	(7)		43	47	(32)
CL(2)	3145	3037	(6)	C(3)	1103	1122	(45)
	432	438	(8)		3737	3718	(47)
	3386	3386	(5)		1430	1444	(28)
CL(3)	3145	3140	(9)	C(4)	4370	4288	(52)
	2500*	2500*			2500*	2500*	
	5400	5420	(6)		7378	7389	(34)
N(1)	1515	1522	(22)	C(5)	4117	4092	(43)
	2500*	2500*			2500*	2500*	
	960	945	(16)		8943	8925	(30)
N(2)	4936	4936	(20)	C(6)	5404	5404	(47)
	2500*	2500*			3906	3947	(52)
	8269	8255	(16)		8434	8437	(26)

* REQUIRED BY SYMMETRY TO BE EXACTLY 0.2500, THEREFORE ESD IS ZERO.

Table IV.4 cont'd

(b) Anisotropic thermal parameters ($\times 10^3$). B_{11} etc are coefficients in the expression for the anisotropic temperature factor

$$\exp\{-(B_{11}h^2+B_{22}k^2+B_{33}\ell^2+2B_{12}hk+2B_{13}h\ell+2B_{23}k\ell)\}$$

ATOM	B	W	JMR	ESD	ATOM	B	W	JMR	ESD
CO*	11	8.01	7.50	(0.6)	C(1)*	11	5.36	2.70	(5.1)
	22	13.30	13.12	(0.6)		22	72.21	48.95	(11.7)
	33	4.09	3.90	(0.2)		33	8.86	10.51	(2.9)
	13	0.04	0.14	(0.3)		13	-1.04	-4.18	(3.3)
CL(1)*	11	6.98	7.15	(1.2)	C(2)*	11	3.80	4.67	(5.4)
	22	22.99	23.09	(1.7)		22	97.61	82.42	(19.9)
	33	7.34	7.22	(0.6)		33	9.01	8.89	(2.8)
	13	0.56	0.07	(0.7)		13	3.17	4.91	(2.9)
CL(2)	11	11.89	12.07	(0.8)	C(3)	11	28.03	27.21	(5.9)
	22	18.86	18.78	(1.1)		22	36.85	35.45	(8.0)
	33	9.13	8.78	(0.4)		33	19.88	17.62	(3.6)
	12	3.26	3.19	(0.7)		12	12.80	4.55	(5.4)
	13	0.72	0.48	(0.5)		13	-1.08	-2.47	(3.7)
	23	-3.24	-3.46	(0.7)		23	-13.07	-11.42	(5.2)
CL(3)*	11	13.73	12.91	(1.5)	C(4)*	11	21.88	33.27	(9.7)
	22	43.42	41.35	(2.8)		22	41.38	41.23	(12.1)
	33	4.42	4.45	(0.5)		33	9.40	9.33	(3.2)
	13	-2.32	-2.24	(0.6)		13	-5.77	-12.46	(4.4)
N(1)*	11	8.71	6.28	(0.3)	C(5)*	11	10.90	14.45	(6.8)
	22	10.18	8.60	(0.3)		22	78.04	75.97	(20.1)
	33	5.14	5.73	(1.3)		33	11.09	7.76	(3.2)
	13	-1.93	-3.08	(2.1)		13	4.65	3.88	(3.5)
N(2)*	11	6.69	4.73	(0.3)	C(6)	11	43.72	42.90	(9.4)
	22	11.02	12.75	(0.4)		22	46.04	47.07	(10.4)
	33	6.18	6.49	(1.6)		33	11.37	12.69	(2.8)
	13	-0.84	-1.00	(1.7)		12	-23.34	-25.96	(8.2)
						13	-7.63	-7.84	(4.3)
						23	2.22	0.22	(5.5)

*B(12) AND B(23) REQUIRED BY SYMMETRY TO BE ZERO

Table IV.5

Atomic parameters for $(Me_4N)_2CuCl_4$.

(a) Positional parameters ($x10^4$).

ATOM	X	Y	Z
CU	2258 (2)	2500 *	4032 (1)
CL 1	467 (4)	2500 *	3689 (4)
CL 2	2736 (4)	315 (5)	3503 (4)
CL 3	3127 (5)	2500 *	5315 (3)
N 1	1305 (11)	2500 *	920 (9)
N 2	5112 (11)	2500 *	8301 (8)
C 1	2535 (15)	2500 *	1106 (21)
C 2	1130 (23)	2500 *	-56 (12)
C 3	814 (19)	3850 (21)	1322 (12)
C 4	4331 (22)	2500 *	7503 (17)
C 5	4465 (28)	2500 *	9085 (24)
C 6	5744 (21)	3859 (25)	8376 (14)

* REQUIRED BY SYMMETRY TO BE EXACTLY 2500, THEREFORE ESD IS ZERO.

Table IV.5 cont'd

(b) Anisotropic thermal parameters ($x10^3$). The expression for the anisotropic temperature factor is given in Table IV.4.

ATOM	B		ESD	ATOM	B		ESD
CU*	11	7.8	(0.2)	C1*	11	5.1	(2.2)
	22	21.0	(0.4)		22	48.1	(8.0)
	33	5.0	(0.1)		33	19.2	(2.8)
	13	0.0	(0.1)		13	-2.8	(1.3)
CL1*	11	7.6	(0.4)	C2*	11	21.1	(3.2)
	22	41.2	(1.6)		22	56.4	(7.8)
	33	8.3	(0.3)		33	3.4	(0.9)
	13	-0.6	(0.3)		13	-2.0	(1.4)
CL2	11	17.4	(0.5)	C3	11	24.6	(3.0)
	22	20.1	(0.8)		22	27.9	(3.8)
	33	17.8	(0.4)		33	15.0	(1.6)
	12	3.1	(0.6)		12	11.8	(2.9)
	13	-4.8	(0.4)		13	4.6	(1.7)
	23	-3.0	(0.5)		23	-8.0	(2.2)
CL3*	11	12.5	(0.6)	C4*	11	14.4	(2.9)
	22	61.2	(2.3)		22	50.8	(7.6)
	33	5.3	(0.3)		33	10.9	(1.6)
	13	-1.8	(0.3)		13	-6.1	(1.9)
N1*	11	7.4	(1.2)	C5*	11	18.4	(3.8)
	22	27.0	(3.2)		22	77.8	(13.9)
	33	5.1	(0.7)		33	15.5	(2.6)
	13	0.2	(0.8)		13	7.6	(2.8)
N2*	11	8.9	(1.4)	C6	11	31.4	(3.7)
	22	23.2	(2.9)		22	36.9	(4.6)
	33	3.6	(0.7)		33	15.1	(1.6)
	13	0.3	(0.7)		12	-19.3	(3.5)
					13	-8.6	(2.1)
					23	8.3	(2.49

* B12 AND B23 REQUIRED BY SYMMETRY TO BE ZERO.

Table IV.6

Atomic parameters for $(Me_4N)_2(Cu,Co)Cl_4$.

POSITIONAL PARAMETERS ($x10^4$)

ATOM	X	Y	Z
CO	2424 (4)	2500 *	4064 (3)
CL1	597 (10)	2500 *	4016 (12)
CL2	3019 (10)	431 (12)	3402 (7)
CL3	3134 (13)	2500 *	5451 (9)
CU	2315 (4)	2500 *	4038 (3)
CL1	513 (11)	2500 *	3702 (12)
CL2	2735 (11)	271 (13)	3556 (10)
CL3	3123 (13)	2500 *	5301 (10)
N1	1406 (11)	2500 *	936 (10)
N2	5019 (13)	2500 *	8279 (10)
C1	2592 (18)	2500 *	1050 (19)
C2	1122 (26)	2500 *	23 (18)
C3	957 (19)	3805 (26)	1399 (16)
C4	4380 (27)	2500 *	7476 (18)
C5	4306 (28)	2500 *	9018 (18)
C6	5626 (23)	3867 (30)	8367 (19)

* REQUIRED BY SYMMETRY TO BE EXACTLY 2500, THEREFORE ESD IS ZERO.

ANISOTROPIC THERMAL PARAMETERS ($x10^3$)

ATOM	B		ESD	ATOM	B		ESD
CO *	11	9.3	(0.5)	CU *	11	7.3	(0.4)
	22	16.6	(0.9)		22	14.6	(0.7)
	33	5.7	(0.3)		33	5.1	(0.2)
	13	0.2	(0.3)		13	0.0	(0.3)
CL1*	11	7.8	(0.8)	CL1*	11	9.1	(0.9)
	22	32.8	(3.0)		22	31.3	(3.0)
	33	10.8	(1.1)		33	8.7	(0.9)
	13	-0.6	(0.9)		13	-1.1	(0.7)
CL2	11	13.1	(0.9)	CL2	11	15.0	(1.3)
	22	21.0	(1.7)		22	16.9	(1.8)
	33	10.1	(0.5)		33	22.5	(1.3)
	12	3.1	(1.1)		12	3.9	(1.3)
	13	2.4	(0.5)		13	-4.1	(1.1)
	23	-5.7	(0.8)		23	-4.8	(1.2)

Table IV.6 cont'd

ATOM	B		ESD	ATOM	B		ESD
CL3*	11	18.9	(1.6)	CL3*	11	17.6	(1.4)
	22	36.4	(3.1)		22	61.4	(4.9)
	33	5.4	(0.7)		33	4.8	(0.7)
	13	-2.1	(0.8)		13	-3.0	(0.8)
N1*	11	8.5	(1.1)	C3	11	23.5	(2.7)
	22	19.2	(3.0)		22	31.7	(4.8)
	33	6.5	(0.8)		33	21.9	(2.2)
	13	2.4	(0.9)		12	10.0	(2.9)
					13	3.7	(1.9)
N2*	11	11.2	(1.5)		23	-15.4	(3.0)
	22	21.1	(3.4)				
	33	6.0	(0.9)	C4*	11	26.1	(4.1)
	13	0.1	(1.0)		22	50.2	(8.4)
					33	8.1	(1.4)
C1*	11	9.9	(2.1)		13	-6.5	(2.1)
	22	40.0	(7.4)				
	33	15.9	(2.3)	C5*	11	21.0	(3.9)
	13	-2.4	(1.9)		22	113.0	(19.0)
					33	6.8	(1.6)
C2*	11	20.8	(3.7)		13	0.0	(2.1)
	22	76.8	(12.7)				
	33	7.5	(1.5)	C6	11	35.3	(4.1)
	13	-4.2	(2.0)		22	35.3	(5.7)
					33	24.9	(2.6)
					12	-24.9	(4.2)
					13	-13.0	(2.8)
					23	11.6	(3.3)

* B12 AND B23 REQUIRED BY SYMMETRY TO BE ZERO.

The expression for the anisotropic temperature factor is given in Table IV.4.

Table IV.7

Bond distances (pm) and angles in $(Me_4N)_2MCl_4$.

CU = $(Me_4N)_2CuCl_4$ etc.

	CU	CO	CUCO
CO-CL(1)		224(1)	224(1)
CO-CL(2)		225(1)	225(1)
CO-CL(3)		227(1)	233(1)
CU-CL(1)	225(1)		228(1)
CU-CL(2)	221(1)		221(1)
CU-CL(3)	223(1)		221(1)
N(1)-C(1)	154(3)	135(3)	147(3)
N(1)-C(2)	151(1)	147(2)	145(1)
N(1)-C(3)	151(4)	148(7)	150(3)
N(2)-C(4)	155(2)	158(4)	148(2)
N(2)-C(5)	145(2)	147(5)	146(3)
N(2)-C(6)	146(2)	144(4)	147(2)
CL(1)-CO-CL(2)		108.3(0.5)	107.9(0.5)
CL(1)-CO-CL(3)		112.6(0.4)	114.0(0.4)
CL(2)-CO-CL(2′)		110.8(0.5)	112.3(0.5)
CL(2)-CO-CL(3)		108.5(0.3)	107.6(0.4)
CL(1)-CU-CL(2)	101.1(0.3)		98.1(0.5)
CL(1)-CU-CL(3)	132.1(0.2)		130.1(0.4)
CL(2)-CU-CL(2′)	126.6(0.3)		131.8(0.5)
CL(2)-CU-CL(3)	100.8(0.2)		101.2(0.4)
C(1)-N(1)-C(2)	108.2(1.4)	112.4(2.1)	111.1(1.5)
C(1)-N(1)-C(3)	108.5(1.4)	106.2(2.9)	107.5(1.4)
C(2)-N(1)-C(3)	109.9(1.7)	113.1(3.0)	112.7(1.8)
C(3)-N(1)-C(3′)	106.6(1.5)	95.7(2.5)	105.1(1.6)
C(4)-N(2)-C(5)	107.7(1.8)	105.9(3.4)	111.1(2.0)
C(4)-N(2)-C(6)	113.5(0.9)	110.7(1.9)	110.5(1.4)
C(5)-N(2)-C(6)	103.3(1.1)	97.9(2.1)	103.9(1.2)
C(6)-N(2)-C(6′)	114.3(1.3)	129.4(2.6)	116.4(1.3)

CHAPTER V

THE FORMATION OF SOLID SOLUTIONS

SOLID SOLUTIONS

This chapter is restricted to a consideration of the formation of solid solutions in systems of one solvent plus two salts having a common ion. This is only a small part of the general field of solid solutions, which also covers alloy formation and formation of solid solutions from melts of salts or organic compounds.

The possibility of solid solution formation has been realized for many years; Beudant[1] in 1818 spoke of a "mélange chimique" in this context. The Law of Isomorphism was stated in 1819, and in 1889 Retgers considered the formation of mixed crystals as a test for isomorphism. Early X-ray work[2] on solid solutions was concerned with the variation of cell dimensions with composition (Végard's Law) and the detection of ordering in the crystals.

The formation of solid solutions of inorganic salts from aqueous solution is of some interest not only to chemists, but also in the understanding of various geological phenomena. The Stassfurt salt deposits[3] are an outstanding example of this. They were formed from complex systems of Mg^{2+}, K^{+}, Na^{+}, Ca^{++}, Cl^{-}, SO_4^{2-} and water, and in order to understand the order of their deposition, their solubility relationships and solid solution formation have been examined over a range of temperatures and pressures.

If, in a system of two salts and water, constant temperature is assumed, there are two possible mechanisms by which solid solutions can be prepared:-

(1) Evaporation of water from a non-saturated solution. This case may be treated for conditions where the solid is not in equilibrium with the solution or where evaporation is so slow that at any stage the surface of the solid may be considered to be in equilibrium with

the solution. These two situations have been described algebraically[4] in terms of the composition of the solid during fractional crystallization. They are not important here because the product in either case consists of non-homogeneous particles of solid solution, which are not useful for studying the variation of physical properties with composition.

(2) The system containing both solid and saturated solution is allowed to attain equilibrium at constant temperature. In the following discussion attainment of this type of equilibrium is always essential.

The types of solid solution formed by salts 1 and 2 having a common ion in water were classified by Roozeboom.[5] The basis of this classification is a plot of mole fraction of salt 1 in the solute (y) against mole fraction of salt 1 in the solid (x), where salt 1 is the more soluble salt. The five types of behaviour found are shown as Roozeboom plots in Fig.V 1(a) and the ternary phase diagrams corresponding to them are shown in Fig.V 1(b). Actual examples of each type are listed below.

Type I	(6)	$KH_2AsO_4 - KH_2PO_4 - H_2O$	
	(7)	$(NH_4)_2SO_4 - K_2SO_4 - H_2O$	Fig.V.2
	(8)	$K_2CrO_4 - K_2SO_4 - H_2O$	Fig.V.3
Type II	(9)	$KBr - KCl - H_2O$	Fig.V.4
Type III	(10)	$PbBr_2 - PbCl_2 - H_2O$	Fig.V.5
Type IV	(11)	$NH_4Cl - KCl - H_2O$	
	(12)	$KClO_3 - TlClO_3 - H_2O$	Fig.V.6
	(13)	$KMnO_4 - RbMnO_4 - H_2O$	Fig.V.7
Type V	(14)	$K_2CuCl_4.2H_2O - (NH_4)_2CuCl_4.2H_2O - H_2O$	
	(15)	$KSO_3.NH_2 - NH_4SO_3NH_2 - H_2O$	Fig.V.8

Two other types of Roozeboom diagram might be expected to exist, namely

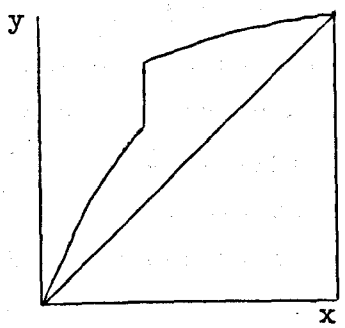

and

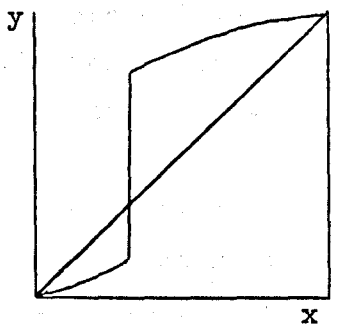

These are theoretically possible, but require that two solutions of different composition are in equilibrium (and also immiscible). This state of affairs is extremely improbable in the case of aqueous solutions, but its existence cannot be ruled out for a system of organic compounds in non-aqueous solvents, although it is still very unlikely.

The classification treats those cases where only one series of solid solutions is formed, and in which the degree of hydration remains constant throughout. Other more complicated examples are known with two or three solid solution phases, differing degrees of hydration and even two distinct continuous series of solid solutions ($CuSO_4$-$MnSO_4$-H_2O[16], where both pentahydrated (triclinic) and heptahydrated (monoclinic) solid solution series are found).

Attempts have been made to interpret these observations, e.g. by Fock.[17] There appears to be no recent treatment of exactly the situation in question, and the most helpful treatment is that of Hill, Durham and Ricci[18] (HDR), which is discussed in some detail. HDR were responsible for some accurate data on systems such as the alums and picromerites, and some of their examples are used to illustrate their treatment.

HDR derived from thermodynamic considerations a relationship between the mole ratio (salt 1/salt 2) in the liquid and solid phases, and the aqueous molar solubilities of the two salts. They then compare this with an empirical equation obtained for alum and picromerite systems. Their treatment is only applicable to those Roozeboom classes in whichthe x-y curves are continuous, i.e. Types I, II and III.

In a system of two phases, the condition for equilibrium is that the chemical potential of each component must be the same in the two phases. If the formulae of the two salts involved are B_bC_c (salt 1) and B'_bC_c (salt 2) they form a series of solid solutions by exchange of B and B'.

At equilibrium $(a_B^b\, a_C^c)_\ell = Ka_1\, (a_B^b\, a_C^c)_s$ and (1)

$$(a_{B'}^b\, a_C^c)_\ell = Ka_2\, (a_{B'}^b\, a_C^c)_s \ , \qquad (2)$$

where Ka is the activity product constant of the salt.
The salts differ only by containing B or B' so that if (1) is divided by (2) the activities of the other components will cancel and hence

$$(a_B/a_{B'})_\ell^b = (Ka_1/Ka_2)(a_B/a_{B'})_s^b \ . \qquad (3)$$

If R_ℓ, R_s are the mole ratios [B]/[B'] in the liquid and solid phases, then in terms of activity coefficients

$$R_\ell (f_B/f_{B'})_\ell = (Ka_1/Ka_2)^{1/b}.R_s.(f_B/f_{B'})_s \ . \qquad (4)$$

It is assumed that for very similar ions, if the total ionic strength in the solutions remains approximately constant , $(f_B/f_{B'})_\ell = 1$. From this,

$$R_\ell = K.R_s.(f_B/f_{B'})_s \ , \qquad (5)$$

where $K = (Ka_1/Ka_2)^{1/b}$.

Equation (5) is the HDR "theoretical" equation for the distribution ratio R_l/R_s.

K can be related to the aqueous molar solubilities by

$$K = (Ka_1/Ka_2)^{1/b} = (S_1 f_1^o / S_2 f_2^o)^{\nu/b} , \qquad (6)$$

where S is the aqueous molar solubility, f^o is the mean ionic activity coefficient at saturation and ν is the total number of ions formed from one molecule of electrolyte.

HDR used experimental results to show the relationship between the mean ionic activity coefficient and ionic strength for the type of solutions they had examined was expressed by

$$f = A + B/\sqrt{\mu} ,$$

in which A was very small and B was similar for all the salts used, so that

$$f_1^o/f_2^o = \sqrt{\mu_2}/\sqrt{\mu_1} = \sqrt{S_2}/\sqrt{S_1} ,$$

and therefore

$$K \approx (S_1/S_2)^{\nu/2b} . \qquad (7)$$

This enables the value of K calculated from equation (7) to be compared with that calculated from equation (5), assuming that the solid solutions are sufficiently ideal for $(f_B/f_{B'})_s \approx 1$.

The most useful form of (5) with the above assumption is

$$\text{Log } R_l = \text{LogK} + \text{Log } R_s . \qquad (8)$$

HDR examined plots of Log R_l vs Log R_s for some alums and picromerites and found that the slope (m) was 1 for alums and Log R_l(Log R_s = 0) = Log K; while for the picromerites straight line plots were obtained with $m < 1$, i.e. obeying the empirical relation

$$\text{Log } R_l = \text{LogK} + m \text{ Log } R_s . \qquad (9)$$

It was then postulated that the appearance of m in equation (9) could be attributed to deviations of $(f_1/f_2)_s$ from unity. Comparison of (9) with (5) gives

$$(f_B/f_{B'})_s = R_s^{m-1} . \qquad (10)$$

With m = 1 the system belongs to Roozeboom type 1, m < 1 gives Type II and m > 1 gives Type III.

The systems examined by HDR obeyed their empirical equation fairly well, as illustrated by the plots of Log R_ℓ vs Log R_s shown in Fig.V.9 which were taken from their data. However their empirical equation is not an accurate representation for many other systems for which data are available; examples are shown in Fig.V.10, and are taken from the systems whose Roozeboom plots were given in Figs.V.2-8. Reasons for this are not fully understood, but are indications of some form of deviation from ideality.

Combining equations (4) and (6),

$$R_\ell.(f_B/f_{B'})_\ell = (S_1 f_1^\circ / S_2 f_2^\circ)^{\nu/b} (f_B/f_{B'})_s \cdot R_s . \qquad (11)$$

This equation contains all the parameters whose variations could lead to non-ideality in the systems. Now S, f_1°, b, ν are constants, and therefore variations in $(f_B/f_{B'})_s$ and $(f_B/f_{B'})_\ell$ must account for any deviations.

In general, whatever the exact form of the relationship, if $(f_B/f_{B'})_\ell$ is not constant it would be expected to vary monotonically with concentration. This would give a non-linear plot of R_ℓ vs R_s; there is no reason why $(f_B/f_{B'})_\ell$ should ever approximate to 1.

The variation of $(f_B/f_{B'})_s$, however, will be dependent on the properties of the lattice. If there is a small concentration of B' in a lattice containing mainly B, then the lattice will be only slightly altered from that of pure BC and vice-versa. In intermediate concentrations greater distortion of the lattice is expected. This will be particularly important in cases where the two salts BC and B'C are not exactly isostructural. A situation is therefore produced in which the behaviour of the solid solution approaches ideality at the extremities of the composition range, and deviates from ideality in the intermediate range.

It is suggested that variations of $(f_B/f_{B'})_s$ are predominant in determining the form of those HDR curves where $m \neq 1$ and is not constant. The HDR plot would then have the form shown in Fig.V.11. Experimental results often do not cover the whole range of Fig.V.11, but only a portion of it. The range of ideality will vary greatly in different systems. If the range of ideality is extremely limited, only the central portion of V.11 may be observed, and this could appear to have the form of a straight line with $m \neq 1$. In the cases of Roozeboom types IV and V a discontinuity in the HDR plot is expected to correspond to that in the Roozeboom diagram, and this is illustrated by the horizontal portion of the curves of Fig.V.10.

If this type of treatment is a reasonable approximation, it might be expected that in the cases where the HDR plot has the form of Fig.V.11 the change in behaviour of the solid solution from ideality to non-ideality might be reflected in changes in the variation of physical properties with composition. A particular example is Végard's law, which states that for a cubic crystal the cell dimension varies linearly with the composition of the solid solution.

This has been verified in various cases. However for non-cubic crystals there is no reason why the cell dimensions should vary linearly with composition.[19] The variation of cell dimensions with composition might in this case be different over the non-ideal range from over the ideal range, and other properties might show similar irregularities in behaviour.

The HDR and Roozeboom plots therefore give a good indication of the ideality of the solid solutions formed, and this will be useful in relating the properties and compositions of the solid solutions containing $CuCl_4^{2-}$, $CoCl_4^{2-}$ and $ZnCl_4^{2-}$.

REFERENCES FOR CHAPTER V

1. Beudant, Ann.des Mines 1818, 3, 239
2(a) Végard Z.physik.Chem. 1921, 5, 17
(b) Havighorst et al. J.A.C.S. 1925, 47, 31
3(a) R. G. Burns "Mineralogical Applications of Crystal Field Theory" O.U.P. 1970
(b) W. C. Blasdale "Equilibria in Saturated Salt Solutions" A.C.S. Monograph, 1927. (Chapter 5).
4(a) A.S.A. Murthy, D. S. Mahadevappa Austral.J.Chem. 1969, 22, 2017
(b) A. Elamayem J.Inorg.Nuc.Chem. 1964, 26, 2159
5. B. Roozeboom Z.physik.Chem. 1891, 8, 521
6. Muthmann & Kuntze Z.Kryst. 1894, 23, 371
7. Seidell "Solubilities of Inorganic Compounds", 1958
8. Amadori & Pampini Atta.Accad.Linc. (V) 1911, 21I, 667
9. ibid. (V) 1911, 20I, 475
10. G. Meyer Rec.Trav.Chim. 1923, 42, 304
11. Uyeda 8th Int.Cong.Appl.Chem. 1912, 22, 237
12. See ref. 7.
13. Muthmann & Kuntze Z.Kryst. 1894, 23, 374
14. Fock Z.physik.Chem. 1893, 12, 658
15. See ref. 7.
16. Hollmann Z.physik.Chem. 1905, 54, 105
17. Fock Z.Kryst. 1897, 28, 353
18. Hill, Durham & Ricci J.A.C.S. 1940, 62, 2723
19. E-An Zen Am.Mineral. 1956, 41, 53

Figure V.1a

The five types of Roozeboom diagram

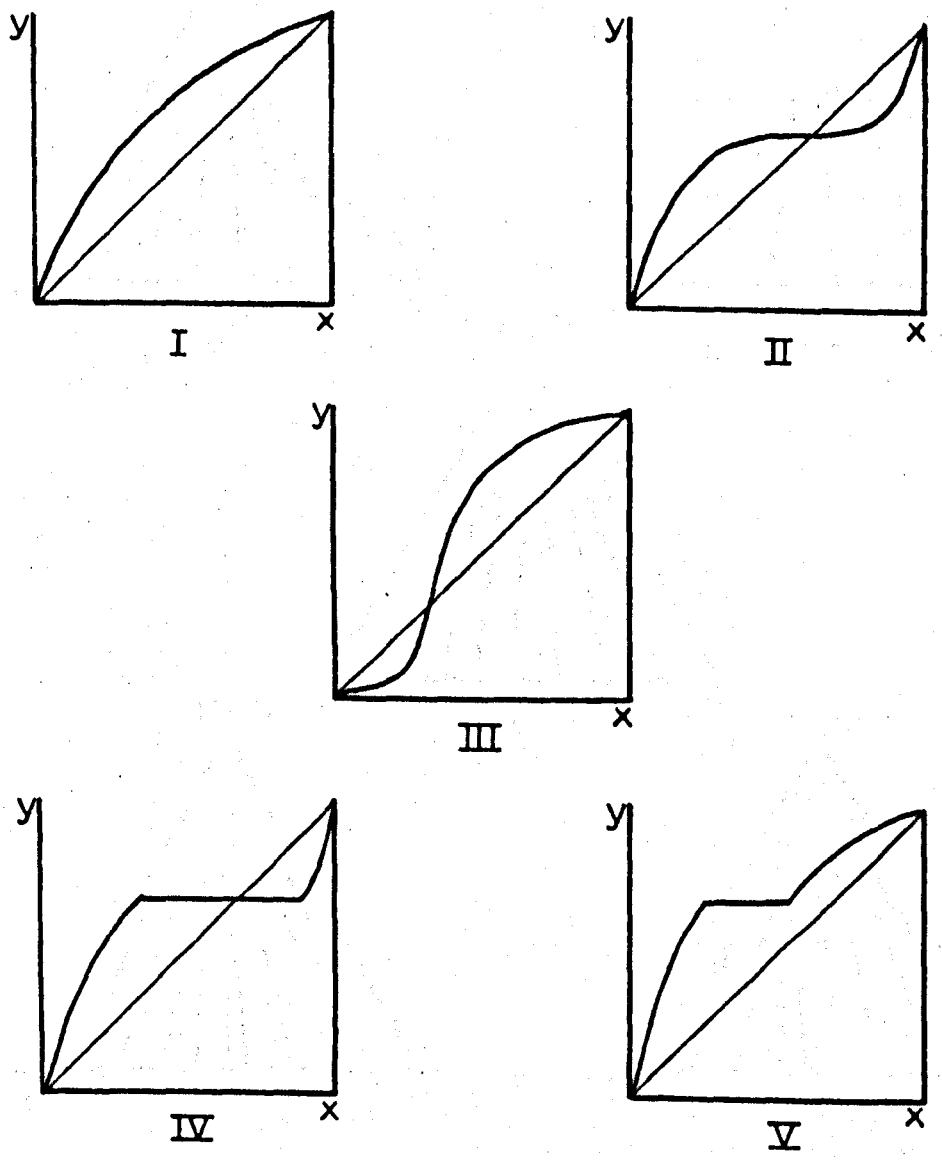

Figure V.1b

Phase diagrams corresponding to the Roozeboom diagrams of Figure V.1a. Dotted lines are lines of constant S1:S2 ratio.

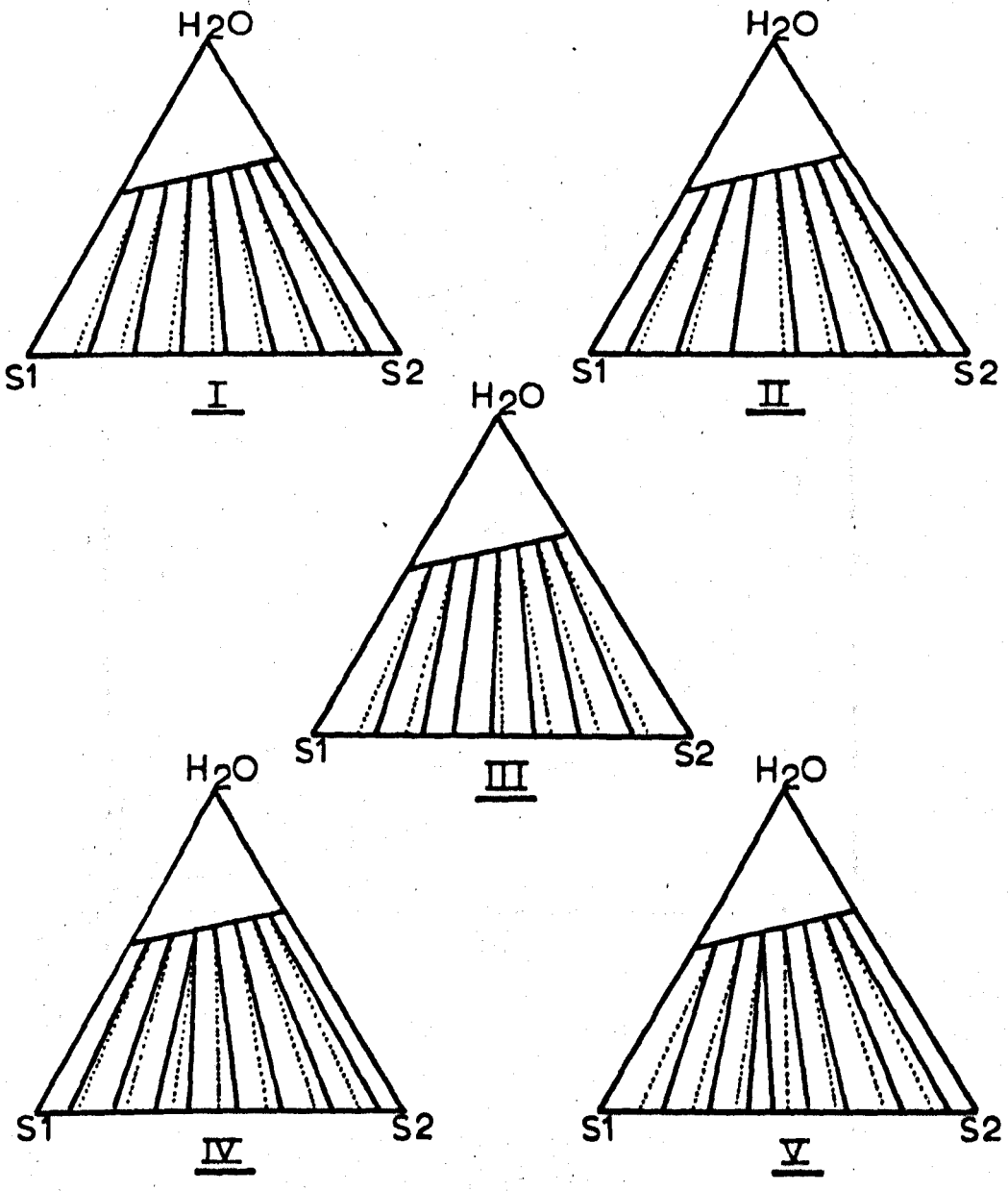

Figure V.2

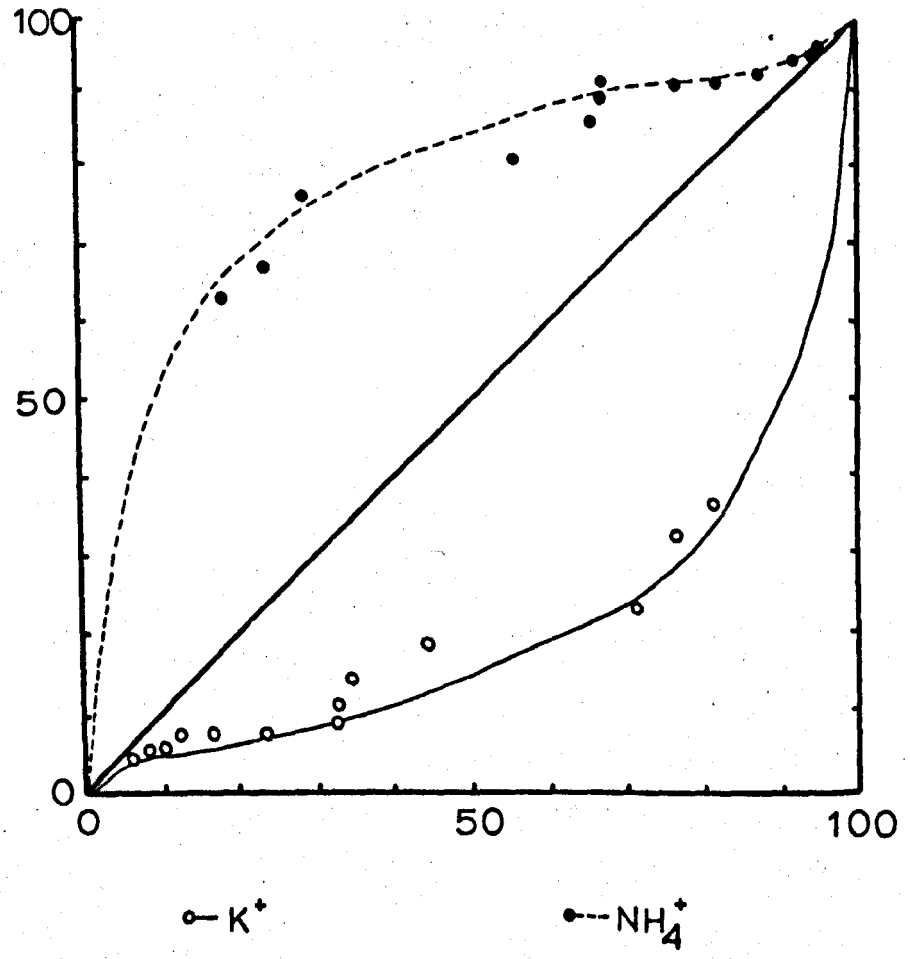

$(NH_4)_2SO_4 - K_2SO_4 - H_2O$

Figure V.3

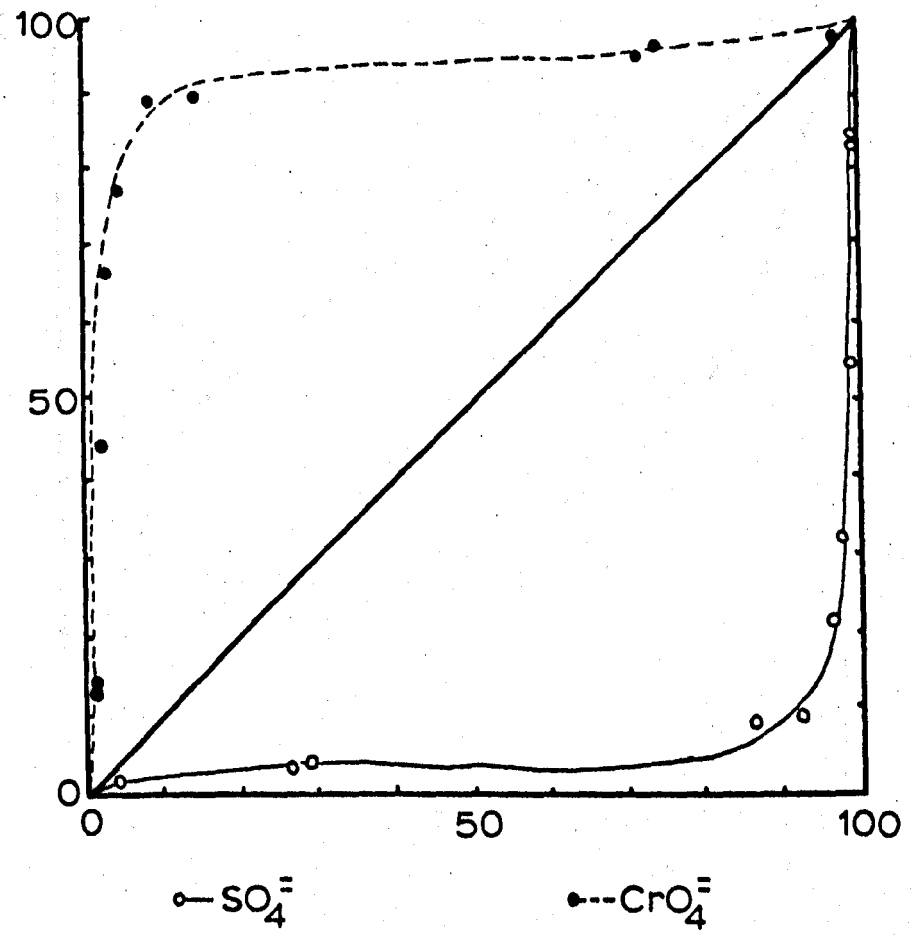

K_2CrO_4 —— K_2SO_4 — H_2O

Figure V.4

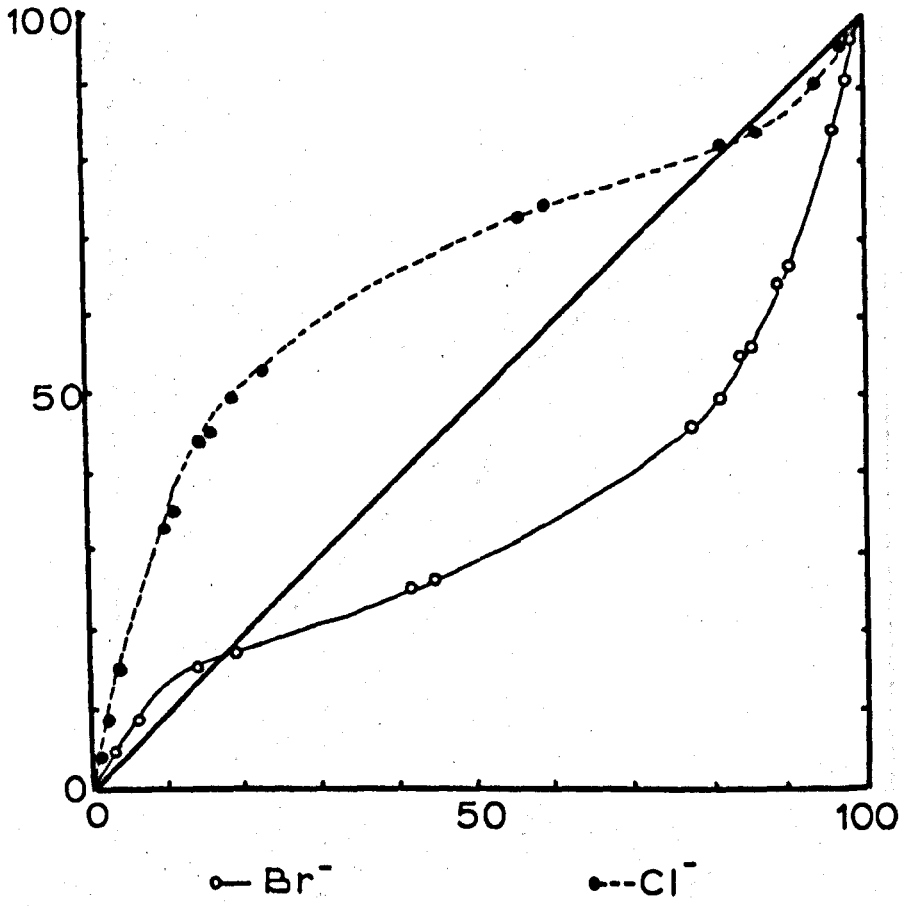

KBr——KCl——H_2O

Figure V.5

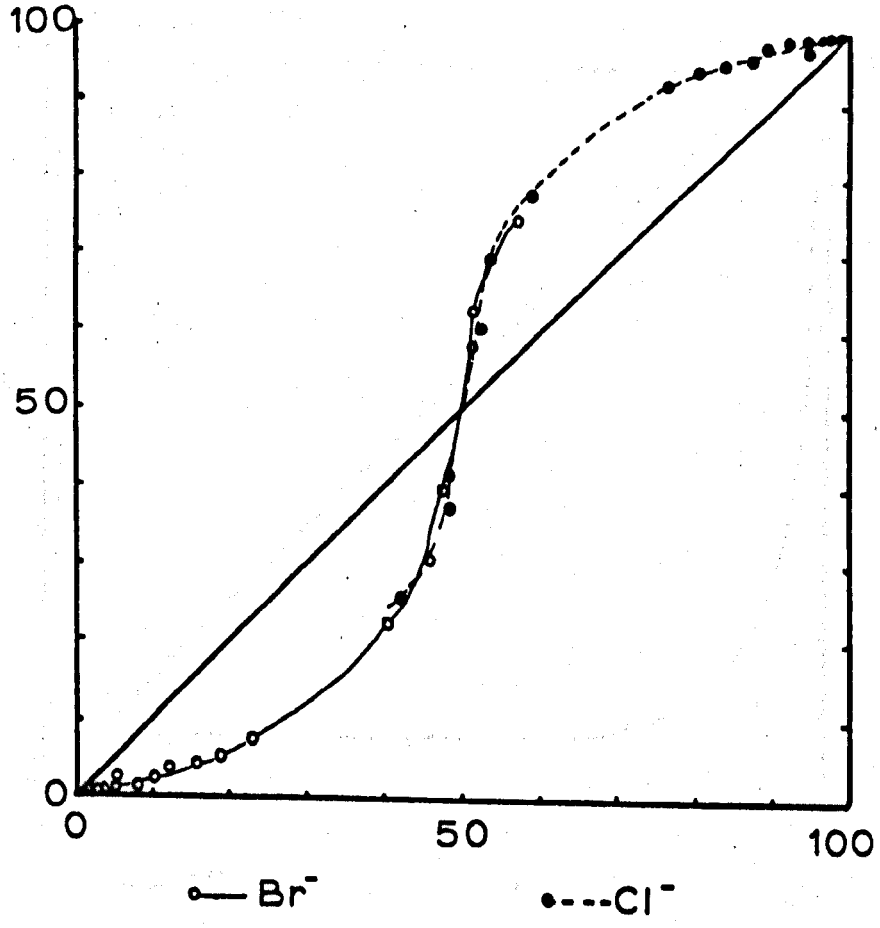

$PbBr_2$—$PbCl_2$—H_2O

Figure V.6

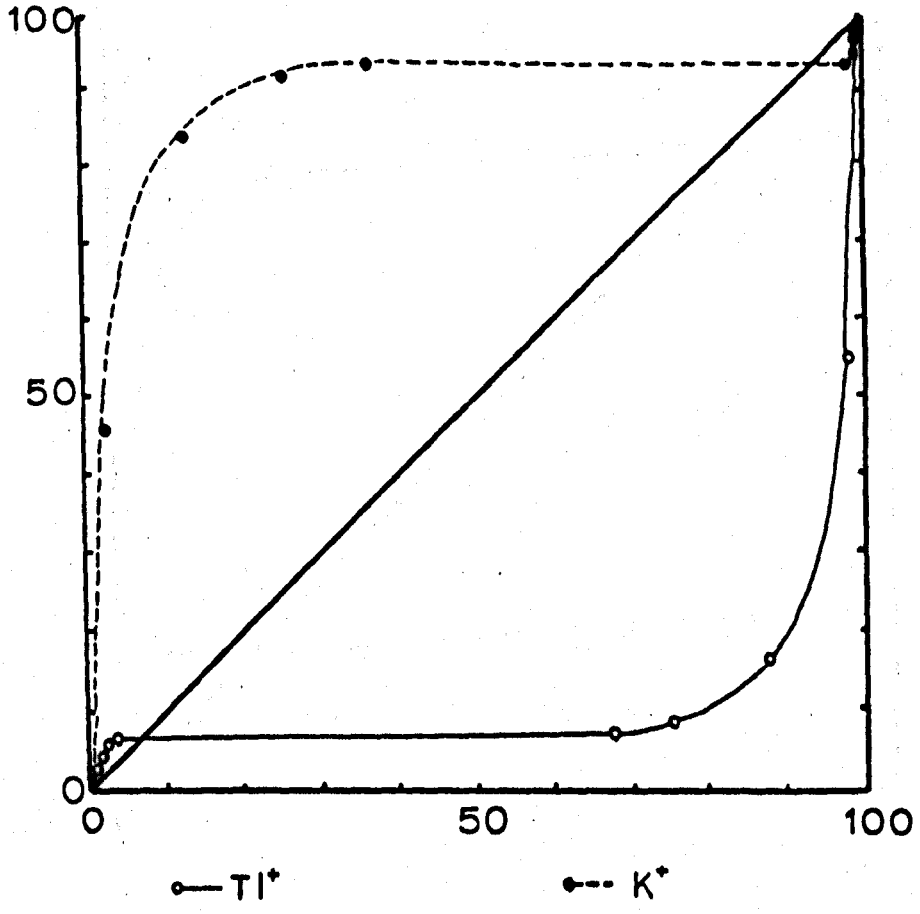

$KClO_3$ — $TlClO_3$ — H_2O

Figure V.7

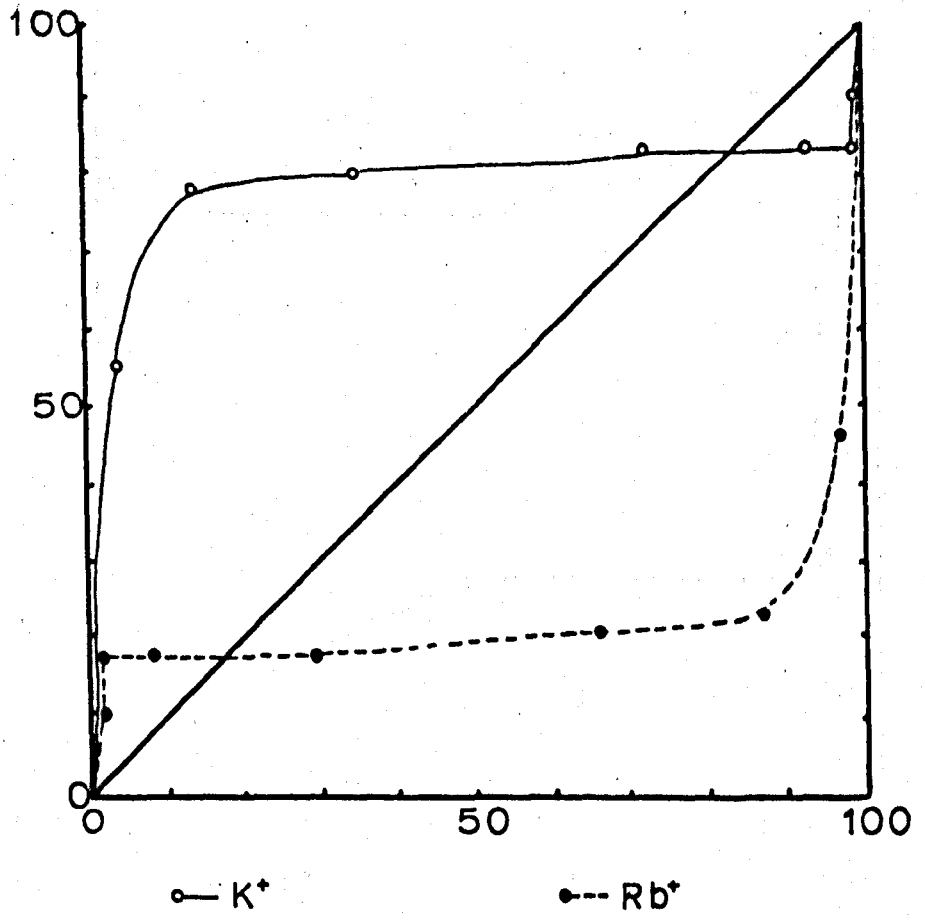

$KMnO_4$—$RbMnO_4$—H_2O

Figure V.8

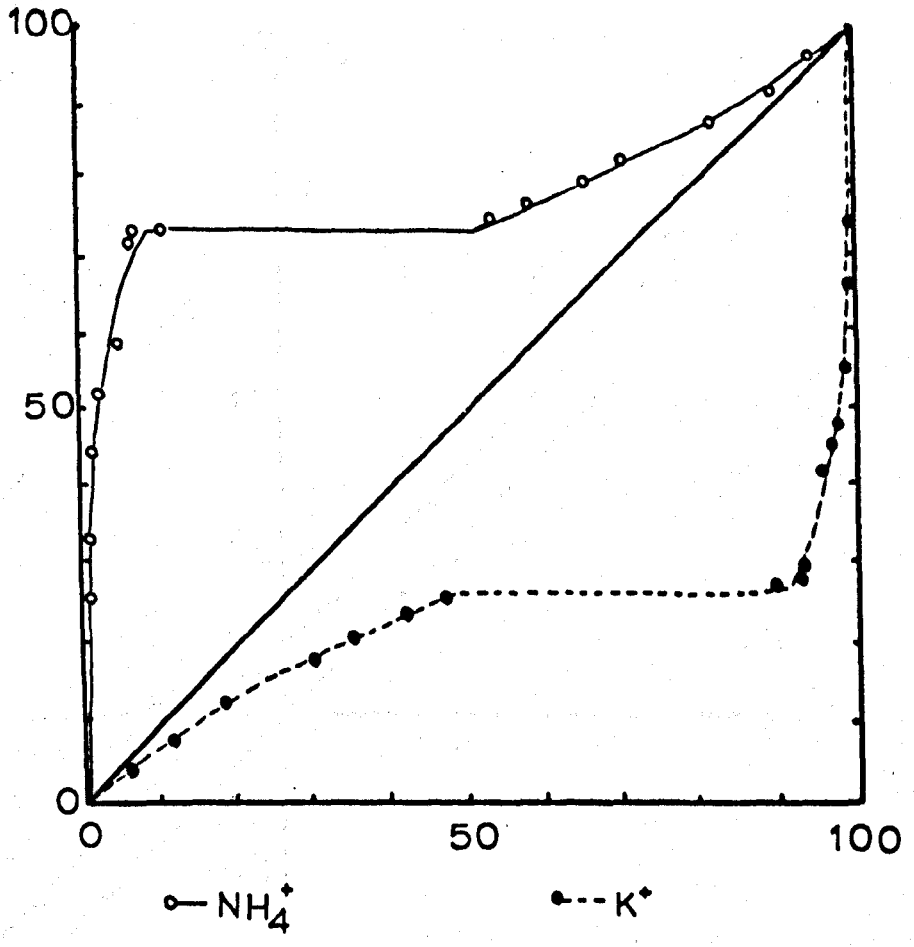

KSO_3NH_2——$NH_4SO_3NH_2$—H_2O

Figure V.9

HDR plots for some alums

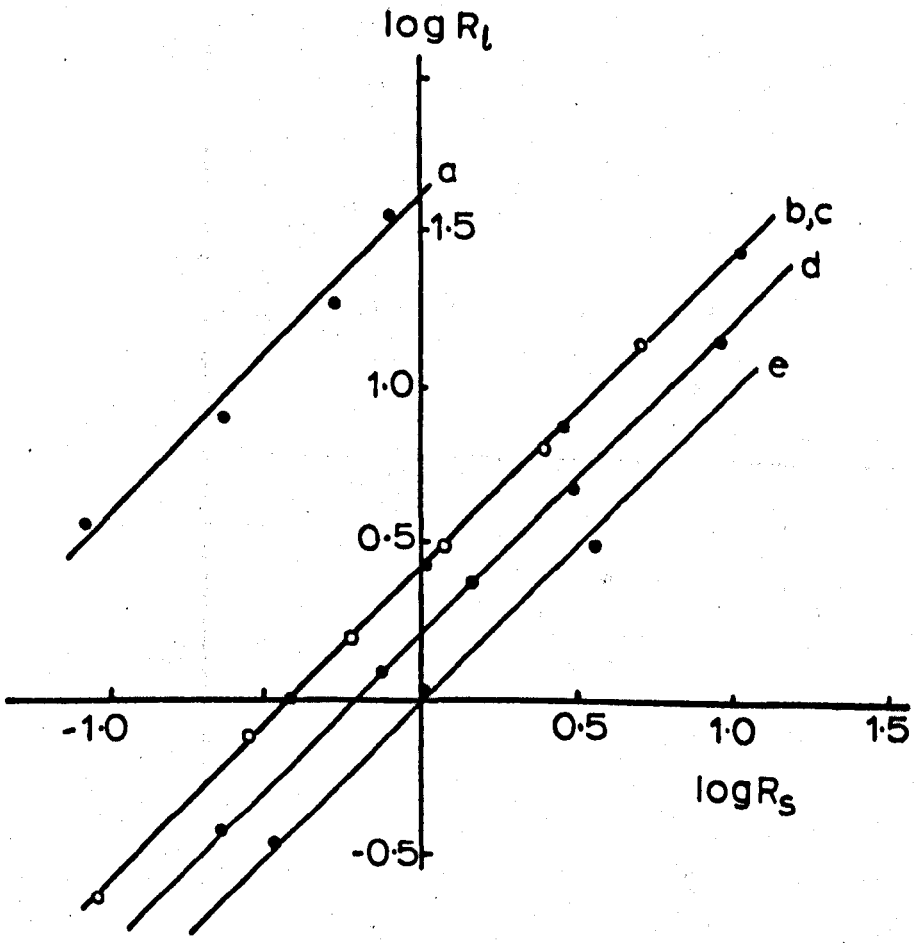

Figure V.10

HDR plots for the systems of Figures V.2 - V.8

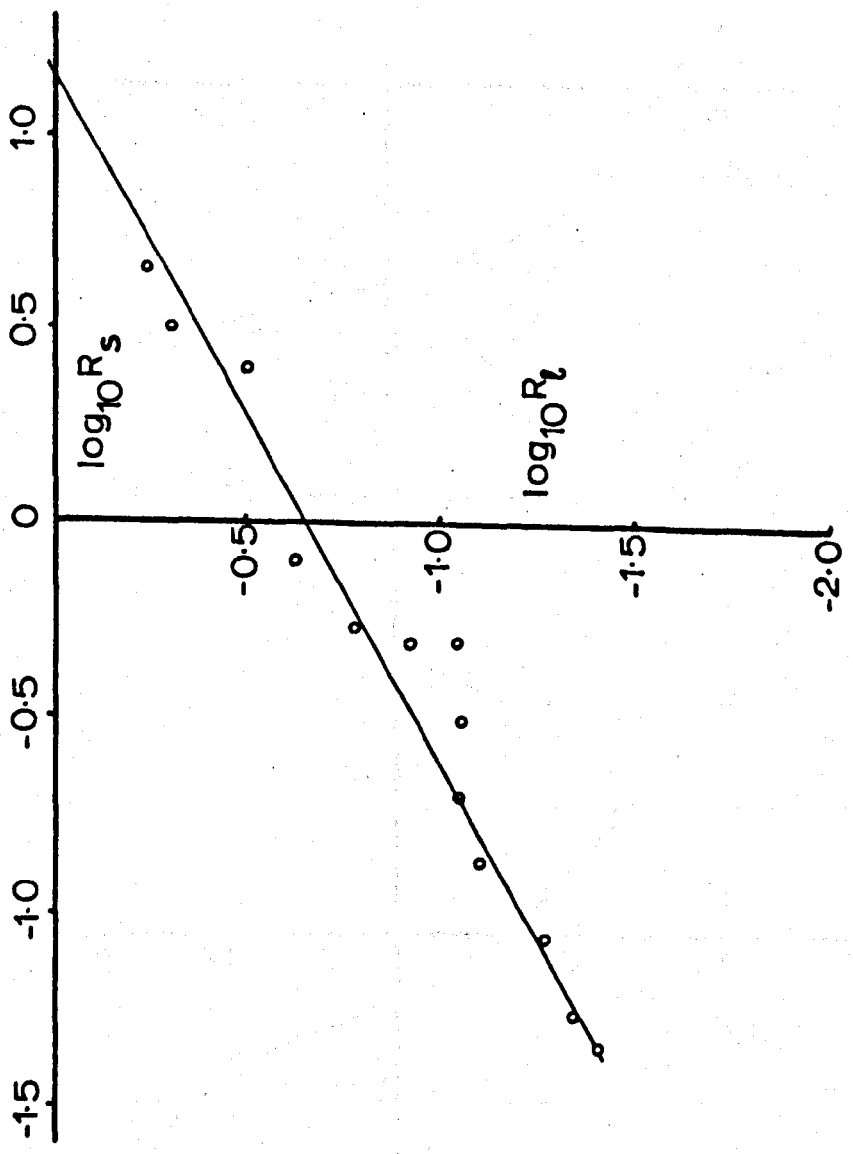

(a) $(NH_4)_2SO_4$—K_2SO_4—H_2O

Figure V.10 cont'd

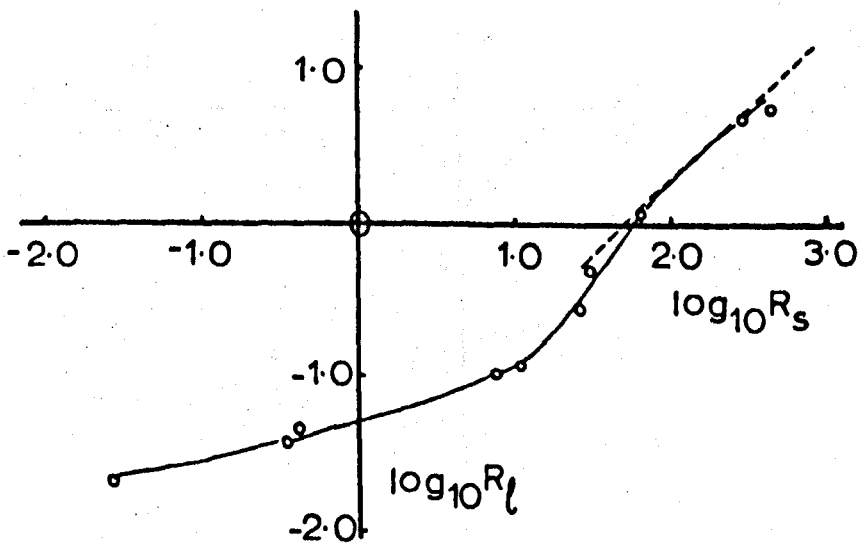

(b) K_2CrO_4—K_2SO_4—H_2O

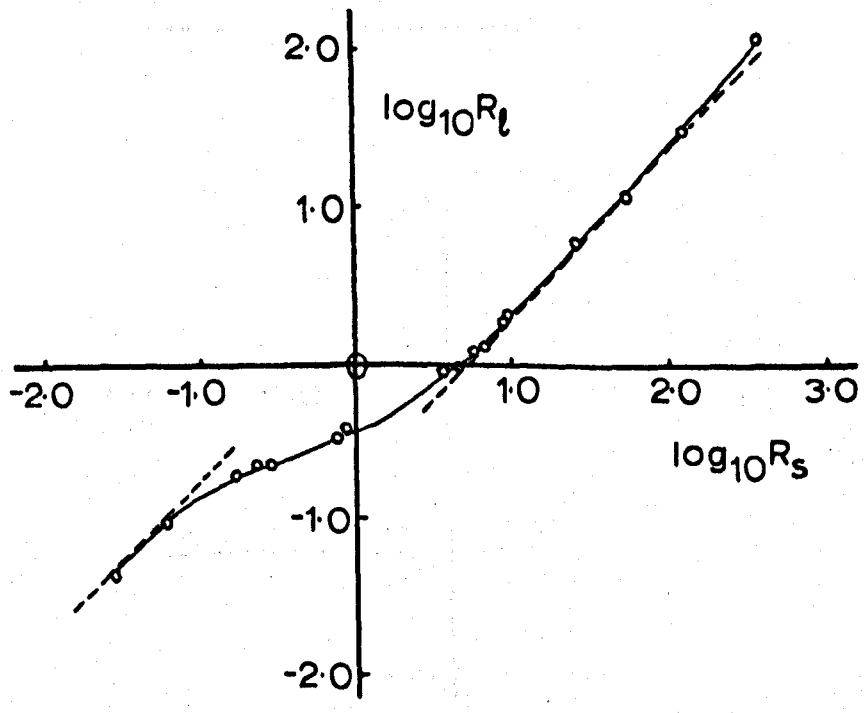

(c) KBr—KCl—H_2O

Figure V.10 cont'd

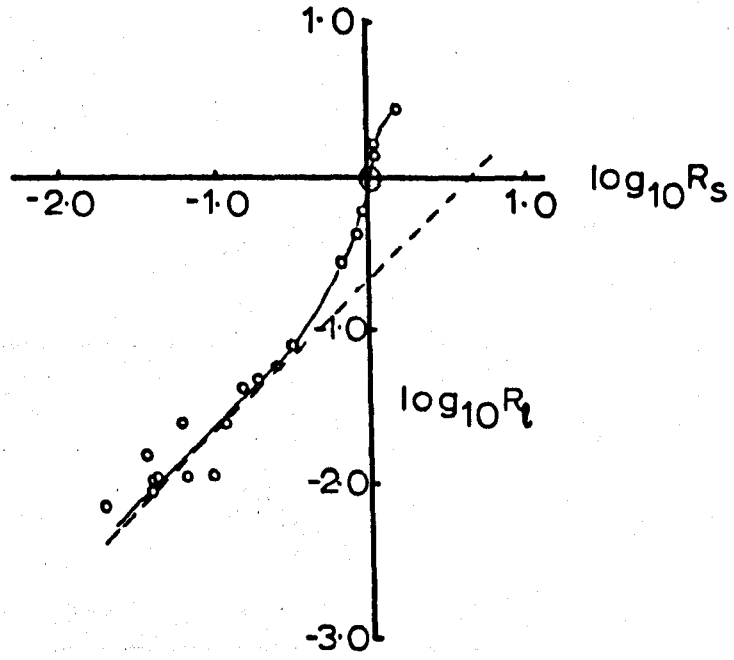

(d) $PbBr_2$—$PbCl_2$—H_2O

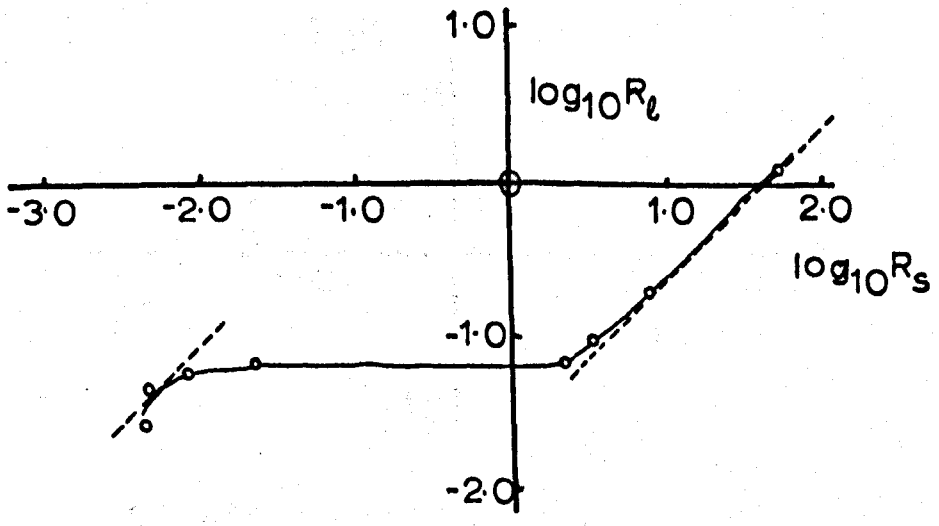

(e) $KClO_3$—$TlClO_3$—H_2O

Figure V.10 cont'd

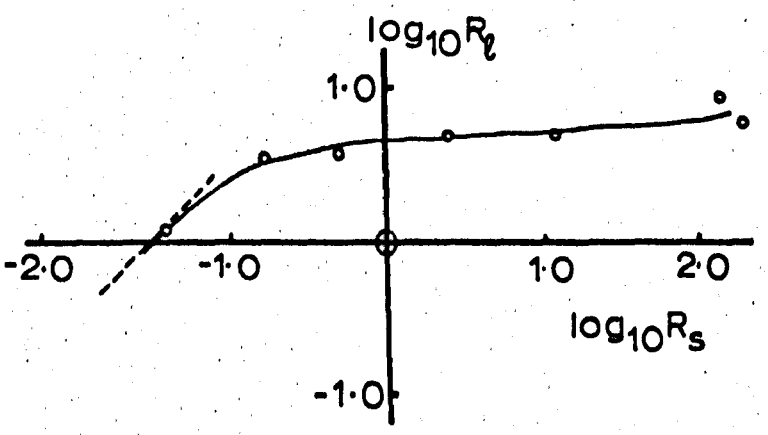

(f) $KMnO_4$—$RbMnO_4$—H_2O

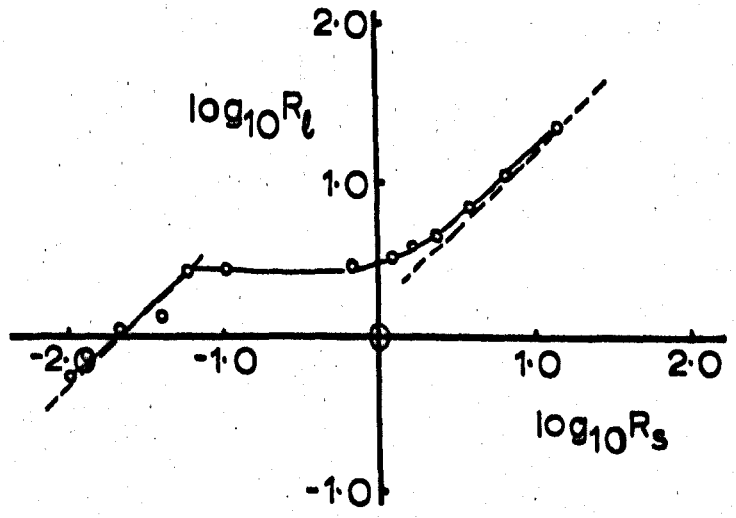

(g) KSO_3NH_2 —$NH_4SO_3NH_2$ —H_2O

Figure V.11

Suggested general form of the HDR plot

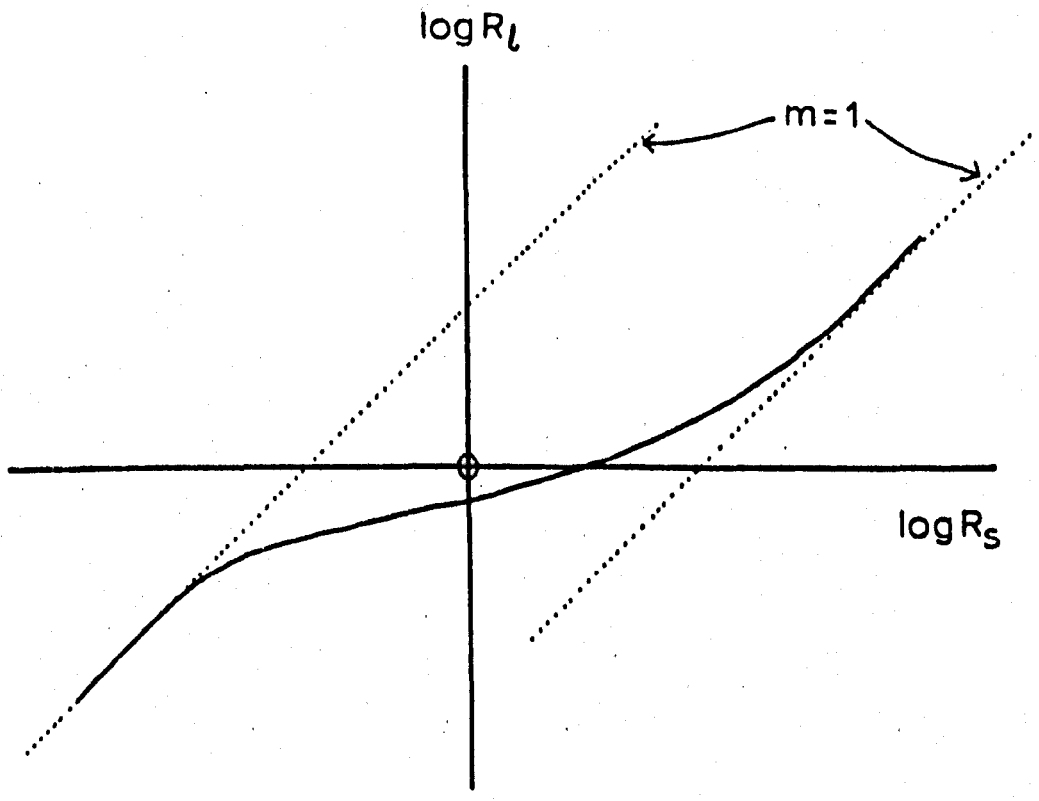

CHAPTER VI

DISCUSSION

DISCUSSION

The stability of chlorocuprate anions in the solid state is strongly dependent on the size and shape of the cation, both crystal packing and hydrogen bonding forces being significant, and it is often possible to interpret the various structures in terms of the properties of the cations. An example is the compounds of stoichiometry $ACuCl_3$, which are of two distinct types (see Chapter I) based either on $(Cu_2Cl_6)^{2-}$ dimers or $(CuCl_3^-)$ chains. There are two different types of dimeric structure, typified by $KCuCl_3$ and $(Me_2NH_2)CuCl_3$, which can be explained by reference to the size and shape of the cation. $KCuCl_3$ contains planar dimers, and since the K^+ ion is small and spherical it does not hinder the formation of a compact arrangement of dimers (Fig.I.2) with dimer-dimer interactions giving the copper atoms distorted octahedral coordination. Where $A = Me_2NH_2^+$ or ½paraquat^{2+},[1] the cation is elongated and not planar, and the non-planar dimers form a less compact arrangement, with square pyramidal coordination for the copper atoms. In both of the latter compounds there is also a N----Cl interaction between the cation and a terminal chlorine atom of the dimer, which can be considered responsible for the deviation of the dimer from planarity. $CsCuCl_3$ has the chain structure discussed in Chapter II, where it was concluded that the packing of the $(CuCl_3^-)_n$ chains determined the overall structure. The packing in $(Me_3NH)_3Cu_2Cl_7$ is also thought to be dominated by the $(CuCl_3^-)_n$ chains. It is not clear, however, why the dimeric structure is preferred for $KCuCl_3$, $Me_2NH_2CuCl_3$ and NH_4CuCl_3, but the chain structure for $CsCuCl_3$. An example where the shape of the chlorocuprate anion is determined by the packing of the cation is $[M(NH_3)_6]CuCl_5$, where M = Cr,Co. The $[M(NH_3)_6]^{3+}$ ions may be regarded as large and spherical, and they tend to form a close-packed type of arrangement; the arrangement of the anion and cation is that of the NaCl structure. $[Cr(NH_3)_6]CuCl_5$ [2] crystallizes in the cubic

space group Fd3c, with the regular octahedral $[Cr(NH_3)_6]^{3+}$ ions occupying sites of $\bar{3}$ symmetry. The pentacoordinated $CuCl_5^{3-}$ ion is forced to occupy sites of 32 symmetry. By contrast $(Me_2NH_2)_3CuCl_5$ [3] and $[(NH_3.CH_2.CH_2)_2NH_2]CuCl_5$ [4] both contain non-spherical cations, and the chlorocuprate anion is in the form $[CuCl_4^{2-} + Cl^-]$, though in the former compound the $CuCl_4^{2-}$ is tetrahedral, and in the latter square planar; this may be due to the difference in chain length in the cations. There is no obvious explanation for the preference for $CuCl_5^{3-}$ over $[CuCl_4^{2-} + Cl^-]$ in $[M(NH_3)_6]CuCl_5$; it is quite possible that a distorted $CuCl_4^{2-}$ ion (of $\bar{4}2m$ symmetry) could be included in a cubic space group, although not in Fd3c.

The chlorocuprate(II) structures can thus be rationalized in terms of crystal packing and hydrogen bonding. It is impossible, however, to predict with any certainty the stoichiometry and structure of the chlorocuprate anions likely to be formed with a particular cation, nor the optimum experimental conditions for their formation.

Another feature of interest in the crystal structures of chlorocuprates is the influence of the Jahn-Teller effect on the coordination of the copper atoms. The $(Me_4N)_2MCl_4$ compounds are a good example of a case in which structures containing different first row transition metals are known to be isomorphous, and of which only $CuCl_4^{2-}$ is expected to show Jahn-Teller distortion. The bond length and angles in the MCl_4^{2-} tetrahedra with M = Co, Ni, Cu, Zn are given in Table VI.1. All the MCl_4^{2-} ions are distorted from $T_d(\bar{4}3m)$ symmetry, and the distortions in $CoCl_4^{2-}$, $NiCl_4^{2-}$ and $ZnCl_4^{2-}$ are attributed to crystal packing forces.[5] These forces will not be significantly different in $(Me_4N)_2CuCl_4$, so the Jahn-Teller effect is responsible for its greater distortion. On the other hand, $CsCoCl_3$,[6] $CsNiCl_3$[7] and $CsCuCl_3$ all contain $(MCl_3^-)_n$ chains, but they crystallize in different space groups, so that the crystal packing forces are not necessarily similar. Also none of the MCl_6 groups has O_h symmetry, and for these reasons the Jahn-Teller effect

is less easy to distinguish. The balance between electronic forces and ligand repulsion in the $CuCl_5^{3-}$ ion of $[M(NH_3)_6]CuCl_5$ is difficult to understand. In a trigonal bipyramid, the axial M-Cl bond lengths are usually expected to be greater than the equatorial bond lengths, to minimise ligand-ligand repulsions. This distortion would satisfy the Jahn-Teller effect; however in $[Cr(NH_3)_6]CuCl_5$ the axial bond lengths are less than the equatorial bond lengths.

A greater number of chlorocuprate anions is formed with Me_3NH^+ than with any other cation. The existence of $Me_3NHCuCl_3$, $Me_3NHCuCl_3.2H_2O$, $(Me_3NH)_2CuCl_4$, $(Me_3NH)_3CuCl_5$ and $(Me_3NH)_3Cu_2Cl_7$ [8] have been confirmed (Chapter III) and Willett has also reported the preparation of $Me_3NHCu_2Cl_5$ [9] (by crystallization from a 10:1 solution of $CuCl_2$ and Me_3NHCl in n-propanol). There is no outstanding feature of Me_3NH^+ which accounts for this, except perhaps the ability to form one strong hydrogen bond, which may be the most important factor. However this would also apply to other R_3NH^+ ions, which do not appear to form the same number of compounds, so the size of Me_3NH^+ may also play a part.

The variety of stoichiometries formed with the Me_3NH^+ cation suggests that a number of chlorocuprate species may coexist in any given solution, and that the species may differ between different solvents. The species are also dependent on the total concentrations of salts in the solution, the chloride ion concentration and the temperature. This work is concerned with solutions which are very close to being saturated, or where solid is in equilibrium with the solution. Attempts were made to study solutions containing $CuCl_2$ and several ACl salts by visible-ultraviolet spectrophotometry, using short pathlength cells (0.1 cm), but the very high absorption coefficients of the solutions prevented the acquisition of any useful information. No X-ray measurements similar to those on concentrated $CoCl_2$ solutions[10] have been reported for $CuCl_2$, and none was made here, mainly because of the unavailability of monochromated X-radiation.

Knowledge of the ~~composition~~ structure of these solutions is therefore extremely sparse, and this imposes a limit on the discussion of solid solution formation.

The $(Me_3NH)_3Cu(Cu,M)Cl_7$ system of solid solutions was the first to be prepared; it is also the most complicated, in that only half of the copper could be replaced by another metal. Where M = Zn, the preliminary experiments suggested that the phase diagram was strongly biased in favour of $Me_3NHCuZnCl_7$; a situation similar to that in the $(Me_4N)(M,Zn)Cl_4$ systems. The ethanol-$(Me_3NH)_3Cu_2Cl_7$-$(Me_3NH)_3CuCoCl_7$ diagram was more symmetrical, and this is why it was used for further experiments. The visible-ultraviolet spectrum (250-700 nm) indicated the presence of $CoCl_4^{2-}$(11) (Chapter III). There is also a gradual decrease in the band at about 470 nm, which is an absorption also found in $(Me_3NH)_2CuCl_4$ and therefore attributed to the $CuCl_4^{2-}$ ion. By analogy the zinc is assumed to be present as $ZnCl_4^{2-}$, although there is no direct spectral evidence for this.

The reasons for the choice of the $(Me_4N)_2MCl_4$ systems for solid solution experiments are given in Chapter III. In retrospect this choice had one additional advantage, namely that the $CuCl_4^{2-}$ ion was in a more typical configuration (D_{2d}) in $(Me_4N)_2CuCl_4$ than in $(Me_3NH)_3Cu_2Cl_7$. This D_{2d} symmetry is shown by all the simple tetrahedral tetrachlorocuprates (Chapter II) whose structures are known. It is interesting to note, however that the absorption bands of $CoCl_4^{2-}$ in $(Me_3NH)_3CuCoCl_7$ are very similar to those in $(Me_4N)_2CoCl_4$ so that any distortion toward C_{3v} symmetry in the former compound is likely to be very slight.

It was found that continuous series of solid solutions were formed between $(Me_4N)_2CuCl_4$, $(Me_4N)_2CoCl_4$ and $(Me_4N)_2ZnCl_4$ in the three possible combinations, but $NiCl_4^{2-}$ did not enter solid solution. The experimental data can be considered in relation to the conclusions of Chapter V on solid solution formation. It was

shown there that the important factors in determining the solubility behaviour of two salts containing a common ion were (1) the solubilities of the two salts, (2) the activity coefficient ratio of the two non-common ions in the liquid phase and (3) the activity coefficient ratio of the two non-common ions in the solid phase. The treatment was only applicable in cases where a continuous series of solid solutions is formed (Roozeboom types I, II and III). Roozeboom type I behaviour is expected from a simple solubility relationship, with the less soluble salt always concentrated in the solid. In types II and III, the portions of the curves above the diagonal may correspond to this solubility relationship, but below the diagonal some other factor must play a part. It is sometimes difficult to distinguish experimentally between type I and types II and III, because the curve may only cross the diagonal close to the limits of the Roozeboom diagram. The possible factors causing this crossover in types II and III were concluded (in Chapter V) to be the activity coefficient ratios in the solid and the solution. These effects may also be present in type I systems, but in this case the solubility effect is dominant. It was further postulated that the activity coefficient ratio in the solid was the more important effect in those systems which had HDR plots similar to Fig.V.11.

The latter postulate appears to be justified in the case of $(Me_4N)_2(M,M')Cl_4$ systems, since the behaviour is similar whether the solvent is water, ethanol or ethanol-water (except for $(Me_4N)_2(Cu,Zn)Cl_4$; see Chapter III). The chlorometallate species in solution are not expected to be the same in all solvents. In concentrated ethanolic solutions of $CoCl_2$ [10] the main species found was $CoCl_4^{2-}$, whereas in aqueous solution it was $Co(H_2O)_6^{2+}$. Spectral examination of $CoCl_2$ in aqueous solution containing Me_4NCl shows the effect of total cobalt concentration; the characteristic deep blue

colour of tetrahedral species disappears as the solution is diluted, giving way to the far less intense pink colour characteristic of octahedral hydrated Co^{2+} species.[12] A variety of chloroaquo complexes may be present at intermediate dilutions, and the species $(Co.6\ solvent)^{2+}$, $(CoX.5\ solvent)^{+}$, $(CoX_2.2\ solvent)$, $(CoX_3.solvent)^{-}$ and CoX_4^{2-} have been postulated in cobalt halide solutions.[13] The equilibrium

$$X^- + [CoX_2.4\ solvent]_{octahedral} \rightleftharpoons [MX_3.solvent]^-_{tetrahedral}$$

has been studied spectroscopically,[14] and evidence was obtained for the existence of $[CoCl_3.H_2O]^-$ and $[CoCl_3.MeOH]^-$ at high halide concentration with solutions about 10^{-2} molar in Co^{2+}.

The solution behaviour of Cu^{2+} is similarly complicated. The species which exist at various concentrations in presence of Cl^- include $[Cu(H_2O)_6]^{2+}$, $[CuCl(H_2O)_5]^{+}$, $[CuCl_2(H_2O)_4]$, $[CuCl_3(H_2O)_3]^-$, $[CuCl_4(H_2O)_2]^{2-}$, $[CuCl_6]^{4-}$, $[Cu(H_2O)_4]^{2+}$, $[CuCl(H_2O)_3]^{+}$, $[CuCl_2(H_2O)_2]$, $[CuCl_3(H_2O)]^-$ and $[CuCl_4]^{2-}$;[15] and similar species in ethanol. The formation constants of $CuCl^+$ and $CuCl_2$ in aqueous solution have been measured.[16] An attempt was made to show, by paper electrophoresis,[17] the existence in aqueous solutions of $CuCl_2$ of $CuCl_6^{4-}$, $CuCl_4^{2-}$, $CuCl_2(H_2O)_2$ and $Cu(H_2O)_4^{2+}$, and the authors claimed to detect characteristically coloured bands for each of these species by varying the $CuCl_2$ concentration between 0.06 and 1.7M.

There is some evidence from work on the Me_4NCl-$NiCl_2$ system[18] that large concentrations of Me_4N^+ promote the formation of tetrahedral $NiCl_4^{2-}$ ions in water, and it is likely that this is true for other metals. However there was not a large excess of Me_4N^+ over MCl_2 in the solid solution experiments, and MCl_4^{2-} is unlikely to have been the dominant species in all the mother liquors produced. There is therefore no reason why the activity coefficient ratio of the two MCl_4^{2-} ions should approach unity; yet the Roozeboom plots for each of the systems $(Me_4N)_2(Cu,Co)Cl_4$, $(Me_4N)_2(Cu,Zn)Cl_4$ and $(Me_4N)_2(Co,Zn)Cl_4$ are similar whichever of the solvents was used.

The remaining factor to be considered is the activity coefficient ratio in the solid. All of the systems examined are compatible with an HDR curve similar to Fig.V.11, although not all of the curve is present in each case. The activity coefficients of the ions in the solids may be considered in relation to the effect of the ions on the lattice energies of the solids. To investigate this a system of two salts of equal solubility will be considered; the salts BC and B'C form a continuous series of solid solutions (B,B')C, and their activity coefficient ratio in solution will be assumed to be close to unity. B' is the ion of smaller ionic radius.

It is then unfavourable to insert B in place of B' into the B'C lattice, since this would necessitate an expansion of the lattice and hence a decrease in lattice energy. However, it is also unfavourable to introduce B' in place of B in the BC lattice, since the gain of lattice energy would be less than for introduction of B; it is therefore energetically advantageous for B' to remain in solution. If the conditions of equal solubility and equal activity coefficient applied strictly, the Roozeboom plot would have the form (i):-

(i)

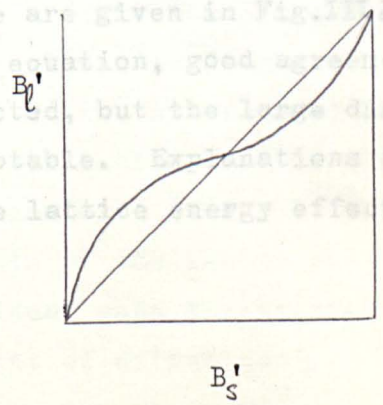

(ii)

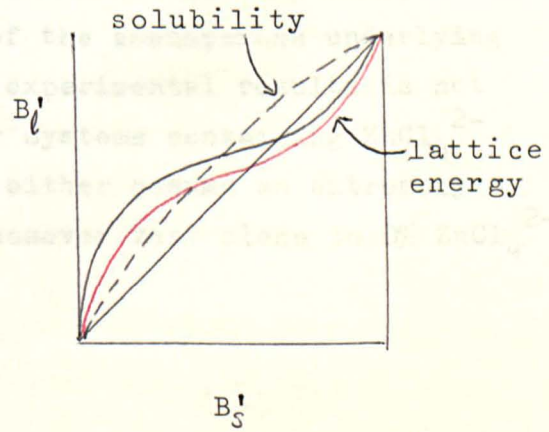

Normally this is superimposed on a solubility curve, as illustrated in (ii), giving a Roozeboom type II curve. A similar result would be expected if differences in shape between B and B' affected the lattice energy. It proved very difficult to find an example in which the solubilities were so similar that only the lattice energy effect could be responsible for the shape of the Roozeboom curve. However this seems an adequate rationalization of the Roozeboom type II systems, in somewhat more explicit terms than those used by Hill, Durham and Ricci, i.e. repulsions in the solid.

The Roozeboom type III system is not amenable to generalization of this type. In contrast to type II there is an attraction in the solid, so that the foreign ion is favoured over that usually found in the lattice. This situation is rather unusual (no example was found in Seidell), and must be related to specific interactions within the solid solution lattice.

The Roozeboom plots for $(Me_4N)_2(Cu,Co)Cl_4$ are of type II; those for $(Me_4N)_2(Cu,Zn)Cl_4$ and $(Me_4N)_2(Co,Zn)Cl_4$ are apparently of type I with a large solubility difference between the two end-compounds in each case; however it is possible that they are type II with a crossover close to the composition limits. The HDR equation

$$\text{Log } R_\ell = \frac{\lambda}{2b}(\text{Log } K) + \text{Log } R_s$$

was used to calculate values of R_ℓ for various values of R_s given the experimental values for the solubilities of the compounds; these are given in Fig.III.2. Because of the assumptions underlying this equation, good agreement with the experimental results is not expected, but the large discrepancy for systems containing $ZnCl_4^{2-}$ is notable. Explanations for this can either assume an extremely large lattice energy effect, with a crossover very close to 0% $ZnCl_4^{2-}$:-

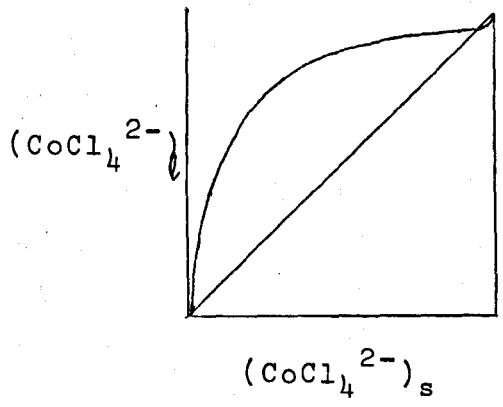

or that in fact the activity coefficient ratio in solution is very important and this is far removed from unity in all the solvents used. This question cannot be resolved, and the evidence from the HDR curves is not conclusive, although it does appear that the behaviour is consistent with Fig.V.11.

If any lattice energy effect is to be detected in these systems it is best sought where the solubility ratio is closest to unity i.e. in $(Me_4N)_2(Cu,Co)Cl_4$. Here, at low $CuCl_4^{2-}$ concentrations the behaviour is that expected from the solubilities, i.e. $CoCl_4^{2-}$ is concentrated in the solid, but at high $CuCl_4^{2-}$ concentration $CuCl_4^{2-}$ is concentrated in the solid. The size of the ions is very similar (Chapter IV), so that the lattice energy effect is most likely caused by the difference in the degree of distortion of the two ions.

The HDR plots for $(Me_4N)_2(Cu,Co)Cl_4$, interpreted in the way outlined in Chapter V, indicate that the solid solutions are ideal at the extremes of composition. It is in exactly this case that the lattice can be described as being essentially that of the pure compound (the salt present in greatest concentration) with small amounts of the second salt incorporated in it. The solid solution is non-ideal when the lattice is so disrupted that it cannot be described as that of either salt. This is in contrast to the behaviour which

might be expected for an ideal type I system (i.e. a system determined entirely by the solubility ratio of the two salts) where a smooth gradation between the structures of the two end-members would be expected. The disruption of the crystal lattice for the middle composition range is apparently at variance with the crystallographic data for $(Me_4N)_2(Cu,Co)Cl_4$, which suggested that the lattice of light atom tetrahedra remained approximately constant throughout the series; however this may be due to a difference in sensitivity between the techniques, since the positional parameters of nitrogen and carbon atoms in presence of copper and chloride are not of high accuracy,[19] (see the standard deviations in Chapter IV), and the disruption needed to show this effect may only be small.

The data for $(Me_3NH)_3Cu(Cu,Co)Cl_7$ shows a type I system, deviating from the "theoretical" curve as for $(Me_4N)_2(Zn,M)Cl_4$, so that $CoCl_4^{2-}$ is always preferred over $CuCl_4^{2-}$ in the lattice. The explanation proposed for this is based on the distortions imposed on the ions by packing forces. From other structures containing $CuCl_4^{2-}$, where it is less constrained by packing than in $(Me_3NH)_3Cu_2Cl_7$, it appears that the preferred symmetry about the copper atom is D_{2d}.[20] To fit into the $(Me_3NH)_3Cu_2Cl_7$ lattice the $CuCl_4^{2-}$ ion is distorted to C_{3v} symmetry, and it is suggested that this requires more energy than distortion from T_d to D_{2d}. The $CoCl_4^{2-}$ ion however, normally adopts symmetry close to T_d and only slight distortion is needed to achieve C_{3v} symmetry; in fact it is not necessary crystallographically to distort the $CoCl_4^{2-}$ ion from T_d symmetry if it is incorporated in the $(Me_3NH)Cu(Cu,Co)Cl_7$ lattice, although it may be distorted by N — H····Cl interactions. It is therefore reasonable to expect that $CoCl_4^{2-}$ will enter the lattice more readily than $CuCl_4^{2-}$, and so for the same reason, will $ZnCl_4^{2-}$.

The crystallographic work on $(Me_4N)_2(Cu,Co)Cl_4$ was described in Chapter IV. There were several possibilities for this

structure. The $CuCl_4^{2-}$ and $CoCl_4^{2-}$ might be distributed in a regular order on lattice sites, i.e. a superlattice might be formed; a phenomenon well-known for several alloys, e.g. $AuCu_3$ after prolonged annealing.[21] Both $CuCl_4^{2-}$ and $CoCl_4^{2-}$ might adopt a conformation intermediate between that of $CuCl_4^{2-}$ in $(Me_4N)_2CuCl_4$ and $CoCl_4^{2-}$ in $(Me_4N)_2CoCl_4$, or each might retain its characteristic conformation, with or without ordering of the solid solution.

The X-ray examination has shown no evidence of long-range order resulting in superlattice formation and although local short-range order probably exists, since a perfectly disordered solid solution is unusual,[22] this would not be evident from the Weissenberg photographs. It is concluded that the structure of $(Me_4N)_2(Cu,Co)Cl_4$ is best described as a random distribution of $CuCl_4^{2-}$ and $CoCl_4^{2-}$ ions, each with approximately the same distortion as that found in the pure compounds, embedded in a lattice of Me_4N^+ groups whose positions are effectively independent of the metal ion present. The persistance of the greater distortion of $CuCl_4^{2-}$ than $CoCl_4^{2-}$ in the solid solution shows the importance of the Jahn-Teller effect in determining the configuration of the $CuCl_4^{2-}$ ion.

The positional disorder found in all the $(Me_4N)_2MCl_4$ compounds, which was suggested to be the result of thermal motion, is discussed later in relation to the DSC measurements on the compounds.

Comparison of the structures of $(Me_4N)_2MCl_4$ (M = Co, Ni, Cu, Zn) prompted an interest in the problem of defining the degree of isomorphism of a group of crystal structures. All the structures belong to the same space group and have closely similar cell dimensions (Table VI.1) and atomic arrangements. However, the detailed atomic arrangements do show differences, particularly in the distortion of the MCl_4^{2-} tetrahedra. The $CuCl_4^{2-}$ ion is more distorted than the other MCl_4^{2-} ions, so that the compounds containing $CoCl_4^{2-}$, $NiCl_4^{2-}$ and $ZnCl_4^{2-}$ are expected to be more isomorphous with each other than with $(Me_4N)_2CuCl_4$.

Ramachandran[23] has examined this problem in relation to the isomorphous replacement method,[24] and his criterion of the degree of isomorphism was adopted. Ramachandran discussed the case of a pair of crystals (of similar cell dimensions and space group), one containing P and one N (= P + C) atoms, where $P < N$. In the present case the whole of each crystal was included, i.e. $P = N$. The condition that all atoms in the crystal should be alike has been disregarded, because this should not be essential if all the atoms are included in the degree of isomorphism parameter. Two extreme cases are possible: the related case, in which all the atoms occupy exactly the same positions in both crystals, and the unrelated case, in which the two sets of atoms are independent of each other. σ_1^2 is defined as σ_P^2/σ_N^2, where the ideal value of σ_P^2 is $\sum_1^P f^2$, i.e. the sum of the squares of the atomic scattering factors. In this case σ_P^2 is approximately equal to σ_N^2, since the only difference is in the scattering factors of the metal ions, and therefore $\sigma_1^2 \approx 1$, and was taken equal to 1 in the following calculations.

The R factor between the structure amplitudes of the two crystals is

$$R = \frac{\sum ||F^{(1)}| - |F^{(2)}||}{\sum |F^{(1)}|}$$

and the degree of isomorphism (γ_r) is defined by

$$\gamma_r = \frac{R_{obs} - R_{unrel}}{R_{rel} - R_{unrel}}$$

where R_{obs} is the R factor between the two observed sets of structure factors, and R_{rel} and R_{unrel} are the R factors for the totally related and totally unrelated cases respectively. Ramachandran gives values for R_{rel} and R_{unrel} for various values of σ_1^2 (between 0 and 1) for both the centrosymmetric and non-centrosymmetric case. For the

structures in question $\sigma_1^2 = 1$, $R_{rel} = 0.00$ and $R_{unrel} = 0.824$, and hence

$$\gamma_r = \frac{R_{obs} - 0.824}{0.00 - 0.824}$$

γ_r is therefore 0 for totally unrelated structures and 1 for totally related structures.

Since the same set of experimentally observed reflections was not available for all the $(Me_4N)_2MCl_4$ compounds, F_{calc} for the structures was used in preference to F_{obs}. It is therefore the isomorphism of the models which is tested, rather than that of the actual structures; however an advantage of this is that the effect of errors in F_{obs} is minimised, which may be important for $(Me_4N)_2CoCl_4$, for which relatively few observed reflections are available. The scaling is also important if F_{obs} of two structures are to be compared.[25] R_{obs} was calculated for two cases: one the conventional R factor as defined above, and the other including the difference in sign between $F^{(1)}$ and $F^{(2)}$ which may occur for some hkl i.e.

$$R = \frac{\sum |F^{(1)} - F^{(2)}|}{\sum |F^{(1)}|}$$

The two R factors show similar trends, and only the conventional R factor has been recorded. The R_{obs} and γ_r for various pairs are given in Table VI.2.

The main limitation of the Ramachandran treatment is the requirement that the cell dimensions should be fairly close. Otherwise γ_r may be close to 1, yet with very different cell dimensions the structures are clearly not as close as if the cell dimensions are similar, and in particular solid solution formation would be difficult in the former case. An attempt was therefore made to define the degree of isomorphism between two structures in terms of atomic positions and cell dimensions. The degree of isomorphism was

empirically defined as the sum of the weighted mean shifts of the atoms between the two structures. To obtain this, both unit cells must have the origin in the same relation to the symmetry elements of the space group, and the axes labelled in the same way. For the nth atom

$$\Delta_n = \sqrt{((x(1)-x(2))^2 + (y(1)-y(2))^2 + (z(1)-z(2))^2)}$$

where x,y,z are orthogonalized real coordinates, and the degree of isomorphism is

$$\gamma_P = \frac{\sum^{\text{unit cell}} A_n \Delta_n}{\sum^{\text{unit cell}} A_n}$$

where A_n is the atomic number of the nth atom.

This takes account of the cell dimension differences, because while an atom at 0,0,0 cannot show a shift, those at a,0,0 0,b,0 and 0,0,c correspond to differences in a,b and c respectively.

The summation $\sum A_n \Delta_n$ should normally be carried out over the whole unit cell. However in the case of the $(Me_4N)_2MCl_4$ compounds, the main cell dimension differences are in c. The coordinates of the atoms in the asymmetric unit were all placed in the region bounded by $x = \frac{1}{2}$, $y = \frac{1}{4}$, $z = 1$ (in fractional coordinates). By only calculating $\sum A_n \Delta_n$ over the asymmetric unit, the calculation is simplified and the differences in c are still included.

γ_P for the various pairs of compounds are given in Table VI.2.

From Table VI.2, it can be seen that both γ_P and γ_r confirm the prediction that $(Me_4N)_2CoCl_4$, $(Me_4N)_2NiCl_4$ and $(Me_4N)_2ZnCl_4$ are more isomorphous with each other than with $(Me_4N)_2CuCl_4$. γ_P and γ_r give the same order i.e. Cu-Ni $>$ Cu-Co $>$ Cu-Zn, although a plot γ_P vs γ_r (Fig.VI.1) does not show a good straight line between the two. It is interesting to note that $NiCl_4^{2-}$ is more distorted than $CoCl_4^{2-}$ or

$ZnCl_4^{2-}$ (Table VI.1) and also most isomorphous with $CuCl_4^{2-}$.

γ_r shows no difference between $(Me_4N)_2(Cu,Co)Cl_4$ containing an average metal ion tetrahedron and $(Me_4N)_2(Cu,Co)Cl_4$ containing $CuCl_4^{2-}$ and $CoCl_4^{2-}$; this comparison is not possible using γ_P, since there are different numbers of atoms in the unit cells. Both γ_r and γ_P indicate that $(Me_4N)_2NiCl_4$ is more isomorphous with $(Me_4N)_2(Cu,Co)Cl_4$ than would be predicted from inspection of the table of bond angles; no explanation is offered for this.

The crystallographic data are of some help in trying to interpret the DSC measurements recorded in Chapter III; for a full interpretation low-temperature crystal data are desirable, but are not available at present.

The information available from a DSC trace is the transition temperature, ΔH for the transition (from the area under the peak) and ΔS ($= \Delta H/T$ for sharp transitions). In this case absolute values of ΔH are not available, for reasons given, but relative measurements are available.

The DSC traces of all the single-metal compounds are seen to be of approximately the same form, showing a broad transition peaking at about room temperature, and a sharper transition at a lower temperature. The heat capacity of $(Me_4N)_2ZnCl_4$ has already been measured by Melia and Merrifield.[26] The DSC curve agrees in general form with this, except that the lower temperature transition obtained from heat capacity measurements is a single peak, whereas it is split into three on the DSC trace. No explanation is offered for this; the DSC curve remained constant for several preparations of the compound both from ethanol and water, with up to five recrystallizations. It therefore seems unlikely that any of the three DSC peaks are caused by trace impurities.

It has been suggested that these thermal transitions are due to the onset of thermal motion of the ions in the crystal. The crystal structures were all determined at room temperature, i.e. above

the peak temperature of the broad transition. At this temperature completely free rotation of the ions does not take place, and from the available data the exact nature of the disorder cannot be determined. It might take the form of either a large librational motion of both cation and anion, or a disordered arrangement of the ions in a number of configurations; or a combination of both of these.

The assumption was tried that the high-temperature and low-temperature transitions could each be assigned to a particular ion in the lattice. The higher temperature DSC transition is at the same temperature whether M = Co, Cu or Zn, and it was therefore postulated that this transition corresponds to the onset of thermal motion of the light atom tetrahedra. The extreme broadening of this transition is not understood, but it is possible that some more drastic change may take place in the lattice apart from thermal motion, since the DSC traces did not return to exactly the same baselines above the transitions, indicating that there had been a change in the heat capacities of the samples. The transitions peaking at lower temperatures were then postulated to correspond to the onset of thermal motion of the MCl_4^{2-} tetrahedra. If this were so, the much higher transition temperature found for $CuCl_4^{2-}$ may be related to the greater distortion of $CuCl_4^{2-}$ causing a greater hindrance to motion. The transition temperatures for $CoCl_4^{2-}$ and $ZnCl_4^{2-}$ are relatively close, and these two anions are very similar in both size and degree of distortion. This assignment of the transitions suffers from the disadvantage that the light atom tetrahedra might be expected to commence rotation at a lower temperature than the heavy atom tetrahedra; however the above assignment appears to agree better with the known experimental facts, and so it is discussed further.

It was hoped that DSC measurements on the solid solutions would help to clarify the behaviour of the single-metal compounds, and in particular whether the assignment of the transitions was reasonable or not. In fact, while not inconsistent with the views outlined above,

they give no conclusive evidence in favour of the assignment; however an explanation of the solid solution behaviour will be attempted. This is somewhat complicated, as shown in Fig.III.7, and includes a number of transitions which appear only at intermediate compositions. The origin of these is completely unexplained, but if they are ignored, the shifts of the two types of transition assigned above can be examined.

There was a variation in the behaviour of the solid solutions, depending upon whether or not they contained $CuCl_4^{2-}$. In the case of $(Me_4N)_2(Co,Zn)Cl_4$ the broad transition remained at constant temperature and ΔH through the whole solid solution series (Fig.III.7), but there were shifts in the sharp transitions. In the cases of $(Me_4N)_2(Cu,Co)Cl_4$ and $(Me_4N)_2(Cu,Zn)Cl_4$ the same types of shift occurred in the sharp transitions, but both ΔH and T for the broad transition decreased to a minimum at about 50:50 composition (Fig.III.8). This corresponds to thermal rotation being easier in the distorted lattice (in the region where non-ideal solid solutions are formed) than in the pure end-members.

The direction ($\pm$ T) of the shift of a peak assigned to a particular MCl_4^{2-} tetrahedron depends on the other anion which is present in the solid solution. The two transitions tend to move towards each other, as illustrated below in an idealized case:-

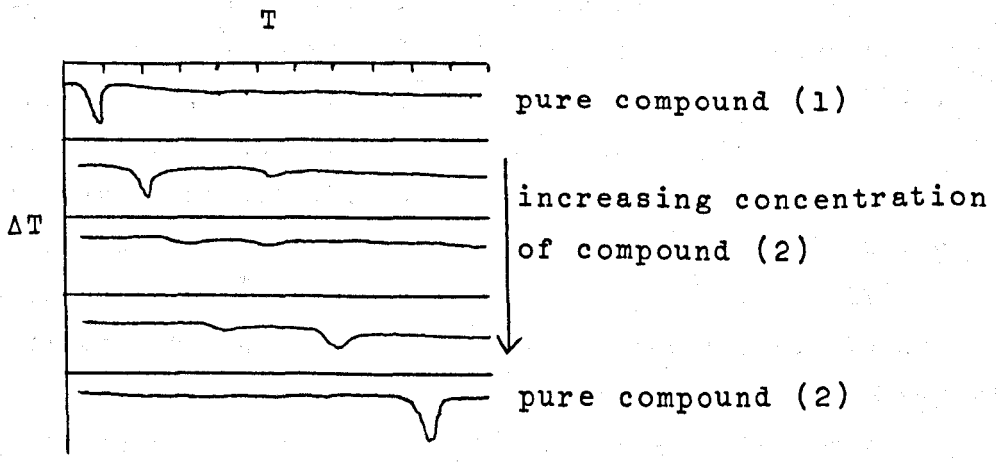

The radii of the MCl_4^{2-} tetrahedra are in the order $CuCl_4^{2-} < CoCl_4^{2-} < ZnCl_4^{2-}$, but the differences are fairly small. An explanation of the shifts is based on the relative sizes of the ions, and also the shape of $CuCl_4^{2-}$. Suppose that A(1) is the compound containing the MCl_4^{2-} ion of smaller size ($M^{(1)}Cl_4^{2-}$) and A(2) contains the ion of large size ($M^{(2)}Cl_4^{2-}$). Then introduction of a small proportion of A(2) into A(1) might be expected to cause slight expansion of the lattice, making movement of $M^{(1)}Cl_4^{2-}$ easier (i.e. a peak shift -T); conversely introduction of A(1) into A(2) would cause contraction of the lattice, so that $M^{(2)}Cl_4^{2-}$ rotates less easily. The size effect alone could explain the behaviour found; however the distortion of $CuCl_4^{2-}$ probably plays a part in causing the much greater difference between $CuCl_4^{2-}$ and the other two ions than between $CoCl_4^{2-}$ and $ZnCl_4^{2-}$.

Solid solution formation finds considerable use in single crystal spectral and esr studies, in which a small amount of paramagnetic compound is introduced into a host lattice so that solid dilution isolates the paramagnetic species from each other. Often the host lattice is that of an isomorphous diamagnetic compound, so that for example the spectra of $CuCl_4^{2-}$ in Cs_2ZnCl_4 [27] and $CoCl_4^{2-}$ in $(Me_4N)_2ZnCl_4$ [28] have been studied. The solid solution spectra in Chapter III were measured from powdered samples, but are in general agreement with the single crystal data. The positions of the bands in $(Me_4N)_2(Co,Zn)Cl_4$ remain constant over the whole range of $CoCl_4^{2-}$ concentration; however this is not always the case, and sometimes extreme changes are found, as when Cu^{2+} replaces Zn^{2+} in $ZnHg(CNS)_4$.[29] The site symmetries of Cu^{2+} in $CuHg(CNS)_4$ and $(Cu,Zn)Hg(CNS)_4$ are different, the former being tetrahedral and the latter tetragonal, and the colour changes found are dramatic. Less extreme differences are found in introducing Cu^{2+} into $ZnK_2(SO_4)_2.6H_2O$,[30] but solid dilution still affects the position of the absorption peaks. Large changes are not expected for $(Me_4N)_2MCl_4$, but this work has been useful in establishing the constancy of the MCl_4^{2-} geometry in the pure

compounds and in the solid solution. No detailed data appear to have been previously published on this topic, although reference has been made to crystallographic work on $Cs_2(Cu,Zn)Cl_4$.[31]

It would otherwise be hard to justify the spectroscopists' method of preparation of solid solution crystals, which typically consists[28] of dropping a few crystals of the paramagnetic salt into a solution of the diamagnetic salt and growing crystals by evaporation. Evaporation produces non-homogeneous crystals, which would be unacceptable if, for example, $CuCl_4^{2-}$ changed slightly in geometry with variations in composition of the solid solution. Since $(Me_4N)_2CuCl_4$ is a typical tetrahedral tetrachlorocuprate, the same general behaviour is expected for other series of compounds, such as Cs_2MCl_4 and $(Et_4N)_2MCl_4$.

It would be interesting to prepare solid solutions of square planar tetrachlorocuprates, but the square planar MCl_4^{2-} ions are less common for other first row transition metals,[32] and ions such as $PtCl_4^{2-}$ or $PdCl_4^{2-}$ would have to be used. The size effect on lattice energy would be more pronounced in this case, so that the solid solutions might be more reluctant to form than in the tetrahedral case.

This work has shown the broad front on which solid solution studies have to be carried on, and more problems have been raised than answered. There is clearly much scope, for example, for further study of chlorometallate ions in concentrated solution, and the dependence of the species formed on the cation present. The subtle changes between the various lattices are not fully understood, particularly in relation to the DSC data; nor are the variations in lattice energy, so that measurement of the excess thermodynamic properties of the solid solutions would also be helpful.

REFERENCES FOR CHAPTER VI

1. P. Murray-Rust, D.Phil. Thesis, 1967.
2. Raymond, Meek and Ibers, Inorg.Chem. 1968, 7, 1111.
3. Colton & Canterford, "Halides of the First Row Transition Elements", Wiley, 1969.
4. Zaslow & Ferguson, Chem.Comm. 1967, 822.
5. Wiesner, Scrivastava, Kennard, D. Vaira & Lingafelter, Acta Cryst. 1967, 23, 565.
6. Seifert, Z.anorg.allgem.Chem. 1960, 307, 137.
7. Stucky, D'Agostino & McPherson, J.A.C.S. 1966, 88, 4828.
8. Remy & Laves, Berichte 1933, 66, 401.
9. Willett & Caputo, private communication.
10. Wertz & Kruh, J.Chem.Phys. 1969, 50, 4313.
11. Figgis, "An Introduction to Ligand Fields", Interscience, 1966.
12. Cotton, Goodgame & Goodgame, J.A.C.S. 1961, 83, 4690.
13. (a) Buffagni & Dunn, J.C.S. 1961, 5105.
    (b) Katzin, J.Chem.Phys. 1962, 36, 3034.
14. Scaife & Wood, Inorg.Chem. 1967, 6, 358.
15. (a) Howald & Keeton, Spectrochim.Acta 1966, 22, 1211.
    (b) Martin, Bull.Soc.Chim. 1966, 1237.
    (c) Antipova-Karataeva & Vainshtein, Zh.Neorg.Khim. 1961, 6, 1115.
    (d) Sergeeva & Dementlev, Zh.Neorg.Khim. 1960, 5, 1601.
    (e) Andreev & Sapozhnikova, Zh.Neorg.Khim. 1965, 10, 2538.
    (f) Furlani & Morpugo, Theoret.Chim.Acta 1963, 1, 102.
16. McConnell & Davidson, J.A.C.S. 1950, 72, 3164.
17. Golgotiu et al., Bull.Inst.Polit .Iasi 1963, 9, 113.
18. Griffiths & Scarrow, Trans.Farad.Soc. 1969, 65, 1727.
19. See Reference 5.
20. See Chapter II.
21. Wooster, "Diffuse X-ray Reflections from Crystals", Clarendon Press, 1962.
22. Guinier, "X-Ray Diffraction", Freeman 1963.
23. Ramachandran, "Crystallography and Crystal Perfection", Academic Press, 1963.

24. Cochran & Lipson, "The Determination of Crystal Structures", Bell, 1966.
25. Srinivasan et al., Acta.Cryst. 1963, 16, 1154.
26. Melia & Merrifield, J.C.S.(A) 1970, 1166.
27. Sharnoff & Reimann, J.Chem.Phys. 43, 2993.
28. Ferguson, J.Chem.Phys. 1963, 39, 116.
29. Forster & Goodgame, Inorg.Chem. 1965, 4, 823.
30. Mathur, J.Phys.Chem.Solids 1968, 29, 2068.
31. Furlani et al., Theoret.Chim.Acta 1967, 7, 375.
32. Cotton & Wilkinson, "Advanced Inorganic Chemistry", Interscience, 1966.

Figure VI.1

Comparison of the two isomorphism parameters for $(Me_4N)_2MCl_4$ compounds

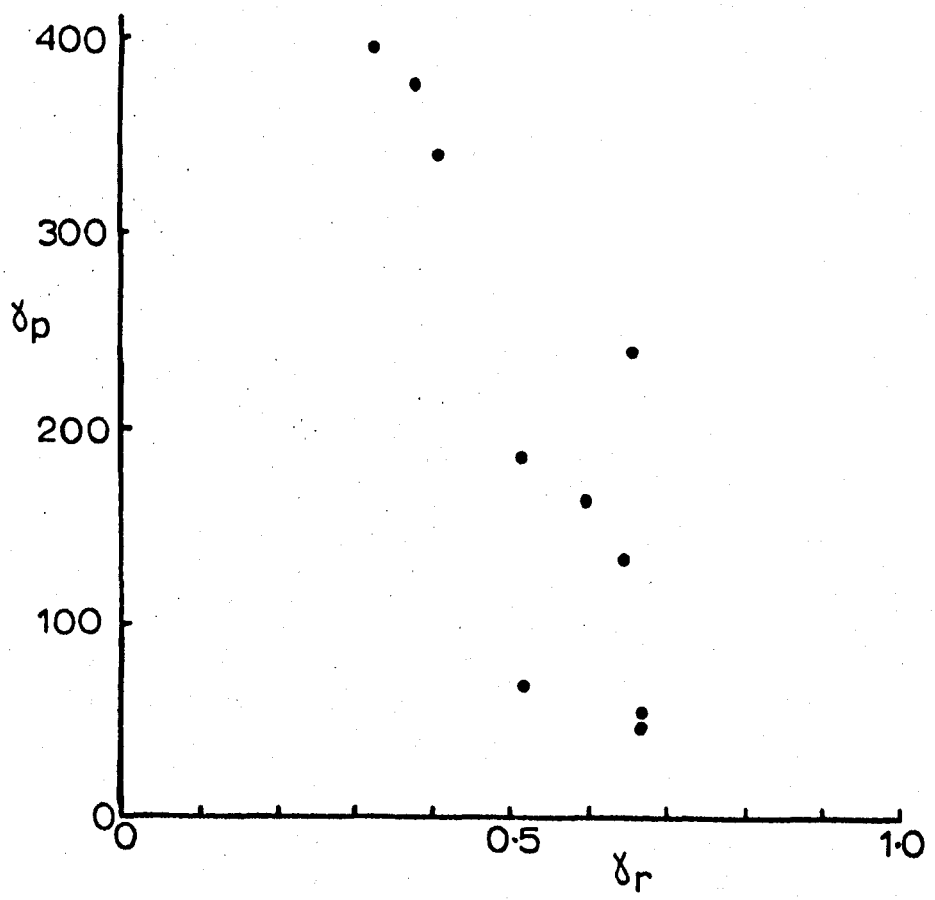

TABLE VI.1

Cell dimensions, bond distances and angles in the isomorphous compounds $(Me_4N)_2MCl_4$

Data for $(Me_4N)_2CuCl_4$ and $(Me_4N)_2CoCl_4$ are given in Chapter IV.

		$(Me_4N)_2ZnCl_4$	$(Me_4N)_2NiCl_4$
Cell dimensions (p.m)	a	1227.6	1226.4
	b	899.8	898.2
	c	1554.1	1548.6
Bond distances (p.m) in MCl_4^{2-}		224.4,224.6,225.3	220.0,224.0,223.4
Bond angles in MCl_4^{2-}		109.1,112.1, 108.4,109.9	107.8,114.4, 107.8,114.4.

TABLE VI.2

(a) The Ramachandran R_{obs} and γ_r (R_{obs}; γ_r)

	CU	CO	NI	ZN	CUCO 1 set	CUCO 2 set
Cu	0;1.00	51.1;0.380	48.9;0.407	55.5;0.327	27.7;0.664	27.6;0.664
Co			27.6;0.665	27.5;0.667		32.9;0.601
Ni				39.3;0.524		29.0;0.649
Zn						39.6;0.519
CUCO 1 set						5.2;0.936

(b) Positional test (γ_p)

Cu	0.0	377	342	395	241	182
Co			54	42	163	91
Ni				66	134	
Zn					185	

Abbreviations used are:

CU = $(Me_4N)_2CuCl_4$ etc.

CUCO 1 set = $(Me_4N)_2(Cu,Co)Cl_4$ with an averaged MCl_4^{2-} tetrahedron

CUCO 2 set = " with both $CuCl_4^{2-}$ and $CoCl_4^{2-}$ tetrahedra.

APPENDIX A

Structure Factors for $(Me_3NH)_3Cu_2Cl_7$

Values given are h,k,ℓ,F_{obs},F_{calc} and α.

H	K	L	FOBS	FCALC	ALFAC	H	K	L	FOBS	FCALC	ALFAC
2	0	0	167.6	173.5	0.3	5	3	0	39.9	63.4	182.5
4	0	0	116.0	99.4	0.6	7	5	0	15.7	12.1	14.6
6	0	0	127.9	128.3	1.3	9	5	0	9.2	7.8	161.9
8	0	0	180.6	162.2	3.6	11	5	0	27.0	25.9	182.6
10	0	0	91.2	84.7	1.4	13	5	0	6.3	8.1	190.4
12	0	0	39.0	39.5	4.8	15	5	0	4.7	2.7	48.3
14	0	0	27.8	28.4	4.7	2	6	0	119.1	98.7	0.3
16	0	0	43.2	41.0	7.0	4	6	0	66.5	65.1	2.1
18	0	0	15.9	19.8	3.2	6	6	0	42.5	49.4	5.2
3	1	0	50.2	35.9	179.3	8	6	0	56.0	52.2	1.4
5	1	0	45.5	39.9	5.5	10	6	0	33.7	36.1	6.9
7	1	0	21.1	23.1	172.4	12	6	0	23.7	24.1	5.5
9	1	0	39.4	38.1	178.1	14	6	0	23.4	20.9	9.5
11	1	0	13.2	11.9	171.2	16	6	0	9.6	11.2	5.8
13	1	0	3.7	4.8	35.5	18	6	0	6.7	8.5	6.8
15	1	0	4.8	6.2	179.3	1	7	0	26.9	26.3	180.9
17	1	0	10.9	10.4	174.7	3	7	0	42.2	38.8	5.1
2	2	0	5.5	12.6	345.4	5	7	0	4.1	6.5	21.2
4	2	0	27.6	27.2	1.5	7	7	0	31.5	30.0	180.2
6	2	0	26.0	22.5	357.6	9	7	0	5.5	7.0	171.3
8	2	0	20.0	18.9	351.0	11	7	0	13.2	11.0	26.0
10	2	0	28.4	24.0	350.7	15	7	0	7.2	5.7	173.1
12	2	0	10.7	11.7	356.0	2	8	0	57.2	44.6	179.7
14	2	0	7.1	4.0	208.5	4	8	0	23.8	19.5	3.1
16	2	0	5.3	4.9	343.8	6	8	0	17.6	15.3	183.4
18	2	0	9.4	9.5	355.4	8	8	0	37.2	30.4	186.9
1	3	0	160.6	174.4	180.5	10	8	0	7.6	6.7	188.3
3	3	0	58.9	54.6	181.6	1	9	0	59.0	55.6	180.6
5	3	0	66.4	63.4	182.5	3	9	0	132.3	125.3	181.3
7	3	0	119.6	101.8	183.8	5	9	0	119.8	100.4	183.2
9	3	0	100.0	89.9	182.9	7	9	0	53.2	49.6	182.0
11	3	0	29.2	30.3	181.3	9	9	0	23.7	25.2	183.7
13	3	0	15.0	14.0	183.4	11	9	0	44.2	40.5	185.9
15	3	0	30.3	24.9	188.0	13	9	0	47.7	42.2	187.0
17	3	0	23.9	22.2	187.0	15	9	0	13.2	12.6	186.2
2	4	0	48.6	38.7	359.4	2	10	0	20.9	19.2	358.2
4	4	0	90.1	79.8	182.8	4	10	0	19.3	20.7	355.7
6	4	0	2.3	3.1	205.0	6	10	0	29.0	25.8	354.9
8	4	0	32.3	28.7	357.1	8	10	0	3.2	5.1	354.0
10	4	0	10.8	9.7	356.1	10	10	0	5.0	7.4	349.8
12	4	0	17.6	14.2	197.2	12	10	0	9.6	7.6	359.3
16	4	0	4.2	5.2	355.5	14	10	0	13.8	13.3	355.9
18	4	0	4.8	5.8	353.8	16	10	0	6.3	7.2	358.1
1	5	0	50.3	36.0	181.0	1	11	0	11.5	10.7	1.8
3	5	0	27.6	30.5	180.8	3	11	0	14.7	17.1	176.7

H	K	L	FOBS	FCALC	ALFAC	H	K	L	FOBS	FCALC	ALFAC
5	11	0	15.5	15.5	172.0	4	18	0	31.0	29.9	359.2
9	11	0	9.7	8.3	10.4	6	18	0	41.1	41.2	2.8
13	11	0	16.1	14.2	175.6	8	18	0	15.5	16.3	5.0
2	12	0	111.6	97.3	0.9	10	18	0	22.0	22.7	6.0
6	12	0	94.7	84.3	0.6	12	18	0	13.1	14.0	1.8
8	12	0	33.7	33.4	2.2	14	18	0	9.8	10.2	1.9
10	12	0	41.3	39.5	2.6	1	19	0	4.8	1.0	15.3
12	12	0	63.6	53.8	4.7	3	19	0	29.6	28.0	180.9
14	12	0	28.8	28.7	2.0	5	19	0	11.3	13.3	177.3
16	12	0	8.0	8.4	358.5	9	19	0	5.0	4.1	179.3
1	13	0	17.4	14.3	6.1	11	19	0	6.5	7.5	176.4
3	13	0	17.2	17.1	176.9	13	19	0	6.8	8.3	175.3
5	13	0	39.5	36.7	180.3	2	20	0	12.8	11.6	185.7
7	13	0	9.3	7.8	168.1	4	20	0	19.1	15.4	183.1
9	13	0	15.0	12.1	19.6	6	20	0	7.3	5.0	176.8
11	13	0	8.9	9.0	175.2	1	21	0	37.9	41.6	182.4
13	13	0	14.4	13.1	174.4	3	21	0	18.1	20.0	178.7
15	13	0	9.0	8.3	168.3	5	21	0	8.9	10.6	176.2
2	14	0	29.7	26.7	3.4	7	21	0	31.3	27.7	184.2
4	14	0	36.8	37.3	358.3	9	21	0	26.0	24.6	187.0
6	14	0	25.0	23.2	354.4	11	21	0	7.6	10.0	180.6
8	14	0	27.0	26.2	3.3	6	22	0	5.1	6.7	193.6
12	14	0	16.1	15.3	355.2	1	23	0	5.2	5.1	188.9
14	14	0	15.2	16.0	359.6	3	23	0	6.3	8.3	6.4
1	15	0	56.2	54.7	180.2	2	24	0	39.1	38.6	358.9
3	15	0	104.5	90.2	181.5	4	24	0	12.2	15.6	4.4
5	15	0	95.5	86.1	181.4	6	24	0	20.1	22.2	2.9
7	15	0	35.5	31.8	180.3	8	24	0	34.4	38.0	3.7
9	15	0	23.8	25.0	185.4	10	24	0	18.1	20.2	3.4
11	15	0	53.7	42.9	186.6	1	25	0	7.9	12.6	179.9
13	15	0	29.5	30.2	183.7	3	25	0	3.5	6.0	5.8
15	15	0	13.9	15.0	180.0	5	25	0	4.7	5.2	17.2
17	15	0	0.8	6.9	191.9	2	26	0	10.6	10.6	355.3
2	16	0	10.7	13.0	359.3	8	26	0	3.7	7.8	355.9
4	16	0	27.4	26.2	354.8	10	26	0	6.9	8.1	356.9
6	16	0	16.4	15.8	355.5	1	27	0	27.7	27.9	178.0
8	16	0	13.0	12.3	194.0	3	27	0	10.7	12.3	180.0
12	16	0	16.8	15.0	357.1	5	27	0	8.6	9.4	186.1
14	16	0	9.7	9.4	354.5	7	27	0	20.7	20.8	183.6
1	17	0	9.0	12.2	174.9	9	27	0	12.2	18.0	181.8
3	17	0	10.3	10.4	178.9	2	28	0	5.8	6.3	1.8
5	17	0	13.3	11.9	175.3	6	28	0	3.4	5.0	2.4
7	17	0	11.3	13.5	177.3	8	28	0	6.9	10.4	358.1
9	17	0	8.1	10.2	184.3	1	29	0	9.6	8.9	175.7
2	18	0	38.4	38.7	3.8	3	29	0	7.6	9.5	180.7

H	K	L	FOBS	FCALC	ALFAC	H	K	L	FOBS	FCALC	ALFAC
2	30	0	9.9	11.3	359.4	2	2	1	85.8	78.6	329.0
4	30	0	5.0	7.5	0.1	2	4	1	35.4	36.8	206.4
6	30	0	2.7	10.2	5.5	2	6	1	11.6	11.6	33.5
1	31	0	4.2	6.5	177.3	2	8	1	35.2	32.2	9.2
0	4	0	4.2	13.5	0.0	2	12	1	18.5	21.0	27.1
0	6	0	59.0	54.3	0.0	2	14	1	16.7	16.3	343.0
0	10	0	37.8	37.3	0.0	2	16	1	31.2	30.6	196.6
0	12	0	38.0	44.1	0.0	2	18	1	20.7	20.2	178.7
0	14	0	33.8	30.5	0.0	-2	2	1	65.3	71.3	317.1
0	16	0	26.5	21.7	180.0	-2	4	1	52.3	61.8	184.3
0	18	0	28.0	33.0	0.0	-2	6	1	15.0	15.7	202.2
0	20	0	9.3	10.3	0.0	-2	8	1	16.0	16.7	47.1
0	24	0	52.3	50.8	0.0	-2	10	1	17.0	17.4	157.2
0	26	0	10.1	10.9	0.0	-2	12	1	18.4	19.5	30.4
0	28	0	13.2	17.5	0.0	-2	14	1	19.7	19.5	348.6
0	30	0	12.6	14.1	0.0	-2	16	1	22.4	21.5	217.0
0	6	1	108.0	107.4	318.5	-2	18	1	10.8	9.6	158.3
0	10	1	18.0	21.5	13.9	-2	20	1	14.7	11.5	5.0
0	12	1	13.9	14.1	320.5	3	1	1	36.6	40.5	21.4
0	16	1	41.0	45.3	226.0	3	3	1	102.7	104.6	315.8
0	18	1	26.9	29.9	148.7	3	5	1	16.7	12.1	329.7
0	20	1	6.6	6.0	230.1	3	7	1	26.4	22.6	29.7
0	22	1	28.6	27.7	140.4	3	9	1	4.3	4.0	154.3
0	26	1	13.7	15.1	318.2	3	11	1	52.2	52.4	131.1
1	5	1	50.4	52.2	190.3	3	13	1	34.4	36.0	311.7
1	7	1	26.3	24.6	169.4	3	15	1	8.0	7.7	133.3
1	9	1	48.0	45.8	150.7	3	17	1	12.2	11.6	209.8
1	11	1	70.2	57.7	175.7	3	19	1	9.2	10.2	333.0
1	13	1	17.8	16.9	357.8	3	21	1	9.5	10.6	123.6
1	15	1	36.7	31.7	316.4	3	23	1	9.5	11.1	204.6
1	17	1	16.8	16.0	6.2	-3	1	1	53.1	51.6	7.2
1	19	1	35.0	32.0	357.0	-3	3	1	106.3	119.0	321.4
1	21	1	9.5	8.0	50.6	-3	5	1	33.6	28.7	357.8
1	23	1	11.7	11.0	122.3	-3	7	1	42.1	36.6	13.5
-1	1	1	28.7	39.4	291.3	-3	9	1	5.9	7.2	339.8
-1	5	1	37.6	37.3	204.4	-3	11	1	51.1	49.1	126.0
-1	7	1	9.0	4.4	131.8	-3	13	1	34.2	32.7	311.6
-1	9	1	47.8	41.5	135.3	-3	15	1	9.7	9.2	145.6
-1	11	1	58.5	55.0	178.9	-3	17	1	19.3	17.8	190.6
-1	13	1	14.8	14.5	351.8	-3	21	1	15.0	13.3	141.1
-1	15	1	32.2	30.4	304.0	-3	23	1	13.3	13.6	194.5
-1	17	1	12.0	11.4	14.9	4	2	1	22.4	19.7	163.9
-1	19	1	27.1	27.7	0.1	4	4	1	120.6	115.5	224.4
-1	21	1	6.6	8.7	75.3	4	6	1	48.3	45.3	146.9
-1	23	1	13.4	14.6	128.5	4	8	1	9.6	10.0	325.0

H	K	L	FOBS	FCALC	ALFAC	H	K	L	FOBS	FCALC	ALFAC
4	10	1	47.8	47.7	126.3	6	10	1	18.3	16.6	176.7
4	12	1	5.3	4.4	358.5	6	14	1	20.1	19.4	343.2
4	14	1	23.8	26.8	309.5	6	16	1	12.8	11.5	266.6
4	16	1	12.1	13.2	144.1	6	20	1	11.7	12.3	16.1
4	18	1	17.0	18.2	315.2	-6	2	1	14.6	14.6	333.8
4	20	1	27.6	27.3	30.8	-6	4	1	49.0	50.7	179.0
4	24	1	9.1	7.9	13.8	-6	6	1	11.3	10.9	89.0
4	28	1	9.8	11.2	218.6	-6	8	1	23.5	23.5	347.3
-4	2	1	20.3	15.7	176.1	-6	10	1	11.8	13.0	148.4
-4	4	1	118.0	123.1	219.2	-6	12	1	11.3	7.7	71.7
-4	6	1	54.3	48.0	146.4	-6	14	1	17.0	18.7	322.9
-4	8	1	7.3	7.3	299.3	-6	16	1	14.2	14.6	227.0
-4	10	1	52.3	47.2	124.1	-6	18	1	9.4	6.0	173.4
-4	12	1	7.3	6.3	354.2	-6	22	1	11.5	10.3	138.1
-4	14	1	25.5	26.7	307.4	7	1	1	47.9	49.6	308.8
-4	16	1	14.7	13.7	137.9	7	3	1	18.6	17.5	25.0
-4	18	1	17.0	17.6	308.1	7	5	1	11.0	10.4	189.9
-4	20	1	26.7	27.0	21.9	7	7	1	5.3	6.5	320.8
-4	28	1	9.8	11.3	210.1	7	9	1	36.0	29.4	128.1
5	1	1	27.5	26.2	18.8	7	11	1	30.2	23.8	211.9
5	3	1	48.3	48.6	333.0	7	13	1	12.2	11.2	28.9
5	5	1	29.9	29.2	10.9	7	15	1	15.8	15.4	297.2
5	7	1	62.8	62.0	358.0	7	19	1	11.7	11.0	28.5
5	9	1	20.4	17.4	27.5	7	23	1	8.7	11.0	134.8
5	11	1	37.4	38.2	143.4	-7	1	1	40.6	46.8	301.7
5	13	1	21.7	21.4	292.0	-7	3	1	13.3	14.3	36.5
5	15	1	6.1	6.6	197.2	-7	5	1	28.9	25.2	164.8
5	17	1	14.3	14.1	236.8	-7	7	1	10.2	9.9	227.2
5	19	1	6.6	4.2	156.4	-7	9	1	35.5	31.5	138.7
5	21	1	20.2	20.7	151.1	-7	11	1	37.2	31.7	192.0
5	23	1	16.0	17.0	174.9	-7	13	1	14.9	13.5	10.0
5	27	1	9.0	8.9	311.1	-7	15	1	20.3	20.0	310.5
-5	1	1	26.9	25.7	31.7	-7	17	1	9.4	7.8	343.7
-5	3	1	47.3	44.1	317.3	-7	19	1	22.4	19.4	11.8
-5	5	1	22.0	20.5	14.3	8	2	1	34.9	36.2	320.6
-5	7	1	53.7	54.0	357.3	8	4	1	19.8	17.5	176.3
-5	9	1	17.7	15.9	32.9	8	6	1	32.9	30.3	317.1
-5	11	1	45.1	43.3	136.8	8	8	1	47.5	43.5	54.9
-5	13	1	23.6	27.7	289.8	8	10	1	15.9	13.7	7.5
-5	17	1	12.8	13.0	230.6	8	12	1	18.8	15.6	354.7
-5	21	1	15.0	17.7	143.9	8	16	1	29.2	28.3	209.1
-5	23	1	14.6	15.4	178.5	8	18	1	19.0	21.7	156.2
6	2	1	6.1	6.9	290.9	8	22	1	12.3	11.4	138.2
6	6	1	21.4	20.6	159.3	-8	2	1	39.6	39.6	316.5
6	8	1	8.6	8.7	359.4	-8	4	1	12.8	14.0	158.8

H	K	L	FOBS	FCALC	ALFAC	H	K	L	FOBS	FCALC	ALFAC
-8	6	1	34.6	31.6	312.9	11	3	1	15.8	16.9	309.6
-8	8	1	52.3	46.9	41.7	11	5	1	6.4	6.4	145.8
-8	10	1	13.2	12.0	6.0	11	7	1	6.6	6.9	37.6
-8	12	1	13.9	13.4	358.1	11	11	1	28.6	27.9	147.4
-8	16	1	32.0	31.4	199.3	11	13	1	11.7	11.8	310.8
-8	18	1	21.3	22.9	150.3	11	23	1	5.9	5.2	220.2
-8	22	1	10.7	12.4	136.0	-11	1	1	14.2	14.2	34.2
9	1	1	19.4	22.7	302.3	-11	3	1	22.1	20.5	315.3
9	3	1	5.7	6.5	265.7	-11	5	1	6.4	5.6	61.4
9	5	1	31.3	26.9	208.2	-11	7	1	20.8	17.5	357.7
9	7	1	15.9	14.7	188.4	-11	9	1	6.6	8.4	276.2
9	9	1	38.2	28.3	149.3	-11	11	1	25.2	25.6	133.3
9	11	1	32.1	27.9	177.3	-11	13	1	9.5	11.3	300.0
9	13	1	9.4	8.4	33.0	-11	21	1	9.1	10.1	130.1
9	15	1	15.0	13.7	324.8	12	4	1	28.4	29.0	212.4
9	17	1	9.5	10.1	8.2	12	6	1	11.7	14.1	142.0
9	19	1	20.6	21.8	359.2	12	8	1	6.8	3.2	335.9
-9	1	1	26.5	28.1	295.2	12	10	1	9.5	11.1	131.8
-9	3	1	5.7	5.8	296.9	12	20	1	11.0	10.1	49.0
-9	5	1	24.3	25.5	202.4	-12	4	1	30.5	33.6	195.7
-9	7	1	10.2	8.3	199.3	-12	6	1	17.7	16.1	144.3
-9	9	1	28.1	26.7	138.4	-12	10	1	11.7	13.3	126.0
-9	11	1	27.0	26.3	181.6	13	1	1	11.7	10.7	27.1
-9	13	1	13.1	10.9	2.8	13	3	1	20.2	22.6	338.2
-9	15	1	11.7	12.0	310.8	13	5	1	6.8	9.8	9.5
-9	17	1	6.8	9.6	23.1	13	7	1	16.3	14.6	22.8
-9	19	1	18.5	20.4	354.3	13	11	1	6.4	6.4	139.0
-9	21	1	8.7	7.5	7.9	13	13	1	10.6	10.8	307.7
10	2	1	17.2	16.0	345.7	13	15	1	8.2	5.5	181.7
10	4	1	12.2	11.0	209.2	-13	1	1	11.7	14.2	23.7
10	6	1	18.8	18.3	3.0	-13	3	1	19.1	20.2	327.7
10	8	1	34.5	29.5	354.9	-13	5	1	6.8	9.4	20.2
10	12	1	6.6	8.2	70.5	-13	7	1	15.0	15.6	12.8
10	16	1	16.3	15.0	198.0	-13	13	1	10.8	12.4	292.8
10	18	1	9.1	11.2	192.5	14	4	1	19.6	22.0	178.6
-10	2	1	16.9	16.7	313.4	14	6	1	11.2	10.8	193.9
-10	4	1	21.9	18.9	188.4	14	8	1	6.3	6.7	151.1
-10	6	1	6.3	7.2	340.4	-14	2	1	9.4	9.1	299.9
-10	8	1	22.0	21.0	2.0	-14	4	1	16.1	16.8	176.9
-10	10	1	6.4	6.6	120.0	15	1	1	10.6	10.2	319.6
-10	12	1	14.9	9.1	70.6	15	3	1	6.1	7.0	15.8
-10	14	1	6.8	7.0	330.2	15	7	1	8.2	7.4	340.1
-10	16	1	9.5	12.3	202.1	-15	1	1	8.9	10.1	306.4
-10	22	1	7.7	6.5	160.1	16	6	1	5.3	9.1	323.2
11	1	1	9.1	11.5	78.7	16	8	1	7.0	10.4	52.2

H	K	L	FOBS	FCALC	ALFAC	H	K	L	FOBS	FCALC	ALFAC
16	10	1	7.7	3.4	347.8	6	2	2	54.0	53.9	355.7
-16	8	1	8.7	13.3	23.8	6	4	2	45.5	50.8	342.3
-16	10	1	10.5	3.0	342.3	-1	7	2	88.9	96.2	169.6
0	4	2	28.8	36.8	329.2	-1	9	2	57.2	64.7	215.1
0	8	2	32.0	33.7	319.3	-1	11	2	29.2	36.3	157.6
0	10	2	59.2	65.1	356.6	-1	13	2	15.3	16.6	115.8
0	12	2	38.8	42.2	9.6	-1	15	2	36.1	30.3	238.8
0	14	2	58.3	62.5	0.6	-1	17	2	42.5	39.9	161.7
0	16	2	27.6	24.7	334.1	-1	19	2	21.7	20.6	155.3
0	18	2	35.8	29.5	42.7	-1	21	2	42.3	35.2	204.0
0	20	2	15.8	17.5	357.4	-1	23	2	6.5	6.1	108.1
0	22	2	13.1	14.0	294.7	-1	27	2	6.2	6.9	204.6
0	24	2	16.6	16.0	24.0	2	2	2	18.6	26.4	315.0
0	26	2	4.7	7.6	226.4	2	4	2	14.3	16.0	324.4
0	30	2	2.0	4.3	76.9	2	6	2	48.2	50.2	26.7
4	0	2	42.6	45.8	29.6	2	8	2	58.2	59.1	332.3
6	0	2	75.5	74.4	40.6	2	10	2	57.7	57.8	353.4
8	0	2	50.9	46.1	31.6	2	12	2	68.6	72.4	28.0
10	0	2	20.5	22.2	115.7	2	14	2	18.1	16.4	354.7
-4	0	2	54.1	52.8	22.2	2	16	2	26.2	23.5	327.7
-6	0	2	51.2	53.9	66.6	2	18	2	30.0	26.1	17.1
-8	0	2	33.2	38.1	32.4	2	20	2	15.9	16.3	315.1
-10	0	2	28.5	26.6	46.4	2	22	2	15.9	14.0	338.1
-12	0	2	27.0	26.2	30.4	2	24	2	16.5	16.7	56.5
-14	0	2	19.7	19.7	29.0	-2	2	2	33.9	47.9	334.4
-16	0	2	6.7	9.2	58.1	-2	4	2	40.1	45.2	347.6
1	5	2	32.1	31.9	160.9	-2	6	2	40.6	52.8	24.8
1	11	2	44.9	50.3	157.6	-2	8	2	33.0	40.2	311.2
1	13	2	32.7	34.0	144.1	-2	10	2	35.5	39.4	357.7
1	15	2	39.3	42.0	217.1	-2	12	2	37.1	41.0	42.3
1	17	2	49.1	41.5	163.0	-2	16	2	10.1	13.0	293.0
1	19	2	24.1	20.9	164.7	-2	18	2	27.6	23.2	21.3
1	21	2	31.3	29.8	210.8	-2	20	2	18.0	18.8	337.1
1	23	2	10.5	9.7	56.8	-2	22	2	20.3	19.8	341.8
1	25	2	8.5	8.9	24.8	-2	24	2	30.0	25.6	31.4
1	27	2	5.3	4.5	259.5	-2	26	2	8.6	10.3	350.3
-1	5	2	33.4	32.0	161.3	3	1	2	12.6	12.6	140.8
-5	13	2	16.5	15.4	44.7	3	3	2	61.7	57.6	217.7
-5	15	2	21.4	22.2	242.5	3	7	2	47.7	51.8	137.2
-5	17	2	15.5	17.7	128.9	3	9	2	64.9	71.2	221.7
-5	19	2	31.3	30.5	173.7	3	11	2	23.1	21.7	91.2
-5	21	2	24.6	21.6	204.6	3	13	2	22.2	20.0	92.5
-5	23	2	10.7	12.2	176.3	3	15	2	44.0	37.5	216.3
-5	25	2	3.3	4.8	165.5	3	17	2	20.1	19.4	139.5
-5	27	2	7.2	9.0	197.7	3	19	2	41.7	31.0	189.1

H	K	L	FOBS	FCALC	ALFAC	H	K	L	FOBS	FCALC	ALFAC
3	21	2	24.7	22.3	208.4	5	7	2	50.8	47.1	161.0
3	23	2	10.4	11.5	151.2	5	9	2	54.6	50.9	215.9
3	25	2	7.6	6.6	124.9	5	11	2	30.9	28.6	62.9
-3	7	2	37.9	48.6	147.7	5	13	2	30.5	21.7	23.2
-3	9	2	48.7	57.8	234.9	5	15	2	23.0	21.7	278.1
-3	11	2	33.6	34.3	46.3	5	17	2	13.8	14.1	128.1
-3	13	2	30.9	28.7	50.1	5	19	2	37.3	29.0	172.7
-3	15	2	27.3	28.4	233.3	5	21	2	28.9	27.7	199.1
-3	17	2	12.2	14.5	130.7	5	23	2	23.0	17.3	179.2
-3	19	2	25.7	30.1	190.7	5	25	2	10.0	10.0	159.9
-3	21	2	33.1	31.0	202.8	5	27	2	17.4	13.3	197.1
-3	23	2	18.8	19.2	154.8	-5	1	2	30.9	36.0	131.1
-3	25	2	13.7	12.3	145.6	-5	3	2	61.1	63.1	217.7
-3	27	2	8.9	10.7	203.8	-5	5	2	59.4	63.3	176.9
-3	29	2	6.5	8.2	183.0	-5	9	2	53.2	64.5	210.4
4	4	2	30.8	32.1	308.6	-5	11	2	19.7	18.3	82.7
4	6	2	75.3	68.1	34.5	6	6	2	44.1	40.0	10.0
4	8	2	53.7	46.5	356.9	6	8	2	24.4	25.7	303.5
4	10	2	27.0	25.7	248.5	6	10	2	8.8	10.0	337.0
4	12	2	52.8	46.6	29.0	6	12	2	25.8	24.8	57.5
4	14	2	23.7	17.9	225.5	6	14	2	5.0	5.0	263.2
4	16	2	8.6	10.7	320.3	6	16	2	11.0	11.4	292.7
4	18	2	16.9	16.7	48.5	6	18	2	24.7	20.5	38.7
4	20	2	12.5	12.3	338.1	6	20	2	15.9	15.2	348.2
4	22	2	32.4	29.5	350.7	6	22	2	23.4	20.1	343.4
4	24	2	22.8	16.8	20.9	6	24	2	27.0	24.3	23.7
4	26	2	22.2	16.8	1.8	6	26	2	11.7	11.1	343.2
4	28	2	4.3	5.0	354.7	-6	2	2	42.3	35.9	352.3
-4	4	2	23.3	26.8	320.8	-6	4	2	33.8	31.6	322.9
-4	6	2	64.5	71.9	34.7	-6	6	2	35.6	38.4	8.9
-4	8	2	47.8	46.3	349.3	-6	8	2	29.3	31.0	327.7
-4	10	2	24.4	25.2	239.1	-6	10	2	17.8	19.8	357.6
-4	12	2	36.7	42.7	30.7	-6	12	2	43.3	46.9	25.4
-4	14	2	25.1	20.5	199.3	-6	14	2	14.7	14.6	330.3
-4	16	2	4.9	6.7	306.8	-6	16	2	16.7	18.2	323.3
-4	18	2	15.6	15.1	37.9	-6	18	2	22.2	22.6	34.8
-4	20	2	14.6	14.3	332.5	-6	20	2	8.4	9.7	339.0
-4	22	2	31.0	31.4	349.6	-6	24	2	12.8	15.2	29.6
-4	24	2	20.5	19.6	21.1	7	1	2	20.2	21.6	85.6
-4	26	2	15.9	18.1	359.2	7	3	2	64.8	65.2	210.6
-4	28	2	4.4	5.6	346.1	7	5	2	33.1	32.2	133.2
-4	30	2	3.6	7.3	31.7	7	7	2	64.6	65.1	179.5
5	1	2	43.9	54.2	145.4	7	9	2	36.7	33.8	231.4
5	3	2	75.6	74.3	212.5	7	11	2	13.6	12.9	133.0
5	5	2	60.1	60.0	177.0	7	13	2	12.8	13.7	122.4

H	K	L	FOBS	FCALC	ALFAC	H	K	L	FOBS	FCALC	ALFAC
7	15	2	12.3	11.0	243.0	9	1	2	28.8	21.4	34.0
7	17	2	33.1	26.2	173.1	9	3	2	32.4	30.1	227.7
7	19	2	13.0	11.9	160.3	9	5	2	20.4	19.0	145.0
7	21	2	27.7	27.1	205.3	9	7	2	52.5	45.4	167.6
7	23	2	9.3	9.9	141.9	9	9	2	36.1	36.2	210.1
7	25	2	4.9	5.0	117.7	9	11	2	34.2	27.5	165.3
7	27	2	14.0	9.2	208.3	9	13	2	24.9	21.5	155.7
-7	1	2	35.8	36.2	39.6	9	15	2	23.9	26.7	213.5
-7	3	2	45.8	44.9	219.4	9	17	2	32.5	25.5	168.1
-7	5	2	20.5	20.6	138.7	9	19	2	15.0	12.6	165.7
-7	7	2	67.8	70.2	179.7	9	21	2	18.9	16.8	207.5
-7	9	2	44.6	47.8	211.3	9	23	2	4.9	6.3	64.5
-7	11	2	29.2	27.2	146.0	9	25	2	3.1	5.3	33.4
-7	13	2	23.0	23.9	153.6	-9	1	2	18.7	16.4	26.5
-7	15	2	21.0	22.3	218.7	-9	3	2	36.4	40.8	212.0
-7	17	2	31.2	28.3	166.6	-9	5	2	19.3	19.8	130.0
-7	19	2	10.6	11.6	164.9	-9	7	2	41.9	46.2	162.7
-7	21	2	23.8	22.3	207.6	-9	9	2	39.6	33.2	220.6
-7	23	2	5.8	4.9	99.6	-9	11	2	23.9	21.7	165.0
-7	25	2	5.8	6.6	28.2	-9	13	2	12.9	15.2	145.7
-7	27	2	4.5	4.7	230.6	-9	15	2	18.1	19.5	210.9
8	4	2	14.4	14.2	348.9	-9	17	2	31.1	25.7	168.4
8	6	2	36.3	39.0	42.5	-9	19	2	6.2	9.4	185.3
8	8	2	29.0	31.2	339.7	-9	21	2	17.9	18.6	202.9
8	10	2	49.4	42.7	346.3	-9	23	2	5.1	4.2	76.1
8	12	2	28.0	25.7	19.9	10	4	2	13.8	16.5	310.6
8	14	2	34.6	27.1	15.3	10	6	2	33.6	27.5	18.0
8	16	2	11.3	10.3	315.9	10	8	2	24.2	28.9	349.6
8	18	2	24.2	20.3	26.0	10	10	2	33.5	24.8	2.9
8	20	2	17.1	15.1	337.5	10	12	2	50.1	40.2	24.5
8	22	2	9.3	9.7	314.1	10	14	2	22.5	18.7	337.1
8	24	2	11.0	11.8	37.2	10	16	2	21.0	17.5	333.2
-8	2	2	21.5	24.5	234.2	10	18	2	17.7	16.4	22.2
-8	4	2	11.8	9.7	354.1	10	20	2	5.5	4.9	303.9
-8	6	2	41.7	40.1	38.9	10	22	2	7.7	7.2	331.4
-8	8	2	36.7	32.3	338.3	10	24	2	5.6	4.8	57.0
-8	10	2	42.0	46.9	345.0	-10	2	2	14.6	14.2	329.5
-8	12	2	27.6	31.7	14.9	-10	4	2	21.0	20.8	330.0
-8	14	2	30.7	32.3	7.0	-10	6	2	29.5	28.7	18.0
-8	16	2	10.0	11.7	329.2	-10	8	2	21.5	20.3	340.6
-8	18	2	21.9	21.8	22.2	-10	10	2	17.0	17.4	358.9
-8	20	2	14.0	12.4	336.0	-10	12	2	27.2	26.7	30.5
-8	22	2	6.7	4.8	289.3	-10	14	2	8.5	8.5	332.8
-8	24	2	7.2	10.6	49.3	-10	16	2	5.2	6.8	304.6
-8	26	2	4.1	5.5	207.8	-10	18	2	13.7	13.5	24.9

H	K	L	FOBS	FCALC	ALFAC	H	K	L	FOBS	FCALC	ALFAC
-10	20	2	5.6	6.4	331.5	13	7	2	16.7	16.3	152.6
-10	22	2	12.2	10.8	343.3	13	9	2	18.2	18.1	229.2
-10	24	2	8.9	11.6	22.1	13	11	2	6.0	7.9	43.8
11	1	2	8.3	10.3	106.8	13	13	2	7.3	8.7	49.0
11	3	2	12.8	13.1	236.5	13	15	2	4.3	4.1	256.7
11	5	2	28.9	28.6	190.2	13	17	2	2.6	4.6	119.8
11	7	2	24.6	23.2	148.5	-13	1	2	9.2	10.6	160.3
11	9	2	42.7	38.2	206.4	-13	3	2	21.9	21.9	203.1
11	11	2	16.0	15.9	136.5	-13	5	2	27.0	27.9	168.8
11	13	2	9.0	8.6	118.5	-13	7	2	9.8	11.5	144.0
11	15	2	23.4	20.7	221.6	-13	9	2	21.6	21.6	217.6
11	17	2	14.3	10.7	129.0	-13	11	2	6.2	4.6	27.9
11	19	2	20.0	15.9	179.1	-13	13	2	4.8	7.9	38.5
11	21	2	10.2	9.8	198.4	-13	15	2	3.1	5.4	221.5
-11	1	2	22.4	21.7	143.4	-13	17	2	11.0	4.9	99.6
-11	3	2	24.2	23.2	210.1	-13	19	2	7.2	9.5	180.5
-11	5	2	32.3	31.9	187.4	14	8	2	8.2	9.8	305.2
-11	7	2	17.9	18.3	160.0	14	10	2	4.5	4.1	347.1
-11	9	2	29.1	28.3	209.1	14	12	2	3.0	4.0	102.8
-11	11	2	14.6	12.7	76.5	14	14	2	5.4	6.0	180.7
-11	13	2	11.2	10.4	25.9	-14	2	2	10.3	11.8	331.6
-11	15	2	16.7	15.6	235.8	-14	4	2	7.2	8.3	2.1
-11	17	2	7.7	7.5	114.0	-14	6	2	15.1	16.7	23.9
-11	19	2	15.2	15.7	177.4	-14	8	2	8.5	9.7	319.0
-11	21	2	12.7	14.8	193.3	-14	10	2	7.5	8.5	347.4
-11	23	2	4.9	5.7	166.5	-14	12	2	7.1	9.5	17.3
12	4	2	12.5	10.9	324.9	-14	14	2	2.9	1.1	115.9
12	6	2	27.2	25.2	32.8	-14	18	2	5.5	6.4	10.6
12	8	2	21.9	18.4	338.0	-15	1	2	4.8	4.1	54.5
12	10	2	8.3	10.5	279.5	-15	3	2	13.0	13.7	208.3
12	12	2	23.7	19.0	22.9	-15	5	2	5.7	5.0	157.4
12	14	2	3.5	5.3	229.1	-15	7	2	21.0	17.7	175.7
12	16	2	7.2	6.3	354.4	-15	9	2	11.9	12.3	201.6
12	18	2	7.1	7.2	28.6	-15	11	2	6.4	6.9	136.4
12	20	2	6.0	6.0	351.2	-15	13	2	5.8	5.5	139.6
-12	2	2	31.2	32.2	351.0	-15	15	2	6.2	6.9	219.0
-12	4	2	14.6	13.8	333.9	-16	2	2	7.3	7.4	207.3
-12	6	2	24.7	26.0	22.4	-16	4	2	6.5	6.0	337.0
-12	8	2	10.7	13.2	337.3	-16	6	2	10.9	12.6	13.3
-12	10	2	8.4	7.5	210.7	-16	8	2	8.0	8.0	347.1
-12	12	2	15.6	13.4	28.2	-16	10	2	11.2	11.9	2.3
-12	16	2	4.7	4.0	334.1	-16	12	2	8.2	8.8	7.8
-12	20	2	6.9	7.1	349.2	-17	1	2	2.5	5.6	27.9
-12	22	2	9.7	13.5	344.7	-17	3	2	9.3	7.8	207.5
13	5	2	26.7	26.5	170.2	-17	7	2	10.7	11.5	162.4

Appendix A

H	K	L	FOBS	FCALC	ALFAC	H	K	L	FOBS	FCALC	ALFAC
-17	9	2	8.2	10.1	201.0	-2	4	3	47.3	47.3	293.4
0	2	3	22.2	24.3	38.3	-2	6	3	30.2	27.4	354.1
0	4	3	44.3	46.8	217.7	-2	8	3	38.4	43.7	65.0
0	6	3	14.3	15.4	265.3	-2	10	3	28.3	28.5	216.8
0	8	3	71.9	66.4	115.8	-2	12	3	10.1	10.0	155.9
0	10	3	47.3	44.9	225.6	-2	14	3	15.6	15.5	60.3
0	12	3	11.0	10.6	252.7	-2	16	3	33.3	28.7	268.9
0	14	3	25.1	25.6	58.2	-2	20	3	21.5	20.4	102.6
0	16	3	31.5	27.1	297.2	-2	22	3	14.0	14.2	201.7
0	18	3	22.5	17.5	31.5	3	1	3	53.6	53.3	93.0
0	20	3	20.4	21.7	27.0	3	3	3	13.1	16.6	280.3
0	22	3	7.6	8.4	228.4	3	5	3	40.2	43.8	261.8
1	1	3	24.3	30.2	42.0	3	7	3	32.8	38.5	62.6
1	3	3	16.1	10.7	340.5	3	9	3	12.2	11.0	352.5
1	5	3	45.1	48.2	281.9	3	11	3	11.9	12.7	222.6
1	7	3	46.7	56.4	53.1	3	13	3	20.8	19.6	66.1
1	9	3	37.3	33.4	33.0	3	15	3	10.3	12.4	197.3
1	11	3	35.0	33.9	290.9	3	17	3	24.7	26.0	248.6
1	13	3	29.3	31.3	80.6	3	19	3	13.5	15.3	95.1
1	15	3	18.7	20.1	252.8	3	21	3	6.0	7.8	105.0
1	17	3	36.8	34.8	217.0	3	23	3	9.2	8.3	274.7
1	19	3	22.8	23.1	129.1	3	25	3	7.6	8.9	66.9
1	21	3	13.5	11.9	176.8	3	27	3	5.2	6.3	305.9
1	23	3	8.8	8.6	202.1	-3	1	3	50.3	42.6	91.8
-1	1	3	14.9	15.0	53.4	-3	3	3	23.4	22.8	227.3
-1	3	3	20.0	21.7	175.1	-3	5	3	55.8	64.7	226.3
-1	5	3	52.4	53.2	253.0	-3	7	3	39.9	33.9	114.1
-1	7	3	45.8	47.6	79.5	-3	9	3	9.9	8.3	167.6
-1	9	3	26.1	23.1	77.2	-3	11	3	22.8	23.4	201.2
-1	11	3	50.2	46.2	278.2	-3	13	3	29.0	26.5	66.0
-1	13	3	35.6	33.4	75.1	-3	15	3	11.1	11.5	302.7
-1	15	3	16.0	16.5	280.8	-3	17	3	28.2	25.7	281.3
-1	17	3	26.0	20.7	221.9	-3	19	3	22.9	22.2	53.0
-1	19	3	18.7	18.5	82.6	-3	21	3	10.4	11.9	41.4
2	2	3	32.9	42.1	46.6	-3	23	3	8.6	9.0	309.8
2	4	3	45.7	56.6	262.2	-3	25	3	5.8	7.4	48.9
2	6	3	20.6	22.1	169.6	4	2	3	36.2	45.3	65.3
2	8	3	25.8	27.2	116.6	4	4	3	60.4	69.6	299.3
2	10	3	46.2	44.0	193.3	4	6	3	29.4	26.4	62.1
2	12	3	18.6	18.0	146.2	4	8	3	34.4	32.0	34.9
2	14	3	22.2	22.9	31.9	4	10	3	23.3	23.6	203.8
2	16	3	27.4	29.5	301.7	4	14	3	12.1	12.0	47.8
2	18	3	24.4	23.4	344.4	4	16	3	13.2	13.3	215.1
2	20	3	25.2	26.0	65.4	4	18	3	14.8	14.4	308.4
2	28	3	8.8	10.0	259.9	4	20	3	18.7	18.7	101.3

H	K	L	FOBS	FCALC	ALFAC	H	K	L	FOBS	FCALC	ALFAC
4	22	3	14.0	15.1	230.1	6	8	3	36.3	36.7	63.3
4	24	3	6.0	7.7	170.1	6	10	3	18.2	16.2	251.1
4	26	3	5.0	7.2	92.1	6	14	3	11.3	11.3	50.7
4	28	3	3.9	9.1	286.5	6	16	3	20.3	21.2	261.6
-4	2	3	50.2	57.7	55.4	6	18	3	6.0	7.1	173.7
-4	4	3	71.6	69.9	299.3	6	20	3	16.1	16.8	121.9
-4	6	3	32.0	29.7	38.8	6	22	3	14.2	15.0	205.1
-4	8	3	37.5	35.6	20.0	6	24	3	6.0	5.1	167.3
-4	10	3	30.6	22.1	195.6	-6	2	3	27.7	27.3	31.2
-4	12	3	5.9	5.0	124.3	-6	4	3	49.0	47.4	261.0
-4	14	3	11.5	11.5	56.7	-6	6	3	26.9	23.3	122.9
-4	16	3	19.9	18.3	214.5	-6	8	3	31.9	29.0	95.2
-4	18	3	13.0	14.3	281.9	-6	10	3	33.9	29.0	204.4
-4	20	3	19.7	20.3	104.5	-6	12	3	6.4	8.3	217.3
-4	26	3	11.8	6.0	79.1	-6	14	3	21.0	18.2	15.2
-4	24	3	6.1	8.6	173.9	-6	16	3	14.7	15.2	296.0
-4	26	3	3.7	6.0	79.1	-6	18	3	9.9	10.9	353.4
5	1	3	28.7	25.2	87.4	-6	20	3	21.0	17.8	67.4
5	3	3	34.1	33.3	220.4	-6	22	3	7.8	10.8	232.9
5	5	3	48.4	54.8	219.0	7	1	3	15.3	14.5	41.3
5	7	3	46.0	42.8	115.3	7	3	3	28.9	28.2	160.9
5	9	3	18.8	17.8	156.8	7	5	3	36.3	38.0	241.3
5	11	3	22.0	24.4	257.5	7	7	3	19.6	19.2	94.4
5	13	3	18.9	16.3	53.9	7	9	3	19.7	17.7	120.4
5	15	3	4.8	5.4	339.6	7	11	3	29.2	27.3	289.1
5	17	3	14.8	15.8	294.3	7	13	3	28.5	28.8	90.1
5	19	3	20.3	20.1	66.3	7	15	3	14.8	15.0	299.0
5	21	3	12.0	10.6	4.7	7	17	3	13.9	16.5	259.8
5	23	3	6.9	8.8	303.4	7	19	3	16.1	15.2	81.2
5	25	3	6.4	8.5	64.2	-7	1	3	30.2	24.4	14.3
-5	1	3	45.9	38.3	89.8	-7	5	3	34.8	29.2	268.5
-5	3	3	25.3	25.0	237.1	-7	7	3	44.4	37.1	44.2
-5	5	3	50.2	41.5	233.8	-7	9	3	22.3	21.1	50.1
-5	7	3	44.2	38.9	83.5	-7	11	3	32.5	27.7	289.0
-5	9	3	3.9	4.1	87.3	-7	13	3	22.2	22.8	83.0
-5	11	3	17.6	18.3	255.3	-7	15	3	14.7	13.7	264.3
-5	13	3	17.1	16.2	34.7	-7	17	3	22.9	23.4	221.3
-5	15	3	3.4	5.1	165.2	-7	19	3	19.8	20.4	122.3
-5	17	3	19.6	18.9	249.1	-7	21	3	7.1	6.4	183.9
-5	19	3	14.0	15.5	70.9	8	2	3	22.2	22.2	67.1
-5	23	3	7.6	7.9	269.9	8	4	3	20.5	17.9	253.7
-5	25	3	7.2	10.5	69.8	8	6	3	16.3	17.0	296.7
6	2	3	39.3	41.4	20.5	8	8	3	29.1	26.0	111.0
6	4	3	39.9	40.7	306.0	8	10	3	19.7	22.3	227.9
6	6	3	23.3	21.0	20.1	8	12	3	12.0	9.7	150.9

H	K	L	FOBS	FCALC	ALFAC
8	14	3	14.4	15.3	74.1
8	16	3	22.7	19.2	286.6
8	18	3	8.8	9.1	14.0
8	20	3	12.0	12.6	39.1
8	22	3	4.7	4.7	190.7
-8	2	3	26.0	24.1	62.4
-8	4	3	27.8	22.9	220.7
-8	6	3	18.3	16.0	245.2
-8	8	3	33.9	27.5	118.9
-8	10	3	29.1	30.7	213.7
-8	12	3	10.2	10.9	156.5
-8	14	3	16.3	18.2	48.0
-8	16	3	20.3	21.4	293.9
-8	18	3	15.5	13.7	10.2
9	1	3	13.8	14.3	54.2
9	3	3	4.6	5.2	14.1
9	5	3	27.7	26.6	296.3
9	7	3	31.4	29.2	48.2
9	9	3	22.6	17.5	31.0
9	11	3	20.3	19.1	292.5
9	13	3	21.5	17.8	92.8
9	15	3	9.1	11.1	236.9
9	17	3	16.7	19.1	217.0
9	19	3	10.0	11.9	136.6
-9	1	3	12.2	13.4	39.7
-9	3	3	9.5	10.6	110.2
-9	5	3	31.4	28.7	269.5
-9	7	3	23.9	22.4	38.0
-9	9	3	15.5	13.1	57.8
-9	11	3	22.9	20.0	278.1
-9	13	3	25.2	25.2	82.2
-9	15	3	10.4	10.9	246.6
-9	17	3	17.1	16.7	221.1
-9	19	3	8.3	8.6	94.4
10	2	3	11.3	11.5	47.0
10	4	3	28.6	28.8	263.9
10	6	3	21.4	19.4	159.6
10	8	3	20.0	20.6	130.6
10	10	3	23.9	24.8	203.4
10	12	3	8.5	7.0	178.6
10	14	3	11.6	11.9	27.9
10	16	3	12.0	11.8	332.4
10	18	3	15.0	16.5	0.6
10	20	3	11.9	12.2	53.5
10	22	3	5.1	6.7	300.6
-10	2	3	18.3	22.1	18.5
-10	4	3	24.3	24.9	284.9
-10	6	3	5.9	4.0	14.4
-10	8	3	24.9	20.5	69.5
-10	10	3	17.8	17.8	212.7
-10	12	3	6.0	6.1	166.6
-10	14	3	6.0	8.7	41.8
-10	16	3	9.4	10.4	255.2
-10	22	3	4.6	6.4	215.4
11	3	3	11.6	12.6	307.3
11	5	3	13.1	14.4	276.0
11	7	3	20.3	21.7	69.6
11	9	3	12.5	12.5	355.1
11	11	3	4.8	8.0	275.4
11	13	3	6.5	6.7	34.0
11	15	3	6.9	9.0	189.0
11	17	3	13.5	12.1	220.6
11	19	3	7.8	9.7	130.5
-11	1	3	13.8	12.8	88.7
-11	3	3	16.6	15.2	245.2
-11	5	3	30.1	26.7	215.7
-11	7	3	27.0	23.0	102.2
-11	11	3	9.8	10.8	225.3
-11	13	3	10.7	9.8	30.3
-11	17	3	7.3	7.1	270.0
-11	19	3	8.8	8.7	54.1
12	6	3	5.9	7.6	89.9
12	8	3	6.7	7.1	56.8
12	10	3	8.0	9.0	201.1
12	14	3	4.1	5.2	53.3
12	16	3	3.8	5.1	275.8
12	18	3	5.1	8.5	318.8
12	20	3	4.5	8.4	97.9
-12	2	3	18.8	20.8	44.1
-12	4	3	22.9	23.0	294.2
-12	6	3	14.7	14.1	46.1
-12	8	3	13.3	15.1	23.3
-12	10	3	10.1	8.1	204.5
-12	16	3	6.9	6.1	203.8
-13	1	3	17.5	17.5	95.0
-13	3	3	8.3	9.8	193.4
-13	5	3	15.5	17.1	217.5
-13	7	3	7.4	9.0	96.5
-14	2	3	10.7	13.7	41.5
-14	4	3	9.0	9.5	259.2

H	K	L	FOBS	FCALC	ALFAC	H	K	L	FOBS	FCALC	ALFAC
-14	6	3	4.4	3.6	22.9	-1	7	4	43.6	39.1	202.8
-14	8	3	4.3	5.6	80.4	-1	9	4	12.6	10.7	155.6
-14	10	3	7.0	8.1	197.0	-1	11	4	36.3	32.7	200.1
-15	1	3	5.8	6.6	9.4	-1	13	4	33.0	29.6	167.4
-15	5	3	6.9	9.3	264.6	-1	15	4	21.7	18.3	132.3
-15	7	3	10.5	9.3	41.4	-1	17	4	30.7	25.0	198.6
-15	9	3	3.6	6.4	42.6	-1	19	4	8.1	7.9	179.8
-15	11	3	5.2	7.7	284.0	-1	25	4	4.9	5.4	174.6
0	4	4	47.7	44.5	12.2	2	2	4	59.5	72.9	12.2
0	6	4	13.6	8.9	298.8	2	4	4	30.9	33.0	351.7
0	8	4	16.1	14.3	316.6	2	6	4	16.0	17.4	249.6
0	10	4	26.8	26.9	354.7	2	8	4	12.2	12.6	23.4
0	12	4	10.0	8.7	285.4	2	10	4	15.0	15.8	20.0
0	14	4	31.7	34.6	26.9	2	14	4	13.5	13.8	333.0
0	16	4	14.6	11.9	7.2	2	16	4	9.3	8.0	7.4
0	18	4	10.5	7.3	270.7	2	20	4	10.2	8.8	354.5
0	20	4	9.2	9.6	353.4	2	22	4	16.5	16.8	6.4
0	24	4	10.1	13.8	8.7	2	24	4	13.4	15.1	351.0
0	26	4	7.5	12.1	9.3	2	26	4	12.3	17.5	15.4
2	0	4	59.8	57.2	353.2	-2	2	4	27.9	26.6	10.5
4	0	4	22.6	21.8	294.8	-2	4	4	18.2	18.0	6.5
6	0	4	14.1	14.8	338.4	-2	6	4	16.8	15.8	230.9
8	0	4	34.6	31.8	16.2	-2	8	4	26.2	20.6	358.4
10	0	4	30.1	35.3	345.2	-2	10	4	46.5	47.5	10.5
12	0	4	14.7	13.2	351.2	-2	12	4	37.0	35.1	0.4
-4	0	4	11.1	12.7	268.4	-2	14	4	44.6	45.3	2.4
-6	0	4	26.3	33.0	338.3	-2	16	4	23.7	22.3	6.0
-8	0	4	33.1	41.0	10.5	-2	20	4	6.5	4.5	340.3
-10	0	4	18.6	16.0	328.8	3	1	4	41.7	48.1	180.2
-14	0	4	11.9	10.4	5.9	3	3	4	21.4	21.2	169.6
1	3	4	40.2	42.6	172.9	3	5	4	39.6	42.0	199.0
1	5	4	33.2	35.0	183.9	3	7	4	10.0	10.6	162.1
1	7	4	35.4	32.8	209.5	3	9	4	12.8	14.1	150.0
1	9	4	12.4	11.7	69.4	3	11	4	12.5	12.1	160.4
1	11	4	6.8	4.7	190.9	3	13	4	16.6	14.4	182.3
1	13	4	8.6	9.3	162.2	3	15	4	17.9	17.3	176.5
1	15	4	9.1	8.7	125.7	3	17	4	12.5	10.7	199.7
1	17	4	17.5	15.8	196.0	3	19	4	17.9	18.1	195.8
1	19	4	11.5	10.6	175.8	3	23	4	8.7	9.5	197.3
1	21	4	9.0	10.0	201.4	3	25	4	11.6	11.3	172.4
1	23	4	9.1	10.1	180.9	-3	1	4	10.4	10.7	179.1
1	25	4	11.4	13.6	180.1	-3	3	4	8.8	9.0	92.3
1	27	4	5.3	12.6	177.9	-3	5	4	33.6	33.2	204.2
-1	3	4	26.9	26.2	173.7	-3	7	4	27.9	26.4	189.6
-1	5	4	18.7	14.3	159.4	-3	9	4	26.8	24.0	152.7

H	K	L	FOBS	FCALC	ALFAC	H	K	L	FOBS	FCALC	ALFAC
-3	11	4	35.7	31.0	170.5	6	8	4	16.9	18.3	350.2
-3	13	4	41.2	37.0	186.7	6	10	4	39.6	40.2	3.1
-3	15	4	35.6	31.3	184.5	6	12	4	33.5	34.8	3.2
-3	17	4	24.0	22.7	185.6	6	14	4	36.5	38.8	8.1
-3	19	4	17.4	15.0	184.2	6	16	4	19.8	21.5	6.0
4	2	4	48.9	44.4	19.5	6	18	4	4.4	5.1	332.8
4	4	4	19.3	18.7	333.9	-6	2	4	41.3	53.1	12.4
4	6	4	8.1	5.1	304.5	-6	4	4	24.9	25.5	13.5
4	8	4	23.1	24.7	20.2	-6	6	4	8.9	8.9	240.9
4	10	4	19.1	20.0	331.7	-6	8	4	11.8	10.6	341.2
4	12	4	29.0	33.1	18.2	-6	10	4	13.9	13.3	327.5
4	14	4	29.5	27.6	3.1	-6	12	4	16.5	14.6	7.7
4	16	4	27.8	25.7	12.6	-6	14	4	18.1	16.4	18.5
4	18	4	11.4	9.6	305.6	-6	16	4	13.3	12.6	25.0
4	20	4	4.4	5.7	323.2	-6	20	4	7.4	6.9	327.6
-4	6	4	10.3	9.4	255.6	-6	22	4	11.5	12.2	5.7
-4	8	4	36.2	31.6	18.4	-6	24	4	6.2	10.3	359.4
-4	10	4	29.2	24.9	356.8	7	1	4	14.0	14.5	140.2
-4	12	4	36.0	37.2	15.1	7	3	4	16.0	16.6	198.7
-4	14	4	29.9	29.6	355.8	7	5	4	8.7	9.0	158.9
-4	16	4	27.3	26.3	8.6	7	7	4	36.1	30.3	212.3
-4	18	4	9.4	8.9	307.8	7	9	4	15.2	16.0	139.3
-4	20	4	4.6	4.1	337.2	7	11	4	26.5	25.5	188.1
5	1	4	13.9	12.9	179.8	7	13	4	29.0	30.1	184.5
5	3	4	12.2	9.0	109.2	7	15	4	18.0	19.2	157.7
5	5	4	17.5	21.5	168.6	7	17	4	21.4	20.3	198.0
5	7	4	20.5	22.8	207.5	7	19	4	5.9	7.3	127.9
5	9	4	26.2	24.8	188.1	-7	1	4	30.9	37.3	177.4
5	11	4	29.5	29.0	185.4	-7	3	4	29.2	28.8	178.2
5	13	4	33.3	32.9	182.5	-7	5	4	24.6	22.5	164.8
5	15	4	25.8	28.3	161.6	-7	7	4	28.3	28.9	215.8
5	17	4	19.8	20.3	192.5	-7	9	4	8.9	7.7	69.6
5	19	4	16.7	15.0	192.5	-7	13	4	8.1	7.3	195.2
-5	3	4	14.4	11.6	149.7	-7	15	4	10.5	8.7	94.5
-5	5	4	36.0	29.8	186.8	-7	17	4	15.1	13.6	197.2
-5	7	4	10.1	9.3	192.7	-7	19	4	6.1	9.1	165.4
-5	9	4	17.3	15.9	187.8	-7	23	4	4.6	7.8	184.1
-5	11	4	19.9	18.3	188.8	8	2	4	19.0	20.5	2.5
-5	13	4	24.5	21.8	173.6	8	4	4	22.2	22.1	354.9
-5	15	4	22.5	19.5	154.6	8	6	4	7.9	8.9	307.3
-5	17	4	13.3	12.5	202.0	8	8	4	10.5	10.9	18.4
-5	19	4	17.6	16.9	200.4	8	10	4	24.0	21.5	9.9
6	2	4	14.8	16.3	23.5	8	12	4	6.6	9.8	336.2
6	4	4	14.0	10.3	22.5	8	14	4	23.5	22.5	8.2
6	6	4	13.9	11.5	250.4	8	16	4	9.9	9.9	336.4

H	K	L	FOBS	FCALC	ALFAC	H	K	L	FOBS	FCALC	ALFAC
8	18	4	4.1	3.5	340.9	12	2	4	21.2	21.4	14.8
8	20	4	5.0	4.9	4.3	12	4	4	9.8	9.8	329.6
-8	2	4	35.7	32.4	7.8	12	8	4	7.1	7.6	9.5
-8	4	4	29.9	26.8	355.9	12	10	4	5.6	5.2	333.0
-8	6	4	8.9	10.7	266.2	12	12	4	9.0	11.5	17.0
-8	10	4	18.1	15.9	15.8	12	14	4	7.3	7.4	353.5
-8	14	4	18.1	16.9	9.4	12	16	4	6.6	9.7	22.4
-8	16	4	7.8	6.1	332.3	-12	2	4	17.2	15.1	24.5
-8	20	4	7.7	7.3	1.4	-12	8	4	11.7	11.4	359.9
9	1	4	30.4	31.8	186.3	-12	10	4	10.4	11.1	344.1
9	3	4	27.2	25.8	180.7	-12	12	4	18.4	18.7	10.0
9	5	4	18.1	15.9	181.4	-12	14	4	11.7	14.8	2.1
9	7	4	13.3	15.0	195.5	-12	16	4	10.2	13.5	16.4
9	17	4	8.9	8.4	203.2	13	1	4	7.0	8.3	146.5
-9	1	4	20.7	22.7	170.7	13	5	4	7.8	7.7	198.2
-9	3	4	23.2	21.6	193.5	13	9	4	7.9	9.9	174.3
-9	5	4	9.1	8.9	188.3	13	11	4	9.2	10.2	182.8
-9	7	4	19.7	20.1	199.0	13	13	4	10.5	13.8	191.9
-9	9	4	10.5	10.6	81.6	13	15	4	5.7	12.4	179.3
-9	11	4	17.0	13.4	182.3	-13	1	4	11.5	10.6	159.5
-9	13	4	18.0	14.4	179.4	-13	5	4	11.3	11.4	201.5
-9	15	4	7.7	6.5	142.2	-13	9	4	5.6	8.8	171.3
-9	17	4	13.9	13.8	205.1	-13	11	4	7.4	9.6	183.7
10	2	4	41.3	38.2	11.1	-13	13	4	8.2	11.1	183.9
10	4	4	20.0	20.5	7.0	-13	15	4	4.9	9.3	171.1
-10	2	4	16.8	16.4	15.6	14	8	4	5.2	6.1	358.4
-10	4	4	10.5	11.7	5.6	14	10	4	11.8	15.4	16.3
-10	8	4	13.3	10.9	12.0	14	12	4	9.2	15.3	3.6
-10	10	4	21.4	20.0	356.7	-14	2	4	14.3	14.9	5.6
-10	12	4	15.8	14.7	7.1	-14	4	4	6.7	6.1	348.6
-10	14	4	18.6	20.2	2.2	-15	1	4	11.8	11.3	183.6
11	1	4	33.5	28.0	186.0	-15	3	4	8.8	9.7	179.6
11	3	4	17.9	17.8	160.7	-15	5	4	7.9	6.6	160.0
11	5	4	22.0	19.5	193.4	-15	7	4	5.2	7.6	210.5
11	19	4	4.9	9.0	207.3	0	2	5	14.5	14.5	146.2
-11	1	4	10.5	9.3	211.8	0	4	5	12.2	10.7	330.8
-11	3	4	8.1	7.3	86.4	0	6	5	13.4	12.8	303.6
-11	5	4	12.4	12.0	181.2	0	8	5	25.0	26.5	136.1
-11	7	4	11.4	10.6	186.6	0	10	5	26.0	23.1	338.4
-11	9	4	12.1	11.0	187.8	0	12	5	10.0	9.8	17.7
-11	11	4	17.8	15.5	182.6	0	14	5	12.0	11.6	124.7
-11	13	4	17.5	15.9	177.0	0	16	5	14.9	17.4	296.7
-11	15	4	14.2	15.2	169.3	0	18	5	10.3	8.4	165.6
-11	17	4	10.5	10.3	181.0	1	1	5	15.6	14.4	129.2
-11	19	4	5.0	8.2	203.9	1	3	5	8.4	8.9	248.3

H	K	L	FOBS	FCALC	ALFAC	H	K	L	FOBS	FCALC	ALFAC
1	5	5	17.4	18.6	287.0	-3	11	5	8.2	8.0	273.4
1	7	5	31.3	29.8	151.3	-3	13	5	14.7	13.5	174.6
1	9	5	18.9	17.9	170.1	-3	19	5	11.4	11.8	146.8
1	11	5	9.8	8.7	251.9	4	2	5	20.7	22.4	148.0
1	13	5	18.0	15.9	154.8	4	4	5	23.3	25.7	328.5
1	15	5	13.7	12.4	348.1	4	6	5	10.8	9.5	174.2
1	17	5	21.8	20.1	341.7	4	8	5	13.8	10.4	141.2
1	19	5	8.0	9.5	63.9	4	10	5	10.2	10.0	322.6
-1	1	5	7.6	10.2	90.8	-4	2	5	24.7	25.4	160.4
-1	3	5	13.0	13.8	15.0	-4	4	5	21.3	23.8	306.9
-1	5	5	30.2	34.6	332.9	-4	6	5	14.3	12.6	162.1
-1	7	5	12.2	15.1	139.1	-4	8	5	16.3	14.6	132.4
-1	9	5	10.3	11.4	162.5	-4	10	5	10.0	6.6	294.3
-1	11	5	16.0	15.5	315.0	-4	14	5	6.2	5.9	144.2
-1	13	5	18.8	17.3	131.8	-4	20	5	11.8	9.4	126.9
-1	17	5	6.0	9.8	291.1	5	1	5	18.3	16.7	94.2
-1	19	5	10.0	10.3	130.2	5	3	5	17.0	17.5	350.6
2	2	5	12.6	14.1	163.9	5	5	5	23.6	25.6	336.9
2	4	5	27.5	32.1	328.2	5	7	5	13.0	12.2	99.5
2	6	5	15.6	13.7	23.0	5	11	5	8.6	9.2	351.4
2	8	5	22.0	23.1	57.6	5	13	5	10.6	8.4	151.5
2	10	5	21.7	23.4	347.8	5	17	5	11.4	11.3	299.3
2	14	5	12.2	13.0	171.6	5	19	5	10.3	11.9	156.6
2	16	5	6.0	9.2	261.7	-5	1	5	22.2	23.5	116.1
2	18	5	8.2	7.7	179.3	-5	3	5	15.8	13.4	329.1
2	20	5	14.3	17.1	160.2	-5	5	5	18.0	18.5	324.3
-2	2	5	19.3	23.6	174.2	-5	7	5	21.3	20.2	141.5
-2	4	5	15.1	14.1	245.3	-5	9	5	13.0	13.2	195.5
-2	6	5	18.8	15.7	202.9	-5	17	5	20.2	16.5	323.6
-2	8	5	29.1	29.8	138.2	-5	19	5	7.6	5.1	104.6
-2	10	5	12.3	13.2	316.0	6	2	5	24.2	22.3	176.5
-2	14	5	8.6	9.3	135.6	6	4	5	19.2	14.6	229.8
-2	16	5	18.3	18.7	323.1	6	6	5	13.2	19.0	202.9
3	1	5	25.0	25.6	131.0	6	8	5	25.6	24.7	148.5
3	3	5	11.1	13.5	305.0	6	14	5	8.4	7.4	115.5
3	5	5	14.5	15.5	315.8	6	16	5	17.9	16.9	327.8
3	7	5	28.1	27.8	141.6	-6	2	5	16.8	13.8	134.4
3	9	5	16.8	16.7	195.0	-6	4	5	21.2	22.3	323.4
3	11	5	6.0	7.7	204.7	-6	8	5	10.2	9.5	80.0
3	17	5	21.4	21.1	343.7	-6	10	5	21.8	18.7	351.4
-3	1	5	14.1	15.4	118.5	7	3	5	10.3	8.1	345.9
-3	3	5	21.4	23.4	335.4	7	5	5	30.8	29.4	342.6
-3	5	5	32.1	33.4	339.4	7	7	5	12.2	12.0	68.8
-3	7	5	21.0	21.9	76.9	7	11	5	10.5	13.1	314.8
-3	9	5	7.6	8.2	26.0	7	13	5	13.2	15.0	157.5

H	K	L	FOBS	FCALC	ALFAC	H	K	L	FOBS	FCALC	ALFAC
7	17	5	8.8	5.8	291.5	8	10	5	15.8	12.7	325.0
-7	1	5	11.4	9.4	95.6	-8	4	5	12.0	11.2	332.4
-7	3	5	10.0	7.3	219.1	-8	6	5	8.6	9.3	336.6
-7	5	5	13.1	12.4	272.0	-8	8	5	17.3	17.1	100.6
-7	7	5	23.2	20.9	151.1	-8	10	5	18.3	16.3	333.4
-7	9	5	17.2	15.4	171.5	9	5	5	13.6	11.7	306.6
-7	11	5	6.2	7.5	292.4	9	7	5	15.8	15.9	156.0
-7	13	5	12.0	11.7	153.9	9	9	5	10.2	10.3	179.6
-7	15	5	8.2	9.9	350.7	9	13	5	11.8	9.3	151.8
-7	17	5	16.3	15.3	336.4	-9	5	5	22.1	18.9	329.1
8	2	5	14.9	13.7	173.7	-9	7	5	10.6	10.4	115.7
8	4	5	6.2	4.7	304.6	-9	11	5	11.8	10.0	276.9
8	8	5	20.2	19.1	133.1	-9	13	5	12.6	11.2	145.9

APPENDIX B

Structure Factors for $(Me_4N)_2CuCl_4$

Values given are h, k, ℓ, F_{obs} and F_{calc}.

H	K	L	FOBS	FCALC	H	K	L	FOBS	FCALC
0	0	2	50.1	40.3	4	0	1	43.8	-46.1
0	0	6	29.4	10.7	4	0	2	5.4	-7.5
0	0	8	54.7	54.2	4	0	3	29.1	31.0
0	0	10	29.8	23.4	4	0	4	116.1	-110.9
0	0	12	15.3	14.9	4	0	5	72.1	65.9
0	0	14	25.5	-20.4	4	0	6	19.7	-20.7
0	0	16	21.3	-19.0	4	0	7	15.1	14.2
1	0	2	133.4	140.5	4	0	8	11.3	10.6
1	0	3	102.9	94.6	4	0	9	23.0	-20.6
1	0	4	17.2	-23.8	4	0	10	14.7	10.4
1	0	5	33.8	31.0	4	0	11	20.7	17.4
1	0	6	95.5	-93.2	4	0	12	10.2	5.4
1	0	7	22.2	-9.5	4	0	13	20.7	24.7
1	0	8	51.6	-55.6	4	0	14	14.4	-11.5
1	0	9	13.3	6.3	5	0	1	17.9	-17.4
1	0	10	22.6	-17.8	5	0	2	107.1	118.6
1	0	12	12.4	11.0	5	0	3	8.1	9.0
1	0	14	18.0	12.4	5	0	4	37.8	35.9
2	0	1	50.2	-51.1	5	0	5	73.4	66.2
2	0	2	82.4	-70.6	5	0	6	47.6	-46.6
2	0	3	91.8	-93.0	5	0	7	20.6	20.6
2	0	4	58.9	49.9	5	0	8	24.0	-21.7
2	0	5	35.6	-37.6	5	0	9	32.5	-31.0
2	0	6	40.1	42.0	5	0	10	10.2	10.2
2	0	7	44.9	42.6	5	0	11	31.3	-32.4
2	0	8	8.7	1.5	5	0	12	16.7	14.9
2	0	9	7.8	-9.1	5	0	14	11.3	8.7
2	0	10	33.1	-34.3	6	0	0	82.6	-81.6
2	0	11	17.5	-19.6	6	0	1	23.8	-22.3
2	0	12	13.1	-8.1	6	0	2	13.1	11.0
2	0	13	9.8	-9.3	6	0	3	59.6	-59.6
2	0	14	20.8	18.0	6	0	4	67.9	71.0
2	0	16	21.8	20.5	6	0	5	31.5	-28.3
3	0	3	27.1	28.7	6	0	6	34.2	28.1
3	0	4	20.3	16.6	6	0	7	40.1	35.8
3	0	5	43.0	-44.3	6	0	8	19.5	-22.7
3	0	6	51.1	53.1	6	0	10	17.7	-14.2
3	0	7	49.0	-48.4	6	0	11	23.9	-22.5
3	0	8	39.7	36.9	7	0	1	30.9	30.7
3	0	9	26.3	24.6	7	0	2	12.4	-12.8
3	0	10	27.4	26.1	7	0	4	18.3	-18.3
3	0	11	17.3	18.5	7	0	5	57.1	-57.8
3	0	12	19.7	-18.0	7	0	6	13.4	-14.4
3	0	14	17.5	-19.5	7	0	7	27.4	-22.3
4	0	0	137.7	145.6	7	0	9	37.2	33.4

H	K	L	FOBS	FCALC
7	0	11	20.5	21.1
7	0	12	13.8	-12.4
8	0	0	9.6	4.1
8	0	3	25.8	23.5
8	0	4	19.8	-23.0
8	0	5	24.1	23.0
8	0	6	14.2	-14.9
8	0	7	25.6	-23.9
8	0	8	9.3	-4.6
8	0	9	21.0	-23.5
8	0	10	18.1	16.4
8	0	12	13.3	12.9
9	0	1	13.0	-12.7
9	0	2	16.7	14.7
9	0	3	17.0	-16.5
9	0	4	9.3	11.1
9	0	5	17.9	17.3
9	0	7	25.4	24.8
9	0	9	15.3	-12.7
9	0	10	15.4	11.2
9	0	11	17.7	-19.2
10	0	3	26.2	-27.0
10	0	4	21.6	22.8
10	0	5	8.9	-5.7
10	0	7	33.1	28.3
10	0	8	13.1	-14.4
10	0	9	19.9	21.0
11	0	1	27.4	27.2
11	0	5	25.4	-22.2
11	0	9	10.8	12.8
0	1	5	87.9	76.5
0	1	7	122.7	129.4
0	1	9	47.0	47.0
0	1	11	10.7	-11.9
0	1	13	10.7	-7.1
1	1	1	106.2	114.4
1	1	2	31.9	-13.2
1	1	3	18.5	-15.8
1	1	4	36.8	33.9
1	1	5	42.7	-42.4
1	1	6	10.0	-9.4
1	1	7	13.4	-12.5
1	1	8	11.3	3.6
1	1	9	14.5	16.9
1	1	10	26.2	30.8

H	K	L	FOBS	FCALC
1	1	11	13.0	15.6
1	1	13	13.1	-13.4
1	1	14	8.2	-4.4
1	1	15	21.3	-23.3
2	1	1	70.7	78.6
2	1	3	56.5	49.9
2	1	4	79.3	84.9
2	1	5	8.7	-8.1
2	1	6	8.1	7.1
2	1	7	61.2	-58.1
2	1	8	17.0	-16.1
2	1	9	64.0	-62.0
2	1	10	24.1	-23.1
2	1	12	9.1	-13.1
2	1	13	34.7	32.1
3	1	1	85.1	-89.0
3	1	2	29.4	-25.8
3	1	3	27.4	-26.0
3	1	4	48.8	-43.3
3	1	5	55.1	54.2
3	1	6	31.8	-32.1
3	1	7	33.5	34.7
3	1	9	27.1	-30.3
3	1	11	34.1	-34.8
3	1	12	21.0	-22.2
3	1	14	9.9	-14.3
3	1	15	19.7	17.8
4	1	0	55.4	-53.5
4	1	2	14.2	-14.9
4	1	3	63.3	-62.9
4	1	4	6.4	-3.4
4	1	6	70.2	-73.3
4	1	7	48.7	46.6
4	1	8	7.2	-9.6
4	1	9	11.7	10.4
4	1	10	32.7	33.0
4	1	11	17.4	-18.5
4	1	12	24.9	21.9
4	1	13	11.4	-12.8
5	1	1	58.2	59.1
5	1	2	61.7	64.8
5	1	3	49.6	-52.7
5	1	4	59.1	58.5
5	1	5	56.3	-55.8
5	1	8	26.8	-25.3

Appendix B

H	K	L	FOBS	FCALC
5	1	9	21.2	20.9
5	1	10	13.3	12.1
5	1	11	14.3	14.4
5	1	12	17.7	19.3
5	1	14	9.4	9.2
6	1	0	32.9	-35.5
6	1	1	38.8	39.3
6	1	2	6.1	7.1
6	1	3	57.9	57.5
6	1	4	66.6	66.7
6	1	6	24.7	23.1
6	1	7	7.4	-7.3
6	1	8	18.7	-18.0
6	1	10	18.5	-18.1
6	1	11	12.9	11.7
6	1	13	14.6	14.1
7	1	1	25.6	23.2
7	1	2	58.4	-57.2
7	1	4	35.2	-34.8
7	1	5	16.4	20.4
7	1	6	17.0	15.9
7	1	7	23.6	24.2
7	1	8	25.1	25.4
7	1	11	17.8	-16.8
7	1	12	14.4	-14.4
8	1	0	21.1	20.8
8	1	2	15.5	19.0
8	1	3	23.0	-23.6
8	1	4	8.7	-9.9
8	1	5	24.8	-26.7
8	1	6	26.4	-28.0
8	1	10	24.4	24.0
8	1	12	10.2	11.4
9	1	3	17.7	-16.4
9	1	4	25.1	27.1
9	1	5	8.5	-7.4
9	1	8	27.7	-30.2
10	1	0	41.1	-42.7
10	1	1	16.5	16.6
10	1	2	16.2	-15.3
10	1	3	12.7	17.2
10	1	4	16.6	17.1
10	1	6	19.0	19.6
10	1	9	9.2	7.7
10	1	10	12.9	-15.5
11	1	2	27.7	-28.7
11	1	6	17.9	18.8
11	1	8	16.4	14.5
12	1	0	22.6	22.0
12	1	1	12.1	10.0
12	1	2	10.9	10.9
12	1	3	11.4	8.0
12	1	4	11.6	-11.6
0	2	2	98.4	-101.6
0	2	4	15.3	21.7
0	2	6	82.8	78.6
0	2	8	20.9	-21.3
0	2	10	45.1	-46.3
0	2	14	17.3	20.6
0	2	16	16.0	15.8
1	2	1	32.9	31.8
1	2	2	25.3	25.3
1	2	3	84.2	-85.2
1	2	4	51.3	-54.9
1	2	5	36.1	-31.8
1	2	6	34.3	34.9
1	2	7	11.1	14.5
1	2	8	79.6	82.1
1	2	10	11.0	14.4
1	2	12	14.5	-18.6
1	2	14	8.4	-9.8
2	2	0	32.3	-32.4
2	2	1	76.3	81.0
2	2	2	86.4	95.5
2	2	3	65.0	65.3
2	2	4	24.4	29.0
2	2	6	82.5	-88.1
2	2	7	15.9	-14.9
2	2	8	10.3	-10.3
2	2	9	9.7	6.6
2	2	10	43.6	47.1
2	2	13	12.7	10.0
2	2	14	14.7	-17.5
2	2	16	15.6	-17.0
3	2	1	28.4	28.5
3	2	2	48.0	-43.2
3	2	3	39.2	37.7
3	2	4	52.5	57.7
3	2	5	26.9	27.6
3	2	6	8.8	8.2

Appendix B

H	K	L	FOBS	FCALC
3	2	7	11.6	16.7
3	2	8	64.0	-68.8
3	2	9	7.8	-9.2
3	2	10	21.0	-25.8
3	2	11	14.2	-13.5
3	2	12	21.5	24.5
3	2	14	12.3	16.3
4	2	0	26.7	-26.1
4	2	1	20.5	-22.2
4	2	2	17.4	-17.1
4	2	3	44.8	-43.8
4	2	4	36.6	33.4
4	2	5	14.5	-16.8
4	2	6	46.7	47.6
4	2	7	16.3	-14.0
4	2	9	11.2	12.6
4	2	10	22.1	-22.8
4	2	11	9.8	-10.7
4	2	13	20.3	-21.2
4	2	14	12.2	12.5
5	2	1	47.3	48.3
5	2	2	45.9	-46.2
5	2	3	56.7	-57.6
5	2	4	50.0	-49.7
5	2	5	38.7	-39.4
5	2	6	18.4	18.0
5	2	8	32.4	34.3
5	2	9	9.0	11.5
5	2	11	29.4	28.9
5	2	12	15.0	-17.6
6	2	0	5.9	5.5
6	2	1	68.4	71.2
6	2	3	59.4	61.0
6	2	4	16.2	-16.2
6	2	5	18.6	-17.7
6	2	6	40.8	-40.9
6	2	7	18.7	-18.3
6	2	8	8.0	5.9
6	2	9	8.4	8.9
6	2	10	18.6	20.6
6	2	11	10.7	11.3
6	2	13	9.5	7.9
7	2	1	53.8	-54.3
7	2	2	13.6	-12.3
7	2	3	34.3	34.6
7	2	4	19.6	19.0
7	2	5	46.9	48.9
7	2	6	23.9	26.1
7	2	9	19.8	-22.6
7	2	11	16.8	-16.0
7	2	12	11.8	13.5
8	2	1	28.8	-27.6
8	2	3	23.3	-26.3
8	2	6	11.8	13.8
8	2	9	15.6	16.2
8	2	10	14.7	-16.5
8	2	12	11.7	-13.1
9	2	1	28.0	28.4
9	2	3	10.7	-11.4
9	2	5	14.5	-14.6
9	2	11	13.7	14.7
10	2	1	20.8	21.7
10	2	3	26.0	30.2
10	2	4	14.5	-14.5
10	2	5	9.9	-7.6
10	2	7	21.8	-22.7
10	2	8	10.1	7.4
10	2	9	13.5	-13.5
11	2	1	28.5	-30.0
11	2	3	12.9	10.6
11	2	5	16.4	19.6
12	2	0	12.7	9.7
12	2	1	18.6	-16.4
12	2	3	14.0	-15.2
13	2	1	12.6	11.5
0	3	1	14.6	13.2
0	3	3	82.8	81.3
0	3	5	6.9	-5.5
0	3	7	88.2	-85.8
0	3	9	42.1	-44.4
0	3	11	14.2	11.9
1	3	1	49.1	-49.5
1	3	2	62.1	-56.8
1	3	3	29.7	-31.1
1	3	5	51.7	53.6
1	3	6	28.4	25.6
1	3	7	25.0	26.4
1	3	8	9.7	-10.6
1	3	9	26.4	-27.5
1	3	10	21.2	-21.1

H	K	L	FOBS	FCALC	H	K	L	FOBS	FCALC
1	3	11	10.4	-15.0	5	3	5	50.1	46.4
1	3	13	12.0	10.8	5	3	7	9.2	12.6
1	3	15	13.6	16.4	5	3	8	16.7	19.2
2	3	0	18.3	22.7	5	3	9	20.6	-22.7
2	3	1	10.2	-7.1	5	3	11	13.3	-14.2
2	3	2	6.5	5.0	5	3	12	13.9	-13.9
2	3	3	37.6	-39.7	5	3	14	9.6	-7.9
2	3	4	34.2	-35.9	6	3	0	50.9	51.6
2	3	5	28.6	-30.4	6	3	1	19.7	-18.7
2	3	6	10.8	-13.9	6	3	2	8.1	-9.5
2	3	7	54.6	56.2	6	3	3	29.9	-30.1
2	3	9	48.3	50.6	6	3	4	55.7	-54.5
2	3	10	14.7	18.2	6	3	6	7.8	-8.0
2	3	12	9.7	10.1	6	3	8	12.1	10.5
2	3	13	24.4	-25.1	6	3	9	9.1	9.8
3	3	1	30.8	31.7	6	3	10	12.3	11.5
3	3	2	33.9	35.3	6	3	11	9.3	-6.9
3	3	3	42.2	41.3	6	3	13	13.4	-12.9
3	3	4	10.8	10.7	7	3	1	16.8	-13.0
3	3	5	31.8	-32.9	7	3	2	72.3	69.3
3	3	6	19.1	17.1	7	3	4	14.1	13.3
3	3	7	43.5	-42.2	7	3	5	14.0	-13.8
3	3	8	8.0	7.0	7	3	6	18.7	-20.9
3	3	9	23.2	22.0	7	3	7	17.1	-17.2
3	3	11	28.0	32.0	7	3	8	13.3	-13.4
3	3	12	13.3	15.1	7	3	11	12.0	12.0
3	3	14	10.1	10.9	7	3	12	11.5	10.5
3	3	15	14.2	-14.7	8	3	0	27.3	-26.9
4	3	0	37.5	-38.3	8	3	2	12.4	-11.1
4	3	1	12.3	12.7	8	3	3	12.6	15.2
4	3	2	20.6	19.9	8	3	4	13.8	14.5
4	3	3	43.8	45.6	8	3	5	20.2	21.3
4	3	4	36.1	36.6	8	3	6	15.5	17.9
4	3	5	11.3	11.4	8	3	10	14.4	-16.7
4	3	6	29.2	28.9	9	3	2	18.4	-18.3
4	3	7	42.5	-42.4	9	3	3	11.1	10.8
4	3	9	10.3	-11.0	9	3	4	15.9	-15.7
4	3	10	19.5	-18.7	9	3	8	19.9	19.3
4	3	11	15.6	16.2	9	3	12	12.0	-7.8
4	3	12	18.6	-16.5	10	3	0	46.7	41.8
4	3	13	9.2	9.1	10	3	1	13.0	-14.1
5	3	1	33.8	-34.0	10	3	2	11.4	8.8
5	3	2	47.7	-49.7	10	3	4	19.0	-20.7
5	3	3	15.2	14.6	10	3	6	13.9	-12.1
5	3	4	36.0	-35.3	10	3	10	12.8	10.8

Appendix B

H	K	L	FOBS	FCALC	H	K	L	FOBS	FCALC
11	3	2	26.4	25.7	4	4	0	84.3	86.6
11	3	6	14.8	-15.1	4	4	3	26.4	27.6
12	3	0	19.5	-19.3	4	4	4	57.9	-59.8
0	4	0	161.4	165.9	4	4	5	25.9	25.3
0	4	2	35.3	32.5	4	4	6	9.5	-7.7
0	4	4	72.0	-69.4	4	4	7	10.5	-9.7
0	4	6	29.6	-29.9	4	4	9	13.1	-13.0
0	4	8	15.3	20.3	4	4	10	11.1	8.1
0	4	10	22.9	23.5	4	4	13	13.3	12.4
0	4	12	13.5	10.8	5	4	1	18.0	-18.0
0	4	14	12.4	-11.8	5	4	2	76.0	74.2
1	4	1	12.7	-15.2	5	4	3	8.9	7.3
1	4	2	95.3	97.9	5	4	4	16.9	17.3
1	4	3	31.7	30.6	5	4	5	26.7	28.7
1	4	5	19.0	22.2	5	4	6	30.1	-33.5
1	4	6	50.8	-49.9	5	4	7	16.0	15.6
1	4	7	7.3	-9.0	5	4	8	14.8	-13.8
1	4	8	27.5	-26.9	5	4	9	16.3	-13.6
1	4	12	9.9	9.4	5	4	11	20.2	-21.2
1	4	14	9.6	8.7	6	4	0	25.3	-26.2
2	4	0	94.0	-95.2	6	4	1	16.0	-15.3
2	4	1	21.9	-22.1	6	4	3	31.2	-31.3
2	4	2	27.0	-26.5	6	4	4	26.3	25.0
2	4	3	29.7	-28.5	6	4	6	20.8	22.8
2	4	4	54.4	53.5	6	4	7	21.7	20.4
2	4	5	16.9	-13.2	6	4	8	8.7	-9.9
2	4	6	31.1	27.6	6	4	10	12.6	-11.6
2	4	7	13.3	13.3	6	4	11	9.8	-9.8
2	4	10	21.5	-21.5	0	5	1	62.3	-63.1
2	4	11	7.7	-6.9	0	5	3	69.4	-63.7
2	4	12	8.6	-6.3	0	5	5	32.3	28.5
2	4	14	11.0	9.1	0	5	7	41.4	39.1
3	4	1	22.9	-22.4	0	5	9	18.7	18.2
3	4	2	40.6	-40.1	0	5	13	12.1	-9.3
3	4	3	12.0	11.0	1	5	1	60.5	61.7
3	4	4	25.0	-24.7	1	5	2	11.3	9.6
3	4	5	18.6	-20.6	1	5	3	38.6	-37.7
3	4	6	18.4	17.8	1	5	4	7.9	5.7
3	4	7	19.5	-20.0	1	5	5	33.0	-31.3
3	4	8	30.8	33.8	1	5	6	9.8	-8.1
3	4	9	11.5	11.6	1	5	10	12.1	9.7
3	4	10	15.6	12.7	1	5	11	11.4	9.7
3	4	11	9.4	9.3	1	5	15	9.4	-9.8
3	4	12	16.7	-14.4	2	5	1	55.9	57.3
3	4	14	15.5	-12.1	2	5	2	12.3	-13.6

H	K	L	FOBS	FCALC
2	5	3	43.4	42.2
2	5	4	13.6	14.1
2	5	5	19.6	-20.7
2	5	6	19.5	20.4
2	5	7	20.6	-21.4
2	5	9	18.0	-17.4
2	5	10	11.6	-12.6
2	5	13	17.3	15.2
3	5	1	49.1	-46.8
3	5	3	19.0	19.3
3	5	4	12.1	-16.4
3	5	5	27.0	26.3
3	5	6	11.3	-8.1
3	5	7	13.9	9.7
3	5	8	10.1	6.9
3	5	9	10.3	-10.7
3	5	11	19.0	-17.8
3	5	15	10.5	9.1
4	5	1	29.4	-29.1
4	5	3	35.8	-33.6
4	5	5	11.3	9.5
4	5	6	29.1	-27.9
4	5	7	21.3	20.6
4	5	10	16.5	14.3
4	5	13	8.8	-5.7
5	5	1	40.7	40.1
5	5	3	31.9	-31.5
5	5	4	37.5	36.7
5	5	5	33.1	-29.3
5	5	8	26.0	-24.6
5	5	9	11.4	10.2
5	5	12	9.5	9.9
6	5	0	13.3	-9.7
6	5	1	23.9	23.6
6	5	2	8.6	-6.7
6	5	3	24.1	25.2
6	5	4	15.7	15.9
6	5	6	20.6	18.1
6	5	10	10.5	-11.7
0	6	0	49.1	-53.1
0	6	2	15.6	-16.5
0	6	4	26.1	26.0
0	6	6	24.6	24.3
0	6	10	16.6	-17.5
1	6	2	13.1	-14.1
1	6	3	14.3	-14.9
1	6	4	15.3	-17.1
1	6	8	21.0	23.4
1	6	12	11.3	-9.6
2	6	0	9.1	9.5
2	6	1	14.4	14.6
2	6	2	16.7	18.3
2	6	3	17.0	18.0
2	6	6	28.1	-27.7
2	6	7	12.6	-10.6
2	6	10	16.2	17.8
3	6	2	15.0	14.4
3	6	4	20.6	19.9
3	6	5	10.0	11.3
3	6	8	22.2	-22.4
3	6	9	8.1	-6.4
3	6	10	10.2	-6.6
3	6	12	11.3	10.2
4	6	0	15.8	-16.9
4	6	1	9.3	-9.0
4	6	3	17.0	-14.2
4	6	4	10.0	10.6
4	6	6	10.9	12.9
5	6	1	21.1	20.3
5	6	2	14.2	-14.9
5	6	3	12.6	-13.3
5	6	4	17.2	-15.2
5	6	5	13.5	-17.9
5	6	8	13.1	13.1
5	6	9	9.2	7.0
6	6	3	18.7	17.8
6	6	6	16.2	-14.5
6	6	7	11.1	-11.9
0	7	3	22.2	23.1
0	7	5	19.1	14.9
0	7	7	24.8	-27.0
0	7	9	15.0	-13.5
1	7	3	11.9	-14.2
1	7	5	15.2	17.1
1	7	7	13.6	15.3
1	7	9	10.0	-10.8
2	7	0	23.3	22.8
2	7	3	11.3	-10.9
2	7	4	18.4	-16.2
2	7	5	12.1	-14.2

Appendix B

H	K	L	FOBS	FCALC	H	K	L	FOBS	FCALC
2	7	7	11.7	13.0	1	8	4	10.5	10.9
2	7	9	12.9	15.2	2	8	0	10.4	-9.9
3	7	2	15.5	15.7	2	8	6	13.1	13.3
3	7	3	10.1	13.3	3	8	2	18.5	-14.9
3	7	5	15.0	-17.4	3	8	4	9.9	-7.1
3	7	7	18.2	-15.0	3	8	6	8.5	6.8
3	7	9	12.3	11.7	4	8	0	10.0	12.1
3	7	11	12.0	9.5	5	8	1	11.2	-8.6
4	7	0	11.4	-12.4	6	8	0	12.0	-10.1
4	7	5	15.2	12.5	0	9	1	16.7	-14.8
4	7	7	14.4	-13.0	0	9	3	14.6	-14.0
5	7	2	23.0	-24.0	1	9	1	12.6	14.4
5	7	5	10.6	10.0	1	9	5	9.4	-8.3
5	7	6	10.7	8.8	2	9	1	13.5	12.9
6	7	0	26.6	24.3	2	9	3	10.3	10.5
6	7	4	15.0	-16.9	3	9	1	13.8	-11.7
0	8	0	19.4	26.3	3	9	3	8.9	8.4
0	8	4	17.4	-17.2	3	9	5	9.7	7.4
0	8	6	9.9	-9.6	4	9	3	9.2	-9.1
1	8	2	12.1	12.2	4	9	7	10.0	5.0

APPENDIX C

Structure Factors for $(Me_4N)_2(Cu,Co)Cl_4$

Values given are h,k,ℓ,F_{obs} and F_{calc}.

Appendix C

H	K	L	FOBS	FCALC
0	0	2	40.8	43.5
0	0	6	18.6	-17.7
0	0	8	25.2	23.7
0	0	10	24.6	24.7
0	0	12	22.0	22.9
0	0	14	24.1	-22.4
0	0	16	21.0	-19.6
1	0	2	114.1	134.2
1	0	3	72.0	66.4
1	0	4	26.0	-29.1
1	0	5	40.8	40.5
1	0	6	87.9	-85.7
1	0	7	9.1	7.9
1	0	8	54.9	-50.8
1	0	10	30.2	-27.6
1	0	12	12.9	12.8
1	0	14	21.0	20.7
2	0	0	117.9	-130.9
2	0	1	41.8	-37.6
2	0	2	70.4	-65.9
2	0	3	91.3	-90.6
2	0	4	59.8	57.1
2	0	5	52.5	-56.1
2	0	6	34.4	33.1
2	0	7	39.8	36.0
2	0	8	11.1	10.7
2	0	10	20.0	-19.1
2	0	11	16.6	-18.3
2	0	12	11.7	-10.1
2	0	14	15.3	11.7
2	0	16	15.3	17.1
3	0	1	138.5	-129.1
3	0	2	134.9	-117.7
3	0	3	61.4	56.1
3	0	4	29.0	26.6
3	0	5	22.0	-22.5
3	0	6	31.1	32.3
3	0	7	39.6	-38.0
3	0	8	26.0	23.6
3	0	9	27.3	25.6
3	0	10	23.8	23.5
3	0	11	7.4	9.4
3	0	12	14.8	-14.8
3	0	14	20.3	-20.4
4	0	0	117.3	115.7
4	0	1	71.1	-69.9
4	0	2	6.4	-2.5
4	0	3	3.7	1.4
4	0	4	86.6	-85.9
4	0	5	62.9	67.1
4	0	6	30.4	-33.4
4	0	7	17.0	18.5
4	0	9	9.1	-9.8
4	0	10	17.8	18.9
4	0	11	12.3	14.6
4	0	12	12.3	12.6
4	0	14	9.8	-10.4
5	0	1	16.6	14.9
5	0	2	115.7	111.6
5	0	3	15.7	-14.2
5	0	4	54.4	58.8
5	0	5	30.6	31.4
5	0	6	34.6	-35.8
5	0	7	14.8	14.5
5	0	8	41.2	-42.8
5	0	9	27.0	-24.5
5	0	11	22.9	-22.9
5	0	12	24.6	23.1
5	0	14	15.7	13.2
6	0	0	82.3	-74.1
6	0	1	9.1	7.9
6	0	2	8.3	-9.9
6	0	3	35.6	-34.6
6	0	4	56.2	58.5
6	0	5	42.2	-40.6
6	0	6	49.2	49.6
6	0	7	29.2	28.6
6	0	8	16.6	-14.5
6	0	10	25.4	-28.5
6	0	11	13.9	-15.4
6	0	12	10.5	-12.1
7	0	1	26.8	24.0
7	0	2	13.4	-16.5
7	0	3	10.5	11.4
7	0	4	36.7	-35.2
7	0	5	45.3	-49.8
7	0	6	7.4	-7.6
7	0	7	19.6	-19.7
7	0	8	15.7	18.6
7	0	9	34.0	31.3

H	K	L	FOBS	FCALC
7	0	11	14.8	15.7
8	0	3	12.9	14.1
8	0	4	13.9	-13.1
8	0	5	15.3	15.4
8	0	6	22.6	-24.3
8	0	7	15.7	-14.9
8	0	9	11.7	-10.3
8	0	10	22.0	22.2
8	0	12	13.4	11.5
9	0	2	10.5	9.6
9	0	3	11.1	-11.1
9	0	4	25.4	22.6
9	0	7	12.3	12.7
9	0	8	11.7	-9.9
9	0	12	10.5	6.8
10	0	0	20.3	-19.1
10	0	2	12.3	-11.6
10	0	3	11.1	-11.1
10	0	4	21.0	20.8
10	0	5	7.4	-3.6
10	0	6	27.8	26.9
10	0	7	14.8	13.1
10	0	8	11.7	-9.9
10	0	9	14.4	11.4
10	0	10	14.8	-14.8
11	0	1	19.3	19.1
11	0	2	10.5	-10.9
11	0	4	13.4	-14.7
11	0	5	18.9	-16.9
11	0	8	9.8	10.4
12	0	1	12.9	12.3
12	0	3	17.4	16.6
12	0	7	14.4	-13.6
13	0	1	10.5	-10.1
0	1	5	60.6	58.9
0	1	7	104.3	111.9
0	1	9	55.8	55.9
0	1	11	8.3	-10.5
0	1	13	22.9	-19.4
0	1	15	11.7	-12.0
1	1	2	38.4	-20.4
1	1	3	13.9	-9.9
1	1	4	49.4	51.8
1	1	5	46.2	-44.0
1	1	7	26.0	-27.4

H	K	L	FOBS	FCALC
1	1	8	6.4	-5.9
1	1	9	6.4	5.5
1	1	10	19.6	20.1
1	1	11	15.3	14.9
1	1	13	9.8	-8.3
1	1	15	20.7	-19.0
1	1	17	9.1	-9.3
2	1	0	63.6	-54.0
2	1	1	95.4	87.1
2	1	2	3.7	1.3
2	1	3	47.1	42.1
2	1	4	51.6	63.8
2	1	5	19.6	-22.1
2	1	6	9.1	8.0
2	1	7	57.0	-55.6
2	1	8	14.8	-14.4
2	1	9	53.4	-52.6
2	1	10	25.2	-24.7
2	1	11	5.2	-4.2
2	1	12	9.1	-9.9
2	1	13	33.8	30.3
2	1	15	9.1	7.3
3	1	1	88.4	-82.0
3	1	2	9.1	-6.6
3	1	3	13.9	-13.6
3	1	4	29.7	-27.8
3	1	5	40.1	42.6
3	1	6	30.2	-33.1
3	1	7	27.5	29.9
3	1	8	22.3	-17.7
3	1	9	12.3	-15.8
3	1	11	29.5	-29.7
3	1	15	13.9	15.2
4	1	0	77.3	-74.9
4	1	1	35.6	-31.9
4	1	2	24.3	-23.2
4	1	3	61.9	-64.4
4	1	4	7.4	8.4
4	1	5	12.9	-12.5
4	1	6	36.4	-41.4
4	1	7	49.9	48.0
4	1	9	22.9	23.0
4	1	10	18.9	21.1
4	1	11	13.4	-13.1
4	1	12	15.7	15.7

H	K	L	FOBS	FCALC
4	1	13	14.8	-16.2
5	1	1	63.6	71.5
5	1	2	30.4	32.5
5	1	3	33.0	-38.8
5	1	4	42.3	49.8
5	1	5	62.4	-69.0
5	1	6	9.1	8.6
5	1	7	17.8	-19.2
5	1	8	13.9	-13.7
5	1	9	27.3	27.0
5	1	10	9.1	9.3
5	1	11	24.9	24.9
5	1	12	8.3	8.3
6	1	0	9.1	-8.1
6	1	1	42.3	45.2
6	1	3	57.5	67.0
6	1	4	35.8	38.9
6	1	6	21.3	21.0
6	1	7	17.0	-16.6
6	1	8	10.5	-12.2
6	1	9	10.5	-12.0
6	1	10	15.3	-16.4
6	1	11	9.1	10.8
6	1	13	14.4	14.6
7	1	2	48.5	-47.5
7	1	4	30.2	-29.7
7	1	5	27.5	29.2
7	1	6	13.9	13.9
7	1	7	17.8	20.1
7	1	8	21.3	21.2
7	1	9	9.8	-11.3
7	1	11	18.6	-18.9
8	1	0	12.9	11.7
8	1	3	30.8	-28.9
8	1	5	25.4	-24.1
8	1	6	9.1	-10.0
8	1	7	10.5	13.6
8	1	9	12.3	10.4
8	1	10	9.1	10.5
9	1	4	13.9	14.4
9	1	5	16.6	-16.5
9	1	8	15.3	-16.4
10	1	0	23.5	-19.8
10	1	1	23.5	19.9
10	1	2	12.3	-10.3
10	1	3	28.7	30.0
10	1	6	9.1	11.7
10	1	7	14.4	-14.5
11	1	1	11.7	-10.4
11	1	2	24.3	-21.8
11	1	5	11.7	10.9
11	1	6	13.4	11.2
11	1	8	11.1	10.4
12	1	0	24.1	22.6
12	1	2	8.3	7.3
12	1	4	12.9	-13.8
12	1	6	11.1	-10.9
0	2	2	113.9	-110.2
0	2	4	15.7	21.8
0	2	6	109.9	107.5
0	2	8	7.4	-7.6
0	2	10	50.2	-49.0
0	2	12	6.4	-10.6
0	2	14	20.7	21.3
0	2	16	17.0	13.7
1	2	2	20.3	27.6
1	2	3	81.0	-76.7
1	2	4	59.8	-56.8
1	2	5	36.2	-33.2
1	2	6	37.1	36.1
1	2	8	85.5	86.4
1	2	10	12.3	14.2
1	2	12	17.0	-20.7
1	2	14	12.3	-12.0
2	2	0	12.9	-16.3
2	2	1	93.7	88.9
2	2	2	104.2	94.0
2	2	3	68.7	70.7
2	2	4	11.1	15.3
2	2	6	89.3	-85.5
2	2	7	7.4	-6.6
2	2	8	9.1	-9.7
2	2	9	7.4	8.4
2	2	10	40.0	36.6
2	2	13	9.1	9.7
2	2	14	8.3	-11.3
2	2	16	15.3	-12.7
3	2	1	23.5	26.2
3	2	2	31.5	-35.5
3	2	3	52.1	50.6

H	K	L	FOBS	FCALC
3	2	4	42.6	45.4
3	2	5	9.1	10.2
3	2	7	7.4	-7.7
3	2	8	52.7	-54.0
3	2	10	12.3	-16.4
3	2	12	14.8	18.7
3	2	14	14.8	14.9
4	2	0	36.4	-35.6
4	2	1	22.9	-23.6
4	2	2	20.3	-18.6
4	2	3	25.2	-26.8
4	2	4	35.4	37.3
4	2	5	8.3	1.4
4	2	6	46.1	51.6
4	2	7	29.5	-28.3
4	2	10	27.8	-24.3
4	2	12	9.8	-8.8
4	2	13	8.3	-6.4
4	2	14	7.4	8.5
5	2	1	31.5	30.0
5	2	2	70.1	-71.7
5	2	3	53.0	-54.6
5	2	4	52.6	-56.9
5	2	5	14.8	-10.6
5	2	6	22.9	23.7
5	2	7	9.1	11.9
5	2	8	40.1	40.5
5	2	11	20.0	20.0
5	2	12	17.0	-19.0
5	2	13	9.8	10.3
5	2	14	13.4	-12.0
6	2	0	43.1	42.0
6	2	1	54.5	62.3
6	2	2	8.3	11.2
6	2	3	44.1	45.3
6	2	4	38.0	-38.6
6	2	5	14.4	-18.0
6	2	6	44.2	-41.5
6	2	7	6.4	-6.7
6	2	8	8.3	9.8
6	2	10	21.6	21.4
6	2	12	11.7	12.2
7	2	1	47.2	-49.9
7	2	2	23.5	21.7
7	2	3	30.2	31.5
7	2	4	24.6	22.0
7	2	5	38.2	39.2
7	2	8	9.8	-9.6
7	2	9	16.2	-16.3
7	2	11	15.7	-13.9
7	2	12	8.3	8.2
8	2	0	21.0	-19.0
8	2	1	18.6	-20.1
8	2	3	15.3	-15.5
8	2	4	18.2	17.4
8	2	6	7.4	9.0
8	2	10	15.3	-13.4
8	2	12	14.4	-14.3
9	2	1	19.6	17.3
9	2	2	23.2	-20.3
9	2	3	9.8	-10.7
9	2	4	7.4	-7.1
10	2	0	32.8	31.0
10	2	1	9.8	10.9
10	2	3	12.9	13.5
10	2	4	23.2	-24.6
10	2	6	12.3	-13.1
10	2	7	9.8	-10.4
10	2	8	7.4	6.1
10	2	9	9.1	-10.5
10	2	10	9.1	8.8
11	2	1	19.3	-19.0
11	2	2	21.0	17.3
11	2	5	13.4	15.1
12	2	0	8.3	-8.3
12	2	1	13.9	-12.1
12	2	3	15.3	-16.1
0	3	3	98.2	95.1
0	3	5	6.4	9.9
0	3	7	87.0	-97.1
0	3	9	49.2	-50.3
0	3	11	21.0	18.2
0	3	13	16.2	14.9
0	3	15	10.5	9.1
1	3	1	57.4	-55.9
1	3	2	69.1	-59.5
1	3	3	40.0	-39.5
1	3	5	66.3	62.5
1	3	6	19.6	18.2
1	3	7	35.8	35.4

Appendix C

H	K	L	FOBS	FCALC
1	3	9	24.9	-25.0
1	3	10	13.4	-12.2
1	3	11	10.5	-11.7
1	3	15	10.5	12.0
2	3	0	22.9	26.4
2	3	1	6.4	-4.2
2	3	3	37.5	-36.8
2	3	4	37.8	-37.5
2	3	5	27.3	-24.2
2	3	7	60.6	60.3
2	3	9	47.4	42.4
2	3	10	16.6	15.4
2	3	12	8.3	11.5
2	3	13	18.9	-21.3
3	3	1	33.0	32.6
3	3	2	36.0	36.1
3	3	3	35.2	32.9
3	3	4	5.2	-8.3
3	3	5	33.8	-34.7
3	3	6	20.7	18.1
3	3	7	36.6	-37.1
3	3	8	24.9	23.8
3	3	9	16.6	17.5
3	3	10	6.4	-6.1
3	3	11	23.8	23.7
4	3	0	28.0	-28.2
4	3	1	20.7	21.9
4	3	2	34.6	35.5
4	3	3	57.4	58.1
4	3	4	28.5	27.5
4	3	5	9.8	10.1
4	3	7	42.3	-44.6
4	3	9	13.4	-15.4
4	3	10	7.4	-8.0
4	3	11	10.5	11.2
4	3	12	13.9	-16.8
4	3	13	10.5	11.4
5	3	1	48.8	-49.8
5	3	2	40.8	-38.5
5	3	3	13.9	15.0
5	3	4	18.6	-18.8
5	3	5	64.7	60.5
5	3	7	17.0	19.3
5	3	9	22.9	-24.5
5	3	11	21.6	-20.3
6	3	0	42.5	39.9
6	3	1	35.8	-37.4
6	3	3	42.2	-45.8
6	3	4	40.0	-39.9
6	3	7	9.1	9.5
6	3	9	12.3	12.6
6	3	10	9.8	9.6
6	3	13	11.7	-13.1
7	3	2	69.0	60.1
7	3	3	17.0	-18.4
7	3	5	18.2	-21.7
7	3	6	12.9	-13.6
7	3	7	7.4	-7.4
7	3	8	8.3	-11.2
7	3	11	14.8	14.9
8	3	0	20.7	-19.2
8	3	1	10.5	12.4
8	3	3	21.6	23.2
8	3	5	11.7	12.8
9	3	1	9.8	-9.4
9	3	2	6.4	-8.8
9	3	3	10.5	12.4
9	3	5	7.4	7.3
9	3	8	10.5	12.5
9	3	12	11.1	-5.1
10	3	0	24.1	18.6
10	3	1	24.9	-24.6
10	3	3	26.8	-24.4
10	3	6	10.5	-10.1
11	3	1	9.1	10.9
11	3	2	16.6	16.6
12	3	0	18.6	-17.4
12	3	4	12.3	11.1
0	4	2	43.8	44.9
0	4	4	83.0	-73.2
0	4	6	47.5	-48.0
0	4	8	7.4	12.2
0	4	10	22.0	21.9
0	4	12	11.7	12.5
0	4	14	11.7	-11.4
0	4	16	12.3	-12.4
1	4	1	10.5	-10.8
1	4	2	84.9	93.5
1	4	3	24.9	24.0
1	4	4	3.7	1.2

H	K	L	FOBS	FCALC
1	4	5	17.8	17.9
1	4	6	56.2	-50.6
1	4	8	34.8	-30.1
1	4	10	8.3	-9.8
1	4	12	7.4	8.8
1	4	14	12.3	13.3
2	4	0	111.3	-97.2
2	4	1	20.0	-17.8
2	4	2	30.4	-30.5
2	4	3	28.5	-26.9
2	4	4	56.3	53.9
2	4	5	26.2	-23.1
2	4	6	32.8	29.9
2	4	7	9.1	9.7
2	4	10	13.4	-15.7
2	4	11	7.4	-7.4
2	4	12	7.4	-7.6
2	4	16	11.1	11.3
3	4	1	29.7	-32.4
3	4	2	36.2	-34.6
3	4	3	7.4	9.8
3	4	4	24.3	-25.8
3	4	5	5.2	-5.3
3	4	6	14.4	16.5
3	4	7	12.3	-12.7
3	4	8	31.3	29.9
3	4	9	8.3	9.0
3	4	10	11.7	12.2
3	4	12	11.7	-11.8
3	4	14	13.9	-13.9
4	4	0	116.7	86.2
4	4	1	20.7	-19.6
4	4	3	8.3	10.4
4	4	4	80.5	-54.9
4	4	5	29.7	27.8
4	4	6	16.2	-17.1
4	4	10	11.7	13.6
4	4	12	11.7	10.2
5	4	2	87.4	78.4
5	4	4	35.0	29.5
5	4	5	7.4	10.1
5	4	6	24.6	-27.0
5	4	7	13.9	15.9
5	4	8	28.3	-25.1
5	4	9	9.1	-9.9
5	4	11	17.0	-17.9
5	4	12	12.9	13.6
5	4	14	9.1	9.6
6	4	0	33.4	-32.4
6	4	1	8.3	-10.2
6	4	2	9.1	-11.9
6	4	3	22.3	-20.8
6	4	4	28.5	28.1
6	4	5	11.1	-10.5
6	4	6	31.7	31.8
6	4	7	10.5	12.2
6	4	8	6.4	-6.1
6	4	9	6.4	5.3
6	4	10	17.4	-18.0
6	4	12	7.4	-8.6
7	4	1	16.2	16.7
7	4	2	21.6	-23.3
7	4	3	5.2	5.6
7	4	4	15.3	-15.0
7	4	5	27.0	-31.0
7	4	7	10.5	-12.8
7	4	8	9.8	11.4
7	4	9	21.3	19.1
7	4	11	8.3	10.2
8	4	0	17.0	17.7
8	4	1	9.1	-3.7
8	4	5	10.5	12.1
8	4	6	11.1	-13.3
8	4	7	9.8	-8.3
8	4	9	9.8	-10.6
8	4	10	13.4	13.7
9	4	2	8.3	8.4
9	4	4	11.1	12.2
9	4	5	7.4	6.7
9	4	7	8.3	7.5
10	4	0	15.3	-17.6
10	4	3	11.1	-10.2
10	4	4	11.7	14.0
10	4	6	12.3	14.6
10	4	7	7.4	11.2
10	4	10	10.5	-9.7
11	4	1	10.5	10.2
11	4	2	9.8	-8.7
11	4	4	9.8	-7.7
11	4	5	11.1	-11.5

Appendix C

H	K	L	FOBS	FCALC
11	4	6	7.4	2.3
12	4	1	7.4	7.7
12	4	3	12.3	11.9
0	5	3	71.4	-71.1
0	5	5	29.7	26.8
0	5	7	41.0	41.7
0	5	9	21.6	25.2
0	5	13	18.9	-15.9
1	5	3	39.1	-38.1
1	5	4	13.9	11.2
1	5	5	28.7	-29.5
1	5	10	9.8	7.7
1	5	11	12.9	13.0
2	5	0	7.4	10.6
2	5	1	60.5	58.9
2	5	2	13.9	-16.1
2	5	3	37.7	39.7
2	5	4	7.4	8.9
2	5	5	22.6	-22.9
2	5	6	26.0	27.0
2	5	7	16.6	-18.9
2	5	8	6.4	-7.0
2	5	9	22.3	-20.1
2	5	10	16.2	-16.4
2	5	13	19.6	17.9
3	5	1	44.4	-45.2
3	5	2	12.3	12.1
3	5	3	20.7	18.0
3	5	4	14.8	-15.9
3	5	5	22.6	24.1
3	5	6	14.4	-14.1
3	5	7	14.8	14.2
3	5	11	18.9	-18.6
4	5	0	24.6	-24.1
4	5	1	23.2	-26.8
4	5	3	38.7	-36.0
4	5	6	23.2	-21.5
4	5	9	10.5	12.1
4	5	10	12.3	13.2
4	5	13	11.1	-10.2
5	5	1	41.0	42.4
5	5	2	9.1	-13.1
5	5	3	22.9	-21.1
5	5	4	41.3	38.8
5	5	5	45.6	-38.9
5	5	7	9.8	-9.9
5	5	8	21.6	-21.5
5	5	9	14.8	15.7
5	5	11	13.9	14.9
6	5	1	21.6	23.3
6	5	2	7.4	-8.1
6	5	3	34.0	31.4
6	5	5	11.7	4.3
6	5	6	18.9	19.0
6	5	7	9.8	-13.2
6	5	9	11.7	-12.7
6	5	10	12.9	-12.1
7	5	2	21.6	-19.6
7	5	4	21.0	-19.6
7	5	5	20.0	16.7
7	5	8	15.3	15.8
7	5	11	9.8	-10.8
8	5	2	9.1	10.3
8	5	3	15.3	-15.9
8	5	5	13.4	-14.5
8	5	6	11.1	-15.1
8	5	7	11.1	13.1
9	5	4	11.1	10.4
9	5	5	9.8	-10.1
9	5	8	11.1	-10.2
10	5	0	12.9	-10.6
10	5	2	7.4	-5.6
10	5	3	17.0	15.2
10	5	6	9.8	7.9
10	5	7	11.7	-10.5
11	5	2	9.8	-10.3
11	5	5	9.1	8.4
12	5	0	11.1	12.5
0	6	0	59.6	-68.5
0	6	2	20.7	-20.3
0	6	4	30.2	30.8
0	6	10	20.7	-20.5
1	6	2	19.3	-19.8
1	6	3	13.9	-14.2
1	6	4	13.4	-13.5
1	6	8	25.7	26.2
2	6	0	19.6	18.9
2	6	1	11.7	13.2
2	6	2	20.7	19.4
2	6	3	21.3	21.5

Appendix C

H	K	L	FOBS	FCALC
2	6	4	8.3	-6.8
2	6	6	32.6	-28.4
2	6	7	13.9	-12.2
2	6	8	8.3	-6.8
2	6	10	20.7	17.7
2	6	12	8.3	7.2
0	7	3	33.0	31.0
0	7	5	19.6	17.4
0	7	7	32.4	-34.7
0	7	9	19.6	-18.9
1	7	1	9.1	-11.5
1	7	3	12.3	-15.9
1	7	5	22.9	22.2
1	7	7	21.0	20.6
1	7	9	12.3	-13.2
1	7	11	9.1	-10.9
2	7	0	26.5	24.6
2	7	3	13.9	-15.6
2	7	4	20.7	-20.1
2	7	5	13.4	-13.8
2	7	7	14.8	17.8
2	7	9	16.6	17.9
0	8	4	24.1	-21.9
0	8	6	21.0	-18.7
1	8	2	13.4	14.8
1	8	4	16.6	17.0
1	8	6	8.3	-11.3
1	8	8	13.4	-16.4
2	8	0	11.7	-15.0
2	8	1	8.3	-8.6
2	8	2	12.3	-12.7
2	8	3	7.4	-7.4
2	8	4	10.5	11.7
2	8	6	20.0	19.2
1	9	1	13.9	18.6
1	9	3	9.8	-11.1